UNIVERSITÀ DEGLI STUDI DI MILANO - BICOCCA

Facoltà di Scienze Matematiche, Fisiche e Naturali

Corso di Dottorato di Ricerca in Informatica - XXVII Ciclo

Continuous Time Bayesian Networks for Reasoning and Decision Making in Finance

Simone Villa

Supervisor:

Prof. Fabio Antonio Stella

Tutor:

Prof. Carlo Batini

Coordinator:

Prof. Stefania Bandini

Submitted in partial fulfillment of the requirements for the degree of

Doctor of Philosophy in Computer Science of

Università degli Studi di Milano - Bicocca,

Academic Year 2013 - 2014.

Ai miei genitori.

Abstract

The analysis of the huge amount of financial data, made available by electronic markets, calls for new models and techniques to effectively extract knowledge to be exploited in an informed decision-making process. The aim of this thesis is to introduce probabilistic graphical models that can be used to reason and to perform actions in such a context.

In the first part of this thesis, we present a framework which exploits Bayesian networks to perform portfolio analysis and optimization in a holistic way. It leverages on the compact and efficient representation of high dimensional probability distributions offered by Bayesian networks and their ability to perform evidential reasoning in order to optimize the portfolio according to different economic scenarios.

In many cases, we would like to reason about the market change, i.e. we would like to express queries as probability distributions over time. Continuous time Bayesian networks can be used to address this issue. In the second part of the thesis, we show how it is possible to use this model to tackle real financial problems and we describe two notable extensions. The first one concerns classification, where we introduce an algorithm for learning these classifiers from Big Data, and we describe their straightforward application to the foreign exchange prediction problem in the high frequency domain. The second one is related to non-stationary domains, where we explicitly model the presence of statistical dependencies in multivariate time-series while allowing them to change over time.

In the third part of the thesis, we describe the use of continuous time Bayesian networks within the Markov decision process framework, which provides a model for sequential decision-making under uncertainty. We introduce a method to control continuous time dynamic systems, based on this framework, that relies on additive and context-specific features to scale up to large state spaces. Finally, we show the performances of our method in a simplified, but meaningful trading domain.

Acknowledgments

I am greatly indebted to my advisor, Prof. Fabio Antonio Stella, for his guidance during my studies. He gave me suggestions, advice and challenging ideas to think over and develop. His strong ethic has been a constant source of commitment and respect for me.

I am thankful to my tutor, Prof. Carlo Batini, for his support during my studies and for providing many suggestions to improve the quality of my research activity.

My sincere thanks also goes to Prof. Christian R. Shelton for giving me the opportunity to work with him and his research group on exciting projects. He was helpful and insightful in discussing research topics on several occasions. A particular thanks to Busra, Juan and Zhen who made me feel welcome and part of their team.

Special thanks go to my colleagues at the department of informatics who shared with me this exciting experience. In particular, I thank my laboratory colleagues Marco and Alessandro for their stimulating discussions and friendship. Thanks to all the master students of my laboratory who worked with me during these years for their commitment on common projects. I thanks all the professors and the administrative personnel at the department of informatics for their high quality service.

I want to thank a number of my friends and colleagues who I have learned from and collaborated with over the last few years. In particular, Michele, Fabrizio, Monica, Edoardo, Paola, Roberto, Luca, Fabio and Emanuele for their in-depth knowledge of financial markets and their countless exchange of views and ideas.

Finally, I would like to thank my sister, my parents and Vika for their understanding, encouragement and support through out all the challenges in my life.

Thank you.

Contents

List of Figures

List of Algorithms

Chapter 1

Introduction

The explosion of the financial data, made available by electronic markets, has started a revolution on data processing and statistical modeling. This revolution forces financial analysts to cope with theoretical and computational challenges. The first main issue in such a complex domain is related to *reasoning*, i.e. to use the available information to draw conclusions. For example, a market practitioner needs to collect information about a company to reach conclusions about the future value of that company.

Probabilistic graphical models, and in particular *Bayesian networks* (Pearl, 1988), are valid tools for reasoning under uncertainty by allowing compact representations of complex domains. The graphical model offers a clear interface by which the domain expert can elicit his knowledge and the skeleton for representing the joint distribution compactly. The availability of inference algorithms, that can answer queries about distributions in an effective way, is the key of the success of these models in many real life contexts. Even if Bayesian networks have been successfully applied to perform portfolio analysis and optimization in a coherent way (Villa and Stella, 2012), they cannot be directly used to answer questions involving distributions over time.

This aspect introduces the second main issue related to the financial context, i.e. how to model the *temporal evolution* of an economic variable. For example, in a high frequency environment the knowledge of the exact time to enter in a position leads to a competitive advantage compared to other market participants given that time is the critical component for the success of a strategy. The classical approach to model structured temporal processes relies on *dynamic Bayesian networks* (Dean and Kanazawa, 1989). Unfortunately, these models suffer from two main drawbacks: the model instability related to the choice of the discretization step and the computational burden related to inference. *Continuous time Bayesian networks* (Nodelman et al., 2002) overcome the previous issues by modeling time directly. These models are based both on homogeneous Markov processes, as they model the transition dynamics of a system, and on Bayesian networks, as they provide a graphical representation over a structured state space. These models can be used in several financial contexts, such as for scenario generation based on historical data, for the analysis of timing and probability related to securities, and for inferring the temporal evolution of an economic variable when its state is not observed.

Two significant extensions of continuous time Bayesian networks have enhanced their expressive power and usability. Firstly, *continuous time Bayesian network classifiers* (Stella and Amer, 2012; Codecasa and Stella, 2014) allow to perform temporal classification in continuous time. Specifically, in the case of complete data, they are effective for performing inference and learning on a huge amount of data (Villa and Rossetti, 2014). In finance, these classifiers can be used to exploit important features of high frequency data, such as the unevenly spaced time data, and to perform the prediction of economic variables, such as the foreign exchange rate (Villa and Stella, 2014). Secondly, *non-stationary continuous time Bayesian networks* allow to represent dependencies which change over time (Stella and Villa, 2014). They can be used to analyze time-series data, such as change-points detection, and reasoning about when and how these dependencies vary.

The third issue in finance is related to the *decision-making* modeling, i.e. how to fruitfully exploit the previous models to make actionable decisions. For example, in the context of trading, the problem is to choose the best action to perform in each possible state of the market in order to maximize the portfolio return. *Structured continuous time Markov decision processes* (Kan and Shelton, 2008) are a useful framework to represent large and structured continuous time systems and they can be solved effectively using approximate linear programming techniques. Unfortunately, this framework requires the full knowledge of the environment, which is a rather strong assumption in finance. *Model-based reinforcement learning using structured continuous time Markov decision processes* relax this assumption allowing the decision-maker to learn the model from the interactions with the unknown environment (Villa and Shelton, 2014a).

1.1 Contributions

This thesis concerns probabilistic graphical models, specifically Bayesian networks, continuous time Bayesian networks and their extensions, for reasoning and decision-making in finance. The contributions of this work can be summarized as follows:

- the interplay between modern portfolio theory and Bayesian networks has been exploited to propose a novel framework for portfolio analysis and optimization (Villa and Stella, 2012). It allows the investor to easily incorporate his market's views and to select the optimal portfolio allocation based on that information;
- an algorithm for learning continuous time Bayesian network classifiers using the MapReduce framework has been designed and developed (Villa and Rossetti, 2014). It scales well in distributed environments and it is able to manage Big Data;
- the prediction of foreign exchange rates has been addressed as a classification problem in which a continuous time Bayesian network classifier has been developed and used to solve it (Villa and Stella, 2014). Empirical results show that these classifiers are more effective and more efficient than dynamic Bayesian network classifiers;
- a definition of structurally non-stationary continuous time Bayesian networks has been provided (Stella and Villa, 2014). The derivation of the Bayesian score, as well as the learning algorithms, have been presented and developed. These models are able to represent statistical dependencies that change over time;
- a model-based reinforcement learning algorithm to control structured continuous time dynamic systems has been described and developed (Villa and Shelton, 2014a). It efficiently manages the exploration-exploitation trade-off and it achieves a sample efficiency which is logarithmic in the size of the problem description;
- an R package that leverages on the C++ engine of continuous time Bayesian networks (Shelton et al., 2010) was designed and developed (Villa and Shelton, 2014b). It provides a valid tool for rapid prototyping and analysis in the R environment;
- some path-breaking examples and insights about the use of continuous time Bayesian networks and their extensions to tackle real financial problems are given.

1.2 Overview

This thesis is organized in eight chapters according to the following structure:

- Chapter 2 presents an overview of the background elements about *Bayesian networks*, their representation ability, the learning algorithms and inference methods. The last part of this chapter presents the interplay between modern portfolio theory and Bayesian networks and how to exploit them in a new framework for portfolio analysis and optimization;

- Chapter 3 covers the fundamental notions about *continuous time Bayesian networks*, their semantics, the problem of parameter and structural learning from data, and the issues of inference using such models. The last part of this chapter is devoted to the discussion about the related models, such as dynamic Bayesian networks, and the presentation of some financial applications;

- Chapter 4 treats the extension of continuous time Bayesian networks to solve the problem of classification. It starts by introducing the basic concepts about temporal classification, then it describes an efficient scalable learning algorithm for Big Data and finally, it presents an application of *continuous time Bayesian network classifiers* to the foreign exchange rate prediction problem in high frequency domain;

- Chapter 5 shows the extension of continuous time Bayesian networks to non-stationary domains. After a brief discussion about the problem of learning in these domains, it gives the formal definition of *non-stationary continuous time Bayesian networks* and it presents the learning framework with three different structural learning settings together with their corresponding learning algorithms. Finally, it provides numerical experiments on synthetic data sets;

- Chapter 6 covers the basic notions about *Markov decision processes* used to model sequential decision-making under uncertainty and it provides the main methods to solve them. Then, it describes their extensions to represent large and structured domains effectively using dynamic Bayesian networks. Finally, it shows how continuous time Bayesian networks are used as basic models of structured continuous time Markov decision processes with some examples in a structured trading domain;

- Chapter 7 presents the background material about reinforcement learning with particular attention to the *model-based reinforcement learning* algorithms. After the introduction on the use of factored Markov decision-making processes in the reinforcement learning environment, it presents a novel algorithm for control continuous time dynamic systems based on structured continuous time Markov decision processes. Finally, it provides numerical experiments on the trading domain, described in the previous chapter, that demonstrate its effectiveness;

- Chapter 8 concludes the thesis with a brief summary and a discussion of future work.

Chapter 2

Bayesian networks

Bayesian networks are sound graphical models that encode probabilistic relationships among random variables. We start this chapter by showing their representation ability, then describe how to perform learning. We move on review the inference methods, then we finish by presenting the interplay between modern portfolio theory and Bayesian networks and how to exploit them in a framework for portfolio analysis and optimization.

2.1 Representation

Bayesian networks are well developed frameworks used for many purposes, such as to model and explain a domain, to update beliefs about states of certain variables when some other variables are observed, to find most probable configurations of variables and to support decision-making under uncertainty. We present the necessary background about Bayesian networks, while we refer to Pearl (1988); Neapolitan (2003); Jensen and Nielsen (2007); Koller and Friedman (2009) for further reference. One of the key aspects of Bayesian networks is the compact description of joint probability distributions. Assume that we would like to represent a joint distribution over a set of N random variables $\boldsymbol{X} = \{X_1, \ldots, X_N\}$. Even in the case of binary variables, the joint distribution requires the specification of the probabilities of 2^N assignments of the values $x_1, \ldots, x_N$. Thus, this explicit representation is unmanageable even for small values of N. Bayesian networks overcome this issue through the use of a *factored* representation which leverages on conditional independence.

2.1.1 Independence properties

The key idea of a factored representation is that, in a given domain, most variables do not directly affect most other variables. Conversely, for each variable only a limited set of other variables influences it. To illustrate this concept, we begin with the definition of marginal independence for random variables.

Definition 2.1. *Marginal independence (Koller and Friedman, 2009). A random variable X with domain of values $Val(X)$ is marginally independent of random variable Y with domain of values $Val(Y)$ if for all $x_i \in Val(X)$ and $y_j, y_k \in Val(Y)$:*

$$P(X = x_i|Y = y_j) = P(X = x_i|Y = y_k) = P(X = x_i). \tag{2.1}$$

In another way, the knowledge of the value of Y does not affect our belief in the value of X. Sometimes two random variables might not be marginally independent. However, they can become independent after we observe a third variable.

Definition 2.2. *Conditional independence (Koller and Friedman, 2009). A random variable X is conditionally independent of random variable Y given random variable Z, denoted as $(X \perp Y|Z)$, if for all $x_i \in Val(X)$, $y_j, y_k \in Val(Y)$, and $z_m \in Val(Z)$:*

$$P(X = x_i|Y = y_j, Z = z_m) = P(X = x_i|Y = y_k, Z = z_m) = P(X = x_i|Z = z_m). \tag{2.2}$$

That is, the knowledge of the value of Y does not affect our belief in the value of X, given the value of Z. Note that, if we use a full parametrization of the joint distribution, the independence structure vanishes because the representation of the joint distribution requires an exponential number of parameters, e.g. 2^N in our previous example.

One approach is to assume some particular distributions of the random variables that admit a *compact representation.* In the previous example, if we assume that each variable has an independent binomial distribution, then the number of independent parameters used to represent the joint distribution is N.

Another way of representing the joint distribution is directly derived by the chain rule of conditional probabilities $P(X, Y) = P(X)P(Y|X)$. Instead of specifying all of the entries of the joint distribution $P(X, Y)$, it is possible to specify the *prior distribution* $P(X)$ and the *conditional probability distribution* (CPD) $P(Y|X)$.

2.1.2 Definition

Bayesian networks effectively combine both qualitative and quantitative components. The qualitative part consists in the graphical model that offers a clear interface by which the domain expert can elicit his knowledge, while the quantitative part consists of *potentials*, i.e. functions over sets of nodes of the graph. The graphical component of the Bayesian network is specified as a *directed acyclic graph* (DAG) whose nodes are the random variables in the domain and edges correspond to direct influence of one node on another. This graph compactly provides both the skeleton for representing the joint distribution and the set of conditional independence assumptions about the distribution.

Definition 2.3. *Bayesian network (BN), (Pearl, 1988). A Bayesian network $\mathcal{B} = (\mathcal{G}, \mathcal{P})$ over a set of N random variables $\boldsymbol{X} = \{X_1, \ldots, X_N\}$, where each X has a finite domain of values $Val(X) = \{x_1, \ldots, x_I\}$, is a representation of a joint probability distribution consisting of two components. The first component is a directed acyclic graph $\mathcal{G}$ where each node is associated with a random variable X and the directed links specify assumptions of conditional dependence and independence between random variables. The second component $\mathcal{P}$ describes a conditional probability distribution $P(X|Pa(X))$ for each variable X as a function of its parent set $Pa(X)$ in the graph $\mathcal{G}$.*

The CPDs form a set of local probability models that can be combined to describe the full joint distribution over the variables $\boldsymbol{X}$ via the chain rule for Bayesian networks.

Definition 2.4. *Chain rule for Bayesian networks, (Pearl, 1988). A Bayesian network $\mathcal{B}$ over a set of N random variables $\boldsymbol{X} = \{X_1, \ldots, X_N\}$ specifies a unique joint probability distribution $P(\boldsymbol{X})$ given by the product of all conditional probability distributions:*

$$P(\boldsymbol{X}) = \prod_{X \in \boldsymbol{X}} P(X|Pa(X)). \tag{2.3}$$

The compactness of Bayesian networks is an example of a more general property of *locally structured systems* in which each subcomponent interacts directly with only a small number K of other components regardless of the total number N of components. Local structure is usually associated with linear rather than exponential growth in complexity. For example, if we assume to use binary random variables, then the amount of information needed to specify the conditional probability distribution for a node will be at most 2^K values, so the complete network can be specified by $N \times 2^K$ values instead of 2^N.

2.1.3 Graph independencies

Dependencies and independencies are important properties of a distribution as they can be exploited to substantially reduce the computational cost of inference. Indeed, BNs can be used to assess how the change of certainty in one variable may change the certainty for other variables. This certainty can be in the form of *hard evidence* if the variable is instantiated, i.e. $X = x_i$, or *soft evidence* otherwise. The graph structure $\mathcal{G}$ can be used to extract independencies that hold for every distribution $\mathcal{P}$ that factorizes over $\mathcal{G}$. A fundamental property is called *d-separation* as it can be used for determining conditional independencies: if two nodes X and Y are d-separated given node Z, then $(X \perp Y|Z)$.

As in Jensen and Nielsen (2007), it is useful to introduce the concept of d-separation analyzing three possible types of connections in a Bayesian network. In the serial connection shown in Figure 2.1 (a), an evidence can be transmitted through it unless the state of the variable in the middle of the connection is known. In the diverging connection depicted in Figure 2.1 (b), an evidence can be transmitted through the connection unless the parent node is instantiated. In the converging connection shown in Figure 2.1 (c), an evidence can be transmitted through it only if either the variable in the connection or one of its descendants has received evidence. The rules for transmission of evidence over the three types of connections can be combined in the following general rule.

Definition 2.5. *D-separation, (Jensen and Nielsen, 2007). Two variables X and Y in a BN are d-separated if for all possible paths between X and Y, there is an intermediate variable Z such that: the connection is serial or diverging and Z is instantiated or the connection is converging, and neither Z nor any descendants of Z have received evidence.*

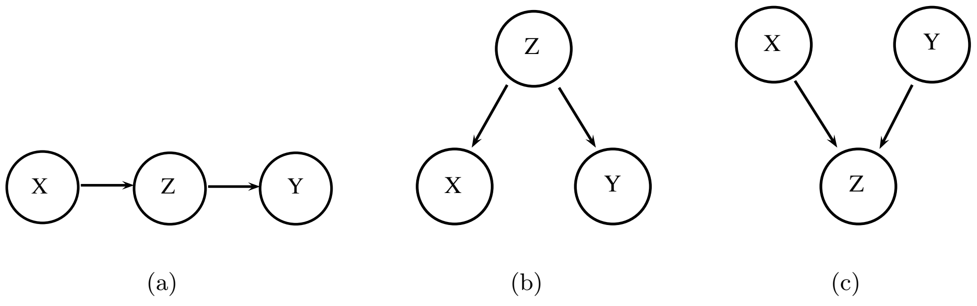

Figure 2.1: Three different connection types in a Bayesian network: serial connection (a), diverging connection (b) and converging connection (c).

From the definition of d-separation, we can introduce the concept of *Markov blanket* of a node X. This notion is important because when the Markov blanket of X is instantiated, X becomes d-separated from the rest of the network.

Definition 2.6. *Markov blanket, (Pearl, 1988). The Markov blanket of a variable X in a Bayesian network is the set consisting of the parents of X, the children of X and the variables sharing a child with X.*

Finally, we mention two useful structures to derive independence statements in a Bayesian network. Firstly, the *moral graph* of a Bayesian network: it is an undirected graph obtained by adding an edge between any two nodes that share a common child in the DAG of the BN and then by dropping the directionality of all edges. The moral graph can be used to check whether X and Y are d-separated given Z. In fact, if all paths connecting X and Y intersect Z, then X and Y are d-separated given Z (Jensen and Nielsen, 2007). Secondly, the *jointree* of a Bayesian network: it is a tree of clusters where each cluster is a set of variables in the Bayesian network sharing two properties. The first one states that every node and its parents must appear in some cluster and the second one states that if a variable appears in two clusters, then it must also appear in every cluster on the path between them. The jointree of a BN can be used to check whether two sets of variables are independent. In fact, any two clusters are independent given any cluster on the path connecting them (Pearl, 1988).

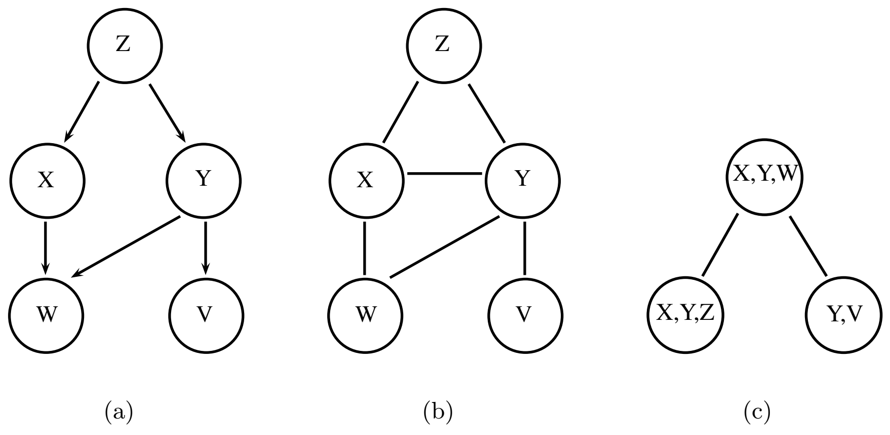

Figure 2.2: A Bayesian network (a), the corresponding moral graph (b) and a jointree (c).

2.2 Learning

Bayesian networks can be learned directly from data. In particular, if we assume that the domain is governed by some underlying distribution and we have a data set of samples from it, then the goal of learning is to construct a BN that captures the original underlying distribution in the best possible way. There are different reasons to learn a BN, such as to perform inference, to solve a classification task and to knowledge discovery, i.e. to reveal some important properties of the domain.

We discuss about the basic notions of parameter and structural learning. *Parameter learning* is concerned with the estimation of the elements of the CPDs when the graph is known, while *structural learning* is concerned with the selection of the graph and the estimation of the CPDs. Parametric and structural learning can be developed for *complete data* or *missing data* arising from partial observability of the random variables. We cover the first case, while we refer to Koller and Friedman (2009) for the second case.

2.2.1 Parameter learning

In the parameter learning case, the graph of the BN is given, e.g. it is constructed ad hoc by a domain expert, and we would like to learn the conditional probabilities from a data set consisting of M complete observations of the random variables $\boldsymbol{X}$, i.e. $\mathcal{D} = \{\boldsymbol{d}_1, \ldots, \boldsymbol{d}_M\}$. There are two main approaches for this estimation: *maximum likelihood estimation* (MLE) and *Bayesian estimation*. The core part of both approaches is the *likelihood function*, i.e. the probability that the BN assigns to the data set $\mathcal{D}$ for a given choice of *parameters* $\boldsymbol{\theta}$:

$$L(\boldsymbol{\theta} : \mathcal{D}) = \prod_{m=1}^{M} P(\boldsymbol{d}_m : \boldsymbol{\theta}). \tag{2.4}$$

The relevant information for computing the likelihood function can be summarized by the *sufficient statistics*. For example, if we consider a multinomial model with a variable X, a sufficient statistic for the data set is the tuple of counts $(M[x_1], \ldots, M[x_I])$ such that $M[x_i]$ is the number of times $\boldsymbol{d}_m[X] = x_i$ appears in the data set.

The structure of the BN allows us to decompose the likelihood function (2.4) by a product of independent terms that reflects each CPD of the network:

$$L(\boldsymbol{\theta} : \mathcal{D}) = \prod_{m=1}^{M} \prod_{X \in \boldsymbol{X}} P(\boldsymbol{d}_m[X] | \boldsymbol{d}_m[Pa(X)] : \boldsymbol{\theta}). \tag{2.5}$$

If we denote by $\boldsymbol{\theta}_{X|Pa(X)}$ the subset of the parameters $\boldsymbol{\theta}$ that determines the CPD $P(X|Pa(X))$, then we can write the equation (2.5) in terms of *local likelihood*:

$$L(\boldsymbol{\theta} : \mathcal{D}) = \prod_{X \in \boldsymbol{X}} L_X(\boldsymbol{\theta}_{X|Pa(X)} : \mathcal{D}). \tag{2.6}$$

This formulation allows us to independently maximize each local likelihood L_X and then to combine them to get the MLE solution. In the case of tabular CPD, called *conditional probability table* (CPT), the parameter $\boldsymbol{\theta}_{X|Pa(X)}$ of each variable X is composed of a set of parameters $\theta_{x_i|pa_u}$ for each $x_i \in Val(X)$ and instantiation of its parents $pa_u \in Pa(X)$. Therefore, the local likelihood can be written as follows:

$$L_X(\boldsymbol{\theta}_{X|Pa(X)} : \mathcal{D}) = \prod_{m=1}^{M} \theta_{\boldsymbol{d}_m[X]|\boldsymbol{d}_m[Pa(X)]} = \prod_{pa_u} \prod_{x_i} \theta_{x_i|pa_u}^{M[x_i,pa_u]}, \tag{2.7}$$

where $M[x_i, pa_u]$ is the number of times $\boldsymbol{d}_m[X] = x_i$ and $\boldsymbol{d}_m[Pa(X)] = pa_u$. That is, we grouped together all the occurrences in the product over all possible instances of pa_u and x_i. These parameters are independent, given an instantiation pa_u, so we can maximize each term in (2.7) independently to obtain the following MLE parameters:

$$\hat{\theta}_{x_i|pa_u} = \frac{M[x_i, pa_u]}{M[pa_u]}, \tag{2.8}$$

where $M[pa_u] = \sum_{x_i} M[x_i, pa_u]$. It is noteworthy to mention that the MLE approach suffers from the sparse data problem: when we have a small number of data from which we estimate the parameters in (2.8), the resulting estimates can be noisy.

Bayesian learning is a valid alternative to MLE. The Bayesian approach requires the use of probabilities to describe the initial uncertainty about the parameters $\boldsymbol{\theta}$, that are treated as random variables, and then use the Bayes rule to take into account new observations. Suppose that we have a network graph $\mathcal{G}$ with parameters $\boldsymbol{\theta}_{\mathcal{G}}$, then we can compute the posterior distribution over parameters given the data set $\mathcal{D}$ as:

$$P(\boldsymbol{\theta}_{\mathcal{G}}|\mathcal{D}) = \frac{P(\mathcal{D}|\boldsymbol{\theta}_{\mathcal{G}})P(\boldsymbol{\theta}_{\mathcal{G}})}{P(\mathcal{D})}, \tag{2.9}$$

where $P(\mathcal{D}|\boldsymbol{\theta}_{\mathcal{G}})$ is the probability of the data set given the parameters $\boldsymbol{\theta}_{\mathcal{G}}$, which is the likelihood function in (2.6), $P(\mathcal{D})$ is the marginal likelihood of the data set that we consider here only as a normalization constant and $P(\boldsymbol{\theta}_{\mathcal{G}})$ is the prior over parameters. This latter term can be computed easily if we make the two following assumptions.

Definition 2.7. *Global parameter independence, (Spiegelhalter and Lauritzen, 1990). The parameters $\boldsymbol{\theta}_{X|Pa(X)}$ associated with each variable X in a network graph $\mathcal{G}$ are independent, so the prior over parameters can be decomposed by variable as follows:*

$$P(\boldsymbol{\theta}_{\mathcal{G}}) = \prod_{X \in \boldsymbol{X}} P(\boldsymbol{\theta}_{X|Pa(X)}|\mathcal{G}). \tag{2.10}$$

Definition 2.8. *Local parameter independence, (Spiegelhalter and Lauritzen, 1990). The parameters associated with each state of the parents of a variable are independent, so the parameters of each variable X are decomposable by parent configuration $pa_u \in Pa(X)$ as follows:*

$$P(\boldsymbol{\theta}_{X|Pa(X)}|\mathcal{G}) = \prod_{pa_u} P(\theta_{X|pa_u}|\mathcal{G}). \tag{2.11}$$

For BNs with discrete variables, it is customary to choose a Dirichlet distribution as prior for the parameters, $P(\boldsymbol{\theta}_{\mathcal{G}}) \sim Dir(\alpha_1, \ldots, \alpha_U)$, which is a *conjugate prior* to the multinomial distribution. In a conjugate prior, the posterior $P(\boldsymbol{\theta}_{\mathcal{G}}|\mathcal{D}) \propto P(\mathcal{D}|\boldsymbol{\theta}_{\mathcal{G}})P(\boldsymbol{\theta}_{\mathcal{G}})$, has the same form as the prior $P(\boldsymbol{\theta}_{\mathcal{G}})$. This property allows us to maintain posteriors in closed form (Geiger and Heckerman, 1997). In fact, if our parameter prior satisfies the assumptions of global (2.10) and local (2.11) parameter independence and:

$$P(\theta_{X|pa_u}|\mathcal{G}) \sim Dir\left(\alpha_{x_1|pa_u}, \ldots, \alpha_{x_I|pa_u}\right), \tag{2.12}$$

then the posterior becomes:

$$P(\theta_{X|pa_u}|\mathcal{G}, \mathcal{D}) \sim Dir\left(\alpha_{x_1|pa_u + M[x_1,pa_u]}, \ldots, \alpha_{x_I|pa_u + M[x_I,pa_u]}\right). \tag{2.13}$$

The posterior (2.13) can be used to predict the next event, averaging out the event probability over the possible values of the parameters, that is equivalent of using the following parameters:

$$\hat{\theta}_{x_i|pa_u} = \frac{\alpha_{x_i|pa_u} + M[x_i, pa_u]}{\alpha_{pa_u} + M[pa_u]}, \tag{2.14}$$

where $\alpha_{pa_u} = \sum_{x_i} \alpha_{x_i|pa_u}$.

Note that the hyperparameters of the Dirichlet distribution can be seen as imaginary counts $\alpha_{x_i|pa_u} = \alpha[x_i, pa_u]$, where $\alpha[x_i, pa_u]$ is the number of times that $\boldsymbol{d}'_m[X] = x_i$ and $\boldsymbol{d}'_m[Pa(X)] = pa_u$ appears in an imaginary data set $\mathcal{D}'$. Clearly, if we consider the data set $\mathcal{D} = \mathcal{D} \cup \mathcal{D}'$, then the parameters (2.14) are equivalent to the MLE parameters (2.8).

2.2.2 Structural learning

Eliciting Bayesian networks from experts can be a laborious task in non trivial networks (Mascherini and Stefanini, 2007). In the case where the network structure in unknown, our goal is to reconstruct it from data. Unfortunately, since the space of all possible BNs is combinatorial, finding the optimal one is NP-hard in the general case (Chickering et al., 1994). However, some methods can be used to solve this task in an approximate way.

One approach is to consider a BN as a representation of independencies and to perform conditional dependency and independency tests in the data in order to find an equivalence class of networks that best explains these relationships. This approach, called *constraint-based structural learning*, is quite intuitive, but it can be very sensitive to failures in individual independence tests (Verma and Pearl, 1992; Cheng et al., 2002).

Another approach is to view a BN as a statistical model and then to address learning as a model selection problem. This approach, called *score-based structural learning*, defines a set of potential structures, a scoring function that measures how well the model fits the data, and a search technique that finds the highest-scoring structure (Spiegelhalter et al., 1993). We discuss this latter approach where the score is represented from a Bayesian perspective. This is similar to what we have presented in the Bayesian parameter learning, but in this context the uncertainty is both over structure and over parameters.

Once we have defined a structure prior $P(\mathcal{G})$, that puts a prior probability on different graphs, and a parameter prior $P(\boldsymbol{\theta}_{\mathcal{G}}|\mathcal{G})$, that puts a probability on different choice of parameters given the graph, we can use the Bayes rule to compute $P(\mathcal{G}|\mathcal{D})$ as follows:

$$P(\mathcal{G}|\mathcal{D}) = \frac{P(\mathcal{D}|\mathcal{G})P(\mathcal{G})}{P(\mathcal{D})}. \tag{2.15}$$

Given that the marginal likelihood of the data does not help us to distinguish between different graphs, we define the *Bayesian score BS* as the logarithm of the numerator in equation (2.15) as follows:

$$BS(\mathcal{G} : \mathcal{D}) = \ln P(\mathcal{G}) + \ln P(\mathcal{D}|\mathcal{G}). \tag{2.16}$$

The first term in (2.16) is the prior over structures that gives us a way of preferring some structures over others in the first stages. However, as it does not grow with the size of the data, a simple prior such as a uniform is often chosen. A key property of this prior is that it must satisfy *structure modularity.*

Definition 2.9. *Structure modularity, (Friedman and Koller, 2000). The prior over structure $P(\mathcal{G})$ decomposes into a product with a term for each variable in the domain:*

$$P(\mathcal{G}) = \prod_{X \in \boldsymbol{X}} P(Pa(X) = Pa_{\mathcal{G}}(X)). \tag{2.17}$$

The second term in (2.16) is the marginal likelihood of the data given the structure and it is computed by marginalizing out the unknown parameters as follows:

$$P(\mathcal{D}|\mathcal{G}) = \int_{\boldsymbol{\theta}_{\mathcal{G}}} P(\mathcal{D}|\boldsymbol{\theta}_{\mathcal{G}}, \mathcal{G}) P(\boldsymbol{\theta}_{\mathcal{G}}|\mathcal{G}) d\boldsymbol{\theta}_{\mathcal{G}}, \tag{2.18}$$

where $P(\mathcal{D}|\boldsymbol{\theta}_{\mathcal{G}}, \mathcal{G})$ is the likelihood of the data given the graph structure $\mathcal{G}$ and its parameters $\boldsymbol{\theta}_{\mathcal{G}}$, while $P(\boldsymbol{\theta}_{\mathcal{G}}|\mathcal{G})$ is the prior over parameters. In structural learning, this prior over parameters is required to satisfy *parameter modularity.*

Definition 2.10. *Parameter modularity, (Geiger and Heckerman, 1997). If a node X has the same parents in two distinct graphs $\mathcal{G}$ and $\mathcal{G}'$, $Pa_{\mathcal{G}}(X) = Pa_{\mathcal{G}'}(X)$, then the probability density functions of the parameters associated with this node must be identical:*

$$P(\boldsymbol{\theta}_{X|Pa_{\mathcal{G}}(X)}|\mathcal{G}) = P(\boldsymbol{\theta}_{X|Pa_{\mathcal{G}'}(X)}|\mathcal{G}'). \tag{2.19}$$

In the case of complete data, $P(\mathcal{D}|\mathcal{G})$ can be computed in closed form by using the *Bayesian-Dirichlet equivalent* (BDe) metric (Heckerman et al., 1995). It assumes that $P(\boldsymbol{\theta}_{\mathcal{G}}|\mathcal{G})$ satisfies global (2.10) and local (2.11) parameter independence, parameter modularity (2.19) and Dirichlet prior (2.12). So, $P(\mathcal{D}|\mathcal{G})$ can be written as follows:

$$P(\mathcal{D}|\mathcal{G}) = \prod_{X \in \boldsymbol{X}} \prod_{pa_u} \frac{\Gamma\left(\alpha_{pa_u}\right)}{\Gamma\left(\alpha_{pa_u} + M[pa_u]\right)} \times \prod_{x_i} \frac{\Gamma\left(\alpha_{x_i|pa_u} + M[x_i, pa_u]\right)}{\Gamma\left(\alpha_{x_i|pa_u}\right)}. \tag{2.20}$$

If we set $\alpha_{x_i|pa_u} = \frac{\alpha}{|x_i| \times |pa_u|}$, then the parameter priors are all controlled by a single hyperparameter α. In this case, formula (2.20) becomes a *uniform BDe* (BDeu) metric.

If the network structure is in the form of tree or we have an ordering over variables, then the search for the optimal structure can be performed polynomially in number of variables (given a fixed number of possible parents for a node). In all other cases, we have to determine how to move through the space of all networks, e.g. with operators of add, delete or reverse an edge (Giudici and Castelo, 2003), and resort to heuristics or sampling strategies for search procedures (Madigan et al., 1995; Chickering et al., 1995).

2.3 Inference

Since a BN defines a joint distribution over variables, it can be used to answer any probabilistic query. For example, we can compute $P(\boldsymbol{Y}|\boldsymbol{E}=\boldsymbol{e})$, where $\boldsymbol{Y}, \boldsymbol{E} \subseteq \boldsymbol{X}$ and $\boldsymbol{e}$ is an instantiation of $\boldsymbol{E}$, dividing $P(\boldsymbol{Y}, \boldsymbol{e})$ by $P(\boldsymbol{e})$. Specifically, each of the instantiations of $P(\boldsymbol{Y}, \boldsymbol{e})$ is a probability $P(\boldsymbol{y}, \boldsymbol{e})$ which can be computed by summing out all entries in the joint that correspond to assignments consistent with $(\boldsymbol{y}, \boldsymbol{e})$, i.e. $P(\boldsymbol{y}, \boldsymbol{e}) = \sum_{\boldsymbol{z}} P(\boldsymbol{y}, \boldsymbol{e}, \boldsymbol{z})$, where the set $\boldsymbol{Z} = \boldsymbol{X} \setminus \{\boldsymbol{Y}, \boldsymbol{E}\}$ and $P(\boldsymbol{e})$ can be computed directly as $P(\boldsymbol{e}) = \sum_{\boldsymbol{y}} P(\boldsymbol{y}, \boldsymbol{e})$.

However, this approach of compute the joint distribution and exhaustively sum out the joint is not efficient, as we incur in the exponential blowup of the inference task. Even if the problem of inference in graphical models is NP-hard (Cooper, 1990), many real-world applications can be tackled effectively using exact or approximate inference algorithms.

2.3.1 Exact inference

The *variable elimination algorithm* (Shachter et al., 1990; Dechter, 1999) addresses the exponential blowup of inference by computing the expressions in the joint distribution that depend on a small number of variables once and by caching the results. The key concept of this algorithm will be useful in the next chapters. As in Koller and Friedman (2009), we use the notion of *factor* ϕ with $Scope[\phi] = \boldsymbol{Y}$, which is a function $\phi : Val(\boldsymbol{Y}) \to \mathbb{R}$.

The basic operation is the factor *marginalization*. Let $\boldsymbol{Y} \subseteq \boldsymbol{X}$, $Z \in \boldsymbol{X} \setminus \boldsymbol{Y}$ and $\phi(\boldsymbol{Y}, Z)$ a factor, the factor marginalization of Z in ϕ is another factor ψ over $\boldsymbol{Y}$ such that $\psi(\boldsymbol{Y}) = \sum_Z \phi(\boldsymbol{Y}, Z)$. We observe that the operations of factor product and summation behave precisely as do product and summation over numbers, specifically, if $X \notin Scope[\phi_1]$, then we can exchange summation and product easily as $\sum_X (\phi_1 \times \phi_2) = \phi_1 \times \sum_X \phi_2$.

For example, if we assume to have a simple BN of four variables, specified as a serial connection, $X_1 \to X_2 \to X_3 \to X_4$, then the marginal distribution over X_4 is:

$$\begin{aligned} P(X_4) &= \sum_{X_3} \sum_{X_2} \sum_{X_1} P(X_1, X_2, X_3, X_4) && (2.21)\\ &= \sum_{X_3} \sum_{X_2} \sum_{X_1} \phi(X_1) \times \phi(X_2) \times \phi(X_3) \times \phi(X_4) && (2.22)\\ &= \sum_{X_3} \phi(X_4) \times (\sum_{X_2} \phi(X_3) \times (\sum_{X_1} \phi(X_2)\phi(X_1))). && (2.23) \end{aligned}$$

These different transformations are justified by the limited scope of each factor.

Any computation of the marginal probability involves taking the product of all the CPDs and doing the summation on all the variables (except the query variables). The elimination order is crucial to speedup the computation and it must ensure that we do the summation on a variable after multiplying in all of the factors that involve that variable.

Algorithm 2.1 shows the computation of the probability query $P(\boldsymbol{Y}|\boldsymbol{E}=\boldsymbol{e})$ using this insight. We simply apply this algorithm to the set of factors in the network, reduced by $\boldsymbol{E}=\boldsymbol{e}$, we eliminate the variables such as $\boldsymbol{Z}=\boldsymbol{X}\setminus\{\boldsymbol{Y},\boldsymbol{E}\}$, and we select an elimination order $\prec$ over $\boldsymbol{Z}$. For each ordered variable $Z\in\boldsymbol{Z}$, we multiply all the factors ϕ such that $Z\in Scope[\phi]$, generating a product factor ψ, and then we sum out the variable Z from this combined factor, generating a new factor υ that we enter into our set of factors Φ to be dealt with. The final product of factors gives us $P(\boldsymbol{Y},\boldsymbol{e})$, while the summation over $\boldsymbol{y}$ gives us the probability of evidence $P(\boldsymbol{e})$. The complexity of this algorithm is $O(N\times\psi_{max})$, where N is the number of random variables of the BN and ψ_{max} is the maximum number of entries of the resulting product factors. This latter term could lead to an exponential blowup of the potentially exponential size of the intermediate factors.

Algorithm 2.1 Inference using the variable elimination method

```
Require: Bayesian network $\mathcal{B}$, query variables $\boldsymbol{Y}$ and evidence $\boldsymbol{E}=\boldsymbol{e}$.
Ensure: $P(\boldsymbol{Y},\boldsymbol{e})$ and $P(\boldsymbol{e})$.
 1: $\Phi \leftarrow factors(\mathcal{B})$
 2: for each $\phi\in\Phi$ do
 3:     $\phi\leftarrow\phi[\boldsymbol{E}=\boldsymbol{e}]$
 4: end for
 5: $\boldsymbol{Z}\leftarrow\boldsymbol{X}\setminus\{\boldsymbol{Y},\boldsymbol{E}\}$
 6: Set an elimination order $\prec$ over $\boldsymbol{Z}$ such that $\forall Z_i,Z_j\in\boldsymbol{Z},Z_i\prec Z_j$ iff $i<j$
 7: for each $Z\in\boldsymbol{Z}$ do
 8:     $\Phi'\leftarrow\{\phi\in\Phi|Z\in Scope[\phi]\}$
 9:     $\psi\leftarrow\prod_{\phi\in\Phi'}\phi$
10:     $\upsilon\leftarrow\sum_Z\psi$
11:     $\Phi\leftarrow\Phi\setminus\Phi'\cup\{\upsilon\}$
12: end for
13: $\phi\leftarrow\prod_{\phi\in\Phi}\phi$
14: $P(\boldsymbol{Y},\boldsymbol{e})\leftarrow\phi(\boldsymbol{Y})$
15: $P(\boldsymbol{e})\leftarrow\sum_{\boldsymbol{y}}\phi(\boldsymbol{y})$
```

We can think the elimination steps 7 - 12 of Algorithm 2.1 as a sequence of graph manipulations induced by the set of factors Φ. Specifically, we have an undirected graph whose nodes correspond to the variables in the $Scope[\Phi]$ and edges (X, Y) iff there exists a factor $\phi \in \Phi : X, Y \in Scope[\phi]$. Step 9 generates edges between all the variables with which Z appears in factors, while step 10 has the effect of removing Z and all of its incident edges from the graph. Every factor that appears in one of the elimination steps is reflected in the graph as a *clique*. Consider the induced graph as the union of the graphs resulting in all the elimination steps, given an elimination order; then its *width* is the number of nodes in the largest clique minus one, and the *tree-width* is the minimal induced width. The tree-width gives us a bound on the performance of Algorithm 2.1 that depends on the elimination order. Finding the optimal order is NP-hard (Arnborg et al., 1987), but some heuristics have been proposed (Reed, 1992; Becker and Geiger, 2001).

An alternative approach is tree clustering, which is also known as the *jointree algorithm* (Lauritzen and Spiegelhalter, 1988; Jensen et al., 1990). The key idea is to organize the set of factors into a jointree and then use this structure to control the process of variable elimination. A third approach of exact inference is based on the concept of *conditioning* (Pearl, 1986; Horvitz et al., 1989; Darwiche, 1995). The key idea is that if we know the value of a variable X, then we can remove edges outgoing from X, modify the CPTs for children of X and then perform inference on the simplified network.

2.3.2 Approximate inference

Exact inference become infeasible for BNs with large tree-width, indeed the computational and space complexity of the clique tree is exponential in the tree-width of the network. We review some approximate inference methods in which the joint distribution is approximated by a set of instantiations to some of the variables in the network, called *particles*.

The simplest approach to generate particles is *forward sampling*. Given M random samples $\mathcal{D} = \{\boldsymbol{d}_1, \ldots, \boldsymbol{d}_M\}$ from the distribution $P(\boldsymbol{X})$, forward sampling estimates the expectation of a target function as empirical mean over samples. If we want to compute $P(\boldsymbol{y})$, then its estimate is the fraction of particles where we have seen the event $\boldsymbol{y}$:

$$\hat{P}(\boldsymbol{y}) = \frac{1}{M} \sum_{m=1}^{M} \mathbf{1}_{\{\boldsymbol{y}\}}(\boldsymbol{d}_m[\boldsymbol{Y}]), \tag{2.24}$$

where $\mathbf{1}$ is the *indicator function* and $\boldsymbol{d}_m[\boldsymbol{Y}]$ is the value of variables $\boldsymbol{Y}$ in the sample $\boldsymbol{d}_m$.

In the case where we are interested in conditional probabilities $P(\boldsymbol{y}|\boldsymbol{e})$, one approach is to generate samples directly from the posterior $P(\boldsymbol{X}|\boldsymbol{e})$ using a method called *rejection sampling.* In practice, it generates samples from $P(\boldsymbol{X})$ as in the previous case, but it rejects any sample that is not compatible with $\boldsymbol{e}$. The problem is that the number of rejected particles can be huge, i.e. proportional to $M \times P(\boldsymbol{e})$.

Another approach is *importance sampling*, a general procedure for estimating the expectation of a function relative to a target distribution from a different distribution, called *proposal distribution*, which is much more simple to sample. In the context of BNs, a simple proposal distribution can be described in terms of a Bayesian network. Specifically, let $\mathcal{B}$ be a BN and $\boldsymbol{y}$ an instantiation of $\boldsymbol{Y}$, then the proposal distribution $\mathcal{B}_{\boldsymbol{y}}$ is the same as $\mathcal{B}$ except that each node $Y \in \boldsymbol{Y}$ has no parents and its CPD gives probability 1 to $Y = y$ and 0 to all other values. The sampling process is similar to forward sampling, but we have weighted particles, i.e. for each sample $\boldsymbol{d}'$ coming from the proposal distribution we have its weight $w(\boldsymbol{d}')$. This weight can be derived from the likelihood of the evidence accumulated throughout the sampling process:

$$w(\boldsymbol{d}') = \frac{P_{\mathcal{B}}(\boldsymbol{d}')}{P_{\mathcal{B}_{\boldsymbol{y}}}(\boldsymbol{d}')} = \prod_{X \in \boldsymbol{Y}} L_X(\boldsymbol{\theta}_{X|Pa(X)} : \boldsymbol{d}'_m) = \prod_{X \in \boldsymbol{Y}} \theta_{\boldsymbol{d}'_m[X]|\boldsymbol{d}'_m[Pa(X)]}. \tag{2.25}$$

Therefore, the weight $w(\boldsymbol{d}')$ is the likelihood contribution of all the variables in $\boldsymbol{Y}$; this approach is also know as *likelihood weighting* (Shachter and Peot, 1989). An estimate of $P(\boldsymbol{y})$ can performed using (unnormalized) importance sampling as follows:

$$\hat{P}(\boldsymbol{y}) = \frac{1}{M'} \sum_{m=1}^{M'} \mathbf{1}_{\{\boldsymbol{y}\}}(\boldsymbol{d}'_m[\boldsymbol{Y}]) w(\boldsymbol{d}'_m), \tag{2.26}$$

while an estimate of $P(\boldsymbol{y}|\boldsymbol{e})$ for a given event $\boldsymbol{e}$ can be computed in two steps. We generate M'' weighted particles from a proposal distribution defined by $\mathcal{B}_{\boldsymbol{y},\boldsymbol{e}}$ and M' weighted particles from a proposal distribution defined by $\mathcal{B}_{\boldsymbol{e}}$, then we compute the following ratio:

$$\hat{P}(\boldsymbol{y}|\boldsymbol{e}) = \frac{M'}{M''} \frac{\sum_{m=1}^{M''} \mathbf{1}_{\{\boldsymbol{y},\boldsymbol{e}\}}(\boldsymbol{d}''_m[\boldsymbol{Y},\boldsymbol{E}]) w(\boldsymbol{d}''_m)}{\sum_{m=1}^{M'} \mathbf{1}_{\{e\}}(\boldsymbol{d}'_m[\boldsymbol{E}]) w(\boldsymbol{d}'_m)}. \tag{2.27}$$

Note that the quality of importance sampling depends largely on how close the proposal distribution is to the target distribution. In fact, if the proposal is very different from the target distribution, then most of the samples will be irrelevant, i.e. with a low weight.

2.4 BNs for portfolio analysis and optimization

Bayesian networks have been widely used in many contexts, such as medicine (Andreassen et al., 1987; Luciani et al., 2003; Lucas et al., 2004), computer science (de Campos et al., 2004; Fagiuoli et al., 2008) and finance (Demirer et al., 2006; Pavlenko and Chernyak, 2010; Rebonato and Denev, 2014). The range of applications is very wide and demonstrates the extensive applicability of Bayesian networks in real life domains.

In this section we present how to exploit the interplay between modern portfolio theory and Bayesian networks to describe the framework for portfolio analysis and optimization introduced by Villa and Stella (2012). This framework leverages on evidential reasoning to understand the behavior of an investment portfolio in different economic and financial scenarios. It allows to formulate and solve a portfolio optimization problem, while coherently taking into account the investor's market views. Some examples of portfolio analysis and optimization on the DJ Euro Stoxx 50 Index, exploiting evidential reasoning on Bayesian networks, are presented and discussed.

2.4.1 Financial context

Portfolio analysis and portfolio optimization are basic problems in computational finance. They have been intensively studied over the last sixty years and several relevant contributions are available in the specialized literature (Elton et al., 2010). Portfolio optimization originates from the seminal paper of Markowitz (1952) who introduced the *mean-variance investment framework*, the first quantitative treatment of the risk-return trade-off. This conventional approach to portfolio optimization consists of two steps. The first one concerns distributional assumptions about the behavior of stock prices, while the second one is related to the selection of the optimal portfolio, depending on some objective function and/or utility function, defined according to the investor's goal. This conceptual model in the past proved to be useful even if many drawbacks have been pointed out by finance practitioners, private investors and researchers. The basic formulation introduced by Markowitz has been extended in the specialized literature by taking into account additional moments of the portfolio's return distribution and by developing necessary conditions on the utility function of investors (Fabozzi et al., 2007).

It is increasingly understood that the investor's experience, i.e. his qualitative and quantitative knowledge on economy, finance and financial markets, is a key factor for success. Indeed, the knowledge of some factors, such as the likelihood of future events, the outlook on finance and economy, the coexistence of different asset pricing theories and the security-driving forces, can be fruitfully exploited to formulate and solve the portfolio optimization problem. The first contribution that exploits investor's market views in a quantitative way is due to Black and Litterman (1991). In their work, they tried to overcome some typical problems of mean-variance investment framework, such as the lack of diversification and instabilities of portfolios on the efficient frontier, by using a Bayesian approach that combines the investor's market views about the expected returns of some assets with those of the market equilibrium defined by the *capital asset pricing model* of Sharpe (1964). Unfortunately, the building of the required inputs is somewhat complex and not intuitive for an investor without quantitative background. Different improvements and extensions of this model have been developed, such as conditional-marginal factorization used to input views on volatilities, correlations and expectations (Qian and Gorman, 2001), the use of market views without any preprocessing (Meucci, 2006) and the use of market views directly on on the risk factors underlying the market instead of the returns of the securities (Meucci, 2009).

2.4.2 Basics of portfolio modeling and optimization

The goal of the portfolio modeling task consists of forecasting and managing the portfolio's profit and loss distribution at the investment horizon. In order to describe this task, we assume to have N securities, a sequence of N-dimensional vectors of *spot prices* $\boldsymbol{S}_t$ indexed by time t sampled at time interval Δt, T is the time when the portfolio allocation decision has to be made and τ is the *investment horizon*. The portfolio modeling task can be accomplished in the following steps according to Meucci (2011).

The first step consists of the identification of the *risk drivers*. A risk driver of a security is modeled with a random variable X, sharing the following two properties: it fully specifies the price of the security at time t and it follows a homogeneous stochastic process. Once the risk drivers have been identified, we have to extract the *invariants* from them. An invariant is a shock that steers the stochastic process associated with the risk driver. The risk driver can be modeled by a set of independent and identically distributed random variables, and it becomes known at time $t + \Delta t$. To connect the invariant Y_t to the risk driver X_t at time t, we use the following relation:

$$Y_t = h(X_t) - h(X_{t-\Delta t}), \tag{2.28}$$

where h is an invertible deterministic function. For example, the risk driver of a stock is the natural logarithm of its price, while the relative invariant is the compounded return.

The second step concerns the estimation of the distribution of the invariants which does not depend on the specific time t because of the invariance property. This task can be accomplished by fitting an empirical distribution from the invariants time-series through multivariate statistical techniques, such as simple historical, maximum likelihood and robust, see Meucci (2005) for an in-depth overview. A dimension reduction technique is fundamental to reduce the number of invariants, such as a *linear factor model* that decomposes the J-dimensional invariants $\boldsymbol{Y}_t$ as follows:

$$\boldsymbol{Y}_t = \boldsymbol{B}_t \boldsymbol{F}_t + \boldsymbol{U}_t, \tag{2.29}$$

where $\boldsymbol{F}_t$ is an M-dimensional vector of *factors* with $M \ll J$, $\boldsymbol{B}_t$ is a $J \times M$ matrix of *factor loadings* which links the factors $\boldsymbol{F}_t$ to the invariants $\boldsymbol{Y}_t$, while $\boldsymbol{U}_t$ is a J-dimensional vector of *residuals*. These factors can be used to synthesize the entire invariants' distribution.

The third step consists of the projection of the invariants' distribution to the investment horizon τ. This projection can be implemented in different ways. If the risk drivers evolve according to a random walk, then the first two moments of the projected distribution can be obtained through recursion (Meucci, 2005), while the projection of the full distribution can be accomplished by the Fourier transform techniques (Albanese et al., 2004).

The fourth step is the pricing of the securities at investment horizon τ:

$$\boldsymbol{S}_\tau = g(\boldsymbol{X}_\tau, tc), \tag{2.30}$$

where g is the *pricing function*, the risk drivers $\boldsymbol{X}_\tau$ are extracted from the projected invariants' distribution and tc are the *terms and conditions* of the securities.

The last step involves the computation of the *profit and loss distribution* at investment horizon A_τ given a portfolio with *holdings* $\boldsymbol{a} = (a_1, \dots, a_N)$ as follows:

$$A_\tau = \boldsymbol{a}'(\boldsymbol{S}_\tau - \boldsymbol{S}_T). \tag{2.31}$$

Once we have estimated the prices at the investment horizon, we can optimize our portfolio using the standard mean-variance portfolio optimization framework. When the investor's objective is the terminal wealth and the initial capital is non-null, the portfolio optimization problem can be formulated in terms of a vector of *linear returns* at investment horizon $\boldsymbol{L}_\tau$ and a vector of *weights* $\boldsymbol{w}$ as follows:

$$\boldsymbol{w}_v^* = \underset{\substack{\boldsymbol{w}\in\Lambda,\\ \boldsymbol{w}'Cov[\boldsymbol{L}_\tau]\boldsymbol{w}=v,}}{\operatorname{argmax}} \left\{ \boldsymbol{w}'\mathbb{E}[\boldsymbol{L}_\tau] \right\}, \tag{2.32}$$

where $\mathbb{E}[\boldsymbol{L}_\tau]$ and $Cov[\boldsymbol{L}_\tau]$ are, respectively, expected value and covariance matrix of linear returns at investment horizon, while v is the desired *level of risk* and Λ is the set of *constraints*. If a budget constraint is introduced ($\boldsymbol{w}'\mathbf{1} = \mathbf{1}$) and short-selling is not allowed ($\boldsymbol{w} \geq \mathbf{0}$), then the optimization problem is quadratic and thus can be solved analytically.

2.4.3 The integrated perspective

The portfolio modeling and optimization tasks can be seen in an integrated perspective. The goal is to preserve the joint probability distribution of the factors and the invariants, as it allows us to perform evidential reasoning on some selected factors; this distribution should be factored properly to avoid the exponential blowup of the full representation. A straightforward way to perform this is to construct a Bayesian network that relates factors to invariants, from the latter it is possible to determine the risk drivers and the prices (or returns) of securities and then to obtain the portfolio distribution from aggregation.

We can think the implementation of this process as a three-layered model. The first is a *Bayesian network layer* that links the key factors with the invariants, while providing a compact description of the market. This layer can be used to perform efficient evidential reasoning. In fact, we can introduce evidences concerning the nodes associated with the factors and then obtain the posterior probability over the nodes associates with invariants. The second is a *transformation layer* that deterministically links the invariants to the risk drivers and prices. This layer is useful because, in general, we are not only interested in analyzing the posterior distribution of the invariants, but rather the distribution of the risk drivers, prices and returns. The last one is an *aggregation layer* that represents the portfolio's securities. This layer links the market securities with those that we have in portfolio, allowing us to perform portfolio analysis and optimization with the given views.

In order to clarify this framework, we show a simple example with two securities, one stock and one call option on this stock, as depicted in Figure 2.3. For the stock, we pick the log-price as risk driver X_1 and its compounded return as invariant Y_1. For the stock option, we select the logarithm of the implied volatility for a given time to expiry as risk drivers (we display only four of them $X_2, \ldots, X_4$) together with the log-price of the underlying, while the invariants are the changes of these risk drivers as in equation (2.28). We assume the existence of two factors relevant to explain the set of invariants, namely F_1 is a common factor driving the market and F_2 is a specific factor for this security. This structure can be learned directly from data, elicited by an expert or by using factor analysis. The set of factors, F_1, F_2, and invariants, $Y_1, \ldots, Y_5$, constitute the Bayesian network layer, while risk drivers, $X_1, \ldots, X_5$, and securities prices, S_1, S_2, represent the transformation layer through deterministic nodes. Finally, the aggregation layer concerns the node A corresponding to the portfolio.

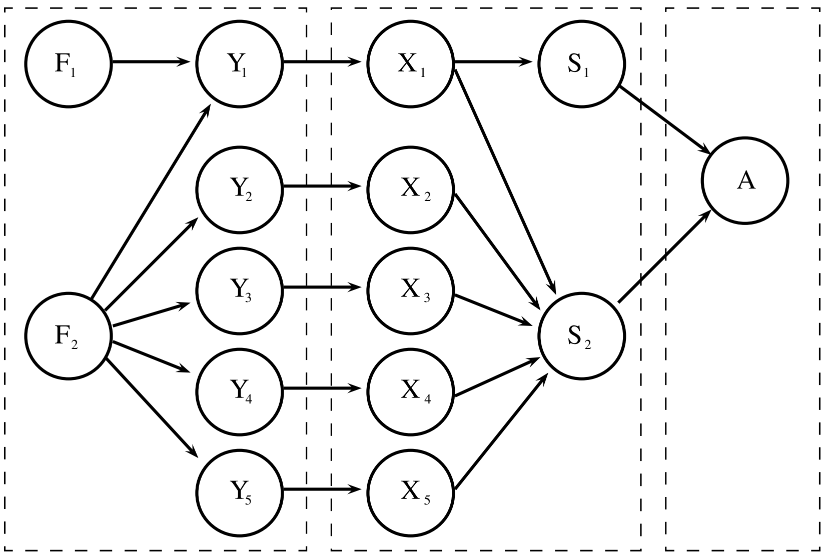

Figure 2.3: An instantiation of the BNs framework for portfolio analysis and optimization with two securities: one stock and one call option on this stock. The dotted lines highlight the three layers, namely Bayesian network, transformation and aggregation. F_1 and F_2 are the factors, $Y_1, \ldots, Y_5$ denote the invariants, $X_1, \ldots, X_5$ are the risk drivers, S_1, S_2 are the securities prices and A denotes the portfolio.

2.4.4 Case study

Villa and Stella (2012) presented a case study about an equity investor interested in analyzing, stress testing and optimizing the tomorrow's return distribution of his portfolio. The eligible universe was the Eurozone Blue-chips forming the DJ Euro Stoxx 50 Index and the available data set consisted of five years of daily prices, spanning from December 30th, 2005, to December 30th, 2010. Note that the basic steps of portfolio modeling are more easily compared to the general case because the risk drivers are the log-prices, the pricing function is the exponential function and it is not needed to project the invariant distribution because of the estimation interval is equal to the investment horizon. So, it is possible to focus only on the estimation of the invariants' distribution and the identification of the underlying factors. The authors have shown how the standard quantitative approach to portfolio analysis and optimization can be seen as an instantiation of the proposed framework and how it can be used to enrich the analysis with investor's market views.

As first case, a *statistical factor model* based on random matrix theory and Monte Carlo simulation with normal copula have been used to generate a panel of 100,000 joint scenarios from the data set (Meucci, 2010). Factor analysis using random matrix theory allows to model the invariants with $M \ll J$ informative factors plus a residual term represented by $J - M$ noise factors (Plerou et al., 2002). The $M = 10$ largest eigenvalues of the empirical covariance matrix have been used. The framework has been instantiated as follows. The BN layer was constructed by discretizing these *estimation factors* into three states (low, medium and high), the invariants into one hundred states and then using MLE for learning the parameters of a fully connected network. The transformation layer deterministically linked the invariants to the risk drivers and then to the securities' returns; finally the portfolio was determined by aggregation of securities' returns.

The first two moments of the projected returns of each security at the investment horizon are depicted in Figure 2.4 (a). Then, the main estimation factor has been evidenced to the state low and the evidence has been propagated by using BNs inference as shown in Figure 2.4 (b). We note that the main estimation factor is associated with a common factor driving the equity market. When this factor is instantiated to the state low, the expected value of each security is negative and the correlation between securities is strong. This could be useful for a quantitative analyst, but less informative for an investor.

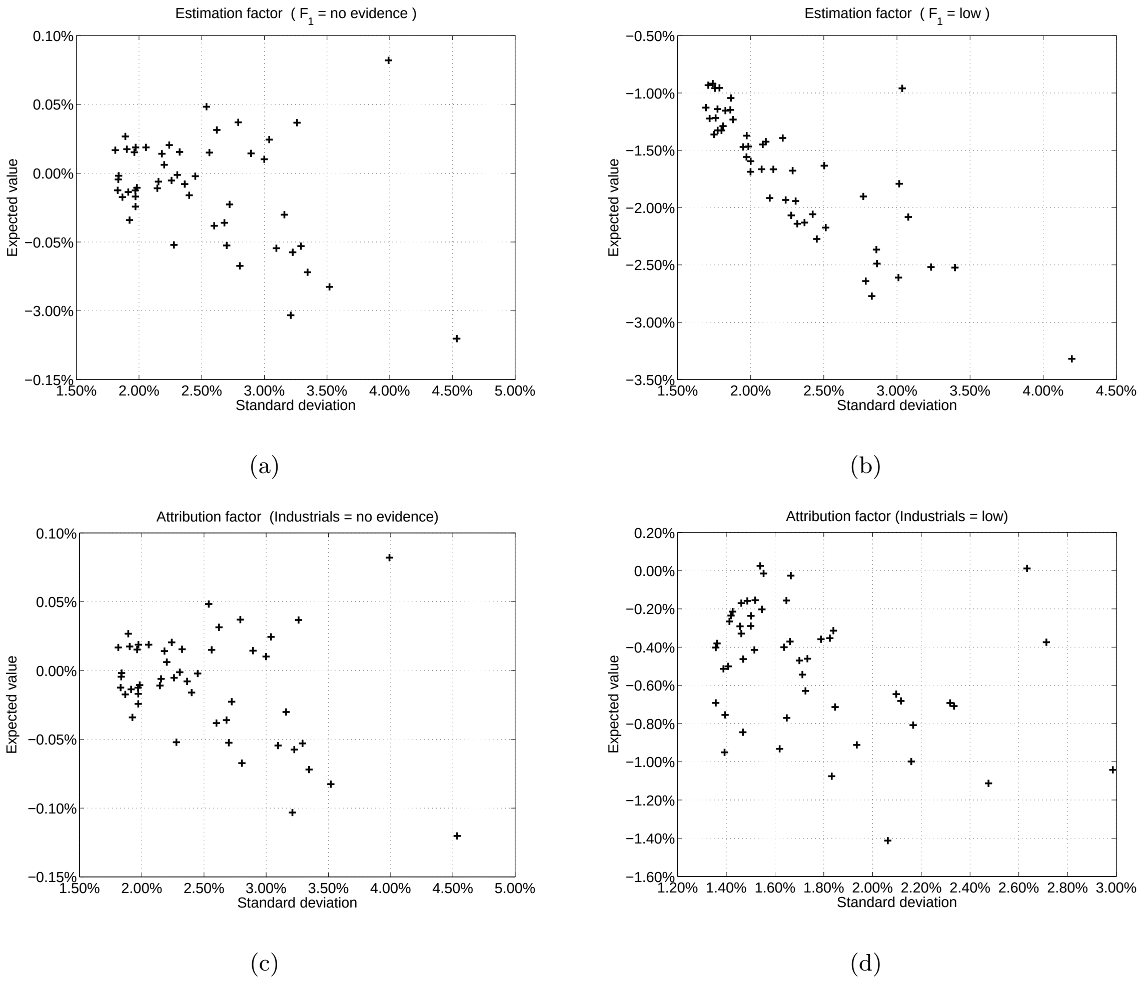

Figure 2.4: Stress tests on estimation and attribution factors. Expected value and standard deviation for the distribution of the returns for the securities of the DJ Euro Stoxx 50 Index where: (a) the first estimation factor has no evidence, (b) the first estimation factor has an evidence on the state low, (c) the Industrials attribution factor has no evidence and (d) the Industrials attribution factor has an evidence on the state low.

As second case, the *Factors on Demand* framework (Meucci, 2010) has been used. It allows us to assign to the portfolio return some *attribution factors*, i.e. random variables correlated with the portfolio return, such as countries and industry factors. These factors give us a way to reason about the securities' returns using factors that are easy to interpret. Thus, the estimation factors have been replaced with the attribution factors associated with the European GICS sectors and evidential reasoning using the factor corresponding to the Industrials GICS sector has been performed. The impacts on the first two moments of the projected returns of the securities are depicted in Figure 2.4 (c) and (d).

The transformation layer allows us to analyze the entire distribution of the projected returns of each security and to assess the impacts of the investor's market views on that distribution. Figure 2.5 shows the cumulative distribution of the projected returns for the first four securities, in alphabetical order, of the DJ Euro Stoxx 50 Index in the case of no evidence and evidence set to the state low for the Industrials attribution factor. Each security reacts to the entered evidence in a different way, that is based on the data used to learn the framework. Some qualitative analysis can be done, for example we can see that the third security is much more influenced by the evidence compared to the fourth one, so we might think to underweight the former instead of the latter.

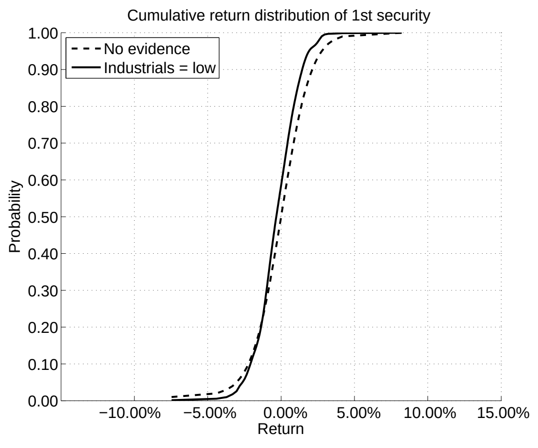

(a)

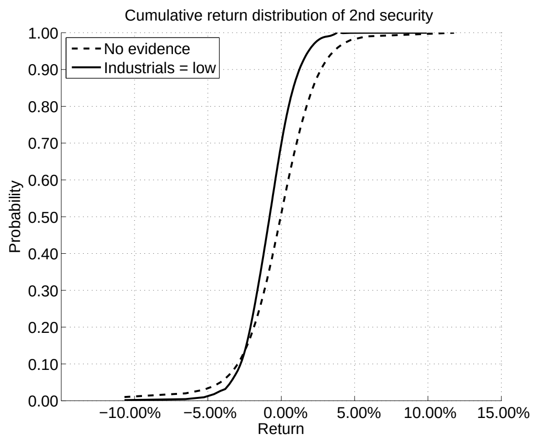

(b)

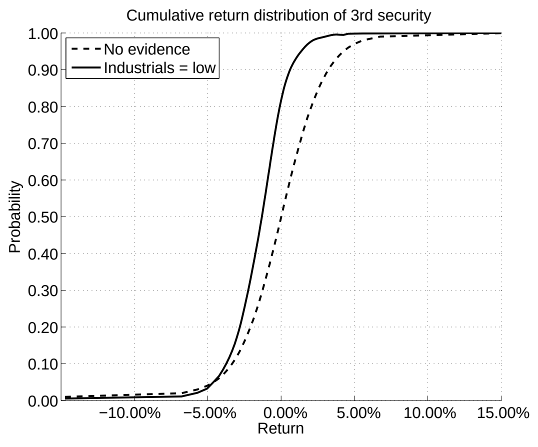

(c)

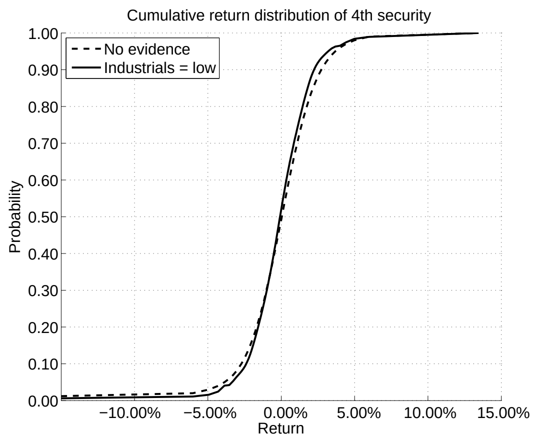

(d)

Figure 2.5: Stress tests on the entire returns' distributions. Cumulative distribution of returns for the first four securities of the DJ Euro Stoxx 50 Index in the case of no evidence and in the case of evidence on the Industrials attribution factor set to the state low.

A more pragmatic approach is the following. Since the posterior distributions of returns has been recovered, we can formulate and solve a portfolio optimization problem using the mean-variance portfolio optimization framework (2.32) in order to have the proper weights of the securities. The efficient frontier together with the optimal portfolio composition when the Industrials attribution factor is evidenced to the state low is shown in Figure 2.6. Therefore, the framework allows to easily construct portfolios with the desired expected return under the analyzed scenarios.

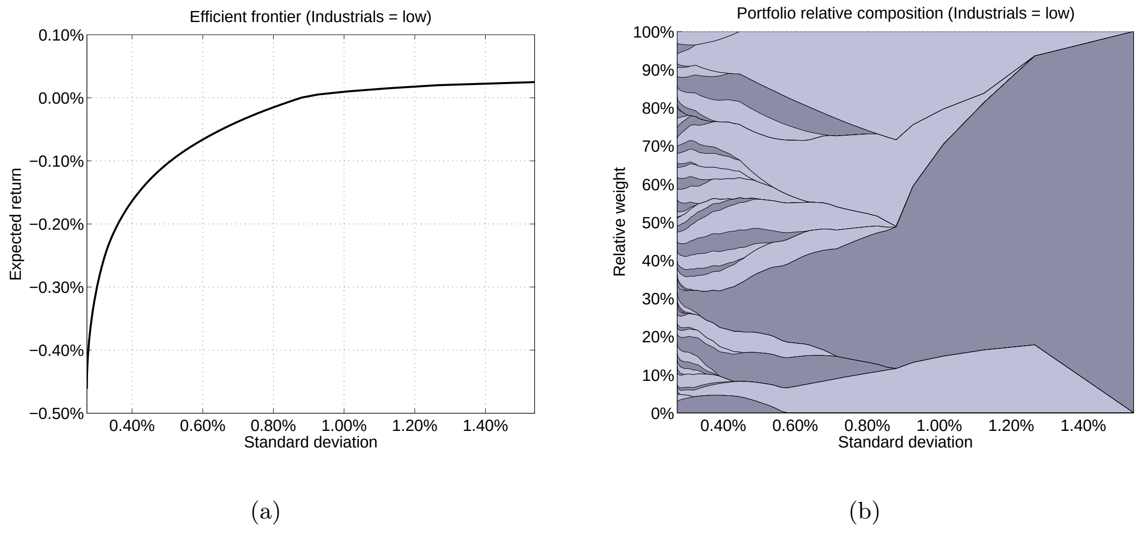

Figure 2.6: Optimal portfolio allocation by using the market views. Efficient frontier (a) and the corresponding portfolio composition (b) where the Industrials attribution factor is evidenced to the state low.

The last point concerns the effectiveness of this framework when the investor's views are correct. Villa and Stella (2012) performed backtesting procedures in order to empirically evaluate the impacts of the views on the performance of the DJ Euro Stoxx 50 Index portfolio. They shown that a correct view is effective in selecting an optimal portfolio, achieving a return which is greater than the one achieved without any market views. Clearly, the formulation of a correct view is a complex task, but this view is restricted to a low number of states of a specific factor which may be well known by the investor. In conclusion, we can state that the proposed framework for portfolio analysis and optimization is a useful tool for those investors who need to integrate their qualitative information (market views) with a quantitative factor model.

2.5 Discussion

In this chapter, we have presented the basic theory about Bayesian networks, a sound probabilistic graphical tool for modeling and reasoning with uncertain beliefs. We have discussed the main characteristics of these models, such as their ability to compactly represent large probability distributions and the availability of inference algorithms that can effectively answer queries about these distributions. We have explored how it is possible to learn Bayesian networks from data and how to use them to perform exact and approximate inference. In the last part of the chapter we have described the interplay between modern portfolio theory and Bayesian networks and how it is possible to exploit them in a novel framework for portfolio analysis and optimization. This framework provides an efficient way to interface models to data and allows efficient evidential reasoning to understand the behavior of the investment portfolio in different economic scenarios.

Chapter 3

Continuous time Bayesian networks

Continuous time Bayesian networks are probabilistic graphical models which describe structured stochastic processes that evolve over continuous time. They are based both on homogeneous Markov processes, as they model the transition dynamics of a system, and on Bayesian networks, as they provide a graphical representation over a structured state space. These models are fundamental to the work developed in this thesis. We start this chapter discussing their representation, we move on to describe how it is possible to perform learning, we continue by reviewing the inference methods and then we finish discussing about the related models and applications.

3.1 Representation

The representation power of continuous time Bayesian networks is inherent to the factorization of the system dynamics in *local Markov processes* that depend on some limited set of state variables and not on the entire state of the system. We present the necessary concepts about continuous time Markov processes that are crucial to understanding the definition and semantics of these models. It should be noted that the first section serves as background material, if a more detailed description is required, we refer to Norris (1997).

3.1.1 Continuous time Markov processes

Markov processes are probabilistic models used to represent dynamic systems. Consider a continuous time random process X, with state space defined as $Val(X) = \{x_1, \ldots, x_I\}$, as a set of random variables indexed by time $t \in [0, \infty)$. Then, the state of the process at time t is defined as a random variable $X(t) \in Val(X)$, while the instantiation of values for $X(t)$ for all t is called *trajectory.* A common assumption is to think that the process is memoryless. More formally, we say that X is a Markov process if it satisfies the *Markov property* $\forall s, t \geq 0$, $\forall x_i, x_j \in Val(X)$:

$$P(X(t+s) = x_j | X(s) = x_i, X(v), v \leq s) = P(X(t+s) = x_j | X(s) = x_i). \tag{3.1}$$

In order to define a Markov process, we have to specify, for each state, the probability of making the next transition to each other state for all transition times. It is common to assume that the process is *time-homogeneous*, i.e. the transition probabilities do not depend on time:

$$P(X(t+s) = x_j | X(s) = x_i) = P_{x_i, x_j}(t) \ \forall t, s \geq 0, \forall x_i, x_j \in Val(X). \tag{3.2}$$

Let us consider the homogeneous transition probabilities as in equation (3.2) and define the *transition probability matrix* $\boldsymbol{P}(t) = [P_{x_i, x_j}(t)]$. This matrix is a stochastic matrix, so we have that $\boldsymbol{P}(t) \geq \mathbf{0}$ and $\boldsymbol{P}(t)\mathbf{1} = \mathbf{1}$, where $\mathbf{1}$ is a I-dimensional column vector of 1's. Moreover, from the Chapman-Kolmogorov equation, we have that:

$$\boldsymbol{P}(s+t) = \boldsymbol{P}(s)\boldsymbol{P}(t) \ \forall t, s \geq 0. \tag{3.3}$$

It follows from equation (3.3) that $\boldsymbol{P}(0) = \boldsymbol{I}$, where $\boldsymbol{I}$ is the identity matrix, which has the physical interpretation that if no time passes, then no transition can occur.

Given that time is continuous, the transition matrix itself cannot give us a tool to calculate probability transitions over time. Thus, we have to resort to the infinitesimal generator matrix $\boldsymbol{Q}$, called *intensity matrix*, defined as the derivative of $\boldsymbol{P}(t)$ at $t = 0$:

$$\boldsymbol{Q} = \lim_{t \to 0^+} \frac{\boldsymbol{P}(t) - \boldsymbol{I}}{t}, \tag{3.4}$$

Given that $\boldsymbol{P}(t)$ is a stochastic matrix, then the diagonal elements of $\boldsymbol{Q}$ are non-positive, the off-diagonal elements are non-negative and the row sums are all zero. This matrix is crucial to introduce the definition of continuous time Markov process.

Definition 3.1. *(finite states, time-homogeneous, continuous time) Markov process, (Norris, 1997). Let X be a random process with a finite domain $Val(X) = \{x_1, \dots, x_I\}$ whose state changes over continuous time. Then X is a Markov process iff its behavior can be specified in terms of a markovian transition model with an intensity matrix*

$$\boldsymbol{Q} = \begin{bmatrix} -q_{x_1} & q_{x_1,x_2} & \cdot & q_{x_1,x_I} \\ q_{x_2,x_1} & -q_{x_2} & \cdot & q_{x_2,x_I} \\ \cdot & \cdot & \cdot & \cdot \\ q_{x_I,x_1} & q_{x_I,x_2} & \cdot & -q_{x_I} \end{bmatrix},$$

where $q_{x_i} = \sum_{j \neq i} q_{x_i,x_j}$ and $q_{x_i,x_j} \geq 0$.

All elements of $\boldsymbol{Q}$ have a practical interpretation: the off-diagonal elements q_{x_i,x_j} can be thought as the "instantaneous probability" of transitioning from x_i to x_j, while the diagonal elements q_{x_i} can be seen as "instantaneous probability" of leaving state x_i.

It is customary to parametrize the intensity matrix $\boldsymbol{Q}$ with two independent sets: $\boldsymbol{q} = \{q_{x_i} : 1 \leq i \leq I\}$, i.e. the set of intensities parameterizing the exponential distributions over *when* the next transition occurs, and $\boldsymbol{\theta} = \{\theta_{x_i,x_j} = q_{x_i,x_j}/q_{x_i} : 1 \leq i, j \leq I, j \neq i\}$, i.e. the set of probabilities parameterizing the distribution over *where* the state transitions.

Consider now the first derivative of the transition probability matrix $\boldsymbol{P}'(t)$. From equation (3.3) and the definition of $\boldsymbol{Q}$ in equation (3.4), we have:

$$\boldsymbol{P}'(t) = \lim_{s \to 0^+} \frac{\boldsymbol{P}(t+s) - \boldsymbol{P}(t)}{s} = \lim_{s \to 0^+} \frac{\boldsymbol{P}(t)\boldsymbol{P}(s) - \boldsymbol{P}(s)}{s} = \lim_{s \to 0^+} \frac{\boldsymbol{P}(s) - \boldsymbol{I}}{s} \boldsymbol{P}(t) = \boldsymbol{Q}\boldsymbol{P}(t), \tag{3.5}$$

which is the *backward* Kolmogorov differential equation. In an analogous way, we can obtain $\boldsymbol{P}'(t) = \boldsymbol{P}(t)\boldsymbol{Q}$, which is the *forward* Kolmogorov differential equation. Its unique solution under the initial condition $\boldsymbol{P}(0) = \boldsymbol{I}$ is given by the following *matrix exponential*:

$$\boldsymbol{P}(t) = \exp(\boldsymbol{Q}t) = \sum_{k=0}^{\infty} \frac{(\boldsymbol{Q}t)^k}{k!}, \ \forall t \geq 0. \tag{3.6}$$

Thus, from equation (3.6), we can work out the transition probability matrix for any future time t. There are different methods to compute the matrix exponential, primarily based on ordinary differential equation solvers, such as the Runge-Kutta-Fehlberg method, and uniformization, a transformation of a continuous time system into a discrete time one, but there are still some numerical difficulties to compute it (Moler and van Loan, 2003).

3.1.2 The CTBN model

Continuous time Bayesian networks provide a factored representation of Markov processes over systems whose state is defined as an assignment to some (possibly large) set of variables. Using the same idea of Bayesian networks, the dynamics of the entire Markov process are decomposed in local dynamics according to a graph structure whose nodes are variables, and the evolution of each variable X depends on the state of its parents $Pa(X)$ in the graph. These local dynamics are modeled using a special type of Markov process defined as follows.

Definition 3.2. *Conditional Markov process, (Nodelman et al., 2002). Let X be a variable whose domain is $Val(X) = \{x_1, \dots, x_I\}$. Assume that X evolves as a Markov process $X(t)$ whose dynamics are conditioned on a set $Pa(X)$ of variables, each of which can also evolve over time. Then, we have a conditional intensity matrix (CIM) $\boldsymbol{Q}_{X|Pa(X)}$ defined as set of intensity matrices, one for each instantiation $pa_u \in Pa(X)$:*

$$\boldsymbol{Q}_{X|pa_u} = \begin{bmatrix} -q_{x_1|pa_u} & q_{x_1,x_2|pa_u} & \cdot & q_{x_1,x_I|pa_u} \\ q_{x_2,x_1|pa_u} & -q_{x_2|pa_u} & \cdot & q_{x_2,x_I|pa_u} \\ \cdot & \cdot & \cdot & \cdot \\ q_{x_I,x_1|pa_u} & q_{x_I,x_2|pa_u} & \cdot & -q_{x_I|pa_u} \end{bmatrix}.$$

Clearly, if $Pa(X) = \emptyset$, then the CIM is the intensity matrix of a standard Markov process. Conditional intensity matrices are the building blocks of the dynamic component of a continuous time Bayesian network, that is defined as follows:

Definition 3.3. *Continuous time Bayesian network (CTBN), (Nodelman et al., 2002). Let $\boldsymbol{X}$ be a set of random variables $X_1, \dots, X_N$. Each X has a finite domain of values $Val(X) = \{x_1, \dots, x_I\}$. A continuous time Bayesian network $\mathcal{N} = (\mathcal{B}, \mathcal{M})$ over $\boldsymbol{X}$ consists of two components: the first is an initial distribution $P^0_{\boldsymbol{X}}$, specified as a Bayesian network $\mathcal{B}$ over $\boldsymbol{X}$, the second is a continuous time transition model $\mathcal{M}$ specified as:*

- *a directed (possibly cyclic) graph $\mathcal{G}$ whose nodes are $X_1, \dots, X_N$;*
- *a conditional intensity matrix, $\boldsymbol{Q}_{X|Pa(X)}$, for each variable $X \in \boldsymbol{X}$.*

3.1.3 Semantics

It is possible to define the semantics of the CTBN model as a single Markov process over the joint state space using a special type of operator called *amalgamation* (Nodelman et al., 2002). This operator takes two CIMs and produces as output a single bigger CIM. Intuitively, given two sets of variables $\boldsymbol{Y} = \boldsymbol{Y}_1 \cup \boldsymbol{Y}_2 \subseteq \boldsymbol{X}$ and $\boldsymbol{Z} = \boldsymbol{Z}_1 \cup \boldsymbol{Z}_2 \subseteq \boldsymbol{X} \setminus \boldsymbol{Y}$, and two CIMs $\boldsymbol{Q}_{\boldsymbol{Y}_1|\boldsymbol{Z}_1}$ and $\boldsymbol{Q}_{\boldsymbol{Y}_2|\boldsymbol{Z}_2}$, the amalgamated CIM $\boldsymbol{Q}_{\boldsymbol{Y}|\boldsymbol{Z}} = \boldsymbol{Q}_{\boldsymbol{Y}_1|\boldsymbol{Z}_1} \times \boldsymbol{Q}_{\boldsymbol{Y}_2|\boldsymbol{Z}_2}$ contains the intensities for the variables in $\boldsymbol{Y}$ conditioned on those in $\boldsymbol{Z}$.

Therefore, a CTBN $\mathcal{N}$ is a factored representation of an homogeneous Markov process described by the *joint intensity matrix*:

$$\boldsymbol{Q}_{\mathcal{N}} = \prod_{X \in \boldsymbol{X}} \boldsymbol{Q}_{X|Pa(X)}, \tag{3.7}$$

where here the symbol $\prod$ refers to the amalgamation operator. We note that $\boldsymbol{Q}_{\mathcal{N}}$ is a square matrix over the entire joint state space with cardinality equals to the product the cardinality of each variable $X \in \boldsymbol{X}$.

The CTBN model can be also seen as a *generative* model over sequences of *events*, where an event is a pair $(t, \boldsymbol{x}[x_n])$ which denotes a transition of the variable X_n to the value $x_n \in Val(X_n)$ at time t. The generative procedure takes the initial distribution, the description of each variable and an end time, and it randomly samples a trajectory for the system from the initial time to end time (Nodelman et al., 2002).

It is noteworthy to mention two important aspects of this model compared to the standard Bayesian networks framework. Firstly, like BNs, the graph of CTBNs provides both a skeleton for representing the joint distribution and a description of the independence properties of this distribution. Unlike BNs, the graph of a CTBN specifies a notion of independence over *entire trajectories* and it can contain cycles because it refers to the dynamic component of the system. In fact, an arc $X \to Y$ implies that the temporal dynamics of Y depends on the value of X, while a loop $X \leftrightarrow Y$ implies that the temporal dynamics of X simultaneously depend on the value of Y and vice versa. Secondly, a fundamental assumption in CTBNs in that, as time is continuous, variables cannot transition at the same instant. Thus, all intensities corresponding to two simultaneous changes are zero (Nodelman, 2007). This assumption will be crucial for the algorithms designed in the next chapters.

3.2 Learning

Continuous time Bayesian networks can be learned directly from data, and then they can be used to perform inference or knowledge discovery. As in the context of the BNs framework, the likelihood of the data is decomposed into local likelihoods and it is summarized in terms of sufficient statistics aggregated over the data. We discuss the basic notions of parameter and structural learning of the dynamic component of a CTBN. Parameter learning is concerned with the estimation of the elements of the CIMs when the graph is known, while structural learning is concerned with the selection of the graph and the estimation of the CIMs. Parametric and structural learning can be developed for complete or missing data arising from partial observability of the trajectory. We cover the first case, while we refer to Nodelman et al. (2003) for the second case.

3.2.1 Parameter learning

In the parameter learning case, the graph $\mathcal{G}$ of the CTBN is given and the goal is to learn each entry of each intensity matrix $\boldsymbol{Q}_{X|pa_u}$ that governs the dynamics of X. Given that a CTBN $\mathcal{N}$ describes a Markov process over the joint state space, we can parametrize it using $\boldsymbol{q}$ and $\boldsymbol{\theta}$, while we use $\boldsymbol{q}_{X|pa_u}$ and $\boldsymbol{\theta}_{X|pa_u}$ to parametrize each intensity matrix.

Given a data set $\mathcal{D} = \{\boldsymbol{\sigma}_1, \ldots, \boldsymbol{\sigma}_M\}$ of M fully observed trajectories, where each $\boldsymbol{\sigma}$ is a complete set of state transitions and the times at which they occurred, then the likelihood function decomposes by variable and parameter as follows:

$$L_{\mathcal{N}}(\boldsymbol{q}, \boldsymbol{\theta} : \mathcal{D}) = \prod_{X \in \boldsymbol{X}} L_X(\boldsymbol{q}_{X|Pa(X)} : \mathcal{D})\ L_X(\boldsymbol{\theta}_{X|Pa(X)} : \mathcal{D}). \tag{3.8}$$

The formulation (3.8) allows us to maximize each local likelihood L_X independently and then to combine them to get the MLE parameters. The likelihood of the data set can be expressed in terms of the following sufficient statistics (Nodelman et al., 2003):

- $T[x_i|pa_u]$: the amount of time spent in the state $X = x_i$ while $Pa(X) = pa_u$;
- $M[x_i, x_j|pa_u]$: the number of transitions from $X = x_i$ to $X = x_j$ while $Pa(X) = pa_u$. From this statistic, we have that $M[x_i|pa_u] = \sum_{x_j \neq x_i} M[x_i, x_j|pa_u]$: the total number of transitions leaving the state $X = x_i$ while $Pa(X) = pa_u$.

The component $L_X(\boldsymbol{\theta}_{X|Pa(X)} : \mathcal{D})$ of equation (3.8) gives us the probability of the sequence of state transitions that depend only on the value of the parents at the instant of the transition. Thus, as done in the BNs context, we can decompose the parameter $\boldsymbol{\theta}_{X|Pa(X)}$ of each variable $X \in \boldsymbol{X}$ by a set of parameters $\theta_{x_i,x_j|pa_u}$ for each $x_i, x_j \in Val(X)$ with $x_j \neq x_i$ and instantiation of its parents $pa_u \in Pa(X)$. Thus, the local likelihood of the parameter $\boldsymbol{\theta}$ can be written as follows:

$$L_X(\boldsymbol{\theta}_{X|Pa(X)} : \mathcal{D}) = \prod_{pa_u}\prod_{x_i}\prod_{x_j \neq x_i} \theta_{x_i,x_j|pa_u}^{M[x_i,x_j|pa_u]}. \tag{3.9}$$

The component $L_X(\boldsymbol{q}_{X|Pa(X)} : \mathcal{D})$ of equation (3.8) gives us the probability that X stays in a state x_i under a specific parent configuration $pa_u \in Pa(X)$. The duration in the state x_i can be determined by a transition of X or a transition of one of its parents. Thus, the local likelihood of the parameter $\boldsymbol{q}$ can be written as follows:

$$L_X(\boldsymbol{q}_{X|Pa(X)} : \mathcal{D}) = \prod_{pa_u}\prod_{x_i} q_{x_i|pa_u}^{M[x_i|pa_u]} \exp\left(-q_{x_i|pa_u} T[x_i|pa_u]\right). \tag{3.10}$$

The maximization of the likelihood in equation (3.8) can be performed using the following MLE parameters as a function of the sufficient statistics (Nodelman et al., 2003):

$$\hat{q}_{x_i|pa_u} = \frac{M[x_i|pa_u]}{T[x_i|pa_u]},\ \hat{\theta}_{x_i,x_j|pa_u} = \frac{M[x_i,x_j|pa_u]}{M[x_i|pa_u]}. \tag{3.11}$$

An alternative to MLE is the Bayesian parameter estimation. This estimation can be performed in a similar way to the BNs case, where $P(\boldsymbol{q}_\mathcal{G}, \boldsymbol{\theta}_\mathcal{G}|\mathcal{D}) \propto P(\mathcal{D}|\boldsymbol{q}_\mathcal{G}, \boldsymbol{\theta}_\mathcal{G})P(\boldsymbol{q}_\mathcal{G}, \boldsymbol{\theta}_\mathcal{G})$. For the prior over parameters $P(\boldsymbol{q}_\mathcal{G}, \boldsymbol{\theta}_\mathcal{G})$, we assume independence between the sets of parameters characterizing the exponential distributions and the set of parameters characterizing the multinomial distributions:

$$P(\boldsymbol{q}_\mathcal{G}, \boldsymbol{\theta}_\mathcal{G}) = P(\boldsymbol{q}_\mathcal{G}|\mathcal{G})P(\boldsymbol{\theta}_\mathcal{G}|\mathcal{G}). \tag{3.12}$$

We assume global parameter independence (2.10), so we have that:

$$P(\boldsymbol{q}_\mathcal{G}, \boldsymbol{\theta}_\mathcal{G}) = \prod_{X \in \boldsymbol{X}} P(\boldsymbol{q}_{X|Pa(X)}|\mathcal{G})P(\boldsymbol{\theta}_{X|Pa(X)}|\mathcal{G}), \tag{3.13}$$

and local parameter independence (2.11), thus we have that:

$$P(\boldsymbol{q}_\mathcal{G}, \boldsymbol{\theta}_\mathcal{G}) = \prod_{X \in \boldsymbol{X}}\prod_{pa_u}\prod_{x_i} P(q_{x_i|pa_u}|\mathcal{G})P(\boldsymbol{\theta}_{x_i|pa_u}|\mathcal{G}). \tag{3.14}$$

For a Markov process, it is customary to choose a Dirichlet distribution as prior for the parameters corresponding to the multinomial distribution, while we choose a gamma distribution as prior for the parameter corresponding to the exponential distribution:

$$P(q_{x_i}) \sim Gamma\left(\alpha_{x_i}, \tau_{x_i}\right), \tag{3.15}$$

$$P(\boldsymbol{\theta}_{x_i}) \sim Dir\left(\alpha_{x_i,x_1}, \ldots, \alpha_{x_i,x_I}\right). \tag{3.16}$$

After conditioning on the data set $\mathcal{D}$, we have:

$$P(q_{x_i}|\mathcal{D}) \sim Gamma\left(\alpha_{x_i} + M[x_i], \tau_{x_i} + T[x_i]\right), \tag{3.17}$$

$$P(\boldsymbol{\theta}_{x_i}|\mathcal{D}) \sim Dir\left(\alpha_{x_i,x_1} + M[x_i, x_1], \ldots, \alpha_{x_i,x_I} + M[x_i, x_I]\right). \tag{3.18}$$

As in the BNs case, these posteriors can be used to predict the next event, averaging out the event probability over the possible values of the parameters, that is equivalent to use the following parameters:

$$\hat{q}_{x_i|pa_u} = \frac{\alpha_{x_i|pa_u} + M[x_i|pa_u]}{\tau_{x_i|pa_u} + T[x_i|pa_u]}, \ \hat{\theta}_{x_i,x_j|pa_u} = \frac{\alpha_{x_i,x_j|pa_u} + M[x_i, x_j|pa_u]}{\alpha_{x_i|pa_u} + M[x_i|pa_u]}, \tag{3.19}$$

where α represents the pseudocount of the number of transitions from one state to another and τ represents the imaginary amount of time spent in each state (Nodelman, 2007).

3.2.2 Structural learning

The problem of learning the structure of a CTBN is simpler then the general BN case because we do not have to satisfy any acyclic constraint. In this case, we resort to a score-based approach defining a Bayesian score and then searching (without constraints) a structure that has the highest score. The Bayesian score is the same as the BNs case (2.16) that we report here for convenience:

$$BS(\mathcal{G} : \mathcal{D}) = \ln P(\mathcal{G}) + \ln P(\mathcal{D}|\mathcal{G}). \tag{3.20}$$

As the prior over structure $P(\mathcal{G})$ does not grow with the size of data, the significant term of the Bayesian score is the marginal likelihood of the data, given the structure $P(\mathcal{D}|\mathcal{G})$. This term is computed by marginalizing out the unknown parameters as follows:

$$P(\mathcal{D}|\mathcal{G}) = \int_{\boldsymbol{q}_\mathcal{G}, \boldsymbol{\theta}_\mathcal{G}} P(\mathcal{D}|\boldsymbol{q}_\mathcal{G}, \boldsymbol{\theta}_\mathcal{G}, \mathcal{G}) P(\boldsymbol{q}_\mathcal{G}, \boldsymbol{\theta}_\mathcal{G}|\mathcal{G}) d\boldsymbol{q}_\mathcal{G} d\boldsymbol{\theta}_\mathcal{G}. \tag{3.21}$$

In the case of no missing values, the probability of the data given a CTBN model $P(\mathcal{D}|\boldsymbol{q}_{\mathcal{G}}, \boldsymbol{\theta}_{\mathcal{G}}, \mathcal{G})$ can be decomposed as a product of likelihoods as shown in equation (3.8):

$$P(\mathcal{D}|\boldsymbol{q}_{\mathcal{G}}, \boldsymbol{\theta}_{\mathcal{G}}, \mathcal{G}) = \prod_{X \in \boldsymbol{X}} L_X(\boldsymbol{q}_{X|Pa(X)} : \mathcal{D})\ L_X(\boldsymbol{\theta}_{X|Pa(X)} : \mathcal{D}). \tag{3.22}$$

Using the global parameter independence assumption (2.10) and the decomposition (3.22), the marginal likelihood $P(\mathcal{D}|\mathcal{G})$ can be written as follows:

$$\begin{aligned} P(\mathcal{D}|\mathcal{G}) &= \prod_{X \in \boldsymbol{X}} \int_{\boldsymbol{q}_{\mathcal{G}}} L_X(\boldsymbol{q}_{X|Pa(X)} : \mathcal{D}) P(\boldsymbol{q}_{X|Pa(X)}) d\boldsymbol{q}_{\mathcal{G}} && (3.23)\\ &\times \prod_{X \in \boldsymbol{X}} \int_{\boldsymbol{\theta}_{\mathcal{G}}} L_X(\boldsymbol{\theta}_{X|Pa(X)} : \mathcal{D}) P(\boldsymbol{\theta}_{X|Pa(X)}) d\boldsymbol{\theta}_{\mathcal{G}} && (3.24)\\ &= \prod_{X \in \boldsymbol{X}} ML_X(\boldsymbol{q}_{X|Pa(X)} : \mathcal{D}) \times ML_X(\boldsymbol{\theta}_{X|Pa(X)} : \mathcal{D}). && (3.25) \end{aligned}$$

It is possible to extend the BDe metric of BNs and to compute the marginal likelihood $P(\mathcal{D}|\mathcal{G})$ in closed form, given the sufficient statistics over the data. Therefore, the closed form solution of the marginal likelihood of $\boldsymbol{q}$ reported in equation (3.23) is:

$$\prod_{pa_u} \prod_{x_i} \frac{\Gamma\left(\alpha_{x_i|pa_u} + M[x_i|pa_u] + 1\right) \left(\tau_{x_i|pa_u}\right)^{(\alpha_{x_i|pa_u}+1)}}{\Gamma\left(\alpha_{x_i|pa_u} + 1\right) \left(\tau_{x_i|pa_u} + T[x_i|pa_u]\right)^{(\alpha_{x_i|pa_u}+M[x_i|pa_u]+1)}}, \tag{3.26}$$

and the marginal likelihood of $\boldsymbol{\theta}$ reported in equation (3.24) is:

$$\prod_{pa_u} \prod_{x_i = x_j} \frac{\Gamma\left(\alpha_{x_i|pa_u}\right)}{\Gamma\left(\alpha_{x_i|pa_u} + M[x_i|pa_u]\right)} \times \prod_{x_i \neq x_j} \frac{\Gamma\left(\alpha_{x_i,x_j|pa_u} + M[x_i, x_j|pa_u]\right)}{\Gamma\left(\alpha_{x_i,x_j|pa_u}\right)}. \tag{3.27}$$

Using the closed form solutions (3.26) and (3.27), under the assumption of structure modularity (2.17), the Bayesian score can be decomposed by variable as follows:

$$\begin{aligned} BS(\mathcal{G} : \mathcal{D}) &= \sum_{X \in \boldsymbol{X}} \ln P(Pa(X) = Pa_{\mathcal{G}}(X)) \\ &+ \ln ML_X(\boldsymbol{q}_{X|Pa(X)} : \mathcal{D}) + \ln ML_X(\boldsymbol{\theta}_{X|Pa(X)} : \mathcal{D}). && (3.28) \end{aligned}$$

Since there are no acyclic constraints, it is possible to optimize the parent set for each variable independently and then combining the results. Thus, the search space over the graph structures can be done in polynomial time, given a maximum number of possible parents per variable. The search can be easily performed enumerating each possible parent set or using a greedy hill-climbing search with operators that add and delete edges in the graph.

3.3 Inference

Since a continuous time Bayesian network is a compact representation of a joint intensity matrix for a Markov process, it can be used to answer any query that we can answer using a state-space model, such as filtering, prediction and smoothing (Murphy, 2002). In the CTBN context, there are two types of possible evidence: *point evidence*, it is an observation of the value x_i of a variable X at a particular instant in time, i.e. $X(t) = x_i$, and *continuous evidence*, it is an observation of the value of a variable throughout an entire interval which we take to be a half-closed interval $[t_1; t_2)$, i.e. $X[t_1 : t_2) = x_i[t_1 : t_2)$.

Using a CTBN model we can ask about the marginal distribution of some variables at a particular time, e.g. the distribution of $X_1(t) = x_1$ and $X_2(t) = x_2$ at $t = 5$, or queries about the timing of a transition, e.g. the distribution over the time that X_1 transitions from x_1 to x_2 in the time interval $[0; 5)$. Other common types of queries are related to the expected sufficient statistics, such as the expected amount of time that a variable X_1 spends in a state x_1, i.e. $\mathbb{E}[T[x_1]]$, and the expected number of times that a variable X_1 transitions from state x_1 to state x_2, i.e. $\mathbb{E}[M[x_1, x_2]]$.

After a brief discussion about the difficulties associated with exact inference (Nodelman et al., 2002), we show how it is possible to perform approximate inference using sampling-based approaches similar to the BNs case (Fan and Shelton, 2008).

3.3.1 Exact inference

Given a series of observations, we can calculate the joint distribution using equation (3.7) at the time of the first observation, conditioned on that observation, and use this new distribution as the initial one from which to compute the joint distribution at the time of the next observation. The limit of this inference procedure is that the generation of the full joint intensity matrix is exponential in the number of variables.

Unfortunately, the graph structure of the CTBN cannot help us to decompose the problem. For example, consider the simplest case of connection depicted in Figure 2.1 (a), $X \to Z \to Y$, where Z is instantiated. In the BN model, if the state of Z is known, then X and Y become independent. Conversely, in the CTBN model, even if the transition intensity of Y depends only on the value of Z at any point in time, as soon as we consider temporal evolution, their states become correlated. This phenomenon, called *entanglement*, is an effect present also in other temporal models which causes independent random variables (considered point in time) to have a dependency (over time) due to frequent updates (Nodelman et al., 2002). Therefore, the only possible conclusion we can make is that X is independent of Y given the *full trajectory* of Z. Unfortunately, also the reconstruction of the full trajectory cannot be performed compactly. Thus, we have to resort to approximate methods to perform inference in a general CTBN model.

3.3.2 Approximate inference

Several approximate algorithms have been proposed in the literature. Nodelman et al. (2005a) introduced the expectation propagation algorithm which allows both point and continuous evidence. Friedman and Kupferman (2006) demonstrated that a separation of time scales between variables can lead to a simpler inference problem. Saria et al. (2007) presented an improved approximate inference method based on expectation propagation. Alternatives are offered by mean field variational approximation (Cohn et al., 2009) and continuous time belief propagation (El-Hay et al., 2010) algorithms. Sampling-based algorithms, such as importance sampling (Fan and Shelton, 2008) and Gibbs sampling (El-Hay et al., 2008; Rao and Teh, 2011) have been introduced. We describe the basic notions of the importance sampling algorithm that has the advantage of being an anytime algorithm, i.e. it is possible to stop it at any time during the computation to obtain an answer and, in the limit, it converges to the true answer.

As in the case of BNs, we can use forward sampling to answer any query that is not conditioned on evidence. This procedure is based on randomly sampling many particles and looking at the fraction that matches the query. Note that, in the context of CTBNs, a particle is a *sampled trajectory.* Formally, given a set $\mathcal{D} = \{\boldsymbol{\sigma}_1, \ldots, \boldsymbol{\sigma}_M\}$ of M trajectories, we can estimate the expectation of any function f by computing:

$$\hat{\mathbb{E}}_{\mathcal{D}}[f] = \frac{1}{M} \sum_{m=1}^{M} f(\boldsymbol{\sigma}_m). \tag{3.29}$$

Thus, if we would like to estimate $P(X(5) = x_1)$, then we can use $f = \mathbf{1}_{\{X(5)=x_1\}}$. The function f can also count the total number of times that X transitions from x_1 to x_2 while $Pa(X) = pa_3$, allowing us to estimate the expected sufficient statistic $M[x_1, x_2|pa_3]$.

If we would like to answer any query that is conditioned on evidence, then we have to resort to other techniques, such as (normalized) importance sampling. Given a set of samples $\mathcal{D}' = \{\boldsymbol{\sigma}'_1, \ldots, \boldsymbol{\sigma}'_M\}$ of M trajectories from a proposal distribution $\mathcal{P}'$, the estimate of the conditional expectation of a function f given an evidence $\boldsymbol{e}$ is:

$$\hat{\mathbb{E}}_{\mathcal{D}}[f|\boldsymbol{e}] = \frac{1}{W} \sum_{m=1}^{M} f(\boldsymbol{\sigma}'_m) w(\boldsymbol{\sigma}'_m), \tag{3.30}$$

where W is the sum of the weights, i.e. the normalization factor.

If the query involves an evidence over some subset of variables $\boldsymbol{Y} \subset \boldsymbol{X}$ for the total length of the trajectory, then we force the behavior of these variables. Specifically, the proposal distribution is obtained by forward sampling the behavior of variables $X \in \boldsymbol{X} \setminus \boldsymbol{Y}$ and inserting the known transitions at known times for variables in $\boldsymbol{Y}$. As in the BNs case, given that the weight is the ratio of the likelihood contributions of all variables $\boldsymbol{X}$ against $\boldsymbol{X} \setminus \boldsymbol{Y}$, then the weight can be computed as:

$$w(\boldsymbol{\sigma}') = \frac{P_{\mathcal{N}}(\boldsymbol{\sigma}')}{P'(\boldsymbol{\sigma}')} = \frac{\prod_{X \in \boldsymbol{X}} \prod_{j=0}^{J} L_X(x[\tau_j : \tau_{j+1}))}{\prod_{X \in \boldsymbol{X} \setminus \boldsymbol{Y}} \prod_{j=0}^{J} L_X(x[\tau_j : \tau_{j+1}))} = \prod_{X \in \boldsymbol{Y}} \prod_{j=0}^{J} L_X(x[\tau_j : \tau_{j+1})), \tag{3.31}$$

where $\tau_0 = 0, \ldots, \tau_{J+1} = T$ are the transition times in the interval $[0; T)$ for a trajectory.

If the query involves evidence where variables are both observed and unobserved, then we force the trajectory to be consistent with it by looking ahead for each variable we sample. If the current state does not agree with the upcoming evidence, then we sample the next transition time Δt from a truncated exponential distribution. Let t_{be} be the time where the evidence begins, $\boldsymbol{\sigma}'_{be}$ be the set for all variables $X \in \boldsymbol{X}$ of intervals $x[\tau_j : \tau_{j+1})$ where the behavior of X is set by the evidence and $\boldsymbol{\sigma}'_{co}$ be the complement of $\boldsymbol{\sigma}'_{be}$ containing the set of intervals of unobserved behavior for all variables. We have that:

$$w(\boldsymbol{\sigma}') = \frac{P_{\mathcal{N}}(\boldsymbol{\sigma}')}{P'(\boldsymbol{\sigma}')} = \prod_{x[\tau_j:\tau_{j+1}) \in \boldsymbol{\sigma}'_{co}} \frac{L_X(x[\tau_j : \tau_{j+1}))}{L'_X(x[\tau_j : \tau_{j+1}))} \times \prod_{x[\tau_j:\tau_{j+1}) \in \boldsymbol{\sigma}'_{be}} L_X(x[\tau_j : \tau_{j+1})). \tag{3.32}$$

We can have four cases. For any variable X whose value is given by the evidence during the interval $[t; t + \Delta t)$, the contribution to the trajectory weight is the likelihood as before. For any variable X whose Δt was sampled from an exponential distribution, the ratio in equation (3.32) is 1. For any variable X whose Δt was sampled from a truncated exponential distribution, if it is involved in the next transition, then the ratio is $1 - \exp(-q(t_{be} - t))$, otherwise the ratio is $\frac{1-\exp(-q(t_{be}-t))}{1-\exp(-q(t_{be}-t-\Delta t))}$ that is almost 1 when Δt is small.

3.4 Related models and applications

Different models have been developed to handle temporal reasoning using the general BNs framework, among them the well known dynamic Bayesian networks. Continuous time Bayesian networks made a significant contribution in this field proving a factored representation of continuous time Markov processes and making available inference and learning algorithms. Some assumption underpinning the CTBN model have been relaxed in order to cover a wider range of systems. The increase of the number of applications to real life problems reveals the effectiveness of the CTBN model. We provide a brief survey about dynamic Bayesian networks, temporal Bayesian networks, and the latest developments and applications of continuous time Bayesian networks.

3.4.1 Dynamic Bayesian networks

Dynamic Bayesian networks (Dean and Kanazawa, 1989) are an extension of BNs to model probability distributions over a collection of random variables $\boldsymbol{X}_0, \boldsymbol{X}_1, \boldsymbol{X}_2, \ldots$. Under the Markov assumption and the time-homogeneity of the transition dynamics, it is possible to compactly represent the probability distribution over infinite trajectories by means of an initial state distribution and a transition model that specifies a conditional probability distribution between current time variables $\boldsymbol{X}$ and next time step variables $\boldsymbol{X}'$.

Definition 3.4. *Dynamic Bayesian network (DBN), (Murphy, 2002). A dynamic Bayesian network over a set of random variables* $\{X_1, \ldots, X_N, X'_1, \ldots, X'_N\}$ *is a pair* $\mathcal{B}_2 = (\mathcal{B}_0, \mathcal{B}_{2T})$, *where* $\mathcal{B}_0$ *is a Bayesian network which defines a prior distribution* $P(\boldsymbol{X})$, *and* $\mathcal{B}_{2T}$ *is a two-slice temporal Bayes network which defines*

$$P(X'|X) = \prod_{X' \in \boldsymbol{X}} P(X'|Pa(X')) \tag{3.33}$$

by means of a directed acyclic graph in which edges can connect nodes between two time slices (inter-time) or nodes in the same time slice (intra-time).

Given a distribution over the initial states, it is possible to *unroll* the network over sequences of a given length in order to create a new BN that induces a distribution over trajectories of that length. DBNs can be learned directly from data and they can be used to perform filtering, prediction and smoothing tasks. Unfortunately, if there are long observation sequences, inference becomes impractical in complex DBNs (Murphy, 2002).

Even if both DBNs and CTBNs allow us to model dynamic systems, they are naturally different. A DBN can be seen as a model of a sequence of observations as it learns a series of snapshots of the system; indeed the learned model can be very sensitive to the granularity of the time step chosen. Conversely, a CTBN can be interpreted as a model of the system as it learns a series of state transitions produced by the system itself. In conclusion, DBNs can be successfully applied in domains where the data is intrinsically time-sliced and where queries about events occurring between time points are not relevant. For all other domains, it is convenient to use CTBNs as they do not require to choose a fixed time step and the number of parameters to estimate is significantly lower compared to DBNs.

3.4.2 Bayesian temporal models

Three main streams of research have attempted to model temporal reasoning in the Bayesian network framework. The first one consists of instant-based formalisms, in which time is discretized in fixed-size intervals and an instance of each random variable is created for each point in time. The models belonging to this group are closely related to DBNs.

The second group are interval-based formalisms, such as *temporal Bayesian networks* (Tawfik and Neufeld, 1994), *temporal nodes Bayesian networks* (Arroyo-Figueroa and Sucar, 1999) and *probabilistic temporal networks* (Santos and Young, 1999). In these models, time is usually discretized into a finite number of intervals that can be of different size and duration for each node, allowing to handle multiple granularity. Each model is based on its own graphical semantics. For example, in temporal nodes Bayesian networks, a node represents an event or a state change of a variable, while an arc between two nodes corresponds to a causal-temporal relation. Conversely, in the probabilistic temporal networks, nodes are temporal aggregates that represent the process changing over time and arcs are the causal-temporal relationships between aggregates.

The last group are formalisms based on a representation of time as continuous variables, such as *networks of dates* (Berzuini, 1989) and *continuous time nets* (Kanazawa, 1992). In these models, the time to occurrence of significant events is generally modeled using continuous time survival analysis, but the temporal distributions generated are not used for modeling state durations of local variables. Therefore, they are more related to the classical event history analysis (Aalen et al., 2008) compared to Bayesian networks.

3.4.3 CTBN extensions and beyond

Even if continuous time Bayesian networks provide a sound framework for temporal reasoning in continuous time, their expressive power is limited by the exponential distribution that models the time duration between state transitions for a single variable. Some extensions have been developed in order to solve this gap. Gopalratnam et al. (2005) extended the CTBN representation by allowing durations to be modeled as Erlang-Coxian distributions, a subclass of general phase-type distributions. Nodelman et al. (2005b) enriched the CTBN model to represent any phase-type distribution, maintaining unchanged the basic structure of the existing algorithms. Portinale and Codetta-Raiteri (2009) extended the CTBN formalist to model continuous time delayed variables, as well as non delayed or immediate variables (which act as standard chance nodes in BNs), and they described the connection between their extension and the generalized stochastic Petri nets model.

There are other related models that allow us to represent continuous time processes. *Poisson networks* (PN) (Rajaram et al., 2005) allow us to represent multivariate structured Poisson processes, where a node of the network represents a Poisson process, and the waiting times of a process are modeled by an exponential distribution with a piecewise constant rate function that depends on the event counts of its parents in the network. *Continuous time noisy-or* (CT-NOR) (Simma et al., 2008) allows us to model the interactions between input and output events as Poisson processes whose intensities are modulated by a parameterized function, taking into account the distance in time between input and output events. *Poisson cascades* (PC) (Simma and Jordan, 2010) are a generalization of CT-NOR models for collections of events, in which each event induces a Poisson process of triggered events. CT-NOR and PC allow us to model event streams, but they require the domain expert to specify a parametric form for temporal dependencies. This limitation has been overcome by *piecewise-constant conditional intensity model* (PCIM) (Gunawardana et al., 2011), which can model the types and timing of events. Specifically, PCIM captures the dependencies of each type of event on events in the past through a set of piecewise-constant conditional intensity functions. This model uses decision trees to represent the dependencies and, given that a closed form for the marginal likelihood is derived, the decision tree induction can be done efficiently. PCIM is closely related to PN, but it is faster then PN to learn, and it can model non-linear temporal dependencies.

3.4.4 Applications

Continuous time Bayesian networks have been successfully used in several real life domains, such as to model the presence of people at their computers (Nodelman and Horvitz, 2003), for dynamic systems reliability modeling and analysis (Boudali and Dugan, 2006), to model failures in server farms (Herbrich et al., 2007), for network intrusion detection (Xu and Shelton, 2008), to model social networks (Fan and Shelton, 2009) and to model cardiogenic heart failure (Gatti et al., 2011). Continuous time Bayesian networks have been also applied as basic models to solve structured continuous time Markov decision processes (Kan and Shelton, 2008), to perform classification (Stella and Amer, 2012), to model non-stationary domains (Stella and Villa, 2014) and to solve a general model-based reinforcement learning problem (Villa and Shelton, 2014a).

Free software implementations of continuous time Bayesian networks are available. Shelton et al. (2010) developed a continuous time Bayesian network reasoning and learning engine (CTBN-RLE) written in C++, while Villa and Shelton (2014b) designed and developed an R package based on CTBN-RLE that allows us to exploit both the power of the C++ engine and the rapid prototyping and analysis offered by the R software.

Note that it is possible to rephrase the scenario analysis of financial securities in the continuous time settings by using CTBNs. In this context, the entire time evolution of a security is considered and the reasoning natively deals with time. Moreover, it is possible to exploit CTBNs to model several financial contexts; we give some insights on them. The first case concerns the generation of scenarios based on historical data. Starting from a historical panel of stock prices, such as that of the previous chapter, we compute the log-returns from the prices, and then we discretize them into bins using discretization techniques, such as quantile-based or interval-based (Dimitrova et al., 2010). After that, a CTBN model is learned from this data set and used as a generative model of time-series. Figure 3.1 (a) shows the discretized daily log-returns of the first security belonging to the DJ Euro Stoxx 50 Index from December 30th, 2005, to December 30th, 2010. Figure 3.1 (b) shows fifty samples, generated by the learned CTBN model, used to compute the possible values that the security can take in twenty business days. These scenarios are useful for the design of hedging or speculative strategies, as well as for the pricing of stock derivatives with path dependent structures.

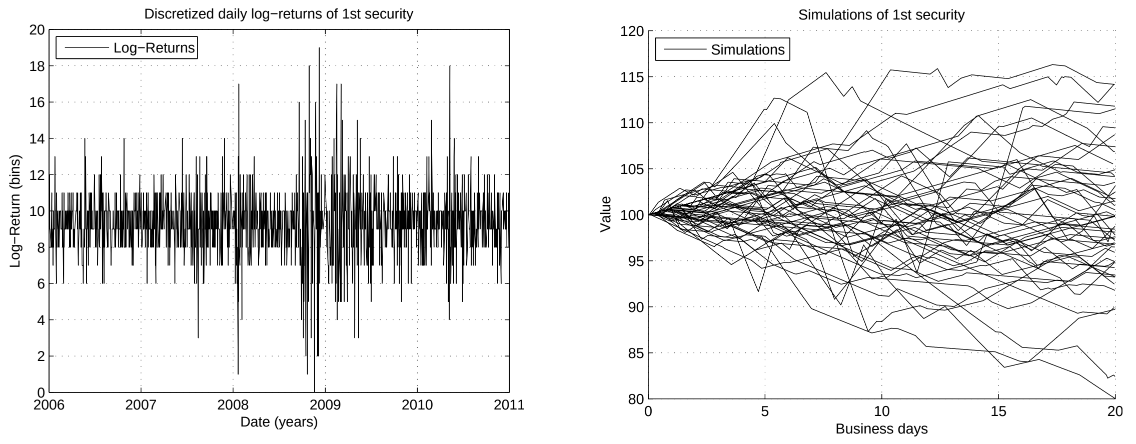

(a) (b)

Figure 3.1: Scenarios generation based on historical data: (a) five years of discretized daily log-returns of the first security belonging to the DJ Euro Stoxx 50 Index and (b) fifty samples generated by the learned CTBN model corresponding to this security.

The second case concerns the reasoning of the learned CTBN model. At a single stock level we can exploit the intensity matrices in order to assess the timing and probability related to the evolutions of the log-prices. Figure 3.2 (a) shows the expected time (in business days) of transitioning (i.e. $1/q_{x_i}$) of each discretized log-return of the first security belonging to the DJ Euro Stoxx 50 Index, while Figure 3.2 (b) shows the relative probability matrix of transition from one state to another state (i.e. θ_{x_i,x_j}).

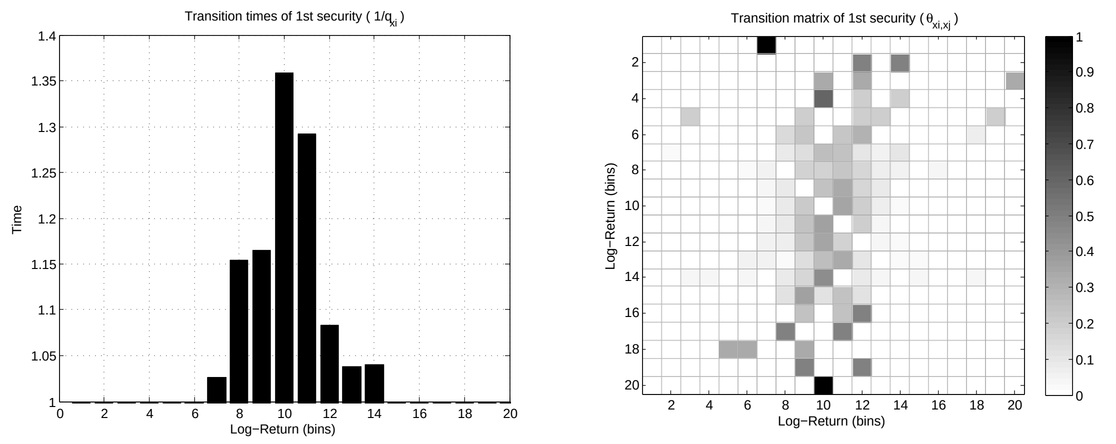

(a) (b)

Figure 3.2: Analysis of the intensity matrix: (a) expected time of transitioning and (b) transition probability matrix of the first security belonging to the DJ Euro Stoxx 50 Index.

We can also perform analysis that involves multiple stocks. For example, we can discretize the previous data set into binary values corresponding to positive (denoted as 1) and negative (denoted as 0) returns, we can select the stocks belonging to one sector, such as the telecommunication sector, and its relative index. A CTBN model is learned from this data set by imposing a loop structure from a security to its index and vice versa. In fact, we assume that a security does not influence all other securities in the same sector, but only the index, which in turn influences the other stocks that compose it. Figure 3.3 (a) shows a possible scenario of the telecommunication stocks belonging to the DJ Euro Stoxx 50 Index. Note that a scenario consists of the full trajectories of the securities and not only a single value as in the static case. Figure 3.3 (b) shows the probability of a positive value of the telecommunication index, given the previous scenario where the index value in unknown. Therefore, it is possible to infer the temporal evolution of the index value when the index is not observed, i.e. we can perform filtering. This is useful in the scenario analysis context where some financial variables are not observed and we would like to asses their values.

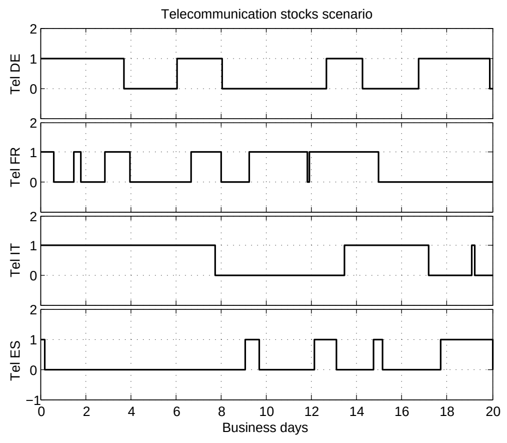

(a)

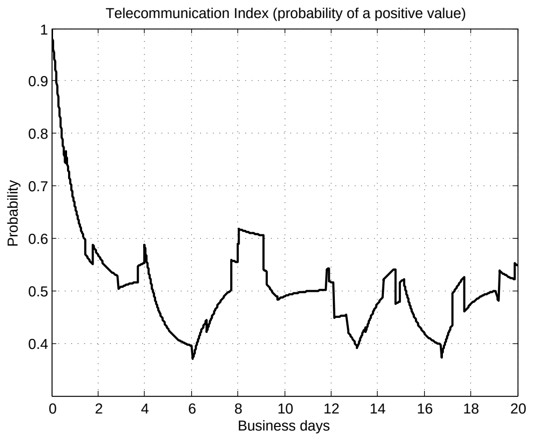

(b)

Figure 3.3: Scenario analysis. (a) a possible scenario of the telecommunication stocks belonging to the DJ Euro Stoxx 50 Index and (b) probability of a positive value of the telecommunication index given the scenario (a) where the index value in unknown.

3.5 Discussion

We have presented the basic theory about continuous time Bayesian networks, a robust modeling language for structured stochastic processes that evolve over continuous time. They allow us to model processes without needing to select a temporal granularity and they make possible the use of cyclic graphs to model mutual influence among random variables. We have explored how it is possible to learn these models directly from data and to use them to perform inference. In this case, structural learning with complete data is simpler then the general Bayesian network case, as there are no acyclic constraints. Thus, the search space over the graph structures can be done in polynomial time, given a maximum number of possible parents per variable. On the other hand, exact inference is limited to the generation of the full joint intensity matrix that is exponential in the number of variables. Thus, we have to resort to approximate methods to perform inference such as sampling-based algorithms. Finally, we have discussed the limitations of continuous time Bayesian networks, their extensions and their applications in several contexts.

Chapter 4

Continuous time Bayesian network classifiers

Continuous time Bayesian networks have been extended to solve the problem of classification on multivariate trajectories evolving in continuous time. We start this chapter by introducing the basic concepts of the classification task and how both Bayesian networks and dynamic Bayesian networks can be seen as classifiers. We continue reviewing temporal classification using continuous time Bayesian network classifiers, we move on to describe an efficient scalable parallel algorithm to learning this latter model from Big Data and then we finish presenting an application of continuous time Bayesian network classifiers to the foreign exchange rate prediction problem in high frequency domain.

4.1 Basics

Supervised learning is a basic task of machine learning and it consists of learning an input-output mapping from a *training data set* of M observations $\mathcal{D} = \{\boldsymbol{d}_1, \ldots, \boldsymbol{d}_M\}$. Each observation is an input-output pair $\boldsymbol{d} = (\boldsymbol{x}, y)$, where the input $\boldsymbol{x}$ is an instantiation of $\boldsymbol{X} = \{X_1, \ldots, X_N\}$ variables called *attributes* (or features), while the output y is an instantiation of the *class variable* Y that can be categorical or scalar. In the first case, the problem is known as *classification*, while in the second case the problem is known as *regression*. We present the necessary concepts and Bayesian models of classification, while we refer to Mitchell (1997); Duda et al. (2000); Murphy (2012) for review.

4.1.1 Classification

Classification is widely used in machine learning to solve many interesting real life problems, such as document classification, image classification and handwriting recognition, and object detection and recognition (Murphy, 2012). We focus on the classification task of input vectors $\boldsymbol{x}$ of discrete-valued features and output $y \in Val(Y) = \{y_1, \ldots, y_C\}$, where C is the number of classes, such that the ultimate goal is to construct a *classifier*. A classifier can be defined as function f that assigns a class label to instances described by a set of attributes, $y_c = f(\boldsymbol{x})$. The learning task concerns the estimation, denoted as $\hat{f}$, of the function f given a training data set. This function must be able to *generalize*, i.e. to make accurate predictions on new (unseen) inputs.

In order to handle ambiguous cases, the classifier has to return a probability distribution over possible classes, given the input vector $\boldsymbol{x}$, $P(Y|\boldsymbol{x}) \propto P(Y)P(\boldsymbol{x}|Y)$. Therefore, given a trained classifier $\hat{f}$, we can compute the most probable class $\hat{y}_c$ using the following equation:

$$\hat{y}_c = \hat{f}(\boldsymbol{x}) = \underset{y_c \in Val(Y)}{\operatorname{argmax}} \left\{P(Y = y_c)P(\boldsymbol{x}|Y = y_c)\right\}. \tag{4.1}$$

The simplest classifiers is the *naïve Bayes classifier* that assumes the features are conditionally independent, given the class value (Duda and Hart, 1973). This assumption allows us to write the class conditional probability, given a choice of parameters $\boldsymbol{\theta}$ as follows:

$$P(\boldsymbol{x}|Y = y_c, \boldsymbol{\theta}) = \prod_{X_n \in \boldsymbol{X}} P(X_n = x_i|Y = y_c, \boldsymbol{\theta}_{nc}). \tag{4.2}$$

In the binary features case, i.e. $Val(X_n) = \{0, 1\}$, we can use a Bernoulli distribution such that $P(x_i|y_c, \boldsymbol{\theta}_{nc}) \sim Ber(x_i|\mu_{nc})$, where μ_{nc} is the probability that the n-th feature occurs in the c-th class. In the categorical features case where a feature can take on one of a limited number of possible values, i.e. $Val(X_n) = \{x_1, \ldots, x_{I_n}\}$, we can use a categorical distribution such that $P(x_i|y_c, \boldsymbol{\theta}_{nc}) \sim Cat(x_i|\boldsymbol{\mu}_{nc})$, where $\boldsymbol{\mu}_{nc}$ is the probability distribution over the I_n possible values for the n-th feature in the c-th class. Even if the naïve Bayes classifier makes a strong assumption about the independence of the attributes given the class, some empirical results show that it performs well in many domains containing clear attribute dependencies (Domingos and Pazzani, 1997). One reason is that the model has $O(C \times N)$ parameters, so it is relatively immune to overfitting (Murphy, 2012).

A naïve Bayes classifier can be learned from data by computing the maximum likelihood estimate for the parameters. The probability for a single data $P(\boldsymbol{x}, y_c|\boldsymbol{\theta})$ is given by

$$P(y_c|\boldsymbol{\theta}_c) \prod_{X_n \in \boldsymbol{X}} P(X_n = x_i|\boldsymbol{\theta}_n) = \prod_{y_c} \theta_c^{(\mathbf{1}_{\{y_c\}}(y))} \prod_{X_n \in \boldsymbol{X}} \prod_{y_c} P(X_n = x_i|\boldsymbol{\theta}_{nc}), \tag{4.3}$$

while the log-likelihood of the entire training set given the parameters is the following:

$$\ln P(\mathcal{D}|\boldsymbol{\theta}) = \sum_{y_c} M[y_c] \ln \theta_c + \sum_{X_n \in \boldsymbol{X}} \sum_{y_c} \sum_{m} \ln P(\boldsymbol{d}_m[X_n]|\boldsymbol{\theta}_{nc}), \tag{4.4}$$

where $M[y_c] = \sum_m \mathbf{1}_{\{y_c\}}(\boldsymbol{d}_m[Y])$ is the number of examples of class y_c in the data set. The MLE for the log-likelihood (4.4) depends on the type of distribution we choose to use for each feature. If all features are binary, then the MLE estimates are:

$$\hat{\theta}_c = \frac{M[y_c]}{M} \qquad \hat{\theta}_{nc} = \frac{M[x_i, y_c]}{M[y_c]}, \tag{4.5}$$

where $M[x_i, y_c]$ is the number of times $\boldsymbol{d}_m[X_n] = x_i$ and $\boldsymbol{d}_m[Y] = y_c$ in the data set.

4.1.2 Performance evaluation

The performance of a classifier can be assessed by analyzing its outcomes over a training set of M input-output pairs. In the case of binary classification, we resort to the construction of the *confusion matrix* by counting the number of true positives (TP), false positives (FP), true negatives (TN) and false negatives (FN) that occur after classification.

	$y = 1$	$y = 0$	
$\hat{y} = 1$	TP	FP	$TP + FP$
$\hat{y} = 0$	FN	TN	$FN + TN$
	$TP + FN$	$FP + TN$	M

From the confusion matrix we can define the following measures: *accuracy* $AC = \frac{TP+TN}{M}$, *precision* $PR = \frac{TP}{TP+FP}$, *true positive rate* $TPR = \frac{TP}{TP+FN} \approx P(\hat{y} = 1|y = 1)$ (this is also known as sensitivity or recall) and *false positive rate* $FPR = \frac{FP}{FP+TN} \approx P(\hat{y} = 1|y = 0)$. Rather than computing TPR and FPR as two single values, it is customary to run the classifier for a set of thresholds and then plot the TPR versus FPR as an implicit function of thresholds. This is called a *receiver operating characteristic* (ROC) curve. The quality of a ROC curve can be summarized as a single number between 0 and 1 using the *area under the ROC curve* (AUC) (Fawcett, 2006).

4.1.3 Bayesian networks as classifiers

Bayesian networks can be used in the context of classification (Friedman et al., 1997). Specifically, we refer to a *Bayesian network classifier* as a BN over a set of random variables $\boldsymbol{X} = \{X_1, \ldots, X_N\} \cup Y$ where $X_1, \ldots, X_N$ are the attributes and Y is the class variable. The graph structure $\mathcal{G}$ is such that the class variable has no parents, $Pa(Y) = \emptyset$, and the attributes can have or not the class variable as parent. Therefore, the problem of learning a Bayesian network classifier can be rephrased as the problem of learning a general Bayesian network. In this context we can rewrite equation (4.1) to compute the most probable class $\hat{y}_c$ as follows:

$$\hat{y}_c = \underset{y_c \in Val(Y)}{\operatorname{argmax}} \left\{ P(Y = y_c) \prod_{X_n \in \boldsymbol{X}} P(X_n = x_i | Pa(X_n) = pa_u) \right\}. \tag{4.6}$$

The naïve Bayes classifier can be seen as a BN classifier, where each attribute X_n has the class variable as its unique parent, $Pa(X_n) = Y$. This classifier has a fixed structure depicted in Figure 4.1 (a), so no structural learning is required. The graph structure encodes the assumption that all the attributes are conditionally independent, given the value of the class. Although this independence assumption is quite restrictive, this classifier outperformed many sophisticated classifiers (Langley et al., 1992). Different extensions of this classifier have been introduced to relax this assumption. We mention the *tree augmented naïve Bayes classifier* (Friedman et al., 1997), which allows additional edges between attributes in order to capture some relations among them. Such relations are restricted to a tree structure as depicted in Figure 4.1 (b).

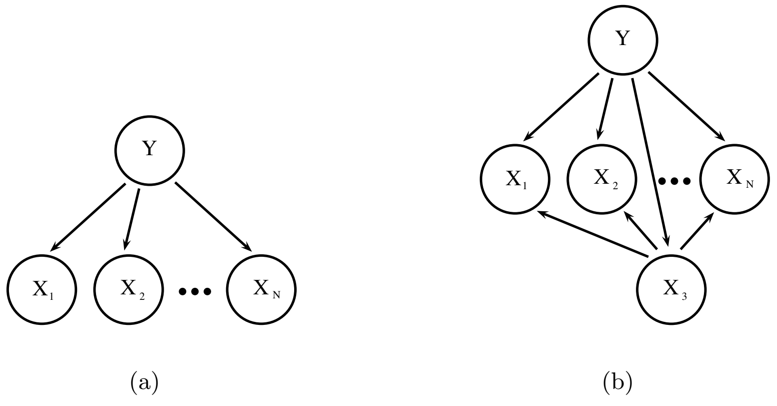

Figure 4.1: The graph structures of common Bayesian network classifiers: (a) naïve Bayes classifier and (b) tree augmented naïve Bayes classifier.

4.1.4 Dynamic Bayesian networks as classifiers

In the same way that BNs can be used for classification, DBNs can be used for *temporal classification*. In this context, we have that an observation is an input-output pair $\boldsymbol{d} = (\boldsymbol{x}^{(0:T)}, y)$, where the input $\boldsymbol{x}^{(0:T)} = (\boldsymbol{x}^{(0)}, \dots, \boldsymbol{x}^{(T)})$ is a sequence of observations of $\boldsymbol{X}^{(t)}$ at the t-th time step, while the output is the class expected to occur in the future (Murphy, 2002). Given a *dynamic Bayesian network classifier*, we can compute the most probable class $\hat{y}_c$ of a sequence $\boldsymbol{x}^{(0:T)}$ as follows:

$$\hat{y}_c = \underset{y_c \in Val(Y)}{\operatorname{argmax}} \left\{ P(Y = y_c) \prod_{t=1}^{T} \prod_{X_n \in \boldsymbol{X}} P(X_n^{(t)} = x_i^{(t)} | Pa(X_n^{(t-1)}) = pa_u^{(t-1)}) \right\}. \tag{4.7}$$

The DBN model $\mathcal{B}_2 = (\mathcal{B}_0, \mathcal{B}_{2T})$ of such classifier allow us to compactly represent the probability distribution over infinite sequences by means of an initial state distribution $\mathcal{B}_0$ and a transition model $\mathcal{B}_{2T}$ that specifies a conditional probability distribution between current time variables and next time step variables. A special case of dynamic Bayesian network classifiers is the *dynamic naïve Bayes classifier* (DBNC-NB). As its static counterpart, it relies on independence assumption among attributes. Figure 4.2 (a) shows the graph of an instance of this classifier where each variable depends on itself at previous time and intra-time relations are allowed. Figure 4.2 (b) shows the graph of an instance of this classifier where only inter-time relations are allowed.

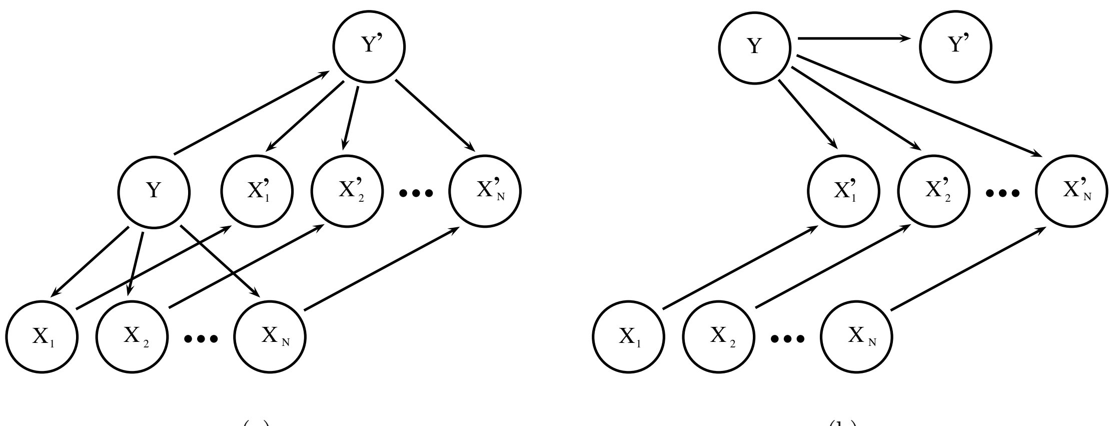

Figure 4.2: The graph structures of two instances of a dynamic naïve Bayes classifier where (a) intra-slice relations are allowed and (b) only inter-time relations are allowed.

4.2 Continuous time Bayesian network classifiers

The continuous time Bayesian network model has been exploited to perform temporal classification in which the attributes explicitly evolve in continuous time and not at fixed-length time step. In this context, we have that an observation is an input-output pair $\boldsymbol{d} = (\boldsymbol{\sigma}, y)$, where $\boldsymbol{\sigma}$ denotes a trajectory that consists of the values of attributes that are measured in continuous time, while the class y is expected to occur in the future.

4.2.1 Definitions

Continuous time Bayesian networks are translated into a class of supervised classification models, the class of continuous time Bayesian network classifiers.

Definition 4.1. *Continuous time Bayesian network classifier (CTBNC), (Stella and Amer, 2012). A continuous time Bayesian network classifier is a pair $\mathcal{C} = (\mathcal{N}, P(Y))$ where $\mathcal{N}$ is a CTBN model with attribute nodes $\boldsymbol{X} = \{X_1, \ldots, X_N\}$, class node Y with marginal probability $P(Y)$ on states $Val(Y) = \{y_1, \ldots, y_C\}$, and $\mathcal{G}$ is the graph, such that the following conditions hold: $\mathcal{G}$ is connected; $Pa(Y) = \emptyset$, the class variable Y is associated with a root node; Y is fully specified by $P(Y)$ and does not depend on time.*

From the previous definition it is possible to specify different types of continuous time Bayesian network classifiers based on the relations among the attribute nodes.

Definition 4.2. *Continuous time naïve Bayes (CTBNC-NB), (Stella and Amer, 2012). A continuous time naïve Bayes is a CTBNC $\mathcal{C}$ such that $Pa(X_n) = Y$, $\forall X_n \in \boldsymbol{X}$.*

Definition 4.3. *Continuous time tree augmented naïve Bayes (CTBNC-TANB), (Stella and Amer, 2012). A continuous time tree augmented naïve Bayes is a CTBNC $\mathcal{C}$ such that the following conditions hold: $Y \in Pa(X_n)$, $\forall X_n \in \boldsymbol{X}$ and the attribute nodes form a tree, i.e. $\exists\, j \in \{1, \ldots, N\} : |Pa(X_j)| = 1$, while for $i \neq j$, $i = 1, \ldots, N : |Pa(X_i)| = 2$.*

Definition 4.4. *Max-k continuous time Bayesian network classifier (CTBNC-Max-k), (Codecasa and Stella, 2014). A max-k continuous time Bayesian network classifier is a couple $(\mathcal{C}, k)$ where $\mathcal{C}$ is a CTBNC such that the number of parents for each attribute node is bounded by a positive integer k. Formally, the following condition holds: $|Pa(X_n)| \leq k$, $\forall X_n \in \boldsymbol{X}$ and $k > 0$.*

4.2.2 Learning

A continuous time Bayesian network classifier $\mathcal{C} = (\mathcal{N}, P(Y))$ can be learned on a training data set $\mathcal{D}$ of input-output pair $\boldsymbol{d} = (\boldsymbol{\sigma}, y)$ using the standard Bayesian learning framework. For continuous time Bayesian network classifiers we have that the model $\mathcal{C}$ consists of three components. The first is the marginal probability associated with the class node $P(Y)$. This marginal probability is independent from the classifier's structure $\mathcal{G}$ and it is not time-dependent. Given a prior probability on the class node, such as a uniform over classes, it can be updated by counting the number of examples of a given class in the available data set. The second is the structure $\mathcal{G}$, as shown in Figure 4.1. The third are the values of the parameters $\boldsymbol{q}_{\mathcal{G}}$ and $\boldsymbol{\theta}_{\mathcal{G}}$ associated with the structure $\mathcal{G}$.

When the graph structure is known, such as for the continuous time naïve Bayes classifier, the parameter learning of each entry of the intensity matrices is based on log-likelihood estimation as for the CTBN case shown in (3.19). When the graph structure is unknown, the dependencies among attributes can be learned using the score-based approach as for CTBNs presented by Nodelman et al. (2003). For example, the learning task for a continuous time tree augmented naïve Bayes can be accomplished evaluating the Bayesian score of different tree structures and searching the structure that has the highest score. We note that the search space over the tree structures can be done in polynomial time given a maximum number of possible parents per variable. This search can be easily performed enumerating each possible tree structure compliant with its definition.

It is noteworthy to mention that the learning goal of a CTBN can be different from that of a CTBNC. In the CTBN case we would like to describe (or generate) the entire data, i.e. we are interested in a *generative* learning. In contrast, in the CTBNC case, we would like to discriminate between different classes, i.e. we are interested in a *discriminative* learning. Generative methods usually maximize the log-likelihood or a score thereof, whereas discriminative methods focus on maximizing the conditional log-likelihood. In this regard, Codecasa and Stella (2014) introduced a conditional log-likelihood scoring function for structural learning of CTBNCs, and they shown that this scoring function combined with Bayesian parameter estimation outperforms the log-likelihood scoring function, in particular when the available data is limited.

4.2.3 Inference

A continuous time Bayesian network classifier computes the most probable class $\hat{y}_c$ of a fully observed trajectory $\boldsymbol{\sigma}$ as follows:

$$\hat{y}_c = \underset{y_c \in Val(Y)}{\operatorname{argmax}} \left\{ P(Y = y_c) P(\boldsymbol{\sigma} | Y = y_c) \right\}, \tag{4.8}$$

where $P(Y = y_c)$ represents the prior probability of the class y_c and $P(\boldsymbol{\sigma}|Y = y_c)$ is the probability of the fully observed trajectory given the class y_c. The latter probability can be decomposed by temporal intervals of the trajectory as follows:

$$P(\boldsymbol{\sigma}|Y = y_c) = \prod_{j=1}^{J} P(\boldsymbol{x}[\tau_{j-1} : \tau_j)|Y = y_c) P(\boldsymbol{x}[x'_n][\tau_j : \tau_{j+1})|\boldsymbol{x}[\tau_{j-1} : \tau_j), Y = y_c), \tag{4.9}$$

where $\tau_0 = 0, \ldots, \tau_{J+1} = T$ are the transition times in the interval $[0; T)$ for the trajectory. The term $P(\boldsymbol{x}[\tau_{j-1} : \tau_j)|Y = y_c)$ represents the probability that $\boldsymbol{X}$ stays in state $\boldsymbol{x}$ during the time interval $[\tau_{j-1}; \tau_j)$ given the class y_c, while $P(\boldsymbol{x}[x'_n][\tau_j : \tau_{j+1})|\boldsymbol{x}[\tau_{j-1} : \tau_j), Y = y_c)$ represents the probability of a transition of the variable X_n from value x_n to the value x'_n ($x_n \neq x'_n$) at time τ_j given the class y_c. This latter probability can be written as follows:

$$P(\boldsymbol{x}[x'_n][\tau_j : \tau_{j+1})|\boldsymbol{x}[\tau_{j-1} : \tau_j), Y = y_c) = \frac{q_{x_n, x'_n|pa_u}}{q_{x_n|pa_u}}, \tag{4.10}$$

where $q_{x_n, x'_n|pa_u}$ is the parameter associated with the transition of variable X_n from state x_n, in which it was during the interval $[\tau_{j-1}; \tau_j)$, to state x'_n, in which it will be during the interval $[\tau_j; \tau_{j+1})$, given the state pa_u of its parents $Pa(X_n)$ during the interval $[\tau_{j-1}; \tau_j)$, while $q_{x_n|pa_u}$ is the parameter associated with the variable $X_n = x_n$, in which it was during the interval $[\tau_{j-1}; \tau_j)$, given the state pa_u of its parents $Pa(X_n)$ during the same interval.

The term $P(\boldsymbol{x}[\tau_{j-1} : \tau_j)|Y = y_c)$ can be further specified for the variable X_n which transitions at time τ_j (i.e. $x_n \neq x'_n$) and for the variables $\boldsymbol{X} \setminus X_n$ that do not change their state at time τ_j (i.e. $x_n = x'_n$) as follows:

$$P(\boldsymbol{x}[\tau_{j-1} : \tau_j)|Y = y_c) = \begin{cases} \exp\left(-q_{x_n|pa_u}(\tau_j - \tau_{j-1})\right) & \text{if } x_n = x'_n, \\ q_{x_n|pa_u} \exp\left(-q_{x_n|pa_u}(\tau_j - \tau_{j-1})\right) & \text{if } x_n \neq x'_n. \end{cases} \tag{4.11}$$

Equations (4.10) and (4.11), when combined with (4.9), allow us to write:

$$P(\boldsymbol{\sigma}|Y = y_c) = \prod_{X_n \in \boldsymbol{X}} \prod_{x_n \neq x'_n} q_{x_n, x'_n|pa_u} \prod_{x_n} \exp\left(-q_{x_n|pa_u}(\tau_j - \tau_{j-1})\right). \tag{4.12}$$

We can compute the most probable class as in (4.8) using the equation (4.12). Thus, a continuous time Bayesian network classifier classifies a fully observed trajectory $\boldsymbol{\sigma}$ by selecting the most probable class $\hat{y}_c$ as follows:

$$\hat{y}_c = \underset{y_c \in Val(Y)}{\operatorname{argmax}} \left\{ P(Y = y_c) \prod_{j=1}^{J} \prod_{X_n \in \boldsymbol{X}} \prod_{x_n \neq x'_n} q_{x_n, x'_n | pa_u} \prod_{x_n} \exp(-q_{x_n | pa_u}(\tau_j - \tau_{j-1})) \right\}. \tag{4.13}$$

Given a continuous time Bayesian network classifier $\mathcal{C} = (\mathcal{N}, P(Y))$ consisting of N attribute nodes $\boldsymbol{X} = \{X_1, \ldots, X_N\}$, a class node Y such that $Val(Y) = \{y_1, \ldots, y_C\}$ and a fully observed trajectory $\boldsymbol{\sigma}$, Algorithm 4.1 computes the posterior probability and returns the most probable class (Villa and Stella, 2014). The *for* statement reported from line 1 to 3 computes the a priori probability for each class, while the core of the algorithm, from line 4 to 13, computes the logarithm of equation (4.13). The three *for* statements range over the C classes (from line 4 to 13), the J temporal intervals of the trajectory (from line 5 to 12) and the N attributes (from line 6 to 11). The most probable class $\hat{y}_c$ is computed by the argmax function in line 14.

Algorithm 4.1 CTBNC Inference

Require: a CTBNC $\mathcal{C} = (\mathcal{N}, P(Y))$ consisting of N attribute nodes, a class node Y such that $Val(Y) = \{y_1, \ldots, y_C\}$ and a fully observed trajectory $\boldsymbol{\sigma}$.

Ensure: the most probable class $\hat{y}_c$ for the fully observed trajectory $\boldsymbol{\sigma}$.

```
1:  for $c \leftarrow 1$ to $C$ do
2:      $lnp(y_c) \leftarrow \ln P(Y = y_c)$
3:  end for
4:  for $c \leftarrow 1$ to $C$ do
5:      for $j \leftarrow 1$ to $J$ do
6:          for $n \leftarrow 1$ to $N$ do
7:              $lnp(y_c) \leftarrow lnp(y_c) - q_{x_n|pa_u}(\tau_j - \tau_{j-1})$
8:              if $(x_n \neq x'_n)$ then
9:                  $lnp(y_c) \leftarrow lnp(y_c) + \ln\left(q_{x_n x'_n | pa(X_n)}\right)$
10:             end if
11:         end for
12:     end for
13: end for
14: $\hat{y}_c \leftarrow \operatorname{argmax}_{y_c \in Val(Y)}\{lnp(y_c)\}$
```

4.3 Learning from Big Data

Parameter and structural learning on continuous time Bayesian network classifiers are challenging tasks when dealing with Big Data. We describe an efficient scalable parallel algorithm introduced by Villa and Rossetti (2014) for parameter and structural learning in the case of complete data using the MapReduce framework.

4.3.1 Introduction

The learning algorithms presented so far have a main limitation: when the data size grows the learning time becomes unacceptable. To overcome this limitation, several parallelization alternatives are available. One approach is to use a system with multiple central processing units (CPUs) and a shared-memory or a distributed-memory cluster made up of smaller shared-memory systems. This method requires vast resources and specialized parallel programming expertise. A recent approach consists of using graphics hardware because the performance increases more rapidly than that of CPUs. Graphics processing units (GPUs) are designed with a high parallel architecture due to the intrinsic parallel nature of graphics computations. For this reason GPUs are transformed into parallel computing devices for a wide range of applications (Owens et al., 2007).

A different approach is to use the *MapReduce* framework (Dean and Ghemawat, 2004). This framework offers the possibility to implement a parallel application without focusing on the details of data distribution, load balancing and fault tolerance. MapReduce programs are expressed as sequences of map and reduce operations performed by the *mapper* and the *reducer* respectively. A mapper takes as input parts of the data set, applies a function (e.g. a partition of the data) and produces as output key-value pairs, while a reducer takes as input a list indexed by a key of all corresponding values and applies a reduction function (e.g. aggregation or sum operations) on the values. Once a reducer has terminated its work, the next set of mappers can be scheduled. Since a reducer must wait for all mapper outputs, the synchronization is implicit in the reducer operation, while fault tolerance is achieved by rescheduling mappers that time out. A free implementation of MapReduce is *Apache Hadoop*, which allows the distributed processing of large data sets across clusters of computers using simple programming models (White, 2009).

4.3.2 MapReduce algorithm design

The design of the learning algorithm is based on some basic patterns used in MapReduce (Lin and Dyer, 2010). The main idea is to exploit the peculiarities of the continuous time Bayesian network classifiers presented in the previous section to parallelize the operations of structural and parameter learning. Through appropriate structuring of keys and values it is possible to use the MapReduce execution framework to bring together all the pieces of data required to perform the learning computation. In our case, the key-value pairs are constructed in order to encode all the information relevant for the description of the classifier, namely the marginal probability of the class, the structure and the parameters associated with the structure. Two types of key-value pairs are used: a key with the identifier of the class node and a value containing the structure for the computation of the marginal probability, and a key with the identifier of the node given its parents and a value containing the structure for the calculation of the sufficient statistics.

The *strips approach* introduced by Lin (2008) is used to generate the output keys of the mapper, instead of emitting intermediate key-value pairs for each interval; this information is first stored in a map denoted as $paMap$. The mapper emits key-value pairs with text as keys and corresponding maps as values. The MapReduce execution framework guarantees that all associative arrays with the same key will be brought together in the reduce step. This last phase aggregates the results by computing the sufficient statistics and the estimation of the parameters of the conditional intensity matrix and of the Bayesian score. It is possible to further increase the performances by means of the use of *combiners*. This approach assumes that the map $paMap$ fits into memory; such condition is reasonable since the number of transitions of each variable, given the instantiation of its parents, is generally bounded.

Chu et al. (2006) demonstrated that when an algorithm does sums over the data, the calculations can be easily distributed over multiple processing units. The key point is to divide the data into many pieces, give each core its part of the data, make calculations and aggregate the results at the end. This is called *summation form* and can be applied to different machine learning algorithms, such as in the field of Bayesian networks. Basak et al. (2012) applied the distributed computing of MapReduce to Bayesian parameter learning both for complete and incomplete data (via the expectation maximization algorithm).

4.3.3 Map, reduce and auxiliary functions

The *Map* function shown in Algorithm 4.2 counts the transitions and the relative amount of time in the fully observed trajectory of each variable X_n given the instantiation pa_u of its parents $Pa(X_n)$. In the case of structural learning, every possible combination of parents for each node must be computed subject to the structure constraints, while in the case of parameter learning the structure $\mathcal{G}$ is given as input. The key-value pairs for the class probability are constructed as textual keys, denoted by $CLASS$, and values containing the id of trajectory and the relative class. The key-value pairs for the parameters are constructed as textual keys encoding the variable name and the names of its parents, i.e. $(X_n|Pa(X_n))$, and values containing a two level association of an id corresponding to the instantiation of parents, another id corresponding to a transition and the count and the elapsed time of that transition, i.e. $< pa_u, < (x_i, x_j), (count, time) >>$.

Algorithm 4.2 Map

```
Require: input-output pair $(id, \boldsymbol{\sigma}, y)$ and structure $\mathcal{G}$ (optional).
Ensure: key-value pairs in the forms: if the key is denoted by $CLASS$, then the value is
    $< id, y >$, while if the key is $(X_n|Pa(X_n))$, then the value is the map $paMap$.
 1: emit $< CLASS, < id, y >>$
 2: for $n \leftarrow 1$ to $N$ do
 3:   for $p \leftarrow 1$ to $N$ do
 4:     $Pa(X_n) \leftarrow (Y, X_p)$
 5:     if $(n = p)$ then
 6:       $Pa(X_n) \leftarrow (Y, \emptyset)$
 7:     end if
 8:     if (AnalyzeParents($Pa(X_n)$)) then
 9:       $paMap \leftarrow Map()$
10:       for $j \leftarrow 2$ to $J$ do
11:         $paMap \leftarrow$ IncrementT($paMap$, $pa(X_n)$, $(x_i, x_j), \tau_j - \tau_{j-1}$)
12:         $paMap \leftarrow$ IncrementM($paMap$, $pa(X_n)$, $(x_i, x_j)$, 1)
13:       end for
14:       emit $< (X_n|Pa(X_n)), paMap >$
15:     end if
16:   end for
17: end for
```

The *Reduce* function shown in Algorithm 4.3 provides the basic elements for the description of the classifier, namely the class probability and the conditional intensity matrices. This function takes as input key-value pairs where the keys can be $CLASS$ or $(X_n|Pa(X_n))$, and the values are collections of data computed by mappers with the same key, while it produces as output key-value pairs for the model description. The values are merged into a single map named *paMap*. If the key is $CLASS$, then the marginal probability of the class node is computed, otherwise the Bayesian score and the CIM are calculated from aggregation of the sufficient statistics.

Algorithm 4.3 Reduce

```
Require: a key and a list of maps $\{paMap_1, \dots, paMap_S\}$, $\alpha$ and $\tau$ hyperparameters.
Ensure: class probability, conditional intensity matrix and Bayesian score.
 1: for $s \leftarrow 1$ to $S$ do
 2:   $paMap \leftarrow$ Merge($paMap$, $paMap_s$)
 3: end for
 4: if ($key = CLASS$) then
 5:   $marg \leftarrow \emptyset$
 6:   for each $y_c \in$ Values($paMap$) do
 7:     $marg(y_c) \leftarrow marg(y_c) + 1$
 8:   end for
 9:   emit $< CLASS, marg >$
10: else
11:   $bs \leftarrow 0$
12:   for each $pa_u \in$ Keys($paMap$) do
13:     $trMap \leftarrow paMap$ [ $pa_u$ ]
14:     $T \leftarrow \emptyset, M \leftarrow \emptyset$
15:     for each $(x_i, x_j) \in$ Keys($trMap$) do
16:       $T[x_i] \leftarrow T[x_i]$ + GetT($trMap$ [ $(x_i, x_j)$ ])
17:       $M[x_i, x_j] \leftarrow M[x_i, x_j]$ + GetM($trMap$ [ $(x_i, x_j)$ ])
18:     end for
19:     $im \leftarrow$ ComputeIM($T$, $M$, $\alpha$, $\tau$)
20:     $bs \leftarrow bs$ + ComputeBS($T$, $M$, $\alpha$, $\tau$)
21:     emit $< CIM, < (key, pa_u), im >>$
22:   end for
23:   emit $< BS, < key, bs >>$
24: end if
```

The Map function relies on *auxiliary* functions in order to compute its output; the main functions are *ComputeIM* and *ComputeBS*. The first function shown in Algorithm 4.4 computes the intensity matrix $\boldsymbol{Q}_{X_n|pa_u}$ of the variable X_n given an instantiation pa_u of its parents $Pa(X_n)$ by means of counting maps according to the formulas reported in equation (3.19). The second function shown in Algorithm 4.5 computes the Bayesian score of the variable X_n given an instantiation pa_u of its parents $Pa(X_n)$ according to equation (3.28). Note that the Bayesian score is computed for every parent configuration; the task of the main function (called *driver*) is to choose the structure that maximizes the Bayesian score subject to the model constraints.

Algorithm 4.4 ComputeIM

```
Require: maps containing the counting values $T$ and $M$ of the node $X_n$ when $Pa(X_n) =$
    $pa_u$, $\alpha$ and $\tau$ hyperparameters.
Ensure: the intensity matrix $\boldsymbol{Q}_{X_n|pa_u}$ for the node $X_n$ when $Pa(X_n) = pa_u$.
 1: for each $(x_i,\, x_j) \in$ Transitions$(X_n)$ do
 2:   if $(x_i \neq x_j)$ then
 3:     $q_{x_i} \leftarrow \frac{M[x_i]\,+\,\alpha_{x_i}}{T[x_i]\,+\,\tau_{x_i}}$
 4:   else
 5:     $q_{x_i,x_j} \leftarrow \frac{M[x_i,x_j]\,+\,\alpha_{x_i,x_j}}{T[x_i]\,+\,\tau_{x_i}}$
 6:   end if
 7: end for
```

Algorithm 4.5 ComputeBS

```
Require: maps containing the counting values $T$ and $M$ of the node $X_n$ when $Pa(X_n) =$
    $pa_u$, $\alpha$ and $\tau$ hyperparameters.
Ensure: Bayesian score $bs$ of the node $X_n$ when $Pa(X_n) = pa_u$.
 1: $bs \leftarrow 0$
 2: for each $(x_i,\, x_j) \in$ Transitions$(X_n)$ do
 3:   if $(x_i \neq x_j)$ then
 4:     $bs \leftarrow bs + \ln\Gamma(\alpha_{x_i,x_j} + M[x_i, x_j]) - \ln\Gamma(\alpha_{x_i,x_j})$
 5:   else
 6:     $bs \leftarrow bs + \ln\Gamma(\alpha_{x_i}) - \ln\Gamma(\alpha_{x_i} + M[x_i])$
 7:     $bs \leftarrow bs + \ln\Gamma(\alpha_{x_i} + M[x_i] + 1) + (\alpha_{x_i} + 1) \times \ln(\tau_{x_i})$
 8:     $bs \leftarrow bs - \ln\Gamma(\alpha_{x_i} + 1) - (\alpha_{x_i} + M[x_i] + 1) \times \ln(\tau_{x_i} + T[x_i])$
 9:   end if
10: end for
```

4.3.4 Numerical experiments

The proposed algorithm has been implemented in Java in the Apache Hadoop framework and its correctness has been tested by comparing the results generated by MapReduce against a sequential version (Stella and Amer, 2012). Moreover, the software performances have been tested for the parameter learning of a continuous time naïve Bayes classifier and for the structural learning of a continuous time tree augmented naïve Bayes. Three types of experiments have been performed changing the data set size, the number of Hadoop nodes and the number of attributes. The data set was composed of a text file containing fully observed trajectories; these trajectories concern transaction data of the foreign exchange market (Villa and Stella, 2014). The tests were performed using *M1 Large* instances of *Amazon EMR*, while the training and output data were stored in *Amazon S3*.

In the first experiment, the performance of the MapReduce algorithm has been measured in the case of parameter learning of a continuous time naïve Bayes classifier. This algorithm used 1 Master instance and 5 Core instances against the sequential algorithm using only one instance. The data set consisted of 1 binary class variable and 6 binary attributes, while the training set size has been varied from 25K to 200K trajectories with steps of 25K. Figure 4.3 (a) illustrates the learning time compared to the data set size. This picture shows the time taken by the algorithms and the regression lines which interpolate the data points. Intuitively, the increase of the size of the training samples leads to increased training time because the MapReduce implementation has a computational overhead, which with few data led to bad performance. Figure 4.3 (b) illustrates the speedup between the sequential and MapReduce algorithms (real) and the speedup between the two regression lines (theoretical). As the data size increases, the speedup grows quickly at the beginning, while it becomes more stable when the data size is already big enough (e.g. with 200K trajectories we have a speedup of about 3).

In the second experiment, the number of Hadoop nodes has been varied to assess the parallel performance of the MapReduce algorithm in the case of parameter learning using the same training set of 200K trajectories. Figure 4.3 (c) shows the changes in the training time using different numbers of Hadoop nodes from 5 to 25 with steps of 5 nodes. As expected, increasing the number of Hadoop nodes significantly reduces the learning time, even if this reduction is not equal to the ratio between the number of nodes.

In the third experiment, the performance of the MapReduce algorithm has been measured in the case of structural learning of a continuous time tree augmented naïve Bayes classifier, varying the number of attributes from 2 to 10 with steps of 2 and using a training set of 100K trajectories. This algorithm used 1 Master instance and 25 Core instances against the sequential one using only one instance. Figure 4.3 (d) illustrates the learning time compared to the number of attributes. In both cases, the trend is quadratic because every possible parent set, given a variable, was analyzed, but the quadratic coefficient for the MapReduce algorithm is only 67.18 against 420.18 of the sequential one.

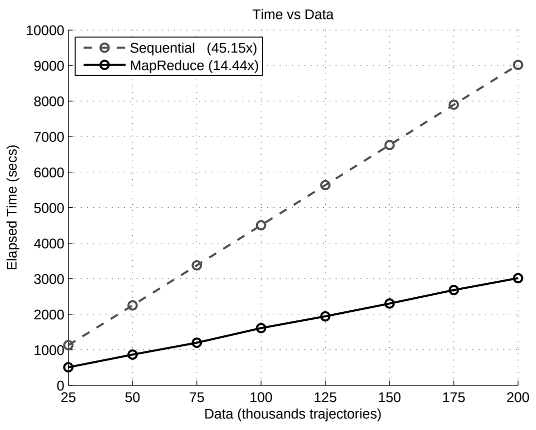

(a)

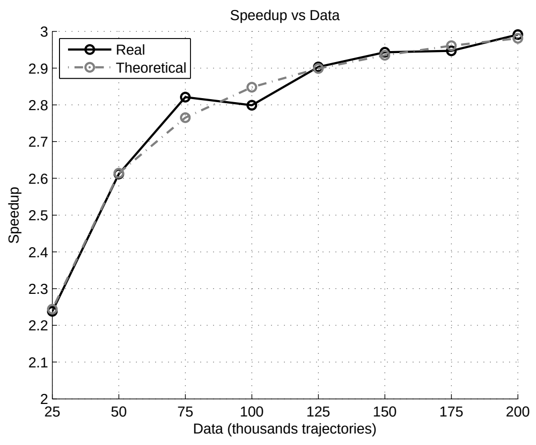

(b)

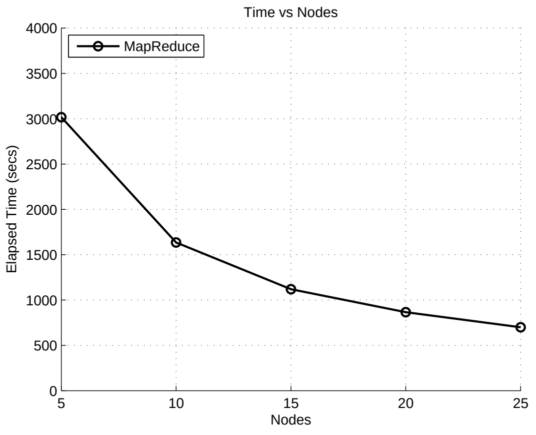

(c)

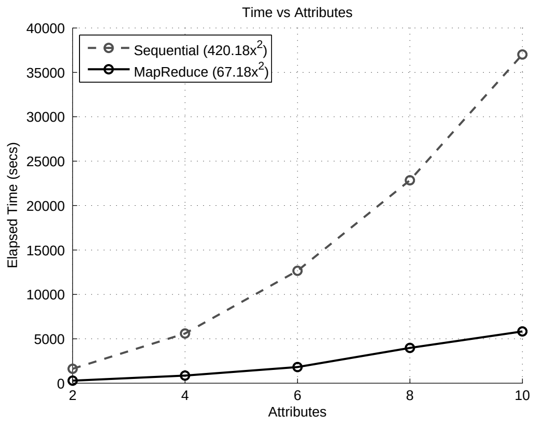

(d)

Figure 4.3: Numerical experiments for MapReduce learning algorithm: (a) parameter learning time versus data set size, (b) parameter learning speedup versus data set size, (c) parameter learning time versus number of Hadoop nodes and (d) structural learning time versus number of attributes.

4.4 The FX forecasting problem

We present how it is possible to exploit continuous time Bayesian network classifiers for the prediction of foreign exchange (FX) spot rates introduced by Villa and Stella (2014). The performance of an instance of these classifiers is analyzed and compared to that of the dynamic Bayesian network by using real tick by tick FX rates. The achieved results based on different metrics show clearly a predictive power of these models for FX rates at high frequencies. These results also show that the proposed classifier is more effective and more efficient than dynamic Bayesian network classifier.

4.4.1 Financial context

High frequency financial data, made available by electronic order driven markets, has started a revolution on data processing and statistical modeling. This revolution forces quantitative analysts to cope with challenging theoretical and computational problems. Indeed, high frequency financial data has to take into account micro structure effects which cannot be appreciated when using longer time intervals (Treleaven et al., 2013).

We focus on high frequency transaction data from the FX market that is the largest and most liquid financial market. Its rapid growth over the last few years has been facilitated by the wider use of electronic trading at both levels, i.e. broker-dealer markets and customer markets deployed through on line trading platforms. The FX market is affected by many correlated economical, political and even psychological factors that make its forecasting a hard task. Researchers and practitioners have been striving for an explanation of the movement of exchange rates. It has long been known that structural models fail to predict exchange rates at short term horizons (Chinn and Meese, 1995; Kilian and Taylor, 2003).

The basic question to be answered is whether it is possible or not to forecast the behavior of an economic variable over a short time interval. The *efficient market hypothesis* (EMH), a fundamental pillar of modern economics (Fama, 1965), states that forecasting is not possible. The weak form of this hypothesis asserts that the asset price reflects all of the information that can be obtained from its history. Accordingly to the EMH, the asset price follows a random walk, and thus the best prediction of the future asset price is given by its current price. Thus, the movement of the price of an asset is unpredictable.

A common myth of traders is that there is a certain predictability of market dynamics. Many efforts have been devoted to proving or disproving the EMH with several works rejecting it with specific reference to intraday data. Zhang (1999) exploited conditional entropy to show that even the most competitive markets are not strictly efficient; Baviera et al. (2000) rejected the random walk hypothesis for high frequency FX returns and proposed a Markovian model which reproduces the available information of the financial series; Renner et al. (2001) found evidence of Markov properties for high frequency exchange rate data; Baviera et al. (2002) found anti-persistent Markov behavior of log-price fluctuations in high frequency FX rates, which in principle allows the possibility of a statistical forecast; Ohira et al. (2002) found that there is a rather particular conditional probability structure in high frequency FX data; Tanaka-Yamawaki (2003) observed stability of a Markovian structure in high frequency FX data; recently, Shmilovici et al. (2009) tested the EMH using a variable order Markov model for twelve pairs of intraday currency exchange rates for one year series with different time granularity. The authors found that intraday currency exchange rates are predictable above the random guess. These empirical evidences reveal that some predictability of high frequency FX rates exists.

The specialized literature describes FX forecasting techniques based on different assumptions and methods. Traditional parametric forecasting methods, such as auto regressive conditional heteroskedastic models and their extensions, were used to capture the salient features of the exchange rate volatility (Vilasuso, 2002). Recent developments in artificial intelligence and machine learning techniques, together with a continuously increasing availability of computational power, have allowed nonparametric models to be applied to FX forecasting. The techniques used in the FX rates forecasting range from artificial neural networks (Yao and Tan, 2000; Leung et al., 2000; Yu et al., 2007), support vector machines (Kamruzzaman et al., 2003), to genetic algorithms (Dempster and Jones, 2001). In the recent literature, hybrid models have also been proposed. Ince and Trafalis (2006) combined parametric and nonparametric techniques to achieve better performance for daily exchange rate forecasting. Gradojevic (2007) combined artificial neural networks and fuzzy logic controllers to obtain the optimal daily currency trading rules. Kablan and Ng (2011) introduced an adaptive neuro-fuzzy inference system for financial trading which learns to predict FX price movements of tick by tick data.

4.4.2 Proposed model

Prediction of foreign exchange rates is addressed as a binary classification problem in which the class is expected to occur in the future, the time flows continuously and the classification decision must be made at any point in time using trained continuous time naïve Bayes classifiers. Our model leverages on an important characteristic of high frequency data: transactions take place irregularly over time. Indeed, the duration between successive trades reflects the intensity of the trading activity (Hautsch, 2004). This characteristic plays a central role when developing continuous time models, as opposed to discrete time models based on fixed time steps.

Specifically, our task consists of predicting if a trajectory, a sequence of FX mid price values, will result in an up movement of the FX spot rate by a fixed amount of υ *pips* (price interest point, i.e. 10^{-4} of an exchange rate) or not. Therefore, the class is a binary variable Y, where $Y = 1$ if the FX spot rate shows an up movement of υ pips and $Y = 2$ otherwise. The attributes used by the classifiers have been selected by exploiting basic concepts of digital signal processing (Proakis and Manolakis, 2006). The moving average technique for smoothing short-term price variation has been used. Moving average involves the computation of the mean value of the past mid price as follows:

$$MA_t^w = \frac{1}{w} \sum_{i=0}^{w-1} p_{t-i}, \tag{4.14}$$

where w represents the length of the moving average window, while p_{t-i} is the mid price at time $t - i$. Although it is possible to associate different weights to different past prices, a simple moving average, assigning the same weight to different past prices, was used. Different moving averages were used to compute a set of moving average triggers. These triggers constitute the attributes of the classifier. A moving average trigger is defined as:

$$X_{w_1,w_2} = \begin{cases} 1 & \text{if } MA_t^{w_1} > MA_t^{w_2}, \\ 2 & \text{if } MA_t^{w_1} \leq MA_t^{w_2}. \end{cases} \tag{4.15}$$

To visualize the concept, an up movement of the mid price for the EUR/USD spot rate is depicted in Figure 4.4 (a), while the smoothed movement obtained through two moving averages with $w_1 = 40$ and $w_2 = 20$ together with their relative trigger $X_{40,20}$ are shown in Figure 4.4 (b).

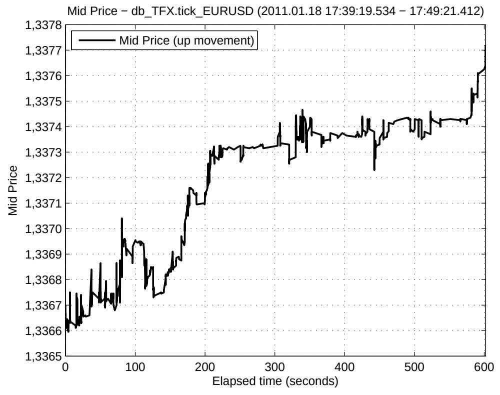

(a)

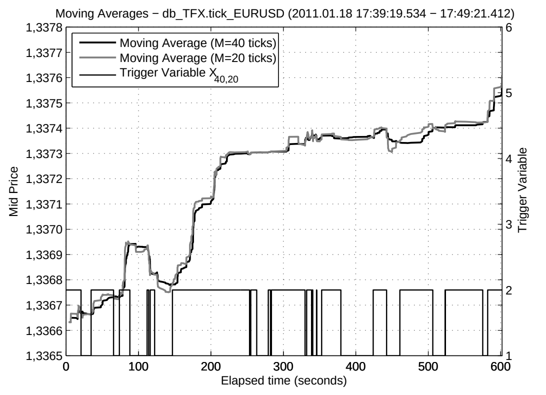

(b)

Figure 4.4: From raw data to attributes: (a) mid price up movement of $\upsilon = 10$ pips of the EUR/USD spot rate and (b) smoothed movement obtained by two moving averages (left axis) and their trigger (right axis).

Preliminary experiments were performed to select the set of moving average triggers. To clarify this selection, we let $\mathcal{W} = \{w_1, \ldots, w_W\}$ be a set of moving averages of window length $w_1, \ldots, w_W$, while $\boldsymbol{X}$ is a set of triggers X_{w_i,w_j} with $w_i, w_j \in \mathcal{W}$ and $w_i > w_j$, e.g. if $\mathcal{W} = \{80, 60, 40, 20\}$, then $\boldsymbol{X} = \{X_{80,60}, X_{80,40}, X_{80,20}, X_{60,40}, X_{60,20}, X_{40,20}\}$. The temporal evolutions of the triggers constitute the input of the classifier, see Figure 4.5 (a), while the output is the class probability computed by Algorithm 4.1, see Figure 4.5 (b).

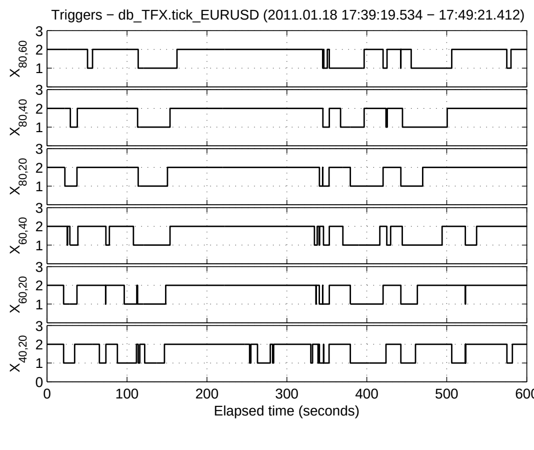

(a)

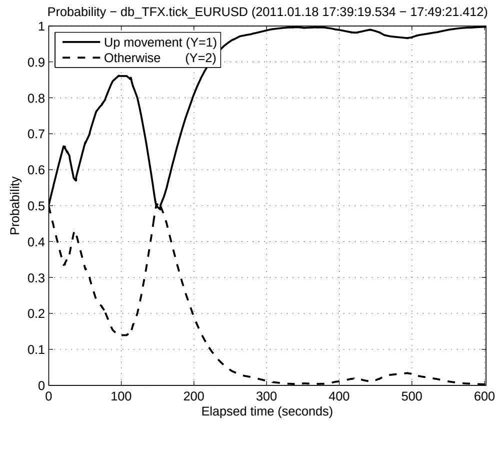

(b)

Figure 4.5: Input and output of the classifier: (a) temporal evolutions of six trigger variables (input) and (b) temporal evolution of the class probability computed by continuous time naïve Bayes classifiers according to Algorithm 4.1 (output).

4.4.3 Benchmarking

The dynamic naïve Bayes classifier was used as benchmark, where the parameter learning task has been performed with the algorithm described by Murphy (2002), while inference has been performed by using the BK algorithm introduced by Boyen and Koller (1998).

Figure 4.6 shows the evolution of the posterior probability associated with the class variable Y (up movement of $\upsilon = 10$ pips) for the EUR/USD spot rate computed by the dynamic classifier. Note that the continuous time classifier allows to obtain the posterior probability of the class variable at each point in time; conversely, the same does not occur for the dynamic classifier, which provides probability values at discrete time points (Δt) computed via the approximate inference algorithm. It is important to note that, for large values of the time slice Δt, the dynamic classifier simply cannot capture the transition dynamics accurately enough to converge to competitive performance.

Villa and Stella (2014) compared the computational effort required for learning and inference with respect to the number of trajectories and they concluded that the continuous time classifier is very efficient versus the dynamic classifier. In fact, the time required for learning the continuous time classifier with 1,000 trajectories is 8 times less than that required for a dynamic classifier with $\Delta t = 60$ secs, while the time required for inference is 182 times less then that required by its discrete counterpart with $\Delta t = 10$ secs.

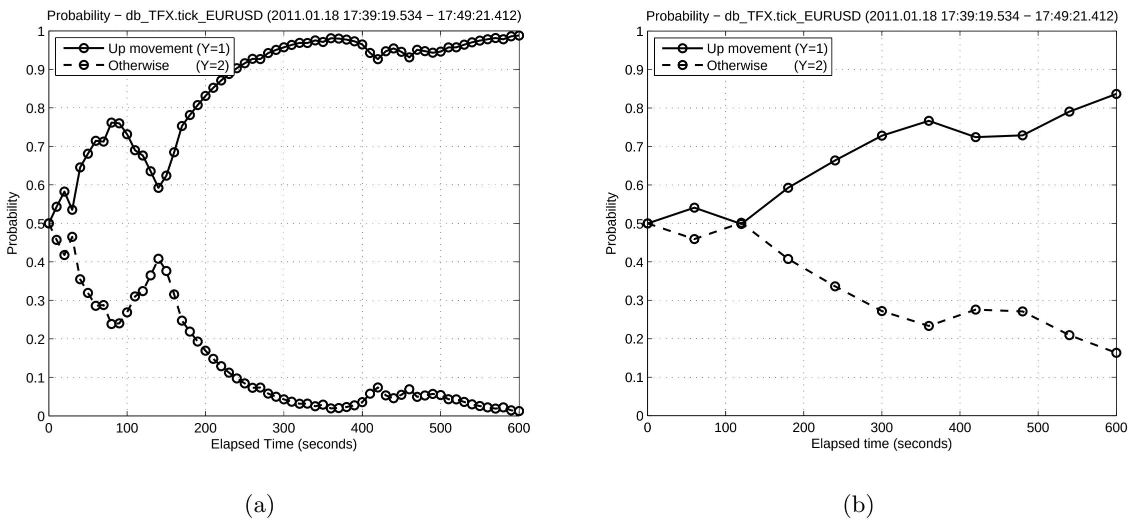

Figure 4.6: Class probability evolutions of a mid price up movement of $\upsilon = 10$ pips using trained dynamic naïve Bayes classifiers with (a) $\Delta t = 10$ secs and (b) $\Delta t = 60$ secs.

4.4.4 Numerical experiments

Numerical experiments were performed by comparing the performances of the continuous time naïve Bayes classifier versus the dynamic naïve Bayes classifier. The database used for these experiments is composed of high frequency transactions coming from three FX trading platforms publicly available over the Internet, denoted as TFX, DKY and GCL. The data set corresponding to each data source is composed of tick by tick bid-ask prices, spanning from January 1st, 2011 to December 30th, 2011 (260 trading days), of three commonly traded currency pairs: EUR/USD, GBP/USD and EUR/CHF. The entire database amounts to 250,346,963 bid-ask observations. Time granularity of TFX and DKY data sets equals 1 millisecond, while the time granularity of the GCL equals 1 second. Furthermore, one year of tick by tick data, generated from a Gaussian random walk (GRW) model, was added to the database for comparison purposes (BMK).

Preliminary experiments were performed in order to select the configuration of pips and moving averages $\{\upsilon, \mathcal{W}\}$ to be used for the next experiments. This selection was based on moving averages most commonly used by traders. Performance values achieved by continuous time and dynamic classifiers for five configurations are depicted in Figure 4.7. Accuracy values are computed by training a classifier on 1,000 contiguous trajectories and by subsequently testing it on the following 1,000 contiguous trajectories, i.e. by using the rolling window schema, on the entire TFX EUR/USD data set.

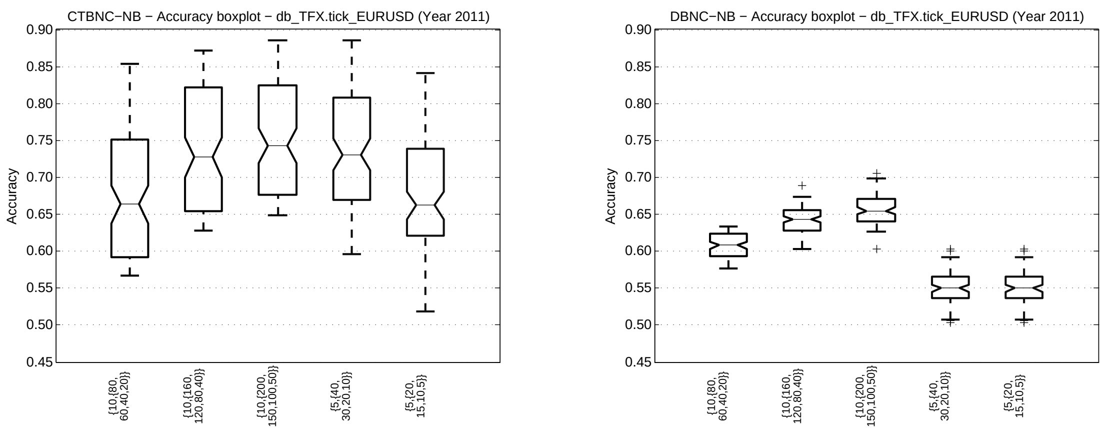

(a) (b)

Figure 4.7: Accuracy comparison across five configurations for the TFX EUR/USD data set for (a) continuous time and (b) dynamic naïve Bayes classifier with $\Delta t = 60$ secs.

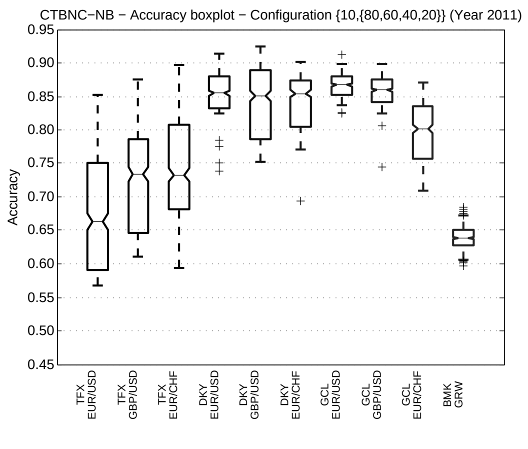

(a)

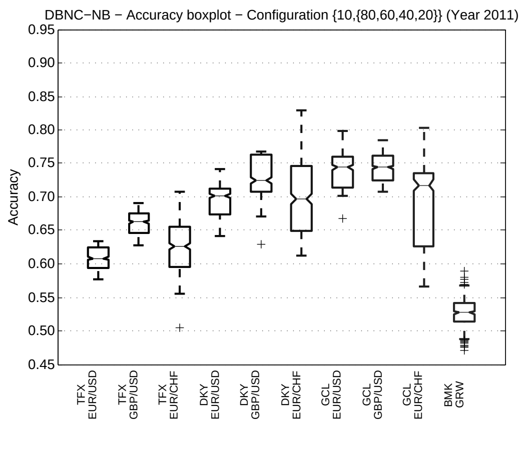

(b)

Figure 4.8: Accuracy comparison across ten data sets of FX spot rates for (a) continuous time and (b) dynamic naïve Bayes classifier with $\Delta t = 60$ secs.

The results obtained from the preliminary experiments suggested the configuration $\{10, \{80, 60, 40, 20\}\}$ to be further studied for performance analysis using different data sets and currency pairs. The first type of performance analysis is related to accuracy. It has been accomplished by using the rolling windows schema used for the preliminary experiments. Multiple rounds have been performed by using different contiguous partitions of the data set. Validation results, averaged over multiple rounds, are summarized in Figure 4.8 by means of box-plots. The empirical findings which emerge from this analysis can be summarized as follows. Firstly, the accuracy values achieved by continuous time and dynamic classifiers are well above the performance value achieved by random guess. Secondly, the accuracy values achieved by the continuous time classifier are greater than the accuracy values achieved by the dynamic classifier on all data sets. Thirdly, the dispersion of the accuracy achieved by the continuous time classifier is greater than the dispersion of the accuracy achieved by the dynamic classifier. This effect could be due to the smoothing effect induced by the time discretization process associated with DBNs.

Performance analysis has been extended through the inspection of the confusion matrices for both classes. This analysis allowed to discover that the performance values of precision and recall achieved by the continuous time classifier are better than those achieved by the dynamic classifier for all data sets. Moreover, the AUC values are all above the random guess for both classifiers.

The ROC curves associated with continuous time and dynamic classifier have been constructed when predicting the class $Y = 1$ (up movement of 10 pips) for the EUR/USD data sets; these curves are depicted in Figure 4.9. This picture shows the fraction of true up movements out of the total number of up movements (i.e. true positive rate) against the fraction of false up movements out of the total number of down movements (i.e. false positive rate) for different probability thresholds. The ROC curves have been computed by vertical averaging, i.e. by taking vertical samples of the ROC curves for fixed false positive rates and by averaging the corresponding true positive rates, as suggested by Fawcett (2006). The ROC curves remark the above random predictions for both classifiers with some differences within classifiers and data sets.

It is important to note that the high values of accuracy reached do not imply that trading profitability has been achieved. For this purpose we highlight at least two relevant aspects. Firstly, the issue of early classification and the study of the trade-off between earliness and accuracy should be considered, see Xing et al. (2009, 2010). Secondly, a dynamic decision strategy which generates trading signals based on the probability evolutions should be designed, such as in Bertsimas et al. (2003).

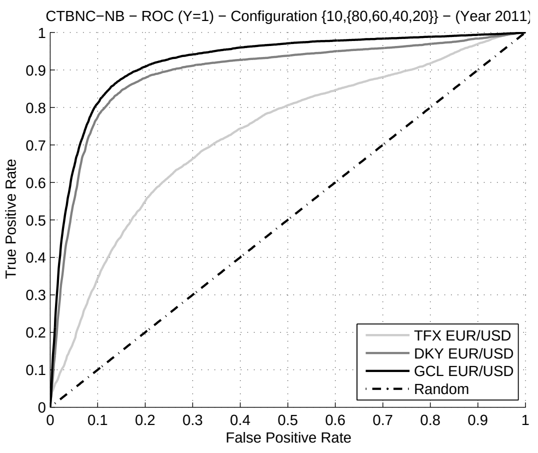

(a)

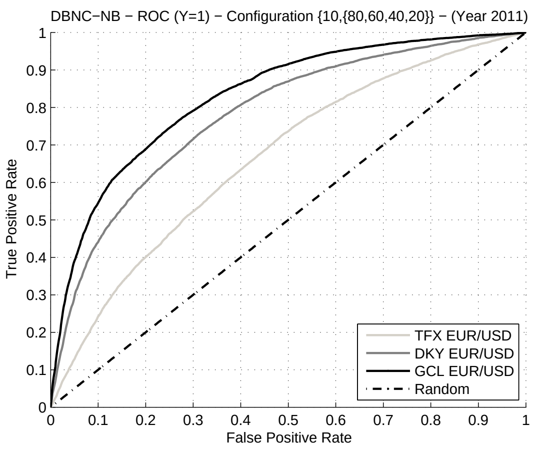

(b)

Figure 4.9: ROC curves using the configuration $\{10, \{80, 60, 40, 20\}\}$ for EUR/USD data sets associated with (a) continuous time naïve Bayes classifier and (b) dynamic naïve Bayes classifier with $\Delta t = 60$ secs.

4.5 Discussion

After a brief introduction about the basic concepts of classification, we have presented the continuous time Bayesian network classifiers and addressed the learning and inference tasks in the case of complete data. We have discussed a MapReduce algorithm for learning in the context of Big Data. Different experiments have shown that this algorithm scales well in the distributed processing environment. The performances can be improved if the algorithms were executed on a huge amount of data using many computational nodes. The advantage of MapReduce depends not only on the size of the input data, but also on the structure of the graph and on the number of states of the variables. In fact, it is not necessary to maintain the counting map in memory, which can be critical in large networks with many states. Furthermore, the algorithm we presented provides a base case for the extension of Big Data learning of continuous time Bayesian networks in both complete and incomplete data. The Big Data phenomenon is well known in finance. In recent years, we have seen a rapid growth of high frequency data as a result of the advancements in computational and mass storage technology. This has led to a high demand of new approaches to data processing and statistical analysis. In the last part of this chapter, we have presented a straightforward application of these classifiers to the FX forecasting problem to natively deal with unevenly spaced time data, i.e. the main characteristic of high frequency data. Extensive experimental tests have shown a strong predictive power of these models and a higher efficiency compared to dynamic Bayesian network classifiers.

Chapter 5

Non-stationary continuous time Bayesian networks

Continuous time Bayesian networks have been extended to the structural non-stationary class of models where the underlying data generating processes are non homogeneous. We start this chapter by discussing the reasons for non-stationary modeling and the common approaches developed in the literature. We continue introducing the definition of non-stationary continuous time Bayesian networks and their structural learning framework. We move on to describe the structural learning algorithms in three different settings based on the available knowledge. We finish by presenting numerical experiments performed to evaluate the correct reconstruction of the graphs sequence provided by these algorithms.

5.1 Stationary versus non-stationary modeling

The identification of relationships and statistical dependencies between components in multivariate time-series concerns many research domains such as biology, finance, traffic engineering and neurology, to mention just a few areas. In biology, for example, it is clear that knowing the gene regulatory network allows to understand complex biological mechanisms ruling the cell. In such a context, Bayesian networks (Friedman et al., 2000; Segal et al., 2005), dynamic Bayesian networks (Zou and Conzen, 2005; Vinh et al., 2012) and continuous time Bayesian networks (Acerbi and Stella, 2014) have been used to reconstruct transcriptional regulatory networks from gene expression data.

While stationarity is a reasonable assumption in many situations, there are cases where this is no longer acceptable. Indeed, in the last few years, researchers from different disciplines have started to be interested in representing relationships and dependencies which change over time. In particular, they have been interested in analyzing the temporal evolution of genetic networks (Ahmed and Xing, 2009; Lèbre et al., 2010), neural information flow networks (Smith et al., 2006) and dependence structure among financial markets during the global financial crisis (Durante and Dunson, 2014). While there have been various efforts to adapt Bayesian networks (Nielsen and Nielsen, 2008) and undirected graphical models (Xuan and Murphy, 2007) to non-stationary domains, relaxing the non homogeneity assumption in dynamic Bayesian networks has become popular in recent years. Specifically, structural learning of dynamic Bayesian networks has been proposed as a principled method for identifying the conditional independence structure in multivariate time-series data (Robinson and Hartemink, 2010).

5.1.1 Structural and parameter non-stationary models

According to Robinson and Hartemink (2010), there are two possible types of models that learn non-stationarities: *structural non-stationary* and *parameter non-stationary.*

Structural non-stationary approaches explicitly model the presence of statistical dependencies between variables and allow them to appear and disappear over time, e.g. they construct directed or undirected networks whose edges change over time. Some examples are *temporal exponential random graph model*, where a structural evolutionary process is modeled with a set of features between adjacent network structures (Hanneke and Xing, 2006) and *non-stationary dynamic Bayesian network*, an extension of the DBN model where the structure is evolving over time (Robinson and Hartemink, 2009).

Modeling short time-series segments with separate networks could lead to inflated inference uncertainty. Parameter non-stationary approaches try to overcome this issue by modeling the evolution of parameters over time while keeping the structure fixed. Some examples are the *switching state-space model* that represents a piecewise-stationary extension of a linear dynamic system (Ghahramani and Hinton, 2000) and the *non-stationary continuous dynamic Bayesian network*, a non-stationary DBN for continuous data where only the parameters are allowed to vary over time (Grzegorczyk and Husmeier, 2009).

5.1.2 Dynamic Bayesian networks in non-stationary domains

Dynamic Bayesian networks have been extended to deal with non-stationary domains as they allow inter-time relationships to be modeled and, under certain assumptions (such as parameter independence and conjugate prior), the parameters can be integrated out in closed form in the likelihood function. The common approaches are the following.

Robinson and Hartemink (2009) introduced the *non-stationary dynamic Bayesian network* model, a structural non-stationary DBN where a Markov chain Monte Carlo (MCMC) sampling algorithm is used to learn the structures from time-series data. Their learning framework is based on the Bayesian-Dirichlet equivalent metric, while the change-points are common to the whole network, i.e. they cannot vary from node to node.

Grzegorczyk and Husmeier (2009) proposed a parameter non-stationary DBN for continuous data, called *non-stationary continuous dynamic Bayesian network*, where the numbers and locations of the change-points are sampled from the posterior distribution. Their learning framework is based on Bayesian Gaussian equivalent (BGe) metric and the patterns of non-stationarity are node-specific, thereby providing extra model flexibility.

Song et al. (2009) introduced the *time-varying dynamic Bayesian network* model, a structural non-stationary DBN for continuous data, where they used a kernel reweighted l_1-regularized autoregressive approach for learning the sequence of networks. Their approach is node-specific, as they estimated the edges for each node separately and then joined these edges to form the overall network.

Lèbre et al. (2010) proposed the *auto regressive time varying* model where a structural non-stationary DBN is used to model the interactions between variables, while a reversible jump MCMC (RJMCMC) is used for inferring simultaneously the times when the network changes and the resulting network topologies. Their method is based on the Bayesian linear regression model which avoids the need for data discretization.

Dondelinger et al. (2013) proposed a model for continuous data based on a *piecewise homogeneous dynamic Bayesian network*. This model is structural non-stationary, as it allows the network structure to change over time, and node-specific, as it allows different penalties for changing edges and non-edges in the network. The values of the parameters are sampled from a posterior distribution computed via an improved version of the RJMCMC algorithm.

5.2 Non-stationary continuous time Bayesian networks

Continuous time Bayesian networks are both structural stationary, as the graph does not change over time, and parametric stationary, as the conditional intensity matrices do not change over time. These stationarity assumptions are reasonable in many situations, but there are cases where the data generating process is intrinsically non-stationary and thus CTBNs cannot be used anymore. We extend CTBNs to cope with non-stationarity with specific reference to the case where the structure of causal dependencies changes over continuous time. In such a setting, the graph of the CTBN is replaced by a *graphs sequence* $\boldsymbol{\mathcal{G}} = (\mathcal{G}_1, \mathcal{G}_2, \ldots, \mathcal{G}_E)$, where a graph $\mathcal{G}_e$ represents the causal dependency structure of the model for the epoch $e \in \{1, 2, \ldots, E\}$. This model is structural non-stationary and it can handle both change-points that are common to the whole network and node-specific.

Following the notations and definitions used by Robinson and Hartemink (2010), we let $\mathcal{T} = (t_1, \ldots, t_{E-1})$ be the *transition times* sequence, i.e. the times at which the causal dependency structure $\mathcal{G}_e$ active at epoch e is replaced by the causal dependency structure $\mathcal{G}_{e+1}$ which becomes active at epoch $e + 1$. An *epoch* is defined as the period of time between two consecutive transitions, i.e. the epoch e is active during the period of time starting at t_{e-1} and ending at t_e. The graph $\mathcal{G}_{e+1}$, which is active during the epoch $e + 1$, differs from graph $\mathcal{G}_e$, which is active during the epoch e, in a set of edges called *set of edge changes* and denoted by $\Delta\mathcal{G}_e$. Figure 5.1 shows a graphs sequence of $\boldsymbol{\mathcal{G}} = (\mathcal{G}_1, \mathcal{G}_2, \mathcal{G}_3, \mathcal{G}_4)$ consisting of $E = 4$ epochs with transition times $\mathcal{T} = (t_1, t_2, t_3)$. Each epoch is associated with a set of edge changes. For example, the graph $\mathcal{G}_2$ differs from the graph $\mathcal{G}_1$ by the following set of edge changes $\Delta\mathcal{G}_1 = \{X_3 \to X_2, X_2 \not\to X_3, X_1 \not\to X_2\}$.

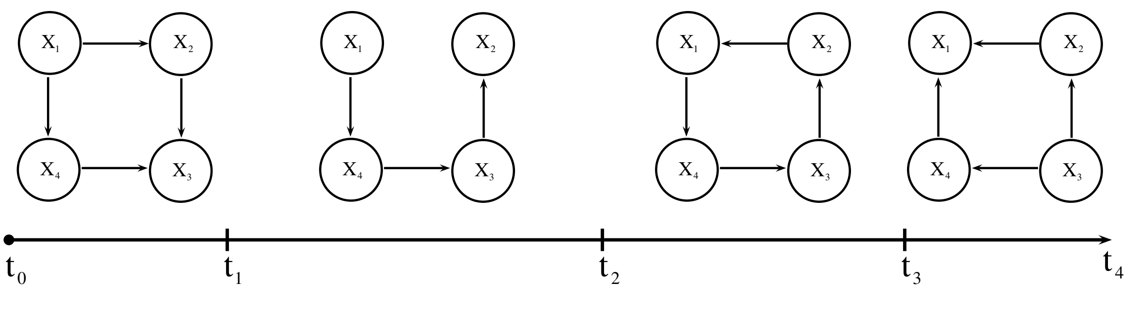

Figure 5.1: A graphs sequence $\boldsymbol{\mathcal{G}} = (\mathcal{G}_1, \mathcal{G}_2, \mathcal{G}_3, \mathcal{G}_4)$ with $E = 4$ epochs and $\mathcal{T} = (t_1, t_2, t_3)$ transition times, where the edges of the graphs sequence are gained and lost over time.

5.2.1 Definition

Non-stationary continuous time Bayesian networks allow each node to have its own sequence of parents sets, each parent set being active at a given epoch. Therefore, we need to introduce the concept of *homogeneous interval* $H(X) = (h_1, \ldots, h_M)$ associated with node X, which is defined as the union of consecutive epochs during which the same parent set $Pa(X)$ is active for the node X. It is important to note that in the case where each epoch is associated with a different parent set, then M is equal to E. We can now introduce the definition of such a model.

Definition 5.1. *(Structural) non-stationary continuous time Bayesian network (nsCTBN), (Stella and Villa, 2014). Let $\boldsymbol{X}$ be a set of random variables $X_1, \ldots, X_N$. Each X has a finite domain of values $Val(X) = \{x_1, \ldots, x_I\}$. A non-stationary continuous time Bayesian network $\mathcal{N}_{ns} = (\mathcal{B}, \mathcal{M}_{ns})$ over $\boldsymbol{X}$ consists of two components: the first is an initial distribution $P^0_{\boldsymbol{X}}$, specified as a Bayesian network $\mathcal{B}$ over $\boldsymbol{X}$, the second is a non-stationary continuous time transition model $\mathcal{M}_{ns}$ specified as:*

- *a sequence of directed (possibly cyclic) graphs $\boldsymbol{\mathcal{G}} = (\mathcal{G}_e)_{e=1}^{E}$ whose nodes are $X_1, \ldots, X_N$ and E is the number of epochs;*
- *a conditional intensity matrix, $\boldsymbol{Q}_{X|Pa_{\boldsymbol{\mathcal{G}}}(X),H(X)}$, $\forall X \in \boldsymbol{X}$, where $Pa_{\boldsymbol{\mathcal{G}}}(X)$ denotes the parents sets of X in $\boldsymbol{\mathcal{G}}$ and $H(X)$ denotes the intervals associated with X.*

In this case, a conditional intensity matrix $\boldsymbol{Q}_{X|Pa_{\boldsymbol{\mathcal{G}}}(X),H(X)}$ consists of a set of intensity matrices, one intensity matrix for each configuration pa_u of the parent set $Pa(X)$ which is active during the interval $h_m \in H(X)$. Thus, an intensity matrix is defined as follows:

$$\boldsymbol{Q}_{X|pa_u,h_m} = \begin{bmatrix} -q_{x_1|pa_u,h_m} & q_{x_1,x_2|pa_u,h_m} & \cdot & q_{x_1,x_I|pa_u,h_m} \\ q_{x_2,x_1|pa_u,h_m} & -q_{x_2|pa_u,h_m} & \cdot & q_{x_2,x_I|pa_u,h_m} \\ \cdot & \cdot & \cdot & \cdot \\ q_{x_I,x_1|pa_u,h_m} & q_{x_I,x_2|pa_u,h_m} & \cdot & -q_{x_I|pa_u,h_m} \end{bmatrix},$$

where $q_{x_i|pa_u,h_m} = \sum_{x_j \neq x_i} q_{x_i,x_j|pa_u,h_m}$. The off-diagonal elements of this matrix can be thought as the "instantaneous probability" of transitioning from x_i to x_j when $Pa(X) = pa_u$ in the interval $H(X) = h_m$, while the diagonal elements can be seen as "instantaneous probability" of leaving state x_i when $Pa(X) = pa_u$ in the interval $H(X) = h_m$.

Learning a nsCTBN from a fully observed data set $\mathcal{D}$ can be done using the standard Bayesian learning framework developed for CTBNs. In such a framework, we must specify a prior probability distribution $P(\boldsymbol{\mathcal{G}})$ over the graphs sequence $\boldsymbol{\mathcal{G}}$ and, for each possible sequence, a density measure over possible values of the parameters $\boldsymbol{q_{\mathcal{G}}}$ and $\boldsymbol{\theta_{\mathcal{G}}}$. Once the prior $P(\boldsymbol{\mathcal{G}})$ and the likelihood $P(\boldsymbol{q_{\mathcal{G}}}, \boldsymbol{\theta_{\mathcal{G}}}|\boldsymbol{\mathcal{G}})$ are given, we can compute the marginal likelihood $P(\mathcal{D}|\boldsymbol{\mathcal{G}})$ and thus the Bayesian score can be evaluated.

It is important to note that we are focused on recovering the graphs sequence and not on detecting possible changes of the parameters. In fact, we identify non-stationarity in the parameters of the model, i.e. the elements of the CIMs, that are significant enough to result in structural changes of the graph. Thus, we assume that other changes are small enough not to alter the graph structure.

5.2.2 Prior probability over the graphs sequence

Unlike the standard learning framework for CTBNs which involves a single graph $\mathcal{G}$, the prior over the nsCTBN's structure $P(\boldsymbol{\mathcal{G}})$ concerns an entire graphs sequence. If the number of epochs E is given, then we can write the prior over the nsCTBN's structure as follows:

$$\begin{aligned} P(\boldsymbol{\mathcal{G}}|E) &= P(\mathcal{G}_1, \ldots, \mathcal{G}_E|E) \\ &= P(\mathcal{G}_1, \Delta\mathcal{G}_1, \ldots, \Delta\mathcal{G}_{E-1}|E) \\ &= P(\mathcal{G}_1)P(\Delta\mathcal{G}_1, \ldots, \Delta\mathcal{G}_{E-1}|E). \end{aligned} \tag{5.1}$$

In this case, we have to define a probability distribution for the initial network $P(\mathcal{G}_1)$ and a probability distribution for the set of edge changes $P(\Delta\mathcal{G}_1, \ldots, \Delta\mathcal{G}_{E-1}|E)$. If some knowledge about particular edges or overall topology is available for the initial network, then we can use an informative prior $P(\mathcal{G}_1)$, otherwise we can resort to a uniform distribution. As in the BNs case, $P(\mathcal{G}_1)$ must satisfy the structure modularity assumption (2.17). The role of the prior on the surviving structures is crucial, since it allows the graphs not to vary dramatically between adjacent epochs. Therefore, the graphs are selected placing some assumptions on the ways by which the edges change through graphs. For example, Robinson and Hartemink (2010) assume that the graph evolves smoothly over time and they use a truncated geometric prior on the number of changes for each each set $\Delta\mathcal{G}_e$.

5.2.3 Prior probability over parameters

The prior over parameters $P(\boldsymbol{q}_{\mathcal{G}}, \boldsymbol{\theta}_{\mathcal{G}} | \mathcal{G}, \mathcal{T})$ is selected in order to satisfy the following standard assumptions: independence between the sets of parameters characterizing the exponential and the multinomial distributions (3.12), parameter modularity (2.19) and parameter independence. For nsCTBNs, the latter assumption is divided into three components: global, interval and local parameter independence.

The *global parameter independence* asserts that the parameters associated with each node in a graphs sequence are independent, so the prior over parameters can be decomposed by variable X as follows:

$$P(\boldsymbol{q}_{\mathcal{G}}, \boldsymbol{\theta}_{\mathcal{G}} | \mathcal{G}, \mathcal{T}) = \prod_{X \in \boldsymbol{X}} P(\boldsymbol{q}_{X|Pa_{\mathcal{G}}(X),H(X)}, \boldsymbol{\theta}_{X|Pa_{\mathcal{G}}(X),H(X)} | \mathcal{G}, \mathcal{T}). \tag{5.2}$$

The *interval parameter independence* states that the parameters associated with each interval of the active parents for each node are independent, so the parameters associated with each X and its parents $Pa(X)$ are decomposable by interval $h_m \in H(X)$ as follows:

$$P(\boldsymbol{q}_{X|Pa_{\mathcal{G}}(X),H(X)}, \boldsymbol{\theta}_{X|Pa_{\mathcal{G}}(X),H(X)} | \mathcal{G}, \mathcal{T}) = \prod_{h_m} P(\boldsymbol{q}_{X|Pa_{\mathcal{G}}(X),h_m}, \boldsymbol{\theta}_{X|Pa_{\mathcal{G}}(X),h_m} | \mathcal{G}, \mathcal{T}). \tag{5.3}$$

The *local parameter independence* states that the parameters associated with each state of a variable in an interval are independent, thus the parameters associated with each X in an interval $h_m \in H(X)$ are decomposable by parent configuration pa_u as follows:

$$P(\boldsymbol{q}_{X|Pa_{\mathcal{G}}(X),h_m}, \boldsymbol{\theta}_{X|Pa_{\mathcal{G}}(X),h_m} | \mathcal{G}, \mathcal{T}) = \prod_{pa_u} \prod_{x_i} P(q_{x_i|pa_u,h_m}, \boldsymbol{\theta}_{x_i|pa_u,h_m} | \mathcal{G}, \mathcal{T}). \tag{5.4}$$

As for CTBNs, we use a Dirichlet distribution as the prior for the parameters of the multinomial distribution and a gamma distribution as the prior for the parameters of the exponential distribution, while the sufficient statistics are modified as follows:

- $T[x_i|pa_u, h_m]$: the amount of time spent in state $X = x_i$ while $Pa(X) = pa_u$ in interval $H(X) = h_m$;
- $M[x_i, x_j|pa_u, h_m]$: the number of transitions from $X = x_i$ to $X = x_j$ while $Pa(X) = pa_u$ in interval $H(X) = h_m$.

The number of times the variable X leaves state x_i while its parents $Pa(X)$ are in state pa_u during interval $H(X) = h_m$ is $M[x_i|pa_u, h_m] = \sum_{x_j \neq x_i} M[x_i, x_j|pa_u, h_m]$.

5.2.4 Marginal likelihood

Given the graphs sequence $\boldsymbol{\mathcal{G}}$ and the transition times $\mathcal{T}$, the marginal likelihood $P(\mathcal{D}|\boldsymbol{\mathcal{G}},\mathcal{T})$ of the data set $\mathcal{D}$, given the graphs sequence and the transition times, can be computed in closed form using the priors and the sufficient statistics previously defined. To derive the Bayesian-Dirichlet equivalent metric for nsCTBNs, we make the same assumptions as those for CTBNs. In this case, the parameter independence assumption is divided into global (5.2), interval (5.3) and local (5.4). Therefore, the marginal likelihood becomes:

$$P(\mathcal{D}|\boldsymbol{\mathcal{G}},\mathcal{T}) = \prod_{X \in \boldsymbol{X}} ML_X(\boldsymbol{q}_{X|Pa_{\boldsymbol{\mathcal{G}}}(X),H(X)}|\mathcal{D}) \times ML_X(\boldsymbol{\theta}_{X|Pa_{\boldsymbol{\mathcal{G}}}(X),H(X)}|\mathcal{D}), \tag{5.5}$$

where the marginal likelihood of $\boldsymbol{q}$ in equation (5.5) is:

$$\prod_{h_m}\prod_{pa_u}\prod_{x_i} \frac{\Gamma\left(\alpha_{x_i|pa_u,h_m} + M[x_i|pa_u,h_m] + 1\right)\left(\tau_{x_i|pa_u,h_m}\right)^{(\alpha_{x_i|pa_u,h_m}+1)}}{\Gamma\left(\alpha_{x_i|pa_u,h_m}+1\right)\left(\tau_{x_i|pa_u,h_m} + T[x_i|pa_u,h_m]\right)^{(\alpha_{x_i|pa_u,h_m}+M[x_i|pa_u,h_m]+1)}}, \tag{5.6}$$

while the marginal likelihood of $\boldsymbol{\theta}$ in equation (5.5) is:

$$\prod_{h_m}\prod_{pa_u}\prod_{x_i=x_j} \frac{\Gamma\left(\alpha_{x_i|pa_u,h_m}\right)}{\Gamma\left(\alpha_{x_i|pa_u,h_m} + M[x_i|pa_u,h_m]\right)} \times \prod_{x_i \neq x_j} \frac{\Gamma\left(\alpha_{x_i,x_j|pa_u,h_m} + M[x_i,x_j|pa_u,h_m]\right)}{\Gamma\left(\alpha_{x_i,x_j|pa_u,h_m}\right)}. \tag{5.7}$$

It is important to note that for nsCTBNs, pseudocounts α as well as imaginary amount of time τ are associated with each interval. This aspect requires a careful choice in order not to be too biased towards these values in the case when small intervals are analyzed. A possible correction is to weight the CTBN's hyperparameters by a quantity proportional to the time interval width $(h_m - h_{m-1})$. Thus, the nsCTBN' hyperparameters can be written as follows:

$$\alpha_{x_i,x_j|pa_u,h_m} = \alpha_{x_i,x_j|pa_u} \times \frac{(h_m - h_{m-1})}{h_M}, \quad \tau_{x_i|pa_u,h_m} = \tau_{x_i|pa_u} \times \frac{(h_m - h_{m-1})}{h_M}, \tag{5.8}$$

where h_M represents the total time. If we want to control the parameter priors using only two hyperparameters α and τ, we can use the uniform BDe for nsCTBNs. In this case, the hyperparameters defined in (5.8) are divided by the number U of possible configurations of the parents of node X times the cardinality I of the domain of X, as follows:

$$\alpha_{x_i,x_j|pa_u,h_m} = \frac{\alpha}{U \times I} \times \frac{(h_m - h_{m-1})}{h_M}, \quad \tau_{x_i|pa_u,h_m} = \frac{\tau}{U \times I} \times \frac{(h_m - h_{m-1})}{h_M}. \tag{5.9}$$

5.3 Structural learning settings

The structural learning of nsCTBNs is addressed as the problem of selecting the graphs sequence $\boldsymbol{\mathcal{G}}$ and the corresponding parameters values which maximize the Bayesian score. To efficiently solve this problem, i.e. to search for the *optimal graphs sequence* $\boldsymbol{\mathcal{G}}^*$, we need to decompose the Bayesian score by variable as done for CTBNs. However, for nsCTBNs, the score decomposition depends on the level of knowledge we have on the transition times. In particular, we take into account the same *learning settings* as those introduced and analyzed by Robinson and Hartemink (2010): *known transitions times*, *known number of epochs* and *unknown number of epochs*.

5.3.1 Known transition times

If the transition times $\mathcal{T}$ are known, then the prior probability over the graphs sequence $P(\boldsymbol{\mathcal{G}})$ decomposes as in equation (5.1). Therefore, from equation (5.5) we obtain that the marginal likelihood decomposes by variable X, while the Bayesian score is the following:

$$\begin{aligned} BS(\boldsymbol{\mathcal{G}} : \mathcal{D}, \mathcal{T}) &= \ln P(\mathcal{G}_1) + \ln P(\Delta\mathcal{G}_1, \dots, \Delta\mathcal{G}_{E-1}|\mathcal{T}) \\ &+ \sum_{X \in \boldsymbol{X}} \ln ML_X(\boldsymbol{q}_{X|Pa_{\boldsymbol{\mathcal{G}}}(X),H(X)}|\mathcal{D}) + \ln ML_X(\boldsymbol{\theta}_{X|Pa_{\boldsymbol{\mathcal{G}}}(X),H(X)}|\mathcal{D}). \end{aligned} \tag{5.10}$$

In such a setting the structural leaning problem of a non-stationary continuous time Bayesian network consists of finding the graph $\mathcal{G}_1$ active during the first epoch ($e = 1$), the $E-1$ sets of edge changes $\Delta\mathcal{G}_1, \dots, \Delta\mathcal{G}_{E-1}$ together with the corresponding parameters values which maximize the Bayesian score defined in equation (5.10). If some knowledge about the structure of the initial graph $\mathcal{G}_1$ is available, then we can use an informative prior for $P(\mathcal{G}_1)$ which must satisfy the structure modularity property (2.17). On the contrary, if no prior knowledge is available, then a uniform distribution is used.

The graphs $\mathcal{G}_2, \dots, \mathcal{G}_E$ are selected by making assumptions on the ways by which the edges change over continuous time. Thus, we have to define prior for $P(\Delta\mathcal{G}_1, \dots, \Delta\mathcal{G}_{E-1}|\mathcal{T})$. We make the same assumption as the one made in Robinson and Hartemink (2010). In particular, we assume that the structural component of the non-stationary continuous time Bayesian network, i.e. the graphs sequence $\boldsymbol{\mathcal{G}} = (\mathcal{G}_1, \mathcal{G}_2, \dots, \mathcal{G}_E)$, evolves smoothly over continuous time.

In such a case, we use a truncated geometric distribution with parameter $p = 1 - \exp(-\lambda_c)$ on the *number of parents' changes* occurring at transition time $e+1$:

$$c_e = \sum_{X \in \boldsymbol{X}} c(Pa_{\mathcal{G}_e}(X), Pa_{\mathcal{G}_{e+1}}(X)), \tag{5.11}$$

where c counts the number of edge changes between two parent sets. If the edge changes $\Delta\mathcal{G}_e$ are assumed to be mutually independent, then the probability for the edge changes through subsequent epochs can be written as follows:

$$P(\Delta\mathcal{G}_1, \ldots, \Delta\mathcal{G}_{E-1}|\mathcal{T}) = \prod_{e=1}^{E-1} \frac{(1-\exp(-\lambda_c))(\exp(-\lambda_c))^{c_e}}{1-(\exp(-\lambda_c))^{c_{max}+1}} \propto \prod_{e=1}^{E-1} (\exp(-\lambda_c))^{c_e}, \tag{5.12}$$

where c_{max} is the *truncation term.* Thus, the Bayesian score (5.10) decomposes by variable:

$$\begin{aligned} BS(\boldsymbol{\mathcal{G}} : \mathcal{D}, \mathcal{T}) &= \sum_{X \in \boldsymbol{X}} \ln P(Pa(X) = Pa_{\mathcal{G}_1}(X)) - \lambda_c \sum_{e=1}^{E-1} c(Pa_{\mathcal{G}_e}(X), Pa_{\mathcal{G}_{e+1}}(X)) \\ &+ \ln ML_X(\boldsymbol{q}, \boldsymbol{\theta}_{X|Pa_{\boldsymbol{\mathcal{G}}}(X), H(X)}|\mathcal{D}), \end{aligned} \tag{5.13}$$

where we grouped together the marginal likelihoods of $\boldsymbol{q}$ and $\boldsymbol{\theta}$. Note that the number of parents' changes for each epoch penalizes the Bayesian score, and thus it discourages sudden variations, while the parameter λ_c regulates the impacts of these changes.

5.3.2 Known number of epochs

If the transition times $\mathcal{T}$ are unknown, then the Bayesian score associated with the nsCTBN can be written as follows:

$$BS(\boldsymbol{\mathcal{G}}, \mathcal{T} : \mathcal{D}) = \ln P(\boldsymbol{\mathcal{G}}, \mathcal{T}) + \ln P(\mathcal{D}|\boldsymbol{\mathcal{G}}, \mathcal{T}). \tag{5.14}$$

In such a setting, to decompose this Bayesian score, we assume that the joint probability $P(\boldsymbol{\mathcal{G}}, \mathcal{T})$ of the evolution of the structural component of the nsCTBNs and the transition times can be decomposed into two independent components: $P(\boldsymbol{\mathcal{G}})$ and $P(\mathcal{T})$. Therefore, the Bayesian score (5.14) can be written as follows:

$$BS(\boldsymbol{\mathcal{G}}, \mathcal{T} : \mathcal{D}) = \ln P(\boldsymbol{\mathcal{G}}) + \ln P(\mathcal{T}) + \ln P(\mathcal{D}|\boldsymbol{\mathcal{G}}, \mathcal{T}). \tag{5.15}$$

If the number of epochs E is known, then the prior probability $P(\boldsymbol{\mathcal{G}})$ over the graphs sequence $\boldsymbol{\mathcal{G}}$ decomposes as in equation (5.1). Therefore, also in this setting, a truncated geometric distribution can be used on the number of parents' changes occurring at each transition time, as we made in the known transition time setting.

Any choice for $P(\mathcal{T})$ can be made to include prior knowledge about the set of transition times. However, if no information is available, then we use a uniform prior on $P(\mathcal{T})$ implying that all possible values of transition times are equally likely for a given number E of epochs. Therefore, in the known number of epochs setting, the Bayesian score can be decomposed by variable as follows:

$$\begin{aligned} BS(\boldsymbol{\mathcal{G}}, \mathcal{T} : \mathcal{D}) &= \ln P(\mathcal{T}) \\ &+ \sum_{X \in \boldsymbol{X}} \ln P(Pa(X) = Pa_{\mathcal{G}_1}(X)) - \lambda_c \sum_{e=1}^{E-1} c(Pa_{\mathcal{G}_e}(X), Pa_{\mathcal{G}_{e+1}}(X)) \\ &+ \ln ML_X(\boldsymbol{q}, \boldsymbol{\theta}_{X|Pa_{\boldsymbol{\mathcal{G}}}(X),H(X)} | \mathcal{D}). \end{aligned} \tag{5.16}$$

5.3.3 Unknown number of epochs

If both the transition times $\mathcal{T}$ and the number of epochs E are unknown, then they must be estimated through the Bayesian score. To accomplish this task, we exploit what we introduced for the known transition times and the known number of epochs settings. In particular, we assume that the structure of the non-stationary continuous time Bayesian network evolves smoothly over continuous time. Such an assumption is incorporated by using a truncated geometric distribution with parameter $p = 1 - \exp(-\lambda_e)$ on the number of epochs. Following what we presented in the known transition times setting, the Bayesian score can be obtained by subtracting the parameter λ_e times the number of epochs E. Therefore, in this setting, the Bayesian score decomposes by variable as follows:

$$\begin{aligned} BS(\boldsymbol{\mathcal{G}}, \mathcal{T} : \mathcal{D}) &= \ln P(\mathcal{T}) - \lambda_e E \\ &+ \sum_{X \in \boldsymbol{X}} \ln P(Pa(X) = Pa_{\mathcal{G}_1}(X)) - \lambda_c \sum_{e=1}^{E-1} c(Pa_{\mathcal{G}_e}(X), Pa_{\mathcal{G}_{e+1}}(X)) \\ &+ \ln ML_X(\boldsymbol{q}, \boldsymbol{\theta}_{X|Pa_{\boldsymbol{\mathcal{G}}}(X),H(X)} | \mathcal{D}). \end{aligned} \tag{5.17}$$

Note that this version of the Bayesian score contains two parameters, namely λ_c and λ_e, which encode our prior belief about the structure of the non-stationary continuous time Bayesian network. Specifically, the parameter λ_c regulates our prior belief about the smoothness of the edge changes (e.g. encouraging or discouraging few edge changes per epoch), while the parameter λ_e regulates our prior belief about the number of epochs (e.g. encouraging or discouraging the creation of few epochs).

5.4 Structural learning algorithms

We introduce three algorithms for structural learning of nsCTBNs, each one tailored to a specific learning setting. A crucial aspect of the structural learning problem of nsCTBNs is that, as it happens for CTBNs, the optimal nsCTBN can be found by separately optimizing the score function component associated with each node. In particular, if the transition times are known, then an exact optimization algorithm based on dynamic programming can be developed. On the contrary, if the transition times are unknown, then we rely on approximated techniques based on simulated annealing.

5.4.1 Known transition times

In this setting, the Bayesian score decomposes by variable as shown in equation (5.13). Therefore, selecting the optimal graphs sequence $\boldsymbol{\mathcal{G}}^*$ for the nsCTBN consists of finding, for each node X of the nsCTBN, the *optimal parents sequence* $Pa_{\boldsymbol{\mathcal{G}}^*}(X)$, i.e. the parents sequence that maximizes the corresponding component of the Bayesian score.

To clarify this problem we consider a sequence of M intervals $H(X) = (h_1, \ldots, h_M)$ and S possible parents $Pa(X) = \{X_1, \ldots, X_S\}$, so we have $Z = 2^S$ possible parents sets. To find the optimal parents sequence $Pa_{\boldsymbol{\mathcal{G}}^*}(X)$, we must compute $M \times Z$ marginal likelihood terms associated with $\boldsymbol{q}$ and $\boldsymbol{\theta}$, one marginal likelihood term for each possible parent set $Pa_z(X)$ and each interval h_m. Then, an optimization algorithm can be used to find the maximum of the components of the Bayesian score associated with the node X. An exhaustive search would be prohibitive as it would require the evaluation of Z^M scores, one for each possible sequence. Unfortunately, a greedy search strategy that selects the parent set, which maximizes the Bayesian score for each interval, is not viable. Indeed, the c function that counts the parent changes used in equation (5.11) binds the choice of the subsequent parents set.

However, the relation between the score $BS_{X|Pa(X),h_m}$, associated with the parents set $Pa(X)$ for the interval h_m of the variable X, and the score $BS_{X|Pa(X),h_{m-1}}$, associated with the parents set $Pa(X)$ for the interval h_{m-1}, can be defined by recursion as follows:

$$BS_{X|Pa(X),h_m} = \max_{Pa_z(X)} \{ BS_{X|Pa_z(X),h_{m-1}} - \lambda_c c(Pa_z(X), Pa(X)) + \ln ML_X(\boldsymbol{q}, \boldsymbol{\theta}_{X|Pa(X),h_m} | \mathcal{D}) \}. \quad (5.18)$$

The equation (5.18) is exploited by the dynamic programming technique shown in Algorithm 5.1. This algorithm takes as input the marginal likelihoods of $\boldsymbol{q}$ and $\boldsymbol{\theta}$ for each interval and parents set, i.e. $ML_X(\boldsymbol{q}, \boldsymbol{\theta}_{X|Pa(X),h_m}|\mathcal{D})$, the prior probability about the initial parent set, i.e. $P(Pa(X) = Pa_{\mathcal{G}_{h_1}}(X))$, the number of parents' changes, i.e. the c function used in equation (5.11), and the parameter λ_c. It ensures the optimal parents sequence $Pa_{\boldsymbol{\mathcal{G}}^*}(X)$ for the node X and its relative optimal Bayesian score.

The core of Algorithm 5.1 is the computation of the $M \times Z$ score matrix, denoted by SC, through the dynamic programming recursion. In the first interval h_1 ($m = 1$), for $1 \leq z \leq Z$, this recursion is defined as follows:

$$SC[1, z] = \ln P(Pa_z(X) = Pa_{\mathcal{G}_{h_1}}(X)) + \ln ML_X(\boldsymbol{q}, \boldsymbol{\theta}_{X|Pa_z(X),h_1}|\mathcal{D}), \tag{5.19}$$

for the subsequent intervals h_m ($m = 2, \ldots, M$), the recursion is defined as follows:

$$SC[m, z] = \max_{1 \leq w \leq Z} \left\{SC[m-1, w] - \lambda_c c(Pa_w(X), Pa_z(X)) + \ln ML_X(\boldsymbol{q}, \boldsymbol{\theta}_{X|Pa_z(X),h_m}|\mathcal{D})\right\} \tag{5.20}$$

After filling the SC matrix, the value $\max_z\{SC[M, z]\}$ is the optimal Bayesian score, while the optimal parents sequence is reconstructed backwards from M to 1 by using the IN matrix. The cost of computing the dynamic programming recursion is $O(M \times Z^2)$, which is polynomial for a fixed number of parents S.

The problem of selecting the optimal parents sequence $Pa_{\boldsymbol{\mathcal{G}}^*}(X)$ has an interesting *graph representation*. Indeed, it is possible to create a graph whose nodes are associated with marginal likelihoods of $\boldsymbol{q}$ and $\boldsymbol{\theta}$ for interval h_m and parents set $Pa_z(X)$, while each node associated with interval h_m is linked with all the nodes associated with interval h_{m+1}. Each arc is associated with a weight computed as the difference between the marginal likelihoods of $\boldsymbol{q}$ and $\boldsymbol{\theta}$ in the interval h_m for the parents set $Pa_z(X)$ and the cost of switching from the parents set of the interval h_{m-1} to the parents set of the interval h_m. To conclude the graph representation, two special nodes are added to represent the start and the end of the optimal parents sequence. Such a graph does not have cycles, thus the selection of the optimal parents sequence for each node can be reduced to a longest path problem from the start node to the end node over a directed acyclic graph, and thus it can be solved using either dynamic or linear programming.

Learning a nsCTBN model can be summarized in four steps: i) compute the sufficient statistics over the data set according to the given transitions times; ii) calculate the marginal likelihoods and fill the MLX matrix for each variable; iii) run Algorithm 5.1 for each variable in order to get the optimal parents sequence; iv) collect the optimal parents sequence of each variable and compute the corresponding CIMs using the sufficient statistics already computed in i). If we allow the intervals to differ from the transition times, i.e. they can be obtained as one of all the possible unions of transition times, then we have to repeat the learning procedure for all the possible $E \times (E-1)/2$ cases. Fortunately, we can speed up this computation. In fact, the sufficient statistics can be aggregated through intervals; in such a way we read the data set once, while the precomputed marginal likelihoods can be stored and reused for the same intervals. Moreover, the computations can be performed in parallel for each variable.

Algorithm 5.1 LearnKTTX

Require: matrix containing the marginal likelihoods of $\boldsymbol{q}$ and $\boldsymbol{\theta}$ $MLX[M,Z]$, vector containing the prior probability about the initial parent set $PR[Z]$, matrix containing the number of parents' changes $C[Z,Z]$ and the parameter for the parent changes λ_c.

Ensure: score matrix $SC[M,Z]$ and index matrix $IN[M,Z]$.

```
1: Initialize $SC[m,z] \leftarrow -\infty, IN[m,z] \leftarrow 0$.
2: for $m \leftarrow 1,\dots,M$ do
3:   for $z \leftarrow 1,\dots,Z$ do
4:     if $(m = 1)$ then
5:       $SC[m,z] \leftarrow \ln MLX[m,z] + \ln PR[z]$
6:     else
7:       for $w \leftarrow 1,\dots,Z$ do
8:         $score \leftarrow SC[m-1,w] + \ln MLX[m,z] - \lambda_c C[w,z]$
9:         if $(score > SC[m,z])$ then
10:          $SC[m,z] \leftarrow score$
11:          $IN[m,z] \leftarrow w$
12:        end if
13:      end for
14:    end if
15:  end for
16: end for
```

5.4.2 Known number of epochs

In this setting, we know the number of epochs, but the transition times are not given, so we cannot directly apply Algorithm 5.1 to solve the structural learning problem. However, once a *tentative allocation* $\hat{\mathcal{T}}$ of the transition times is given, we can apply Algorithm 5.1 to obtain the optimal solution. This optimal solution assumes that $\hat{\mathcal{T}}$ is not too different from the true and unknown transition times $\mathcal{T}$.

We developed and applied the *simulated annealing* (SA) algorithm (Kirkpatrick et al., 1983; Cerny, 1985) to find the allocation $\hat{\mathcal{T}}^*$ which is as close as possible to $\mathcal{T}$. We give a brief description of this technique. SA is a stochastic algorithm that attempts to find the global optimum of a given function $f(\boldsymbol{x})$ where $\boldsymbol{x}$ represents the current solution, also referred to as *state*. SA is an iterative algorithm that, at each step, samples a new state $\boldsymbol{x}'$ according to some *proposal distribution* $\mathcal{P}'(\cdot|\boldsymbol{x})$. Once the new state $\boldsymbol{x}'$ has been proposed, the following quantity is computed $\alpha = \exp\left(-\frac{f(\boldsymbol{x})-f(\boldsymbol{x}')}{CT}\right)$, where CT denotes the *computational temperature*. SA accepts the proposed state $\boldsymbol{x}'$ with probability equal to $\min\{1, \alpha\}$, thus moving from state $\boldsymbol{x}$ to state $\boldsymbol{x}'$, otherwise the current state $\boldsymbol{x}$ does not change. SA always accepts any proposed state $\boldsymbol{x}'$ where $f(\boldsymbol{x}') > f(\boldsymbol{x})$, while it accepts the proposed state $\boldsymbol{x}'$ when $f(\boldsymbol{x}') < f(\boldsymbol{x})$ with probability α.

The computational temperature CT reduces over iterations according to a *cooling schedule*. It has been shown that if one cools *sufficiently slowly*, then the algorithm will provably find the global optimum (Kirkpatrick et al., 1983). However, it is not clear how to implement this in practice. An approach is to use an *exponential cooling schedule* defined as follows: $CT_k = CT_0 \times \zeta^k$, where CT_0 represents the *initial temperature* typically set to 1.0, ζ is the *cooling rate* usually set to be close to 0.8 and k is the current step (Murphy, 2012). The best cooling schedule is difficult to determine: if it cools too quickly, then it risks getting stuck in a local optimum, while if cools too slowly, then it wastes time. This is the main drawback of simulated annealing (Bertsimas and Tsitsiklis, 1993).

In the case of nsCTBNs the state $\boldsymbol{x}$ is the tentative allocation $\hat{\mathcal{T}}$, while the function $f(\boldsymbol{x})$ to be optimized is the Bayesian score (5.16). Algorithm 5.2 solves the structural learning problem in the known number of epochs setting for a given node by ensuring the optimal tentative allocation $\hat{\mathcal{T}}^*$ and its Bayesian score. It takes as input the sufficient statistics, the parameters used to run Algorithm 5.1 and the parameters regarding the SA technique. These latter parameters are the tentative allocation $\hat{\mathcal{T}}$ selected according to the discrete uniform distribution, the initial temperature CT_0, the cooling rate ζ and the number of iterations $Iters$. The proposal distribution is the truncated normal distribution with a *truncation parameter* z and a *standard deviation* σ, while the proposed state is chosen according to Algorithm 5.3.

Algorithm 5.2 LearnKNEX

```
Require: sufficient statistics $SuffStatsX$, prior probability $PR[]$, number of parent changes $C[,]$, parameter $\lambda_c$, tentative allocation $\hat{\mathcal{T}}$, initial temperature $CT_0$, cooling rate $\zeta$, number of iterations $Iters$, truncation parameter $z$ and standard deviation $\sigma$.
Ensure: optimal tentative allocation $\hat{\mathcal{T}}^*$ and best Bayesian score $bestSC$.
 1: Initialize $k \leftarrow 0$, $\hat{\mathcal{T}}^* \leftarrow \hat{\mathcal{T}}$.
 2: $bestSC \leftarrow$ LearnKTTX(GetMLX($SuffStatsX$, $\hat{\mathcal{T}}$), $PR[], C[,], \lambda_c$)
 3: while ($k < Iters$) do
 4:   $\hat{\mathcal{T}} \leftarrow$ TentativeAllocation($\hat{\mathcal{T}}^*$, $z$, $\sigma$)
 5:   $tentSC \leftarrow$ LearnKTTX(GetMLX($SuffStatsX$, $\hat{\mathcal{T}}$), $PR[], C[,], \lambda_c$)
 6:   $CT \leftarrow CT_0 \times \zeta^k$
 7:   $accProb \leftarrow \min\left\{1, \exp\left(-\frac{(bestSC-tentSC)}{CT}\right)\right\}$
 8:   $ur \leftarrow$ UniRand()
 9:   if ($ur \leq accProb$) then
10:     $\hat{\mathcal{T}}^* \leftarrow \hat{\mathcal{T}}$
11:     $bestSC \leftarrow tentSC$
12:   end if
13:   $k \leftarrow k + 1$
14: end while
```

Algorithm 5.3 TentativeAllocation

```
Require: tentative allocation $\hat{\mathcal{T}}$, truncation parameter $z$ and standard deviation $\sigma$.
Ensure: new tentative allocation $\hat{\mathcal{T}}'$.
1: $t \leftarrow$ UniRandDiscr($\hat{\mathcal{T}}$)
2: $\hat{\mathcal{T}}' \leftarrow \hat{\mathcal{T}} \setminus t$
3: $nr \leftarrow$ StdNormRand()
4: if (($nr < -z$) or ($nr > z$)) then
5:   $nr \leftarrow z$
6: end if
7: $t \leftarrow t + nr \times \sigma$
8: $\hat{\mathcal{T}}' \leftarrow \hat{\mathcal{T}} \cup t$
```

5.4.3 Unknown number of epochs

In this setting, the number of epochs is unknown, thus the structural learning algorithm must be able to change the number of epochs, as well as the corresponding transition times. Also in this case, we used the simulated annealing technique, where the state $\boldsymbol{x}$ is the tentative allocation $\hat{\mathcal{T}}$ and the function $f(\boldsymbol{x})$ to be optimized is the Bayesian score shown in equation (5.17). The cooling schedule is set to be the same as the one used for the known number of epochs setting.

The proposal distribution differs from the one of the previous case as it uses two additional operators, namely *split* and *merge*. The split operator allows to split a given interval $[t_m; t_{m+1})$ into two subintervals $[t_m; t)$ and $[t; t_{m+1})$, where $t_m, t_{m+1} \in \hat{\mathcal{T}}$. The merge operator allows to merge contiguous intervals $[t_{m-1}; t_m)$ and $[t_m; t_{m+1})$ to form the wider interval $[t_{m-1}; t_{m+1})$, where $t_{m-1}, t_m, t_{m+1} \in \hat{\mathcal{T}}$. The new state $\boldsymbol{x}'$ is obtained by sampling the number of epochs changes *ec* from a multinoulli distribution with parameters (p_1, p_2, p_3), where p_1 represents the probability that the current number of epochs $|\hat{\mathcal{T}}|$ is decreased by one, p_3 represents the probability that the current number of epochs $|\hat{\mathcal{T}}|$ is increased by one, and p_2 represents the probability that the current number of epochs $|\hat{\mathcal{T}}|$ does not change. If *ec* is equal to 2, then the Algorithm 5.2 is invoked. If *ec* is equal to 1, then the merge operator is applied before running the Algorithm 5.2. If *ec* is equal to 3, then the split operator is applied before running the Algorithm 5.2.

Algorithm 5.4 solves the structural learning problem in the unknown number of epochs setting for a given node X by ensuring the optimal tentative allocation $\hat{\mathcal{T}}^*$ and its corresponding Bayesian score. This algorithm is basically the same as the one in the known number of epochs settings, but it uses Algorithm 5.5 to perform the two additional operators. Specifically, the split operator is implemented as follows: a time interval $[t_m; t_{m+1})$, selected according to a discrete uniform distribution, is evenly splitted to obtain two equal width intervals, i.e. $[t_m; t)$ and $[t; t_{m+1})$ where t is the mid point in $[t_m; t_{m+1})$. The merge operator is implemented as follows: a transition time t_m belonging to $\hat{\mathcal{T}}$ is sampled according to a discrete uniform distribution, then the contiguous time intervals $[t_{m-1}; t_m)$ and $[t_m; t_{m+1})$ are merged.

Algorithm 5.4 LearnUNEX

```
Require: sufficient statistics $SuffStatsX$, prior probability $PR[]$, number of parent changes $C[,]$, parameter $\lambda_c$, parameter $\lambda_e$, tentative allocation $\hat{\mathcal{T}}$, initial temperature $CT_0$, cooling rate $\zeta$, number of iterations $Iters$, truncation parameter $z$, standard deviation $\sigma$, split probability $sp$ and merge probability $mp$.
Ensure: optimal tentative allocation $\hat{\mathcal{T}}^*$ and best Bayesian score $bestSC$.
 1: Initialize $k \leftarrow 0$, $\hat{\mathcal{T}}^* \leftarrow \hat{\mathcal{T}}$.
 2: $bestSC \leftarrow$LearnKTTX(GetMLX($SuffStatsX$, $\hat{\mathcal{T}}$), $PR[], C[,], \lambda_c$) $-\lambda_e\ |\hat{\mathcal{T}}|$
 3: while ($k < Iters$) do
 4:   $\hat{\mathcal{T}} \leftarrow$ SplitMerge($\hat{\mathcal{T}}^*$, $sp$, $mp$)
 5:   $\hat{\mathcal{T}} \leftarrow$ TentativeAllocation($\hat{\mathcal{T}}$, $z$, $\sigma$)
 6:   $tentSC \leftarrow$ LearnKTTX(GetMLX($SuffStatsX$, $\hat{\mathcal{T}}$), $PR[], C[,], \lambda_c$) $-\lambda_e\ |\hat{\mathcal{T}}|$
 7:   $CT \leftarrow CT_0 \times \zeta^k$
 8:   $accProb \leftarrow \min\left\{1, \exp\left(-\frac{(bestSC - tentSC)}{CT}\right)\right\}$
 9:   $ur \leftarrow$ UniRand()
10:   if ($ur \leq accProb$) then
11:     $\hat{\mathcal{T}}^* \leftarrow \hat{\mathcal{T}}$
12:     $bestSC \leftarrow tentSC$
13:   end if
14:   $k \leftarrow k + 1$
15: end while
```

Algorithm 5.5 SplitMerge

```
Require: tentative allocation $\hat{\mathcal{T}}$, split probability $sp$ and merge probability $mp$.
Ensure: new tentative allocation $\hat{\mathcal{T}}'$.
 1: $\hat{\mathcal{T}}' \leftarrow \hat{\mathcal{T}}$
 2: $p \leftarrow$ UniRand()
 3: if ($p < mp$) then
 4:   $t \leftarrow$ UniRandDiscr($\hat{\mathcal{T}}$)
 5:   $\hat{\mathcal{T}}' \leftarrow \hat{\mathcal{T}} \setminus t$
 6: else
 7:   if ($p < (mp + sp)$) then
 8:     $t \leftarrow$ UniRandDiscr($\hat{\mathcal{T}} \cup T$)
 9:     $nt \leftarrow \text{left}(t) + \frac{t - \text{left}(t)}{2}$
10:     $\hat{\mathcal{T}}' \leftarrow \hat{\mathcal{T}} \cup nt$
11:   end if
12: end if
```

5.5 Numerical experiments

Numerical experiments were performed to evaluate the effectiveness of the proposed algorithms. Before applying them to real world data sets, where ground truths are often not available, we relied on simulated (controlled) experiments to provide reference performance values. Specifically, we have studied the performance of the proposed algorithms using data sets varying different parameters, such as the number of observations, the number of nodes, the number of epochs and the simulated annealing parameters. In each experiment we performed multiple simulations and sensitivity analysis to ensure that our results were robust to possible artifacts. For brevity, we present the results based on two data sets, while we refer to Stella and Villa (2014) for further details.

Data set A is generated from the non-stationary process shown in Figure 5.2 (a). It is composed by three epochs and three nodes with different domain size, while the observations consist of 100 trajectories sampled from 0 to 20 time units. Data set B is generated from the non-stationary process depicted in Figure 5.2 (c). It has five epochs and three nodes, and it consists of 100 trajectories sampled from 0 to 30 time units.

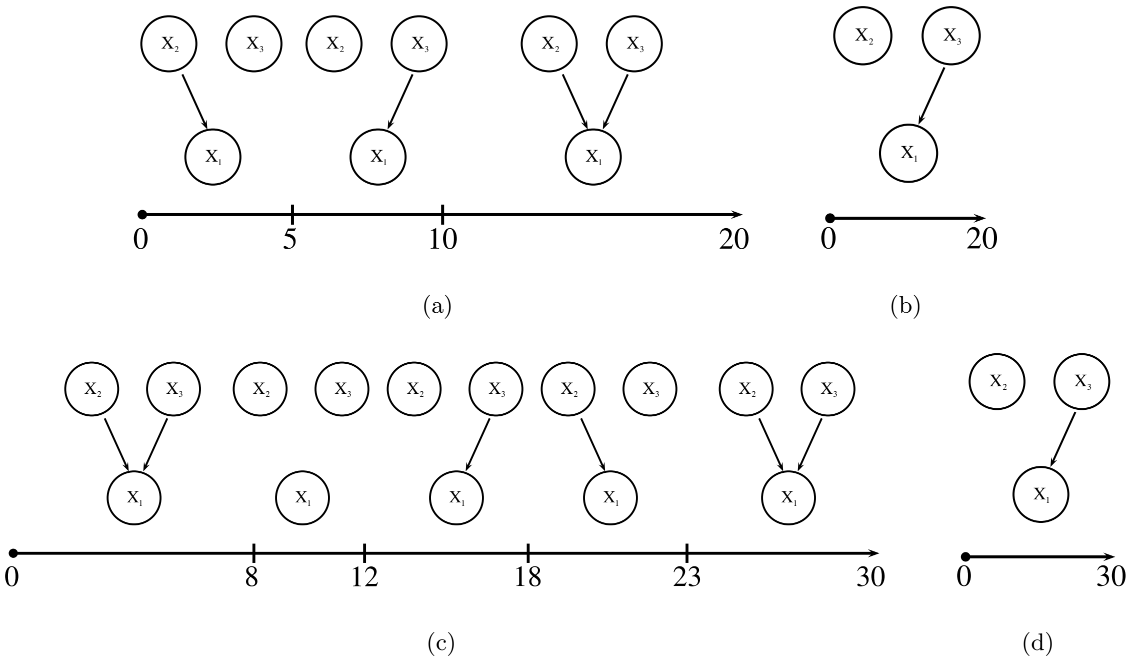

Figure 5.2: Data-generation processes used for the experiments: (a) true non-stationary process of data set A and its stationary counterpart (b) learned by a CTBN; (c) true non-stationary process of data set B and its stationary counterpart (d) learned by a CTBN.

5.5.1 Known transition times

The first set of experiments was focused on two aspects: the ability of Algorithm 5.1 to reconstruct the correct graphs sequence and the analysis of the impacts of the parameter λ_c that regulates the creation of new edges. In the case where there are no restrictions on the evolution of the graphs sequence, i.e. $\lambda_c = 0$, the optimal graphs sequence is obtained acting greedily. Therefore, we partitioned the data sets according to the transitions times and we applied the standard structural learning algorithm for CTBNs on each partition. Then, the results were compared against those of Algorithm 5.1 (with $\lambda_c = 0$) and we ascertained that the reconstructed graphs sequences were identical.

In the case where there are some restrictions on the evolution of the graphs sequence, i.e. $\lambda_c > 0$, we analyzed the behavior of the optimal graphs sequence over time varying the value of the parameter λ_c. Figure 5.3 shows the optimal graphs sequence of four nsCTBNs reconstructed using data set A with different values of λ_c. In the first case ($\lambda_c = 0$) the resulting graphs sequence has 3 edge changes, i.e. $\Delta\mathcal{G}_1 = \{X_2 \not\rightarrow X_1, X_3 \rightarrow X_1\}$ and $\Delta\mathcal{G}_2 = \{X_2 \rightarrow X_1\}$. In the second case ($\lambda_c = 20$) we have 2 edge changes, i.e. $\Delta\mathcal{G}_1 = \{X_2 \not\rightarrow X_1, X_3 \rightarrow X_1\}$ and $\Delta\mathcal{G}_2 = \emptyset$. In the third case ($\lambda_c = 50$) we have only one edge change, i.e. $\Delta\mathcal{G}_1 = \{X_3 \rightarrow X_1\}$ and $\Delta\mathcal{G}_2 = \emptyset$. In the last case ($\lambda_c = 70$) the cost of change an edge is so high that we have no changes.

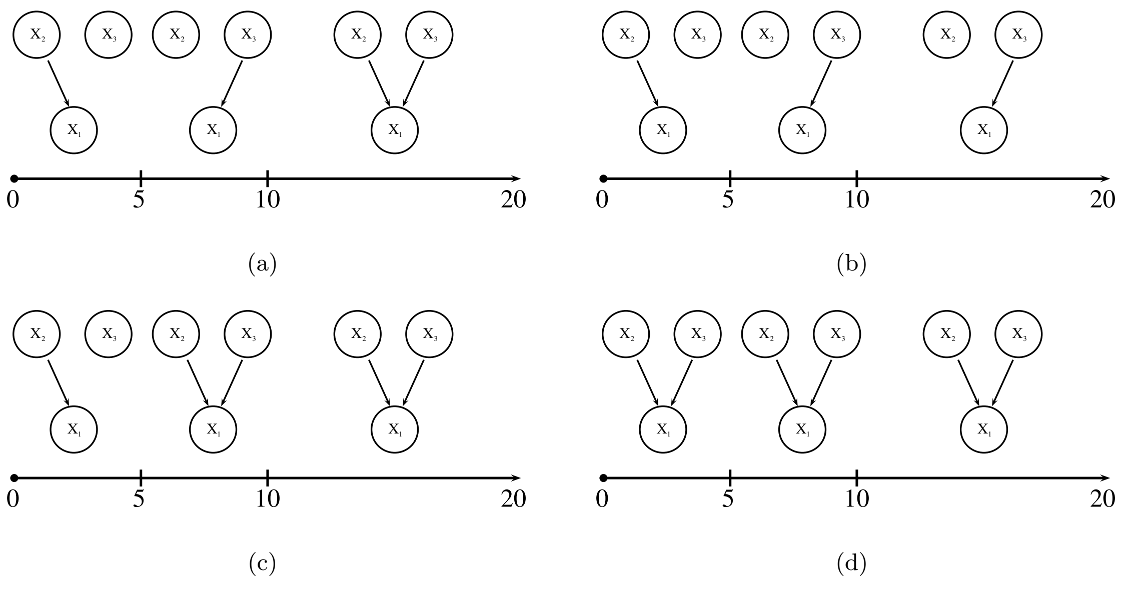

Figure 5.3: Optimal graphs sequence over time for data set A varying the parameter λ_c: (a) $\lambda_c = 0$, (b) $\lambda_c = 20$, (c) $\lambda_c = 50$ and (d) $\lambda_c = 70$.

5.5.2 Known number of epochs

The second set of experiments was focused on the empirical evaluation of the effectiveness of the simulated annealing technique to find the allocation which is as close as possible to the true and unknown transition times. We have performed different tests to assess the sensitivity of the parameters used by the SA technique. Specifically, to provide robust results we have tried different settings of the cooling schedule, the number of iterations and the parameters of the proposal distribution.

We run Algorithm 5.2 one hundred times using an exponential cooling schedule (with initial temperature $CT_0 = 1,000$, that is in line with the size of the Bayesian score, and cooling rate $\zeta = 0.8$), for 300 iterations and $\lambda_c = 1$. The proposal distribution was the truncated normal distribution (with a truncation parameter $z = 3$ and a standard deviation $\sigma = 1$), while the first tentative allocation was selected according to the discrete uniform distribution. Figure 5.4 shows the retrieved transition times (gray) versus the true transition times (black) for data set A and data set B respectively. Given that time is continuous, the retrieved transition times were grouped in ten bins for each transition time to draw a meaningful distribution. The results are very encouraging as the proposed algorithm is able to find transition times very close to true ones on synthetic data sets.

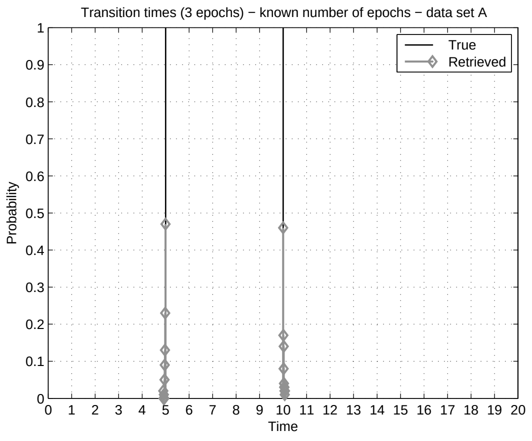

(a)

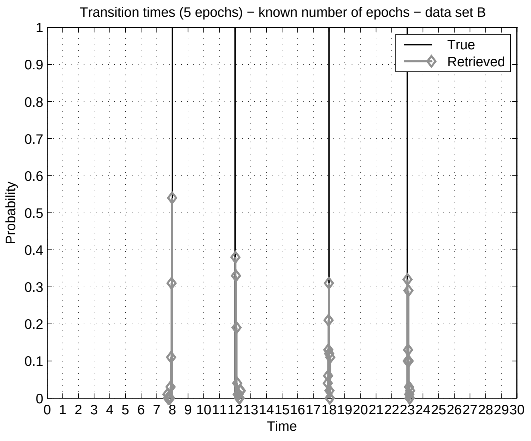

(b)

Figure 5.4: Retrieved transition times (gray) versus the true transition times (black) for data set A (a) and data set B (b) coming from one hundred runs of Algorithm 5.2.

5.5.3 Unknown number of epochs

The third set of experiments was performed to test the case where the number of epochs is unknown as addressed by Algorithm 5.4. We have used the same configuration of the simulated annealing technique previously described, and we have performed different tests to assess the behavior of the split and merge operators, as well as the impacts of the parameter λ_e that regulates the creation of new epochs.

We run Algorithm 5.4 one hundred times using the SA settings previously defined, split and merge probability equal to 0.20, and $\lambda_e = 1$. The first tentative allocation was selected to contain only the end time. Figure 5.5 shows the retrieved transition times corresponding to the most probable number of epochs, the distribution of the number of epochs and the average Bayesian score for each epoch for data set A and B respectively. For the data set A, the proposed algorithm provides the true number of epochs, transition times very close to the true ones and the correct graphs sequence. For the data set B, the algorithm provides a distribution over the number of epochs, where the most probable number of epochs is the correct one, the corresponding transition times are close to the true ones and the correct graphs sequence. In the other cases, it recovers only the strongest changes, specifically the transition time $t_2 = 12$ is the most difficult to identify.

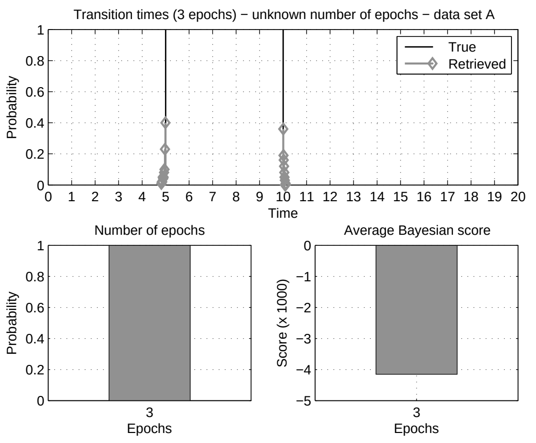

(a)

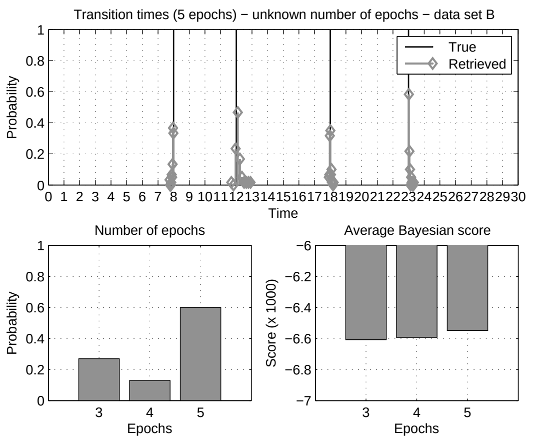

(b)

Figure 5.5: Retrieved transition times corresponding to the most probable number of epochs, distribution of the number of epochs, and average Bayesian score for each epoch for data set A (a) and data set B (b) coming from one hundred runs of Algorithm 5.4.

5.6 Discussion

After a brief introduction of the motivations of non-stationarity modeling and the state-of-the-art methods in this context, we have presented the structural non-stationary continuous time Bayesian networks. These models allow us to represent dependencies which change over continuous time; this aspect makes them particularly suitable to in-depth analyze time-series data. We have provided the formal derivation of the Bayesian score for learning these models, and we have designed and implemented three learning algorithms of increasing complexity based on the available knowledge. Finally, we have tested the proposed algorithms on synthetic data sets and illustrated their effectiveness in the reconstruction of the correct graphs sequence.

Chapter 6

Markov decision processes

The probabilistic graphical models described in the previous chapters can be used within the Markov decision process framework, which provides a model for sequential decision-making under uncertainty. We begin by reviewing the basic concepts and algorithms, then we move on describing factored Markov decision processes and then we conclude the chapter discussing structured continuous time Markov decision processes with some examples in a simplified, but meaningful trading domain.

6.1 Basic concepts

Markov decision processes have been widely used in modeling stochastic sequential decision problems, such as many economic problems involving choices made over time and under uncertainty, see for example Derman et al. (1975); Mendelssohn and Sobel (1980); White (1993); Bäuerle and Rieder (2011). We describe the basics of fully observable Markov decision processes, while we refer to Bertsekas (1987); Puterman (1994); Boutilier et al. (1999) for further material on these models.

Definition 6.1. *Markov decision process (MDP), (Puterman, 1994). A MDP is defined as a tuple* $(\boldsymbol{X}, \boldsymbol{A}, R, P)$ *where:* $\boldsymbol{X}$ *is a finite set of states;* $\boldsymbol{A}$ *is a finite set of actions;* R *is a (bounded) reward function* $R : \boldsymbol{X} \times \boldsymbol{A} \rightarrow [0, R_{max}]$ *such that* $R(\boldsymbol{x}, a)$ *represents the reward obtained in state* $\boldsymbol{x}$ *after taking action* a*; and* P *is a Markovian transition model such that* $P(\boldsymbol{x}'|\boldsymbol{x}, a)$ *represents the probability of going from state* $\boldsymbol{x}$ *to state* $\boldsymbol{x}'$ *after taking action* a.

6.1.1 Policy

A policy describes a course of action to be adopted by the decision-maker to control the system. We are interested in Markovian, since the action choice at any state does not depend on the system history, and stationary policies, since action choice does not depend on the stage of the decision problem. More precisely, we define a policy as follows.

Definition 6.2. *(Deterministic, stationary, Markovian) policy, (Puterman, 1994). A policy π for an MDP is a mapping $\pi : \boldsymbol{X} \rightarrow \boldsymbol{A}$, where $\pi(\boldsymbol{x})$ is the action the decision-maker takes in the state $\boldsymbol{x}$.*

6.1.2 Value function

An optimality criteria is used to measure the value of a policy which evaluates the rewards accumulated by the decision-maker, as it goes through the state space executing π. The decision-maker seeks to maximize the expected return, where the return is defined as some specific function of the reward sequence. We focus on infinite-horizon problems where the decision-maker is trying to maximize two types of expected returns: discounted and average. In the discounted return case, the current value of a reward received in the future is discounted by γ with $\gamma \in [0, 1)$, a *discount factor* γ close to 0 leads to myopic evaluation, while close to 1 leads to far-sighted evaluation. In the average return case, the decision-maker is interested in maximizing the average reward received per time step.

Definition 6.3. *Value function, (Puterman, 1994). The value function of a state $\boldsymbol{x}$ under a policy π, denoted by $V^{\pi}(\boldsymbol{x})$, is the expected return when starting in $\boldsymbol{x}$ and following π.*

The value function for the *infinite-horizon discounted return* is:

$$V^{\pi}(\boldsymbol{x}) = \lim_{T\rightarrow\infty} \mathbb{E}_{\pi}\left[\sum_{t=0}^{T} \gamma^{t} R(\boldsymbol{X}^{(t)}, \pi(\boldsymbol{X}^{(t)}))|\boldsymbol{X}^{(0)} = \boldsymbol{x}\right], \tag{6.1}$$

while for the *infinite-horizon average return ρ^{π}*, the value function is:

$$V^{\pi}(\boldsymbol{x}) = \lim_{T\rightarrow\infty} \frac{1}{T}\mathbb{E}_{\pi}\left[\sum_{t=0}^{T} R(\boldsymbol{X}^{(t)}, \pi(\boldsymbol{X}^{(t)}))\right] = \rho^{\pi}, \tag{6.2}$$

where $\boldsymbol{X}^{(t)}$ is a random variable representing the state of the system after t steps. In equation (6.2) we assume that for any policy π, the resulting Markov chain $P(\boldsymbol{x}'|\boldsymbol{x}, \pi(\boldsymbol{x}))$ is ergodic, and hence the average return ρ^{π} is unique, independent of the starting state (Puterman, 1994).

6.1.3 Bellman operators

Value functions allow us to define a partial ordering over policies: a policy π is better than or equal to another policy π' if its expected return is greater than or equal to that of π' for all states, i.e. $\pi \geq \pi'$ if and only if $V^{\pi}(\boldsymbol{x}) \geq V^{\pi'}(\boldsymbol{x})$ for all $\boldsymbol{x} \in \boldsymbol{X}$. There is at least one *optimal policy* π^* that is better than or equal to all other policies; its value function is the *optimal value function* V^* and is defined as:

$$V^*(\boldsymbol{x}) = \max_{\pi}\{V^{\pi}(\boldsymbol{x})\}, \forall \boldsymbol{x} \in \boldsymbol{X}. \tag{6.3}$$

The optimal value function and the optimal policy are related to the Bellman (1957) operators. The Bellman operators allow us to express relationships between the value of a state and the values of its successor states: the value of the start state $\boldsymbol{x}$ is equal to the immediate reward plus the (discounted) value of the successor state $\boldsymbol{x}'$.

Definition 6.4. *Bellman operator, (Bellman, 1957). The Bellman operator, denoted as $\mathcal{F}^{\pi} : \mathbb{R}^{|\boldsymbol{X}|} \to \mathbb{R}^{|\boldsymbol{X}|}$, for a policy π is defined as follows:*

$$(\mathcal{F}^{\pi}V)(\boldsymbol{x}) = R(\boldsymbol{x}, \pi(\boldsymbol{x})) + \gamma \sum_{\boldsymbol{x}'} P(\boldsymbol{x}'|\boldsymbol{x}, \pi(\boldsymbol{x}))V(\boldsymbol{x}'). \tag{6.4}$$

The value function of a policy π is the fixed point of $\mathcal{F}^{\pi}$ such that $V^{\pi} = \mathcal{F}^{\pi}V^{\pi}$.

As reported in equation (6.3), the optimal value function is defined by a set of non-linear equations; thus, the value of a state must be the maximal expected value achievable by any policy starting at that state.

Definition 6.5. *Bellman optimality operator, (Bellman, 1957). The Bellman optimality operator, denoted as $\mathcal{F}^* : \mathbb{R}^{|\boldsymbol{X}|} \to \mathbb{R}^{|\boldsymbol{X}|}$, is defined as:*

$$(\mathcal{F}^*V)(\boldsymbol{x}) = \max_{a}\left\{R(\boldsymbol{x}, a) + \gamma \sum_{\boldsymbol{x}'} P(\boldsymbol{x}'|\boldsymbol{x}, a)V(\boldsymbol{x}')\right\}. \tag{6.5}$$

The optimal value function V^* is the fixed point of $\mathcal{F}^*$ such that $V^* = \mathcal{F}^*V^*$.

We can define the policy obtained by acting greedily relative to V as follows:

$$greedy(V)(\boldsymbol{x}) = \arg\max_{a}\left\{R(\boldsymbol{x}, a) + \gamma \sum_{\boldsymbol{x}'} P(\boldsymbol{x}'|\boldsymbol{x}, a)V(\boldsymbol{x}')\right\}. \tag{6.6}$$

The *greedy policy* relative to the optimal value function V^* is the optimal policy $\pi^* = greedy(V^*)$.

6.2 Solving Markov decision processes

Solving a Markov decision process consists of constructing an optimal policy π^*. There are different algorithms to compute optimal policies in MDPs; we present two most popular dynamic programming methods, namely *policy iteration* and *value iteration*, and then we introduce the *linear programming* method.

6.2.1 Policy iteration

The policy iteration algorithm iterates over policies, producing an improved policy at each iteration. This algorithm consists of two components, called *policy evaluation* and *policy improvement*, and it can be shown to converge to the optimal policy (Howard, 1960; Bertsekas and Tsitsiklis, 1996). This algorithm can be described as follows.

For the policy evaluation part (lines 3 - 10 of Algorithm 6.1), consider a sequence of value functions $V_0, V_1, \ldots$, each mapping $\boldsymbol{X}$ to $\mathbb{R}$. The initial value function, V_0, is chosen arbitrarily, and the successive value functions are obtained by using the Bellman operator (6.4) as an update rule for each state $\boldsymbol{x} \in \boldsymbol{X}$. The sequence $(V_j)_{j=0}^{\infty}$ converges to V^π because of the Bellman operator; thus, $V_\infty = V^\pi$ is a fixed point for this update rule. In practice, it is possible to stop the policy evaluation part when the Bellman error of V_j is less then a small amount $\epsilon > 0$, i.e. $err(V_j) = ||\mathcal{F}^* V_j - V_j||_\infty = \max_{\boldsymbol{x}}\{\mathcal{F}^* V_j(\boldsymbol{x}) - V_j(\boldsymbol{x})\} < \epsilon$. To produce successive approximation V_{j+1} from V_j, the iterative policy evaluation updates the value of one state based on the values of all possible successor states (rather than on a sample of the next state), so it performs a so called *full backup*.

Once we have determined the value function V^π for an arbitrary policy π, we can perform the policy improvement procedure (lines 12 - 18 of Algorithm 6.1) by selecting the greedy policy for each state $\boldsymbol{x}$ according to equation (6.6).

Each policy evaluation part is started with the value function from the previous policy. This typically results in a great increase of the speed of convergence of policy evaluation, so the algorithm converges in a few iterations, but in $O(|\boldsymbol{X}|^2 \times |\boldsymbol{A}| + |\boldsymbol{X}|^3)$ (Littman et al., 1995). Mansour and Singh (1999) gave an upper bound on the number of iterations equal to $|\boldsymbol{A}|^{|\boldsymbol{X}|}/|\boldsymbol{X}|$, while Ye (2011) proved that policy iteration is a strongly polynomial-time algorithm for solving MDPs with a fixed discount factor.

6.2.2 Value iteration

Value iteration (Bellman, 1957) can be seen as a special case of the policy iteration when the policy evaluation step is stopped after just one *sweep* (i.e. one backup of each state). Thus, the value iteration algorithm effectively combines in each of its sweeps one sweep of policy evaluation and one sweep of policy improvement (lines 4 - 8 of Algorithm 6.2). Unlike policy iteration, there is no explicit policy, so the intermediate value functions may not correspond to any policy. Like policy iteration, value iteration requires an infinite number of iterations to converge to V^*. In practice, it is possible to stop the algorithm once the value function changes by only a small amount $\epsilon > 0$ in a sweep (Sutton and Barto, 1998). Value iteration approximates the optimal value function by successive iterations that can be performed in $O(|\boldsymbol{X}|^2 \times |\boldsymbol{A}|)$, but the number of iterations required can grow exponentially in the discount factor (Condon, 1992).

Algorithm 6.1 Policy iteration

```
Require: MDP $(\boldsymbol{X}, \boldsymbol{A}, R, P)$, $\epsilon > 0$.
Ensure: optimal policy $\pi^*$.
1: Initialize $V(\boldsymbol{x})$, $\pi(\boldsymbol{x})$ $\forall \boldsymbol{x} \in \boldsymbol{X}$
2: repeat
3:   repeat
4:     $\Delta \leftarrow 0$
5:     for each $\boldsymbol{x} \in \boldsymbol{X}$ do
6:       $v \leftarrow V(\boldsymbol{x})$
7:       $V(\boldsymbol{x}) \leftarrow (\mathcal{F}^{\pi} V)(\boldsymbol{x})$
8:       $\Delta \leftarrow \max\{\Delta, |v - V(\boldsymbol{x})|\}$
9:     end for
10:  until $(\Delta < \epsilon)$
11:  $stable_{\pi} \leftarrow true$
12:  for each $\boldsymbol{x} \in \boldsymbol{X}$ do
13:    $a \leftarrow \pi(\boldsymbol{x})$
14:    $\pi(\boldsymbol{x}) \leftarrow greedy(V)(\boldsymbol{x})$
15:    if $(a \neq \pi(\boldsymbol{x}))$ then
16:      $stable_{\pi} \leftarrow false$
17:    end if
18:  end for
19: until $(stable_{\pi})$
```

Algorithm 6.2 Value iteration

```
Require: MDP $(\boldsymbol{X}, \boldsymbol{A}, R, P)$, $\epsilon > 0$.
Ensure: optimal policy $\pi^*$.
1: Initialize $V(\boldsymbol{x})$ $\forall \boldsymbol{x} \in \boldsymbol{X}$
2: repeat
3:   $\Delta \leftarrow 0$
4:   for each $\boldsymbol{x} \in \boldsymbol{X}$ do
5:     $v \leftarrow V(\boldsymbol{x})$
6:     $V(\boldsymbol{x}) \leftarrow (\mathcal{F}^{*} V)(\boldsymbol{x})$
7:     $\Delta \leftarrow \max\{\Delta, |v - V(\boldsymbol{x})|\}$
8:   end for
9: until $(\Delta < \epsilon)$
10: for each $\boldsymbol{x} \in \boldsymbol{X}$ do
11:   $\pi(\boldsymbol{x}) \leftarrow greedy(V)(\boldsymbol{x})$
12: end for
```

6.2.3 Linear programming

Linear programming provides an alternative method compared to value iteration and policy iteration for solving MDPs, where the problem of finding a value function is formulated as a linear program (LP), see D'Epenoux (1963). Let S be the number of possible states of system, then the LP variables are $V_1, \dots, V_S$, where each V_s represents $V(\boldsymbol{x}_s)$, i.e. the value of starting at the s-th state of the system. The linear program is defined as follows:

$$\text{vars}: \; V_1, \dots, V_S \tag{6.7}$$

$$\min: \; \sum_{s=1}^{S} \alpha(\boldsymbol{x}_s) V_s \tag{6.8}$$

$$\text{s.t.}: \; V_s \geq R(\boldsymbol{x}_s, a) + \gamma \sum_j P(\boldsymbol{x}_j | \boldsymbol{x}_s, a) V(\boldsymbol{x}_j), \; \forall \boldsymbol{x}_s \in \boldsymbol{X}, \forall a \in \boldsymbol{A}, \tag{6.9}$$

where $\alpha(\boldsymbol{x}_s)$ are positive *state relevance weights*. Note that the policy is implicitly represented by the slack variables of the LP. In fact, for each $\boldsymbol{x}_s$ there is at least one action a for which the corresponding state value constraint is tight, i.e. the optimal action for $\boldsymbol{x}_s$.

There are several algorithms for solving LPs (Vanderbei, 2001), among which the well known *simplex* algorithm introduced by Dantzig (1963). This algorithm starts at a vertex of the polyhedron corresponding to the LP and then follows edges of the polyhedron that lead to vertices of lower value, until an optimal vertex is reached, or an edge along which the objective function is unbounded from below is found. The choice of which edge to follow is controlled by a pivoting rule; for example, the Dantzig's pivoting rule asserts that the non-basic variable with the most negative reduced cost is chosen to enter the basis.

There is a close connection between policy iteration method, which updates actions in multiple states simultaneously, and the simplex algorithm, which updates an action in only one state at a time. In fact, a violated constraint in the LP formulation provides an opportunity for policy improvement by pivoting on the corresponding variable in a simplex algorithm for the dual problem (Ye, 2011).

The simplex method is very efficient in practice and, even if its worst-case complexity is exponential (Klee and Minty, 1972), it has been proved to be strongly polynomial when used to solve MDPs with any value of the discount factor (Post and Ye, 2013).

6.3 Factored Markov decision processes

One of the main problems with MDPs is that the number of possible states becomes very large when they are used to model real life domains. In fact, these domains can have a significant internal structure that MDPs are not able to model. We refer to two main types of structure: *additive*, i.e. large scale systems can often be decomposed into a combination of locally interacting components, and *context-specific*, i.e. large systems may be influenced directly by only a small number of parts at any given point in time.

Factored MDPs are one approach to represent large and structured domains effectively (Boutilier et al., 1995). In this framework, a state is described implicitly as an assignment of values to some set of state variables and a dynamic Bayesian network is then used as a compact representation of the transition dynamics.

Definition 6.6. *Factored MDP, (Boutilier et al., 1995). A factored MDP is an MDP* $(\boldsymbol{X}, \boldsymbol{A}, R, P)$ *where: the set of states* $\boldsymbol{X}$ *is described via a set of random variables* $\boldsymbol{X} = \{X_1, \ldots, X_N\}$*;* $\boldsymbol{A}$ *is the finite set of actions; R is the reward function and it is factored additively into a set of L localized functions:* $R(\boldsymbol{x}, a) = \sum_{l=1}^{L} R_l(\boldsymbol{L}_l^a, a) \in \mathbb{R}$ *in which the* $Scope[R_l]$ *is restricted to* $\boldsymbol{L}_l^a \subseteq \boldsymbol{X}$*; the transition model P is a set of dynamic Bayesian networks, one network* $\mathcal{B}_2^a$ *for each action* $a \in \boldsymbol{A}$*. The transition graph of a DBN is a two-layer directed acyclic graph* $\mathcal{G}_{\mathcal{B}_{2T}^a}$ *whose nodes are* $\{X_1, \ldots, X_N, X'_1, \ldots, X'_N\}$*. Each node* X' *is associated with a conditional probability distribution* $P_{\mathcal{B}_{2T}^a}(X'|Pa(X'))$*. The transition probability is then defined as* $P(\boldsymbol{x}'|\boldsymbol{x}, a) = \prod_{X'} P_{\mathcal{B}_{2T}^a}(X' = x'_n|Pa(X') = pa_u)$*.*

Factorization allows a very large MDP to be represented compactly; however, solving it exactly may still be intractable: exact solution algorithms require the manipulation of the value function, whose representation is linear in the number of states, but exponential in the number of state variables. Moreover, factored dynamics and rewards do not ensure that the value function has a factored representation (Koller and Parr, 1999). Dynamic programming methods have been adapted to factored representations, such as *structured policy iteration* (Boutilier et al., 1995) and *structured value iteration* (Boutilier et al., 2000), that exploit the context-specific structure in the value function using decision trees manipulations. Approximate linear programming methods have emerged as promising approaches to solve them efficiently (Guestrin et al., 2003).

6.3.1 Approximate linear programming

A key to performing efficient computations over the exponentially-sized state spaces encountered in factored MDPs is the use of an approximate value function. A very popular choice for this approximation is by using linear regression (Bellman and Dreyfus, 1959; Tsitsiklis and van Roy, 1996; Koller and Parr, 1999), where the space of allowable value functions is specified via a set of basis functions.

Definition 6.7. *Factored linear value function, (Koller and Parr, 1999). A factored linear value function over a set of basis functions $\boldsymbol{H} = \{h_1, \ldots, h_K\}$ is a function V that can be written as $V(\boldsymbol{x}) = \sum_{k=1}^{K} w_k h_k(\boldsymbol{x})$ for some coefficients $\boldsymbol{w} = (w_1, \ldots, w_K)'$.*

Once the set of basis functions $\boldsymbol{H}$ has been selected, the problem becomes one of finding values for the weights $\boldsymbol{w}$ such that $\boldsymbol{Hw}$ will yield a good approximation to the true value function. One efficient approach to solving this problem is based on the LP formulation defined in (6.7)-(6.9). Specifically, Schweitzer and Seidmann (1985) restricted the space of allowable value functions to the linear space spanned by K basis functions. The *approximate linear program* (ALP) formulation for factored MDPs is:

$$\text{vars}: \; w_1, \ldots, w_K \tag{6.10}$$

$$\text{min}: \; \sum_{\boldsymbol{x}} \alpha(\boldsymbol{x}) \sum_{k=1}^{K} w_k h_k(\boldsymbol{x}) \tag{6.11}$$

$$\text{s.t.}: \; \sum_{k=1}^{K} w_k h_k(\boldsymbol{x}) \geq R(\boldsymbol{x}, a) + \gamma \sum_{\boldsymbol{x}'} P(\boldsymbol{x}'|\boldsymbol{x}, a) \sum_{k=1}^{K} w_k h_k(\boldsymbol{x}'), \; \forall \boldsymbol{x} \in \boldsymbol{X}, \forall a \in \boldsymbol{A}. \tag{6.12}$$

This ALP is guaranteed to be feasible if a constant function, i.e. a function with the same constant value for all states, is included in the set of basis function (Guestrin et al., 2002). We have to point out two aspects of this ALP formulation. Firstly, the choice of state relevance weights $\alpha(\boldsymbol{x})$ becomes important because, unlike the exact case, the solution obtained may differ for different choices of the positive weights. Secondly, in general, there is no guarantee about the quality of the greedy policy generated from the approximation $\boldsymbol{Hw}$. However, de Farias and van Roy (2003) provided an analysis of the error relative to that of the best possible approximation in the subspace and some guidance about the selection of $\alpha(\boldsymbol{x})$ in order to improve the quality of the approximation.

6.3.2 Backprojection function

A key component of the ALP formulation is the computation of the one-step lookahead function, called *backprojection*, $g_k^a(\boldsymbol{x})$ of the basis function h_k for the action a:

$$g_k^a(\boldsymbol{x}) = \sum_{\boldsymbol{x}'} P(\boldsymbol{x}'|\boldsymbol{x}, a) h_k(\boldsymbol{x}'). \tag{6.13}$$

This computation is performed efficiently when the transition model is factored using a DBN, and each basis functions h_k has scope restricted to a small set of variables, i.e. $Scope[h_k] = \boldsymbol{C}_k$. In fact, the scope of the backprojection g_k^a through a DBN $\mathcal{B}_2^a$ is the set of parents of $\boldsymbol{C}'_k$ in the transition graph $\mathcal{G}_{\mathcal{B}_{2T}^a}$, i.e. the $Scope[g_k^a] = \bigcup_{X'_n \in \boldsymbol{C}'_k} Pa_{\mathcal{B}_{2T}^a}(X'_n) = \boldsymbol{B}_k^a$ (Guestrin et al., 2003). The advantage is that each backprojection can be computed by only enumerating settings of variables in $\boldsymbol{B}_k^a$, rather than settings of all variables $\boldsymbol{X}$. The cost of the computation depends linearly on $|Val(\boldsymbol{B}_k^a)|$, which depends on $\boldsymbol{C}_k$, and on the complexity of the process dynamics. The backprojection of the basis function h_k is then computed as follows:

$$g_k^a(\boldsymbol{x}) = \sum_{\boldsymbol{c}' \in \boldsymbol{C}'_k} \prod_{X'_n \in \boldsymbol{C}'_k} P_{\mathcal{B}_2^a}(\boldsymbol{c}'[X'_n]|\boldsymbol{b}_k^a, a) h_k(\boldsymbol{c}'),\ \forall \boldsymbol{b}_k^a \in \boldsymbol{B}_k^a, \tag{6.14}$$

where $\boldsymbol{c}'[X'_n]$ denotes the value of variable X'_n in the instantiation $\boldsymbol{c}'$.

6.3.3 Efficient constraints representation

The ALP formulation has the effect of reducing the number of free variables in the linear program from $|\boldsymbol{X}|$ to K, but the number of constraints remains $|\boldsymbol{X}| \times |\boldsymbol{A}|$. However, given that the functionals in the constraints (6.12) have restricted scope, i.e. the constraints can be satisfied in a structured form and without being enumerated exhaustively, it is possible to use some methods to exploit this peculiarity.

Guestrin et al. (2003) observed that the constraints (6.12) are all in the form:

$$0 \geq R(\boldsymbol{x}, a) + \sum_{k=1}^{K} w_k F_k(\boldsymbol{x}, a),\ \forall \boldsymbol{x} \in \boldsymbol{X}, \forall a \in \boldsymbol{A}, \tag{6.15}$$

where $F_k(\boldsymbol{x}, a) = \gamma g_k^a(\boldsymbol{x}) - h_k(\boldsymbol{x})$ has the scope restricted to $\boldsymbol{C}_k \cup \boldsymbol{B}_k^a$. Thus, it is possible to replace the entire set of constraints (6.15) by $|\boldsymbol{A}|$ equivalent non-linear constraints:

$$0 \geq \max_{\boldsymbol{x}} \left\{ R(\boldsymbol{x}, a) + \sum_{k=1}^{K} w_k F_k(\boldsymbol{x}, a) \right\},\ \forall a \in \boldsymbol{A}. \tag{6.16}$$

The approximate linear program formulation reported in (6.10)-(6.12) becomes:

$$\text{vars} : w_1, \ldots, w_K \tag{6.17}$$

$$\min : \sum_{k=1}^{K} \alpha_k w_k \tag{6.18}$$

$$\text{s.t.} : 0 \geq \max_{\boldsymbol{x}} \left\{ R(\boldsymbol{x}, a) + \sum_{k=1}^{K} w_k \left(\gamma g_k^a(\boldsymbol{x}) - h_k(\boldsymbol{x}) \right) \right\}, \ \forall a \in \boldsymbol{A}. \tag{6.19}$$

The basis weights α_k are defined as $\alpha_k = \sum_{\boldsymbol{c}_k \in \boldsymbol{C}_k} \alpha(\boldsymbol{c}_k) h_k(\boldsymbol{c}_k)$, where $\alpha(\boldsymbol{c}_k)$ represents the marginal of the state relevance weights over $Val(\boldsymbol{C}_k)$ of the basis function h_k.

The new set of non-linear constraints (6.19) can be implemented by a set of linear constraints using a construction that follows the structure of the variable elimination algorithm in BNs (Guestrin et al., 2003). The main idea is maximizing over variables one at a time instead of summing all functions and then doing the maximization. Note that computing the optimal elimination order is an NP-hard problem (Arnborg et al., 1987); however, good heuristics have been introduced (Reed, 1992; Becker and Geiger, 2001).

Schuurmans and Patrascu (2001) solved the constraints satisfaction problem by the *cutting plane method* (Bertsekas and Tsitsiklis, 1996). The approach iteratively searches for the most violated constraint for each action a:

$$\arg\max_{\boldsymbol{x}} \left\{ R(\boldsymbol{x}, a) + \sum_{k=1}^{K} w_k^{(i)} F_k(\boldsymbol{x}, a) \right\}, \tag{6.20}$$

with respect to the solution $\boldsymbol{w}^{(i)}$ of a relaxed ALP in the i-th iteration. The most violated constraint is added to the ALP, which is then solved for a new vector $\boldsymbol{w}^{(i+1)}$. This procedure is iterated until no violated constraint is found; the last vector $\boldsymbol{w}^{(i)}$ is then an optimal solution to the ALP problem.

The space complexity of both methods is exponential in the tree-width of the constraints space. However, such problems can be still solved approximately. For example, de Farias and van Roy (2004) proposed Monte Carlo approximations of the constraints space. Kveton and Hauskrecht (2005) introduced a Markov chain Monte Carlo sample for searching the most violated constraints. Kveton and Hauskrecht (2008) described a different ALP based on the inner approximations to the feasible region; in particular, they decomposed the constraints space into a set of low dimensional spaces without an exponential dependence on the tree-width of the original constraints space.

6.4 Structured continuous time Markov decision processes

In a factored MDP the system evolves at a fixed-size temporal instant and the decision maker can choose actions only at discrete points in time. In this section we consider the extension of this model, called *structured continuous time MDP* (Kan and Shelton, 2008), in which the system evolves in continuous time and the actions are chosen at every transition (note that the time between decisions follows an exponential distribution). The system is assumed to have a structure that can be exploited by continuous time Bayesian networks. We restrict our attention to infinite-horizon models and assume all models have time homogeneous transition probabilities and rewards. We refer to Hu and Yue (2007); Guo and Hernandez-Lerma (2009) for material on continuous time MDPs.

Definition 6.8. *Structured CTMDP, (Kan and Shelton, 2008). A structured continuous time MDP is an MDP $(\boldsymbol{X}, \boldsymbol{A}, r, P)$ where: the set of states $\boldsymbol{X}$ is described via a set of random variables $\boldsymbol{X} = \{X_1, \ldots, X_N\}$ where each X has a finite domain of values $Val(X) = \{x_1, \ldots, x_I\}$; $\boldsymbol{A}$ is the finite set of actions; r is the reward rate while taking action $a \in \boldsymbol{A}$ in state $\boldsymbol{x} \in \boldsymbol{X}$ and it is factored additively into a set of L localized functions: $r(\boldsymbol{x}, a) = \sum_{l=1}^{L} r_l(\boldsymbol{L}_l^a, a) \in \mathbb{R}$ in which the $Scope[r_l]$ is restricted to $\boldsymbol{L}_l^a \subseteq \boldsymbol{X}$; the transition model P is a set of continuous time Bayesian networks, one network $\mathcal{N}^a$ for each action $a \in \boldsymbol{A}$. The transition graph of a CTBN is a directed graph $\mathcal{G}_{\mathcal{N}^a}$ whose nodes are $\{X_1, \ldots, X_N\}$. Each node X is associated with a conditional intensity matrix $\boldsymbol{Q}^a_{X|Pa(X)}$ that consists of a set of intensity matrices, one intensity matrix for each instantiation pa_u of its parents $Pa(X)$ is:*

$$\boldsymbol{Q}^a_{X|pa_u} = \begin{bmatrix} -q^a_{x_1|pa_u} & q^a_{x_1,x_2|pa_u} & \cdot & q^a_{x_1,x_I|pa_u} \\ q^a_{x_2,x_1|pa_u} & -q^a_{x_2|pa_u} & \cdot & q^a_{x_2,x_I|pa_u} \\ \cdot & \cdot & \cdot & \cdot \\ q^a_{x_I,x_1|pa_u} & q^a_{x_I,x_2|pa_u} & \cdot & -q^a_{x_I|pa_u} \end{bmatrix},$$

where $q^a_{x_i,x_j|pa_u}$ is the intensity of transitioning from x_i to x_j under action a when $Pa(X)$ is set to the configuration pa_u, while $q^a_{x_i|pa_u} = \sum_{x_j \neq x_i} q^a_{x_i,x_j|pa_u}$. If $X(0) = x_i$, then the system stays in state x_i for an amount of time exponentially distributed with parameter $q^a_{x_i|pa_u}$. Upon transitioning, X shifts to state x_j with probability $q^a_{x_i,x_j|pa_u}/q^a_{x_i|pa_u}$.

6.4.1 From discrete to continuous time

The theory introduced for factored MDPs can be extended to structured CTMDPs. Specifically, we revise the reward model, the optimality criteria for each policy and initial state and the Bellman operators in the continuous time case.

The reward model is a function $r(\boldsymbol{x}, a)$ that represents the (bounded) reward rate while taking action a in state $\boldsymbol{x}$. There may also be an instantaneous reward for transitioning from one state to another, but we assume it is equal to zero for simplicity. The rewards can be discounted exponentially in time at a rate of $\beta > 0$; this means that the present value of 1 unit received t time units in the future equals $e^{-\beta t}$. By setting $e^{-\beta t} = \gamma$, where γ denotes the discrete time discount factor, we have that $\gamma = 0.95$ corresponds to $\beta = -\log(\gamma) = 0.05$ (Puterman, 1994).

The value function for infinite-horizon discounted return in continuous time is:

$$V^{\pi}(\boldsymbol{x}) = \mathbb{E}_{\pi}\left[\int_0^{\infty} e^{-\beta t} r(\boldsymbol{X}(t), \pi(\boldsymbol{X}(t)))dt \mid \boldsymbol{X}(0) = \boldsymbol{x}\right]. \tag{6.21}$$

In a structured CTMDP, the transition rates and the reward rates are both bounded, and the action set and the states are both finite; this allows us to derive the Bellman operators in continuous time from the discrete time case (Kakumanu, 1977). Thus, the Bellman operator that defines the relationship between the value of a state and the values of its successor states is:

$$(\mathcal{F}^{\pi}V)(\boldsymbol{x}) = \frac{r(\boldsymbol{x}, \pi(\boldsymbol{x}))}{\beta + q_{\boldsymbol{x}}^{\pi(\boldsymbol{x})}} + \frac{q_{\boldsymbol{x}}^{\pi(\boldsymbol{x})}}{\beta + q_{\boldsymbol{x}}^{\pi(\boldsymbol{x})}} \sum_{\boldsymbol{x}' \neq \boldsymbol{x}} \frac{q_{\boldsymbol{x},\boldsymbol{x}'}^{\pi(\boldsymbol{x})}}{q_{\boldsymbol{x}}^{\pi(\boldsymbol{x})}} V(\boldsymbol{x}'). \tag{6.22}$$

This Bellman operator is similar to its discrete time counterpart (6.4) with a reward equal to $\frac{r(\boldsymbol{x},\pi(\boldsymbol{x}))}{\beta+q_{\boldsymbol{x}}^{\pi(\boldsymbol{x})}}$, a discount factor equal to $\frac{q_{\boldsymbol{x}}^{\pi(\boldsymbol{x})}}{\beta+q_{\boldsymbol{x}}^{\pi(\boldsymbol{x})}}$ and transition probabilities equal to $\frac{q_{\boldsymbol{x},\boldsymbol{x}'}^{\pi(\boldsymbol{x})}}{q_{\boldsymbol{x}}^{\pi(\boldsymbol{x})}}$.

The Bellman optimality operator in continuous time is defined as follows:

$$(\mathcal{F}^{*}V)(\boldsymbol{x}) = \sup_a \left\{ \frac{r(\boldsymbol{x}, a)}{\beta + q_{\boldsymbol{x}}^{a}} + \frac{q_{\boldsymbol{x}}^{a}}{\beta + q_{\boldsymbol{x}}^{a}} \sum_{\boldsymbol{x}' \neq \boldsymbol{x}} \frac{q_{\boldsymbol{x},\boldsymbol{x}'}^{a}}{q_{\boldsymbol{x}}^{a}} V(\boldsymbol{x}') \right\}. \tag{6.23}$$

The existence of a solution V^* and of an optimal stationary policy π^* was shown by Howard (1960); Kakumanu (1971). Note that for some continuous time Markov control processes (such as controlled diffusion), the optimal value function is called the *Hamilton-Jacobi-Bellman* equation (Lions, 1983).

The value function for infinite-horizon average return in continuous time is:

$$V^{\pi}(\boldsymbol{x}) = \lim_{T\to\infty}\inf \frac{1}{T}\, \mathbb{E}_{\pi}\left[\int_0^T r(\boldsymbol{X}(t), \pi(\boldsymbol{X}(t)))dt \mid \boldsymbol{X}(0) = \boldsymbol{x}\right]. \tag{6.24}$$

In this case, the optimal policy π^* is characterized by a set of fixed point equations:

$$\frac{\rho^*}{q^a_{\boldsymbol{x}}} + V^*(\boldsymbol{x}) = \sup_a \left\{ \frac{r(\boldsymbol{x}, a)}{q^a_{\boldsymbol{x}}} + \sum_{\boldsymbol{x}' \neq \boldsymbol{x}} \frac{q^a_{\boldsymbol{x},\boldsymbol{x}'}}{q^a_{\boldsymbol{x}}} V(\boldsymbol{x}') \right\}, \tag{6.25}$$

which is different from the discrete time case because of the denominator $q^a_{\boldsymbol{x}}$. The existence of a solution for equation (6.25) is guaranteed under some standard assumptions, specifically the ergodicity condition of the resulting continuous time Markov chain (Guo and Hernandez-Lerma, 2003).

6.4.2 Uniformization

Instead of tackling the continuous time MDP directly, it is possible to convert the continuous time into a discrete time MDP using the *uniformization* technique (Bertsekas, 1987; Puterman, 1994). If the transition rates from each state are bounded by some constant κ such that

$$\sup_{\boldsymbol{x},a}\{q^a_{\boldsymbol{x}}\} \leq \kappa < \infty, \tag{6.26}$$

then this method can be seen as an equivalent process in which the system state is observed at random times exponentially distributed with parameter κ. The new transition model $\tilde{P}$ is then adjusted as follows:

$$\tilde{P}(\boldsymbol{x}'|\boldsymbol{x}, a) = \begin{cases} \kappa - q^a_{\boldsymbol{x}} & \text{if } \boldsymbol{x}' = \boldsymbol{x}, \\ q^a_{\boldsymbol{x},\boldsymbol{x}'} & \text{if } \boldsymbol{x}' \neq \boldsymbol{x}, \end{cases} \tag{6.27}$$

while the new reward function $\tilde{r}$ for the discounted case is:

$$\tilde{r}(\boldsymbol{x}, a) = r(\boldsymbol{x}, a)\frac{\beta + q^a_{\boldsymbol{x}}}{\beta + \kappa}. \tag{6.28}$$

As highlighted by Kan and Shelton (2008), this conversion is not the same as constructing the discrete time MDP corresponding to a fixed sample rate. In fact, the uniformization technique constructs a new discrete time MDP in which each time step corresponds to a single transition in the continuous time domain, that does not correspond to a fixed amount of time in the original process. Moreover, even simple sparse CTBNs can lead to fully connected DBNs, if they are sampled at a uniform rate.

6.4.3 Approximate linear programming

If a factored linear value function can be used to approximate well the value function, then it is possible to solve efficiently the structured CTMDP by approximate linear programming (Kan and Shelton, 2008). We derive the ALP formulation from that of factored MDPs. Recall the ALP formulation for expected discounted return in factored MDPs (6.10)-(6.12) and the Bellman optimality operator in continuous time (6.23). Thus, the set of constraints for the structured CTMDP becomes:

$$\sum_{k=1}^{K} w_k h_k(\boldsymbol{x}) \geq \frac{r(\boldsymbol{x}, a)}{\beta + q_{\boldsymbol{x}}^a} + \frac{q_{\boldsymbol{x}}^a}{\beta + q_{\boldsymbol{x}}^a} \sum_{\boldsymbol{x}' \neq \boldsymbol{x}} \frac{q_{\boldsymbol{x},\boldsymbol{x}'}^a}{q_{\boldsymbol{x}}^a} \sum_{k=1}^{K} w_k h_k(\boldsymbol{x}'),\ \forall \boldsymbol{x} \in \boldsymbol{X}, \forall a \in \boldsymbol{A}. \tag{6.29}$$

By multiplying both sides of the inequality (6.29) by $\beta + q_{\boldsymbol{x}}^a$, moving everything from the left hand side to the right hand side and rearranging, we obtain the following set of constraints:

$$0 \geq r(\boldsymbol{x}, a) + \sum_{k=1}^{K} w_k(-\beta h_k(\boldsymbol{x}) - q_{\boldsymbol{x}}^a h_k(\boldsymbol{x}) + \sum_{\boldsymbol{x}' \neq \boldsymbol{x}} q_{\boldsymbol{x},\boldsymbol{x}'}^a h_k(\boldsymbol{x}')),\ \forall \boldsymbol{x} \in \boldsymbol{X}, \forall a \in \boldsymbol{A}. \tag{6.30}$$

This formulation can be simplified in structured CTMDPs. In fact, in the underlying continuous time Bayesian network model, the system stays in state $\boldsymbol{x}$ for an amount of time exponentially distributed with parameter $q_{\boldsymbol{x}}$:

$$q_{\boldsymbol{x}} = \sum_{\boldsymbol{x}'} q_{\boldsymbol{x},\boldsymbol{x}'} = \sum_{X_n \in \boldsymbol{X}} \sum_{x_n' \neq x_n} q_{x_n,x_n'|pa_u}^a, \tag{6.31}$$

and only one single variable change state at any single instant. Moreover, given the values of the parents, the rate at which a variable transitions is independent of all the other variables. Therefore, we can rewrite the set of constraints (6.30) $\forall \boldsymbol{x} \in \boldsymbol{X}$, $\forall a \in \boldsymbol{A}$ as:

$$\begin{aligned} 0 \geq r(\boldsymbol{x}, a) + \sum_{k=1}^{K} w_k(-\beta h_k(\boldsymbol{x}) \\ &- \sum_{X_n \in \boldsymbol{C}_k} \sum_{x_n' \neq x_n} q_{x_n,x_n'|pa_u}^a h_k(\boldsymbol{x}) - \sum_{X_n \notin \boldsymbol{C}_k} \sum_{x_n' \neq x_n} q_{x_n,x_n'|pa_u}^a h_k(\boldsymbol{x}) \\ &+ \sum_{X_n \in \boldsymbol{C}_k} \sum_{x_n' \neq x_n} q_{x_n,x_n'|pa_u}^a h_k(\boldsymbol{x}[x_n']) + \sum_{X_n \notin \boldsymbol{C}_k} \sum_{x_n' \neq x_n} q_{x_n,x_n'|pa_u}^a h_k(\boldsymbol{x})), \end{aligned} \tag{6.32}$$

where $\boldsymbol{x}[x_n']$ denotes the state assignment that is the same as $\boldsymbol{x}$ except that X_n equals x_n' and then we delete the two components over $X_n \notin \boldsymbol{C}_k$ obtaining the following:

$$0 \geq r(\boldsymbol{x}, a) + \sum_{k=1}^{K} w_k(-\beta h_k(\boldsymbol{x}) + \sum_{X_n \in \boldsymbol{C}_k} \sum_{x_n' \neq x_n} q_{x_n,x_n'|pa_u}^a (h_k(\boldsymbol{x}[x_n']) - h_k(\boldsymbol{x}))). \tag{6.33}$$

The ALP for infinite-horizon discounted return in structured CTMDPs is the following:

$$\text{vars}: \; w_1, \dots, w_K \tag{6.34}$$

$$\min: \; \sum_{k=1}^{K} \alpha_k w_k \tag{6.35}$$

$$\text{s.t.}: \; 0 \geq \max_{\boldsymbol{x}} \left\{ r(\boldsymbol{x}, a) + \sum_{k=1}^{K} w_k \left(g_k^a(\boldsymbol{x}) - \beta h_k(\boldsymbol{x}) \right) \right\}, \forall a \in \boldsymbol{A}, \tag{6.36}$$

where we use the max operator to combine the constraints (6.33) for the same action a, obtaining $|\boldsymbol{A}|$ non-linear constraints. The scope of the backprojection g_k^a through a CTBN model $\mathcal{N}^a$ is the set of variables in $\boldsymbol{C}_k$ plus their parents in the transition graph $\mathcal{G}_{\mathcal{N}^a}$, i.e. the $Scope[g_k^a] = \bigcup_{X_n \in \boldsymbol{C}_k} X_n \cup Pa_{\mathcal{N}^a}(X_n) = \boldsymbol{B}_k^a$, while the backprojection is:

$$g_k^a(\boldsymbol{x}) = \sum_{X_n \in \boldsymbol{C}_k} \sum_{x'_n \neq x_n} q^a_{x_n, x'_n | \boldsymbol{b}_k^a[Pa(X_n)]} (h_k(\boldsymbol{x}[x'_n]) - h_k(\boldsymbol{x})), \tag{6.37}$$

where $\boldsymbol{b}_k^a[Pa(X_n)]$ denotes the value of the parents of X_n in the instantiation $\boldsymbol{b}_k^a$. This ALP can be solved through the same techniques used for factored MDPs, such as the variable elimination algorithm (Guestrin et al., 2003) and the cutting plane algorithm (Schuurmans and Patrascu, 2001). The comparison between discrete and continuous time models is shown in Figure 6.1. Using DBNs, the inter-time relationships are modeled with two nodes for the same random variable at current X and next time X', while using CTBNs, the two nodes are collapsed in one.

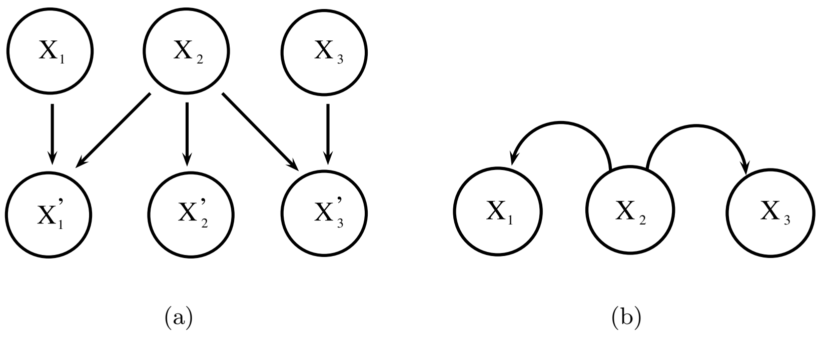

Figure 6.1: Discrete time (a) vs continuous time (b) representation three random variables $\boldsymbol{X} = \{X_1, X_2, X_3\}$. If the scope of the 1st basis function is $Scope[h_1] = \{X_1, X_2\} = \boldsymbol{C}_1$, then in the case (a) the scope of its backprojection is $Scope[g_1^a] = \bigcup_{X'_n \in \boldsymbol{C}'_1} Pa_{\mathcal{B}^a_{2T}}(X'_n) = \{X_1, X_2\}$, whereas in the case (b) it is $Scope[g_1^a] = \bigcup_{X_n \in \boldsymbol{C}_1} X_j \cup Pa_{\mathcal{N}^a}(X_n) = \{X_1, X_2\}$.

The revised version of the cutting plane algorithm introduced by Schuurmans and Patrascu (2001) is shown in Algorithm 6.3. It requires a structured CTMDP model and a maximum violation tolerance $\epsilon > 0$, and it ensures an optimal policy π^*. Given a solution $\boldsymbol{w}^{(i)}$ at iteration i, the additional violated constraints are found by selecting, for each action a, the state $\boldsymbol{x}$ which maximizes the violation magnitude (line 5 of Algorithm 6.3), where $F_k(\boldsymbol{x}, a) = g_k^a(\boldsymbol{x}) - \beta h_k(\boldsymbol{x})$. All violated constraints are added to the ALP formulation, which is then solved to obtain the next decision vector $\boldsymbol{w}^{(i+1)}$ (line 9 of Algorithm 6.3). This procedure is repeated until the maximum violated magnitude is less than the violation tolerance (lines 2 - 10 of Algorithm 6.3). The vector $\boldsymbol{w}$ obtained at the last iteration represents the best approximate solution of the ALP formulation and it is used to compute the optimal greedy policy (lines 11 - 13 of Algorithm 6.3).

The crucial part of this algorithm is due to the maximization problem solved in line 5. Note that the reward rate function r, the basis h_k and its backprojection g_k^a are functions that depend only on a small set of variables. Therefore, for a fixed vector $\boldsymbol{w}$, it is possible to compute the maximum over $\boldsymbol{x}$ using a cost network, while the computational efficiency depends on the elimination order of the network (Dechter, 1999).

Algorithm 6.3 Cutting plane algorithm for solving structured CTMDPs

```
Require: structured CTMDP $(\boldsymbol{X}, \boldsymbol{A}, r, P)$ and maximum violation tolerance $\epsilon > 0$.
Ensure: optimal policy $\pi^*$.
 1: Initialize $\boldsymbol{w} \leftarrow \mathbf{0}$, $consts \leftarrow \emptyset$
 2: repeat
 3:     $\Delta \leftarrow -\infty$
 4:     for each $a \in \boldsymbol{A}$ do
 5:         $sol \leftarrow \arg\max_{\boldsymbol{x}}\{r(\boldsymbol{x}, a) + \sum_{k=1}^{K} w_k F_k(\boldsymbol{x}, a)\}$
 6:         $consts \leftarrow consts \cup \text{ViolatedConstraint}(sol)$
 7:         $\Delta \leftarrow \max\{\Delta, \text{MaxViolation}(sol)\}$
 8:     end for
 9:     $\boldsymbol{w} \leftarrow \arg\min_{\boldsymbol{w}}\{\sum_{k=1}^{K} \alpha_k w_k\}$ subject to $consts$
10: until $(\Delta < \epsilon)$
11: for each $\boldsymbol{x} \in \boldsymbol{X}$ do
12:     $\pi(\boldsymbol{x}) \leftarrow greedy(\boldsymbol{H}\boldsymbol{w})(\boldsymbol{x})$
13: end for
```

6.5 Trading in structured continuous time domains

We consider the continuous time version of a simplified trading domain in which a portfolio manager has to construct a portfolio choosing among N securities. These securities can rise or fall randomly, and at any point in time the portfolio manager has to choose to buy, sell or be neutral about one of them in order to maximize the expected discounted return. In this context, it is possible to exploit both the additive feature of the domain, as it can be decomposed into individual securities, and the context-specific feature, as we consider that each security is influenced directly by only a small number of other securities that we call *neighbors*. Note that a similar problem has been presented by Strehl et al. (2007) where they used a factored MDP to model a simple stock trading domain.

6.5.1 Market dynamics

The continuous time domain is composed of a set of N securities $\boldsymbol{Y}$ and a set of N security-owner variables $\boldsymbol{Z}$; so the total state variables are $\boldsymbol{X} = \boldsymbol{Y} \cup \boldsymbol{Z}$ with $N \times 2$ variables. Each security Y_n is modeled as a binary random variable, $Y_n = 1$ means that the security is rising, while $Y_n = 0$ is falling. The security-owner variable Z_n is also binary, if the portfolio manager holds the n-th security, then $Z_n = 1$, otherwise $Z_n = 0$.

The market dynamics implement the basic idea that a falling security induces its neighbors to fall more quickly: the amount of time a securities Y_n is rising until it falls follows an exponential distribution with parameter $q_1 = q_1^{id} + q_1^{sys} \times$ number of falling neighbors / total neighbors, while the amount of time a securities Y_n is falling until it rises follows an exponential distribution with parameter: $q_0 = q_0^{id} + q_0^{sys} \times$ number of rising neighbors / total neighbors. Both q_1 and q_0 are composed of an idiosyncratic part, q^{id}, specific of each security plus a systematic part, q^{sys}, that depends on the local market conditions. Note that the idea of distinguishing between idiosyncratic and systematic components is widely accepted in finance (Elton et al., 2010).

At any point in time the portfolio manager must choose to buy (B_n) or sell (S_n) a security Y_n, or do nothing ($Nothing$), so we have $\boldsymbol{A} = \{B_1, S_1, \dots B_N, S_N, Nothing\}$ with $|\boldsymbol{A}| = (N \times 2) + 1$. The security-owner variables $\boldsymbol{Z}$ are used to control the exposures, i.e. it is not possible to buy a security already owned, or sell a security not owned.

The portfolio manager receives a global reward rate defined as the sum of N local reward rate functions, one for each security, such that $r(\boldsymbol{x}, a) = \sum_{l=1}^{N} r_l(Y_l, Z_l, a) \in \mathbb{R}$ with $Scope[r_l]$ restricted to $\{Y_l, Z_l\} \subseteq \boldsymbol{X}$. The portfolio manager receives a reward based on the ownership of rising and falling securities according to the following definition:

$$r_l(Y_l, Z_l) = \begin{cases} 2.0 & \text{if } Y_l = 1 \text{ and } Z_l = 1, \\ 1.5 & \text{if } Y_l = 0 \text{ and } Z_l = 0, \\ 0.5 & \text{if } Y_l = 1 \text{ and } Z_l = 0, \\ 0.0 & \text{if } Y_l = 0 \text{ and } Z_l = 1. \end{cases} \tag{6.38}$$

6.5.2 Proposed solution

A structured CTMDP can be used to model this dynamic context and it can be solved by the ALP (6.34)-(6.36) formulation. In order to apply this ALP we have to specify four elements: a CTBN model for each action, the basis functions, the backprojections of the basis functions and the basis weights.

For each action, we construct a CTBN model where the securities $\boldsymbol{Y}$ are identified as nodes. These nodes are connected according to a given structure that models the behavior of the interactions among securities. The entries of the conditional intensity matrices can be the same for all securities or be different as specified in the market dynamics section.

We use $K = N$ basis functions with $Scope[h_k] = \{Y_k\} = \boldsymbol{C}_k$ to approximate the value function. Each basis function h_k is defined as follows:

$$h_k(Y_k) = \begin{cases} 1.0 & \text{if } Y_k = 1, \\ 0.0 & \text{if } Y_k = 0. \end{cases} \tag{6.39}$$

The scope of the backprojection g_k^a is $\{Y_k\} \cup \{Y_n | Y_n \in neighbors(Y_k)\} = \boldsymbol{B}_k^a$, while the backprojection of the k-th basis function h_k is defined as follows:

$$g_k^a(\boldsymbol{x}) = q^a_{y_k, y'_k | \boldsymbol{b}_k^a[neighbors(Y_k)]}(h_k(\boldsymbol{x}[y'_k]) - h_k(\boldsymbol{x})). \tag{6.40}$$

For the basis weight $\alpha_k = \sum_{\boldsymbol{c}_k \in \boldsymbol{C}_k} \alpha(\boldsymbol{c}_k) h_k(\boldsymbol{c}_k)$, we use uniform state relevance weights, so $\alpha(\boldsymbol{c}_k) = \frac{1}{|\boldsymbol{C}_k|} = \frac{1}{2}$. Finally, it is possible to solve the ALP problem using the same techniques used for factored MDPs, such as the variable elimination algorithm and the cutting plane algorithm defined in the previous sections.

6.5.3 Examples with different structures

We consider two examples with different structures using the solution previously described.

In the first scenario, we assume to have only two securities, Y_1 and Y_2, so the set of states is $\boldsymbol{X} = \{Y_1, Y_2, Z_1, Z_2\}$ and the set of actions is $\boldsymbol{A} = \{B_1, S_1, B_2, S_2, Nothing\}$. We use two basis functions: h_1 with $Scope[h_1] = \{Y_1\}$ and h_2 with $Scope[h_2] = \{Y_2\}$ both defined as in (6.39). The CTBN model depicted in Figure 6.2 (a) is used to represent the interactions among the two securities and this structure is maintained for all actions. For the security Y_1, we assume that $q_1^{id} = 1.0$, $q_1^{sys} = 2.0$, and $q_0^{id} = 0.5$, $q_0^{sys} = 2.0$, so its intensity matrices are defined as follows:

$$\boldsymbol{Q}_{Y_1|Y_2=0} = \begin{bmatrix} -0.5 & 0.5 \\ 3.0 & -3.0 \end{bmatrix}, \ \boldsymbol{Q}_{Y_1|Y_2=1} = \begin{bmatrix} -2.5 & 2.5 \\ 1.0 & -1.0 \end{bmatrix}. \tag{6.41}$$

For security Y_2, we assume that $q_1^{id} = 1.2$, $q_1^{sys} = 1.8$, and $q_0^{id} = 0.7$, $q_0^{sys} = 1.8$, so its intensity matrices are the following:

$$\boldsymbol{Q}_{Y_2|Y_1=0} = \begin{bmatrix} -0.7 & 0.7 \\ 3.0 & -3.0 \end{bmatrix}, \ \boldsymbol{Q}_{Y_2|Y_1=1} = \begin{bmatrix} -2.5 & 2.5 \\ 1.2 & -1.2 \end{bmatrix}. \tag{6.42}$$

The backprojections defined in (6.40) are used to set and solve the ALP (6.34)-(6.36). The optimal policy extracted from its solution is shown in Figure 6.2 (b) in which for each possible state, grouped by $\{Y_1, Z_1\}$ and $\{Y_2, Z_2\}$, we have the optimal action to perform.

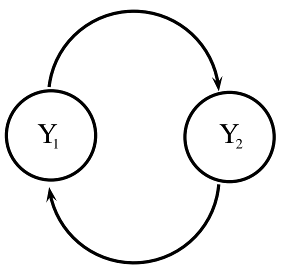

(a)

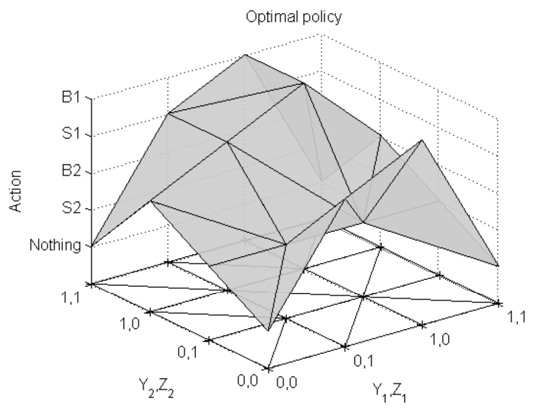

(b)

Figure 6.2: CTBN model (a) underpinning the structured CTMDP using two securities and the optimal policy (b) extracted from the ALP solution of the structured CTMDP.

In the second case, we assume a bidirectional ring structure underpinning the CTBN model, where each security Y_n is connected with its neighbors Y_{n-1} and Y_{n+1} (if $n = 1$, then $Y_{n-1} = Y_N$, and if $n = N$, then $Y_{n+1} = Y_1$). The set of states is composed of $N \times 2$ securities; the set of actions is constituted by $(N \times 2)+1$ actions and $K = N$ basis functions are used with $Scope[h_k] = \{Y_k\}$ as defined in (6.39). For securities in an odd position we use $q_1^{id} = 1.0$, $q_1^{sys} = 2.0$, and $q_0^{id} = 0.5$, $q_0^{sys} = 2.0$, while for securities in an even position we use $q_1^{id} = 1.2$, $q_1^{sys} = 1.8$, and $q_0^{id} = 0.7$, $q_0^{sys} = 1.8$. For example, the conditional intensity matrix $\boldsymbol{Q}_{Y_n|Y_{n-1},Y_{n+1}}$ when n is odd consists of four intensity matrices:

$$\boldsymbol{Q}_{Y_n|Y_{n-1}=0,Y_{n+1}=0} = \begin{bmatrix} -0.5 & 0.5 \\ 3.0 & -3.0 \end{bmatrix}, \ \boldsymbol{Q}_{Y_n|Y_{n-1}=0,Y_{n+1}=1} = \begin{bmatrix} -1.5 & 1.5 \\ 2.0 & -2.0 \end{bmatrix}, \quad (6.43)$$

$$\boldsymbol{Q}_{Y_n|Y_{n-1}=1,Y_{n+1}=0} = \begin{bmatrix} -1.5 & 1.5 \\ 2.0 & -2.0 \end{bmatrix}, \ \boldsymbol{Q}_{Y_n|Y_{n-1}=1,Y_{n+1}=1} = \begin{bmatrix} -2.5 & 2.5 \\ 1.0 & -1.0 \end{bmatrix}. \quad (6.44)$$

An instantiation of the bidirectional ring structure with $N = 4$ securities is shown in Figure 6.3 (a). The optimal policy extracted from the solution of the ALP (6.34)-(6.36) is shown in Figure 6.3 (b), where for each possible state, grouped by $\{Y_1, Z_1, Y_2, Z_2\}$ and $\{Y_3, Z_3, Y_4, Z_4\}$, we have the optimal action to perform.

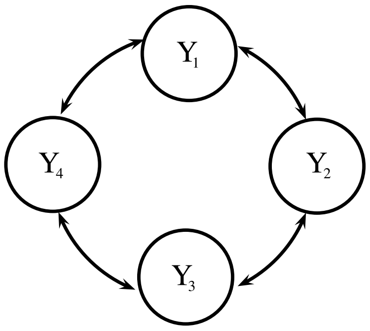

(a)

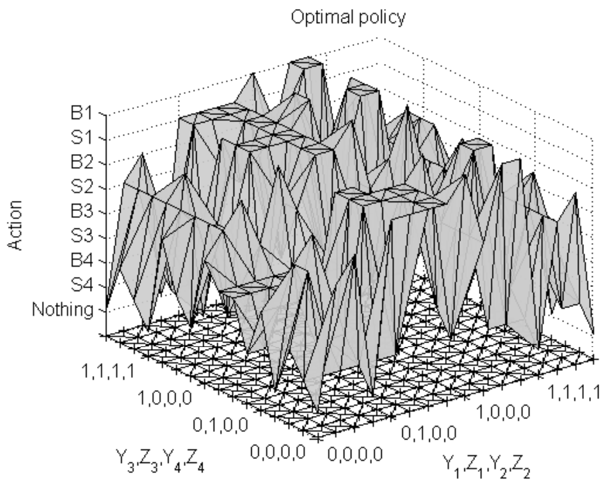

(b)

Figure 6.3: CTBN model (a) underpinning the structured CTMDP using four securities connected as a bidirectional ring and the optimal policy (b) extracted from the ALP solution of the structured CTMDP.

6.6 Discussion

After a brief introduction about the basic concepts, we have presented the Markov decision process framework in factored discrete time and structured continuous time domains and solved them via approximate linear programming. Both models can scale up to large problems by exploiting the additive and context-specific structures of complex systems and by using linear value function approximations. We have discussed differences and similarities of the two models in a comprehensive vision. A new formulation of a trading problem in structured continuous time domains has been presented, and different instantiations of this problem have been implemented and solved.

Chapter 7

Model-based reinforcement learning

Reinforcement learning is a broad area of machine learning that addresses the problem of how a decision-maker can learn a behavior through trial and error interactions with an uncertain environment. We focus on the specific area called model-based reinforcement learning in which the decision-maker uses his experience to construct a model of the environment. This model can then be used to predict the outcome of the decision-maker's actions in order to enhance his learning performance. We start this chapter introducing the general reinforcement learning framework, we continue describing the model-based reinforcement learning techniques in factored MDPs and a novel extension to structured CTMDPs, then we finish analyzing the trading problem discussed in the previous chapter.

7.1 General model

In the standard reinforcement learning model, a decision-maker learns from interactions with the environment or, in other terms, from repeated simulation. Specifically, at each interaction, the decision-maker receives the current state of the environment, he chooses an available action and then he performs it. The action causes the state transition of the environment and the value of this state transition is revealed to the decision-maker via a *reinforcement signal*. The goal of the decision-maker is to find a policy in order to maximize an expected return over the reinforcement signals (Kaelbling et al., 1996).

We assume that the current state of the environment is observed (i.e. full observability) and that the environment is stationary, so that the probabilities of the state transitions, as well as the corresponding reinforcement signals, do not change over time. We refer to Bertsekas and Tsitsiklis (1996); Sutton and Barto (1998); Wiering and van Otterlo (2012) for further material on this framework.

Definition 7.1. *Reinforcement learning (RL) model, (Kaelbling et al., 1996). A RL model consists of a tuple* $(\boldsymbol{X}, \boldsymbol{A}, \boldsymbol{S})$ *where:* $\boldsymbol{X}$ *is a finite set of states;* $\boldsymbol{A}$ *is a finite set of actions;* $\boldsymbol{S}$ *is a set of (bounded) reinforcement signals, where* $\boldsymbol{S} = \{s : s \in [0, s_{max}]\}$*.*

RL is defined by characterizing a learning problem not a learning method. Thus, any method that is well suited to solving this problem can be considered a RL method. For example, when the model of the environment is described as a Markov decision process and it is known, then dynamic programming methods and linear programming can be used to solve it. On the contrary, when a model of the environment is not available, then Monte Carlo methods can be used. These methods require only experiences (samples) of sequences of states, actions and rewards from on-line or simulated interactions with the environment. Rather than using a model to compute the value of a given state, they simply average many returns obtained starting in that state. Unfortunately, the variance of the returns can be high, which slows convergence (Fishman, 2003).

Reinforcement learning is primarily concerned with how to obtain an optimal policy when a model of the environment is not known in advance. The decision-maker must interact with the environment directly to obtain information which can be processed to produce an optimal policy. At this point he can learn a controller without learning a model (*model-free*) or learn a model and use it to derive a controller (*model-based*).

It is important to note that RL differs from the problem of supervised learning in many ways. Firstly, there is no presentation of input-output pairs, in fact the RL decision-maker is not told which actions to take, but he must discover which actions yield the most reward by trying them. Secondly, it is an interactive problem in which the evaluation of the system is often concurrent with learning. Thirdly, there is the exploration of the environment, in fact the RL decision-maker has to exploit what he already knows in order to obtain a reward, but he also has to explore in order to make better action selections in the future (Sutton and Barto, 1998; Wiering and Schmidhuber, 1998).

7.1.1 Exploration versus exploitation

One of the main challenges that arises in reinforcement learning is the trade-off between exploration and exploitation. The *exploration task* is performed by an action taken for the purpose of gathering new information, while the *exploitation task* is performed by an action tried in the past and found to be effective in producing rewards. In order to receive a near-optimal return, a balance between these two types of actions must be achieved.

There are different exploration heuristics used in RL; we present the most used ones (Thrun, 1992). The simplest action selection strategy is called *e-greedy*, and it consists of selecting the greedy action by default, but with probability e to choose an action at random from a uniform distribution. There are some variants of this strategy that start with a large value of e to encourage initial exploration and then slowly decrease, such as the *Boltzmann exploration*. If the parameter of e-greedy is made a function of time and the resulting sequence is tuned with care, then it can be made competitive with more sophisticated strategies. However, the best choice is problem dependent, and there is not a general way of obtaining good results with e-greedy and its variants (Auer et al., 2002).

Another action selection strategy is *optimism in the face of uncertainty* in which actions are selected greedily, but strongly optimistic prior beliefs are put to their payoffs so that strong negative evidences are used to discard actions (Lai and Robbins, 1985). Many RL techniques use this idea, such as the exploration bonus in *dyna* (Sutton, 1990), *curiosity-driven exploration* (Schmidhuber, 1991) and the exploration mechanism in *prioritized sweeping* (Moore and Atkeson, 1993). Actions can be also chosen based on *interval estimation* (Kaelbling, 1993); in this case, the number of successes and the number of trials are used to construct confidence intervals on the success probability of each action.

There are algorithms which define unique optimal solutions. *Bayesian reinforcement learning* provides an optimal solution in the Bayesian context by taking all possible models weighted by their posteriors into account at once (Poupart et al., 2006; Kolter and Ng, 2009). An alternative approach is provided by the *probabilistically approximately correct* (PAC-MDP) framework for model-based reinforcement learning methods (Kakade, 2003). The seminal algorithms E^3 (Kearns and Singh, 1998) and *R-max* (Brafman and Tennenholtz, 2001) execute near-optimal actions in all but a polynomial number of steps. We will discuss some advances of these algorithms in the next sections.

7.1.2 Model-free methods

Temporal-difference methods are suitable for solving the reinforcement learning problem; they combine the Monte Carlo idea, as they learn from experience without a model of the environment, and the dynamic programming idea, as they *bootstrap*, i.e. they update estimates from previous estimates without waiting for the final outcome. The general idea of temporal-difference algorithms can be explained as follows. Consider an experience $(\boldsymbol{x}, a, s, \boldsymbol{x}')$ summarizing a single transition of the environment, where $\boldsymbol{x}$ is the decision-maker's state before the transition, a is his choice of action, s is the reinforcement signal received and $\boldsymbol{x}'$ is the resulting state. The update rule of the value function in the case of discounted return is:

$$V(\boldsymbol{x}) = (1-\eta)V(\boldsymbol{x}) + \eta(s + \gamma V(\boldsymbol{x}')), \tag{7.1}$$

where η is the *learning rate*. The key idea is that $s + \gamma V(\boldsymbol{x}')$ is a sample of the value of $V(\boldsymbol{x})$ and it is likely to be correct because of the incorporation of the reinforcement signal s. If the learning rate η is slowly decreased and the policy is held fixed, then the temporal-difference converges to the optimal value function (Sutton, 1988). A generalization of this algorithm applies the update rule (7.1) to every state according to its *eligibility* rather than just to the immediately previous state. This generalization is computationally more expensive, but it often converges faster (Dayan, 1992).

Probably one of the best known temporal-difference algorithms is *Q-Learning* (Watkins, 1989; Watkins and Dayan, 1992). It is an *off-policy* method because it learns the value of the optimal policy independently of the decision-maker's actions. In order to illustrate Q-Learning, we have to introduce some additional notation. For control purposes, rather than the value of each state, it is easier to consider the value of each action in each state. Let $Q(\boldsymbol{x}, a)$ be the expected return starting from state $\boldsymbol{x}$, taking action a, and then following the actual policy. In this case we have that $V^*(\boldsymbol{x}) = \max_a Q^*(\boldsymbol{x}, a)$. Note that we are assuming that both states and actions are finite, and they can be stored explicitly in a lookup table. Since the Q function makes the action explicit, we can estimate the Q values online using essentially the same update rule (line 6 of Algorithm 7.1) as temporal-difference:

$$Q(\boldsymbol{x}, a) = (1-\eta)Q(\boldsymbol{x}, a) + \eta(s + \gamma \max_{a'} Q(\boldsymbol{x}', a')). \tag{7.2}$$

Under the assumption that every state-action pair is visited infinitely often and appropriate learning rates are used, the Q values converge to Q^* (Jaakkola et al., 1994b). Q-Learning can also be adapted in the case of average return (Schwartz, 1993) and convergence properties can be guaranteed (Jaakkola et al., 1994a). When the state and action spaces become very large, i.e. they cannot be stored in a lookup table anymore, then some generalizations of Q-Learning have been introduced. For example, *function approximation* techniques have been used, but few convergence results under rather restrictive conditions have been proved (Melo et al., 2008). *State aggregation* techniques have been also introduced, for example interpolation based Q-Learning has been proved to converge if the assumption about the interpolation property is satisfied (Szepesvari and Smart, 2004). Another strategy for dealing with large state spaces is to treat them as *hierarchical* problems, this strategy introduces slight sub-optimality in performance, but potentially gain a good efficiency in learning time and space (Barto and Mahadevan, 2003).

Another well known temporal-difference algorithm is *SARSA* (Rummery and Niranjan, 1994). Unlike Q-Learning, it is an *on-policy* method because it learns the value of the policy being carried out by the decision-maker including the exploration steps. The update rule is given in line 7 of Algorithm 7.2. As Q-Learning, it has been proved to converge to optimal values (Singh et al., 2000). In some cases, such as in the case of function approximations, an on-policy algorithm like SARSA can be more effective than Q-Learning (Gosavi, 2009).

Algorithm 7.1 Q-Learning (tabular)

```
Require: learning rate $\eta > 0$.
Ensure: optimal $Q$ function $Q^*$.
1: Initialize $Q(\boldsymbol{x}, a)$ $\forall \boldsymbol{x} \in \boldsymbol{X}$, $\forall a \in \boldsymbol{A}$
2: $\boldsymbol{x} \leftarrow$ startingState()
3: repeat
4:     $a \leftarrow$ chooseAction($\boldsymbol{x}, Q$)
5:     $(s, \boldsymbol{x}') \leftarrow$takeAction($a$)
6:     $Q(\boldsymbol{x}, a) \leftarrow (1-\eta)Q(\boldsymbol{x}, a) +$
           $\eta(s + \gamma \max_{a'} Q(\boldsymbol{x}', a'))$
7:     $\boldsymbol{x} \leftarrow \boldsymbol{x}'$
8: until (isTerminal($\boldsymbol{x}$))
```

Algorithm 7.2 SARSA (tabular)

```
Require: learning rate $\eta > 0$.
Ensure: optimal $Q$ function $Q^*$.
1: Initialize $Q(\boldsymbol{x}, a)$ $\forall \boldsymbol{x} \in \boldsymbol{X}$, $\forall a \in \boldsymbol{A}$
2: $\boldsymbol{x} \leftarrow$ startingState()
3: $a \leftarrow$ defaultAction()
4: repeat
5:     $(s, \boldsymbol{x}') \leftarrow$ takeAction($a$)
6:     $a' \leftarrow$ chooseAction($\boldsymbol{x}', Q$)
7:     $Q(\boldsymbol{x}, a) \leftarrow (1-\eta)Q(\boldsymbol{x}, a) +$
           $\eta(s + \gamma Q(\boldsymbol{x}', a'))$
8:     $\boldsymbol{x} \leftarrow \boldsymbol{x}'$
9:     $a \leftarrow a'$
10: until (isTerminal($\boldsymbol{x}$))
```

7.1.3 Model-based methods

Model-free methods presented in the previous section do not exploit the knowledge of the environment gathered during exploration. Although many of these methods are guaranteed to find optimal policies and use little computation time per experience, they require a huge amount of data to achieve good performance (Kaelbling et al., 1996). A different class of reinforcement learning methods, called model-based, do not assume knowledge of the model of the environment in advance, but they try to learn it from experience.

The simplest model-based RL method is *certainty equivalence* (Kumar and Varaija, 1986). In this framework, the decision-maker maintains an estimated model of the environment as an MDP with transition model $\hat{P}$ and reward function $\hat{R}$. For each experience $(\boldsymbol{x}, a, s, \boldsymbol{x}')$, the decision-maker updates the estimated model and solves it to obtain a policy that would be optimal if the estimated model was true, and he acts according to that policy. A common approach is to use the empirical distribution of observed state transitions and rewards for the estimated model. For instance, if action a has been attempted $C(\boldsymbol{x}, a)$ times in state $\boldsymbol{x}$ and on $C(\boldsymbol{x}, a, \boldsymbol{x}')$ of these times the state $\boldsymbol{x}'$ has been reached, then the estimate of true probability $P(\boldsymbol{x}'|\boldsymbol{x}, a)$ is $\hat{P}(\boldsymbol{x}'|\boldsymbol{x}, a) = C(\boldsymbol{x}, a, \boldsymbol{x}')/C(\boldsymbol{x}, a)$. If $C(\boldsymbol{x}, a) = 0$, then a prior distribution is used (Dearden et al., 1999). The drawbacks of this method are the continuous interactions with the environment and the computational burden of resolving the model for each update of $\hat{P}$ and $\hat{R}$.

A common solution to speed up the learning procedure is provided by the dyna framework (Sutton, 1990). The key idea is to use the acquired experience to construct a model of the environment and then use it for updating the value function without having to interact with the environment. This updating is performed in the same spirit of temporal-difference algorithms, e.g. using the equation (7.2), but for a limited number of iterations.

Several variations of dyna have been developed to improve its performance, such as prioritized sweeping (Moore and Atkeson, 1993). This approach does not uniformly select the state-action pairs to update equation (7.2), but it focuses on state-action pairs that are likely to be useful. As shown in Algorithm 7.3, a priority queue is maintained for every state-action pair whose estimated value would change substantially if backed up, ordered by the size of the change. When the top of the queue is backed up, the effect on each of its predecessor pairs is computed, so the effects of the changes are propagated backward.

Algorithm 7.3 Prioritized sweeping

```
Require: learning rate $\eta > 0$, error threshold $\upsilon$ and max number of iterations $Iter_{max}$.
Ensure: optimal $Q$ function $Q^*$.
 1: Initialize $Q(\boldsymbol{x}, a)\ \forall \boldsymbol{x} \in \boldsymbol{X}, \forall a \in \boldsymbol{A}, model, pQueue$.
 2: $\boldsymbol{x} \leftarrow$ startingState()
 3: repeat
 4:   $a \leftarrow$ chooseAction($\boldsymbol{x}, Q$)
 5:   $(s, \boldsymbol{x}') \leftarrow$ takeAction($a$)
 6:   $model \leftarrow (\boldsymbol{x}, a, s, \boldsymbol{x}')$
 7:   $err \leftarrow |s + \gamma \max_{a'} Q(\boldsymbol{x}', a') - Q(\boldsymbol{x}, a)|$
 8:   if $(err > \upsilon)$ then
 9:     $pQueue \leftarrow$ push($pQueue, (\boldsymbol{x}, a), err$)
10:   end if
11:   $i \leftarrow 0$
12:   while ($pQueue \neq \emptyset$ and $i < Iter_{max}$) do
13:     $(\boldsymbol{x}, a) \leftarrow$ pop($pQueue$)
14:     $(\hat{s}, \hat{\boldsymbol{x}}') \leftarrow model(\boldsymbol{x}, a)$
15:     $Q(\boldsymbol{x}, a) \leftarrow (1 - \eta) Q(\boldsymbol{x}, a) + \eta(\hat{s} + \gamma \max_{a'} Q(\hat{\boldsymbol{x}}', a'))$
16:     $i \leftarrow i + 1$
17:     for each $(\hat{\boldsymbol{x}}, \hat{a}, \hat{s})$ predicted by $model$ to lead to $\boldsymbol{x}$ do
18:       $err \leftarrow |\hat{s} + \gamma \max_a Q(\boldsymbol{x}, a) - Q(\hat{\boldsymbol{x}}, \hat{a})|$
19:       if $(err > \upsilon)$ then
20:         $pQueue \leftarrow$ push($pQueue, (\hat{\boldsymbol{x}}, \hat{a}), err$)
21:       end if
22:     end for
23:   end while
24:   $\boldsymbol{x} \leftarrow \boldsymbol{x}'$
25: until (isTerminal($\boldsymbol{x}$))
```

Extensions of prioritized sweeping to large state space using linear function approximation has been developed. Specifically, Sutton et al. (2008) have established that dyna-style planning with reinforcement learning update rules converges under weak conditions. Even if the idea of prioritized sweeping of focusing search on the states believed to have changed in value can speed up its convergence, the overhead of managing the priority queue can be prohibitively high (Wingate and Seppi, 2005; Dai and Hansen, 2007).

7.2 Model-based RL in factored MDPs

Model-based RL methods are important in applications where computation is considered to be cheap and real world experience costly as they can speed up their convergence with a better use of experience. However, they must be able to efficiently manage the exploration-exploitation trade-off and scale up to large state spaces in order to be successfully used to solve non trivial problems. In order to deal with these two issues, explicit exploration strategies have been developed and factored MDPs have been used.

7.2.1 Prioritized sweeping-based algorithms

Generalized prioritized sweeping (Andre et al., 1998) is an extension of prioritized sweeping with two important contributions: they use a parametrized version of the value function and a compact representation of the environment by using a factored MDP. Like prioritized sweeping, their method aims to perform only the most beneficial value propagations. In particular, when performing value propagations, the decision-maker updates the value function by updating its parameters. In order to estimate the change in the Bellman error without computing it for each state, they use the gradient of the Q function. For the environment representation, they assume that the DBNs structures underpinning the factored MDP model are given, and they learn the conditional probability entries using Dirichlet priors for each multinomial distribution.

Structured prioritized sweeping (Dearden, 2001) is an extension of generalized prioritized sweeping in which the factored MDP is represented by DBNs with tree-structured conditional probability tables. This algorithm maintains a structured value function and updates the values of aggregate states. It applies the techniques used in the *structured policy iteration* algorithm (Boutilier et al., 1995), such as the regression operator computed in a structured way where the value function is represented as a tree and the result is another tree in which each leaf corresponds to a region of the state space. An advantage of this algorithm is that the DBNs structure can be unknown.

Both generalized prioritized sweeping and structured prioritized sweeping take advantage of the structure of the factored MDP to improve learning, but they do not take into account the issue of exploration in such domains.

7.2.2 Factored E^3

The E^3 algorithm (Kearns and Singh, 1998) is a model-based RL method that provides an explicit handling of the exploration-exploitation trade-off. As the certainty equivalence method, E^3 keeps an estimated model of the environment as an MDP that is updated during execution. Upon arriving in a state it has never visited before, it takes an arbitrary action, otherwise it takes the action it has tried the fewest times from that state.

A key notion of E^3 is that of *known-state MDP*, that is an MDP where all transitions between known states are preserved, while all other transitions are redirected to an absorbing state that represents all of the unknown and unvisited states. This known-state MDP is not directly accessible to the algorithm, but it is possible to have a good approximation of it according to the *simulation lemma* introduced by Kearns and Singh (1998). The authors also defined the *explore or exploit lemma*, which formalizes that either the optimal (T-step) policy achieves its high return by staying, with high probability, in the set of currently known states (so it can perform exploitation), or the optimal policy has significant probability of leaving the currently known states within T steps (so it can perform exploration that quickly reaches the absorbing state). Thus, by performing two polynomial-time computations on the known-state MDP off-line, the algorithm is guaranteed to either find a way to get near-optimal return or find a way to improve its estimates.

The E^3 algorithm makes no assumptions about the structure of the MDP, so the resulting polynomial dependence on the number of states makes E^3 impractical in the case of large MDPs. Kearns and Koller (1999) derived a generalization of E^3, called *factored E^3*, where the underlying model can be represented as a factored MDP in which the structure is known, but the parameters are unknown. In their work, the concept of known-state is extended to the idea of *known-transition*, that is known if all of its CPT entries of the underlying DBN are known. The core part of factored E^3 is essentially the same as of that E^3. After some number of steps, one or more transitions become known by the *Pigeonhole principle* (Fletcher and Patty, 1995). When it reaches a known state (one where all the transitions are known), it performs approximate off-line policy computations for two different factored MDPs. The first corresponds to attempted exploitation and the second to attempted exploration. Factored E^3 has a polynomial dependence not on the number of states, but on the number of CPT parameters in the factored MDP.

7.2.3 Factored R-max

R-max is a more general algorithm than E^3, which can attain near-optimal return in polynomial time (Brafman and Tennenholtz, 2001). It uses the idea of certainty equivalence as the decision-maker maintains a complete, but possibly inaccurate model of the environment and acts based on the optimal policy derived from this model. The action selection strategy follows the optimism in the face of uncertainty principle. In particular, the action selection step is always to choose the action that maximizes the current action value, $\max_a Q(\boldsymbol{x}, a)$, while the model update step is to solve the following set of equations:

$$Q(\boldsymbol{x}, a) = \begin{cases} \hat{R}(\boldsymbol{x}, a) + \gamma \sum_{\boldsymbol{x}'} \hat{P}(\boldsymbol{x}'|\boldsymbol{x}, a) \max_{a'} Q(\boldsymbol{x}', a') & \text{if } C(\boldsymbol{x}, a) \geq c, \\ R_{max} & \text{otherwise,} \end{cases} \tag{7.3}$$

where $\hat{R}(\boldsymbol{x}, a)$ and $\hat{P}(\boldsymbol{x}'|\boldsymbol{x}, a)$ are the empirical estimates for the reward and transition distribution of state-action pair $(\boldsymbol{x}, a)$ using only data from the first c counts of $(\boldsymbol{x}, a)$. Strehl et al. (2009) demonstrated that c can be defined as a function of the input parameters in the PAC-MDP framework in order to make theoretical guarantees about its efficiency.

Any implementation of R-max must choose a technique for solving the set of equations (7.3) such as dynamic programming and linear programming. Following the generalization of E^3 to factored E^3, Guestrin et al. (2002) introduced the *factored R-max* in which the environment is modeled as a factored MDP and solved (7.3) using the approximate linear programming approach (6.17)-(6.19). Strehl (2007) proposed a similar algorithm that takes into account the empirical estimates for the transition components.

Different extensions of the R-max algorithm have been introduced that do not assume knowledge of the structure of the factored MDP in advance. Strehl et al. (2007) proposed *SLF-R-max* that learns the structure as part of the reinforcement learning process requiring as input only an upper bound in-degrees of the underlying DBN. It behaves near optimally, with high probability, in all but a polynomial number of time steps. The sample complexity of this algorithm has been improved by Diuk et al. (2009) with their *Met-R-max*. Chakraborty and Stone (2011) studied the case when a prior knowledge in-degrees of the underlying DBN is unavailable for an ergodic factored MDP. Given a big enough time T, their *LSE-R-max* algorithm provably achieves a return sufficiently close to the optimal one with high certainty and polynomial complexity.

7.2.4 Algorithm-directed factored reinforcement learning

Both factored E^3 and factored R-max suffer from some limitations, e.g. the concept of known state is quite limiting, given that many visits are required before a state becomes relevant to the plan. Guestrin et al. (2002) proposed an alternative approach, called *algorithm-directed factored reinforcement learning*, that uses an ALP as planning algorithm. Their approach only learns the critical parts of the model needed for the ALP and it achieves a sample efficiency which is logarithmic in the size of the problem description. They assumed that the decision-maker is interested in maximizing the infinite-horizon average return ρ and is trying to obtain a linear approximation of the optimal value function using the average return version of the ALP (6.17)-(6.19) defined as follows:

$$\text{vars}: \ \rho, w_1, \dots, w_K \tag{7.4}$$

$$\text{min}: \ \rho \tag{7.5}$$

$$\text{s.t.}: \ 0 \geq \max_{\boldsymbol{x}} \left\{ -\rho + R(\boldsymbol{x}, a) + \sum_{k=1}^{K} w_k \left(g_k^a(\boldsymbol{x}) - h_k(\boldsymbol{x}) \right) \right\}, \ \forall a \in \boldsymbol{A}. \tag{7.6}$$

They defined an *ϵ-optimal algorithm-directed approximation* as a factored MDP which yields $|\rho^*_{alp} - \hat{\rho}| < \epsilon$, for some $\epsilon > 0$, where ρ^*_{alp} is the *exact-model average return* obtained by solving the ALP (7.4)-(7.6) with the true-model, while $\hat{\rho}$ is the *estimated-model average return* obtained by solving the same ALP with the estimates $\hat{P}(\boldsymbol{x}'|\boldsymbol{x}, a)$ and $\hat{R}(\boldsymbol{x}, a)$.

The key idea of their approach is the construction of two ALPs (7.4)-(7.6), one uses all lower bounds on reward functions and backprojections, and it provides a solution $\underline{\rho}$, while the other one uses all upper bounds on the same functions and returns a solution $\overline{\rho}$. These bounds are updated during execution and they are constructed such that $\underline{\rho} \leq \rho^*_{alp} \leq \overline{\rho}$ with probability at least $(1 - \alpha_\rho)$. Both lower $\underline{\rho}$ and upper $\overline{\rho}$ solutions are important because they provide two types of information: a stopping criterion $\overline{\rho} - \underline{\rho} < \epsilon$, in order to obtain an ϵ-optimal algorithm-directed approximation, and which states need to be explored to make the bounds tighter, i.e. the *active states* of the two ALPs.

As factored R-max, this algorithm assumes that the structure of the factored MDP is known. During execution, it maintains lower and upper bounds on reward functions and backprojections. After solving the two ALPs described above, it verifies whether the stopping criterion has been reached. If not, it collects the active state-action pairs of the two ALPs and it drives the exploration toward the relevant active states.

7.3 Model-based RL using structured CTMDPs

Model-based reinforcement learning algorithms using factored MDPs have been used to scale up to large state spaces and techniques to solve them have been widely developed. However, when the system does not evolve natively in discrete time, it is necessary to resort to some forms of discretization, leading to the same problems incurred in DBNs.

We present a novel model-based reinforcement learning approach for control continuous time dynamic systems based on structured CTMDPs (Villa and Shelton, 2014a). Our approach extends the algorithm-directed factored RL in the continuous time case allowing us to manage the exploration-exploitation trade-off via an ad-hoc ALP formulation for infinite-horizon average return in continuous time. We also maintain a sample efficiency logarithmic in the size of the problem description.

7.3.1 Approximate linear program

As we are interested in maximizing the infinite-horizon average return, we have to derive the ALP formulation for structured CTMDPs in this case. This task can be accomplished in the same way as the infinite-horizon discounted return, where we derived the ALP formulation from that of factored MDPs.

Recall the set of constraints (6.12) of the ALP formulation for discounted return in discrete time and the Bellman optimality operator (6.25) in continuous time for average return. Then, the set of constraints for average return can be written as follows:

$$\frac{\rho}{q^a_{\boldsymbol{x}}} + \sum_{k=1}^{K} w_k h_k(\boldsymbol{x}) \geq \frac{r(\boldsymbol{x}, a)}{q^a_{\boldsymbol{x}}} + \sum_{\boldsymbol{x}' \neq \boldsymbol{x}} \frac{q^a_{\boldsymbol{x},\boldsymbol{x}'}}{q^a_{\boldsymbol{x}}} \sum_{k=1}^{K} w_k h_k(\boldsymbol{x}'),\ \forall \boldsymbol{x} \in \boldsymbol{X}, \forall a \in \boldsymbol{A}. \tag{7.7}$$

By multiplying both sides of the inequality (7.7) by $q^a_{\boldsymbol{x}}$, moving everything from the left hand side to the right hand side and rearranging, we obtain the following set of constraints:

$$0 \geq -\rho + r(\boldsymbol{x}, a) + \sum_{k=1}^{K} w_k(-q^a_{\boldsymbol{x}} h_k(\boldsymbol{x}) + \sum_{\boldsymbol{x}' \neq \boldsymbol{x}} q^a_{\boldsymbol{x},\boldsymbol{x}'} h_k(\boldsymbol{x}')),\ \forall \boldsymbol{x} \in \boldsymbol{X}, \forall a \in \boldsymbol{A}. \tag{7.8}$$

Given that only one single variable changes state at any single instant (6.31) and the rate at which a variable transitions is independent of all the other variables given the values of the parents, then the inequality (7.8) can be simplified $\forall \boldsymbol{x} \in \boldsymbol{X}, \forall a \in \boldsymbol{A}$ as follows:

$$0 \geq -\rho + r(\boldsymbol{x}, a) + \sum_{k=1}^{K} w_k(\sum_{X_n \in \boldsymbol{C}_k} \sum_{x'_n \neq x_n} q^a_{x_n, x'_n | pa_u} (h_k(\boldsymbol{x}[x'_n]) - h_k(\boldsymbol{x}))). \tag{7.9}$$

Then, the ALP for infinite-horizon average return in structured CTMDPs is defined as:

$$\text{vars}: \ \rho, w_1, \dots, w_K \tag{7.10}$$

$$\min: \ \rho \tag{7.11}$$

$$\text{s.t.}: \ 0 \geq \max_{\boldsymbol{x}} \left\{ -\rho + \sum_{l=1}^{L} r_l(\boldsymbol{x}, a) + \sum_{k=1}^{K} w_k g_k^a(\boldsymbol{x}) \right\}, \forall a \in \boldsymbol{A}, \tag{7.12}$$

where we use the max operator to combine the constraints (7.9) for the same action a, while g_k^a is the backprojection of the k-th basis function h_k for action a as defined in equation (6.37) with $Scope[g_k^a] = \boldsymbol{B}_k^a \subseteq \boldsymbol{X}$. The reward rate function is composed of a set of L localized functions, $r(\boldsymbol{x}, a) = \sum_{l=1}^{L} r_l(\boldsymbol{L}_l^a, a) \in [0; R_{l_{max}}]$ with $Scope[r_l] = \boldsymbol{L}_l^a \subseteq \boldsymbol{X}$.

Given a set of basis functions $\boldsymbol{H} = \{h_1, \dots, h_K\}$ where $0 \leq h_k(\boldsymbol{x}) \leq H_{max}, \forall k, \boldsymbol{x}$, and a model defined as a structured CTMDP, it is possible to solve the ALP (7.10)-(7.12) and obtain the continuous time version of the exact-model average return ρ^*_{alp}. In the context of RL, the conditional intensities as well as the reward rate functions of the structured CTMDP are unknown. We are interested in estimating them and providing an ϵ-optimal algorithm-directed approximation of the exact-model as in Guestrin et al. (2002).

7.3.2 Lower and upper bounds

The main part of the algorithm is to provide lower $\underline{\rho}$ and upper $\overline{\rho}$ bounds on the exact-model average return such that:

$$P(\underline{\rho} \leq \rho^*_{alp} \leq \overline{\rho}) \geq (1 - \alpha_\rho). \tag{7.13}$$

As first step, we would like to maintain lower and upper bounds on the unknown components in (7.12), namely the reward rate functions $r_l(\boldsymbol{x}, a)$ and backprojections $g_k^a(\boldsymbol{x})$.

Given an experience occurred along the path $\chi = ((t, \boldsymbol{x}), a, s(\boldsymbol{x}, a), (t', \boldsymbol{x}[x'_n]))$ where only the variable X_n has changed its state, if $X_n \in \boldsymbol{L}_l^a$, then it can be used to estimate the local reward rate function as follows:

$$\underline{r}_l(\boldsymbol{x}, a) = \frac{1}{C(\chi_{\boldsymbol{l}_l^a})} \sum_{\chi_{\boldsymbol{l}_l^a}} s(\boldsymbol{x}, a) - \sqrt{\frac{R^2_{l_{max}}}{2C(\chi_{\boldsymbol{l}_l^a})} \ln\left(\frac{2L|\boldsymbol{A}||\boldsymbol{L}_{max}|}{\alpha_r}\right)}, \tag{7.14}$$

$$\overline{r}_l(\boldsymbol{x}, a) = \frac{1}{C(\chi_{\boldsymbol{l}_l^a})} \sum_{\chi_{\boldsymbol{l}_l^a}} s(\boldsymbol{x}, a) + \sqrt{\frac{R^2_{l_{max}}}{2C(\chi_{\boldsymbol{l}_l^a})} \ln\left(\frac{2L|\boldsymbol{A}||\boldsymbol{L}_{max}|}{\alpha_r}\right)}, \tag{7.15}$$

where $\chi_{\boldsymbol{l}_l^a}$ denotes the experience where the state $\boldsymbol{x}$ is consistent with $\boldsymbol{l}_l^a$ and $C(\chi_{\boldsymbol{l}_l^a})$ is the number of such experiences. If $C(\chi_{\boldsymbol{l}_l^a}) = 0$, then $\underline{r}_l(\boldsymbol{x}, a) = 0$ and $\overline{r}_l(\boldsymbol{x}, a) = R_{l_{max}}$. Given that there are L localized functions for $|\boldsymbol{A}|$ actions with at most $|\boldsymbol{L}_{max}|$ assignments each, where $|\boldsymbol{L}_{max}|$ is the maximum reward rate function scope size $|\boldsymbol{L}_{max}| = \max_{\boldsymbol{x},l} |\boldsymbol{L}_l^a|$, the entire reward rate function can be bounded with probability at least $(1 - \alpha_r)$ by the application of Hoeffding and Union bounds, as shown in equations (7.14) and (7.15).

Consider the other component of the set of constraints (7.12), we would like to maintain lower and upper bounds on the backprojections such that $\underline{g}_k^a(\boldsymbol{x}) \leq g_k^a(\boldsymbol{x}) \leq \overline{g}_k^a(\boldsymbol{x})$ holds. From equation (6.37), we note that each backprojection is essentially an expectation over a small set of states $\boldsymbol{b}_k^a \in \boldsymbol{B}_k^a \subseteq \boldsymbol{X}$ that yields a backprojected basis reward over time. We can estimate these bounds by doing an empirical mean computation of the rewards obtained divided by the empirical mean time of occurrence. Therefore, we introduce two elements: the mean value $\widehat{gv}_k^a(\boldsymbol{x})$ and the mean time $\widehat{gt}_k^a(\boldsymbol{x})$ backprojections.

Given an experience occurred along the path $\chi = ((t, \boldsymbol{x}), a, s(\boldsymbol{x}, a), (t', \boldsymbol{x}[x'_n]))$ where only the variable X_n has changed its state, if $X_n \in \boldsymbol{B}_k^a$, then it can be used to estimate the two elements of the backprojection $\widehat{gv}_k^a(\boldsymbol{x})$ and $\widehat{gt}_k^a(\boldsymbol{x})$ as follows:

$$\widehat{gv}_k^a(\boldsymbol{x}) = \frac{1}{C(\chi_{\boldsymbol{b}_k^a})} \sum_{\chi_{\boldsymbol{b}_k^a}} (h_k(\boldsymbol{x}[x'_n]) - h_k(\boldsymbol{x})), \tag{7.16}$$

$$\widehat{gt}_k^a(\boldsymbol{x}) = \frac{1}{C(\chi_{\boldsymbol{b}_k^a})} \sum_{\chi_{\boldsymbol{b}_k^a}} (t' - t), \tag{7.17}$$

where $\chi_{\boldsymbol{b}_k^a}$ denotes the experience where the state $\boldsymbol{x}$ is consistent with $\boldsymbol{b}_k^a$ and $C(\chi_{\boldsymbol{b}_k^a})$ is the number of such experiences. The lower and upper bounds for the mean value backprojection which will hold with high probability are: $\underline{gv}_k^a(\boldsymbol{x}) = \widehat{gv}_k^a(\boldsymbol{x}) - \epsilon_{\widehat{gv}_k^a}$ and $\overline{gv}_k^a(\boldsymbol{x}) = \widehat{gv}_k^a(\boldsymbol{x}) + \epsilon_{\widehat{gv}_k^a}$ respectively, where the error parameter $\epsilon_{\widehat{gv}_k^a}$ is given by:

$$\epsilon_{\widehat{gv}_k^a} = \sqrt{\frac{2H_{max}^2}{C(\chi_{\boldsymbol{b}_k^a})} \ln\left(\frac{4K|\boldsymbol{A}||\boldsymbol{B}_{max}|}{\alpha_g}\right)}. \tag{7.18}$$

The lower and upper bounds for the mean time backprojection which will hold with high probability are: $\underline{gt}_k^a(\boldsymbol{x}) = \widehat{gt}_k^a(\boldsymbol{x}) - \epsilon_{\widehat{gt}_k^a}$ and $\overline{gt}_k^a(\boldsymbol{x}) = \widehat{gt}_k^a(\boldsymbol{x}) + \epsilon_{\widehat{gt}_k^a}$ respectively, where the error parameter $\epsilon_{\widehat{gt}_k^a}$ is given by:

$$\epsilon_{\widehat{gt}_k^a} = \sqrt{\frac{T_{max}^2}{2C(\chi_{\boldsymbol{b}_k^a})} \ln\left(\frac{4K|\boldsymbol{A}||\boldsymbol{B}_{max}|}{\alpha_g}\right)}. \tag{7.19}$$

The errors reported in (7.18) and (7.19) are constructed such that all backprojections are bounded with probability at least $(1-\alpha_g)$ by Hoeffding and Union bounds with the following two assumptions. Firstly, we assume that all the possible differences of the backprojections $(h_k(\boldsymbol{x}') - h_k(\boldsymbol{x}))$ belong to the interval $[-H_{max}; H_{max}]$. Secondly, we also assume that all the possible time differences $(t' - t)$ are in the interval $[0; T_{max}]$. The Union bound is used since there are 2 elements for K basis functions for $|\boldsymbol{A}|$ actions with at most $|\boldsymbol{B}_{max}|$ assignments each, where $|\boldsymbol{B}_{max}|$ is the maximum backprojection scope size $|\boldsymbol{B}_{max}| = \max_{\boldsymbol{x},k} |\boldsymbol{B}_k^a|$. The lower and the upper bounds on the backprojections can be then computed using the rule of *uncertainty propagation* (Taylor, 1996) as follows:

$$\underline{g}_k^a(\boldsymbol{x}) = \frac{\widehat{g_v}_k^a}{\widehat{g_t}_k^a}\left(1 - \sqrt{\left(\frac{\epsilon_{\widehat{g_v}_k^a}}{\widehat{g_v}_k^a}\right)^2 + \left(\frac{\epsilon_{\widehat{g_t}_k^a}}{\widehat{g_t}_k^a}\right)^2}\right), \tag{7.20}$$

$$\overline{g}_k^a(\boldsymbol{x}) = \frac{\widehat{g_v}_k^a}{\widehat{g_t}_k^a}\left(1 + \sqrt{\left(\frac{\epsilon_{\widehat{g_v}_k^a}}{\widehat{g_v}_k^a}\right)^2 + \left(\frac{\epsilon_{\widehat{g_t}_k^a}}{\widehat{g_t}_k^a}\right)^2}\right). \tag{7.21}$$

As second step, we show that the proposed bounds on reward rate functions and backprojections can be used to ensure that inequality (7.13) holds.

Let $\underline{\rho}$ be the *estimated-model average return* obtained by solving the ALP (7.10)-(7.12) using the lower bounds of the reward rate functions $\underline{r}_l(\boldsymbol{x}, a)$ and backprojections $\underline{g}_k^a(\boldsymbol{x})$ and let $\overline{\rho}$ be the estimated-model average return by solving the same ALP using the upper bounds of the reward rate functions $\overline{r}_l(\boldsymbol{x}, a)$ and backprojections $\overline{g}_k^a(\boldsymbol{x})$. Then, for any $\alpha_\rho > 0$, we have that $\underline{\rho} \le \rho^*_{alp} \le \overline{\rho}$ holds with probability at least $(1-\alpha_\rho)$.

We can prove this proposition in two parts following the work of Guestrin et al. (2002). Firstly, we note that all sources of uncertainty of the ALP are bounded with high probability by construction of the error parameters. Thus, the lower and upper bounds hold with probability at least $(1-\alpha_\rho)$ by setting $\alpha_r = \alpha_\rho/2$ and $\alpha_g = \alpha_\rho/2$. Secondly, we note that if we use the lower bounds $\underline{r}_l(\boldsymbol{x}, a)$ and $\underline{g}_k^a(\boldsymbol{x})$ instead of true values $r_l(\boldsymbol{x}, a)$ and $g_k^a(\boldsymbol{x})$, then the feasible region becomes larger, therefore the return ρ^*_{alp} is still feasible. Thus, using the same set of basis weights as the ones in the solution provided when the model is known, we can decrease the objective function obtaining a smaller return $\underline{\rho}$ compared to ρ^*_{alp}. Similarly, if we replace the upper bounds $\overline{r}_l(\boldsymbol{x}, a)$ and $\overline{g}_k^a(\boldsymbol{x})$ with the true values $r_l(\boldsymbol{x}, a)$ and $g_k^a(\boldsymbol{x})$, then the feasible region becomes smaller, therefore the return ρ^*_{alp} may not be longer feasible, so the upper bound return $\overline{\rho}$ cannot be smaller than ρ^*_{alp}.

7.3.3 Exploration strategy

The lower and upper bounds in (7.13) obtained by solving two ALPs (7.10)-(7.12) using the lower and upper bounds of the reward rate functions and backprojections give us two types of information. Firstly, the stopping criterion, i.e. if $\overline{\rho} - \underline{\rho} < \epsilon$, then we have obtained the ϵ-optimal approximation with probability at least $(1 - \alpha_\rho)$. Secondly, the exploration strategy, i.e. which states need to be explored to make the bounds tighter.

These critical states can be found in the solutions of the ALPs. Specifically, a solution of an ALP problem provides active constraints that correspond to the critical state-action pairs $(\boldsymbol{x}, a)$ for which the inequality constraints (7.12) become active. If we denote as Prc the set of state-action pairs with precise backprojections and reward rate functions, i.e. $Prc = \{(\boldsymbol{x}, a) : \underline{g}_k^a(\boldsymbol{x}) = \overline{g}_k^a(\boldsymbol{x}), \underline{r}_l(\boldsymbol{x}, a) = \overline{r}_l(\boldsymbol{x}, a), \forall k, l\}$, and all active state-action pairs of the ALP are in Prc, then its solution is equal to ρ^*_{alp} with probability at least $(1 - \alpha_\rho)$ as proved by Guestrin et al. (2002). Therefore, the exploration strategy is guided toward the active states of the ALPs because precise estimates of these states are sufficient to obtain an ϵ-optimal approximation. It is important to note that it is not possible to construct the Prc set in practice because of the uncertainty of the bounds; thus, we have to rely on LP sensitivity analysis to determine error bars for which small changes in the backprojections and reward rate functions do not impact the ALP solution.

7.3.4 Algorithm

The algorithm-directed reinforcement learning approach for structured CTMDPs is shown in Algorithm 7.4. As in factored R-max, we assume that the structure of the structured CTMDP is given, but its parameters are unknown; moreover, we require a value $\epsilon > 0$, a confidence level of $(1 - \alpha_\rho)$ and a set of basis functions $\boldsymbol{H}$. The result is a near-optimal policy $\hat{\pi}^*$ obtained as an ϵ-optimal algorithm-directed approximation of the exact-model.

During execution, the algorithm maintains two models, denoted as *models*, that contain the lower and upper bounds on the reward rate functions and the backprojections. For each experience occurred along the path, the algorithm updates these models and solves the relative ALPs defined in (7.10)-(7.12), (lines 6 - 7 of Algorithm 7.4). If the stopping criterion is not met, then the active states of the two ALPs are collected. These active states are crucial given that their exploration makes the ALPs bounds tighter.

A straightforward implementation of the exploration strategy is through a priority queue which gives a higher priority to the active states incurred along the path, preferring the most non-precise ones. At the beginning, the exploration is guided toward the unknown active states; as time passes the relevant active states become precise until their exploration is sufficient enough. If the current state is included in the priority queue, then an exploration action according to that state is given, otherwise an action is extracted from the current policy (lines 14 - 19 of Algorithm 7.4). This algorithm directs exploration toward the domain uncertainties that affect the results of the ALP planner and it makes a good use of the data collected as the estimates of the two models depend logarithmically in the size of the problem description.

Algorithm 7.4 Algorithm-directed RL using structured CTMDPs

```
Require: $\epsilon > 0$, confidence $(1 - \alpha_\rho)$, $\boldsymbol{H} = \{h_1, \ldots, h_K\}$, structured CTMDP definition.
Ensure: near-optimal policy $\hat{\pi}^*$ and error $\epsilon_\rho$.
 1: Initialize $models, pQueue, finished \leftarrow false$.
 2: $(t, \boldsymbol{x}) \leftarrow$ startingState()
 3: $a \leftarrow$ defaultAction()
 4: repeat
 5:    $(s(\boldsymbol{x}, a), (t', \boldsymbol{x}[x'_n])) \leftarrow$ takeAction($a$)
 6:    $models \leftarrow ((t, \boldsymbol{x}), a, s(\boldsymbol{x}, a), (t', \boldsymbol{x}[x'_n]))$
 7:    $sols \leftarrow$ solveALP($models$)
 8:    $\boldsymbol{x} \leftarrow \boldsymbol{x}[x'_n]$
 9:    $\epsilon_\rho \leftarrow sols.\overline{\rho} - sols.\underline{\rho}$
10:    if $(\epsilon_\rho < \epsilon)$ then
11:       $finished \leftarrow true$
12:    else
13:       $pQueue \leftarrow$ push($pQueue, sols$)
14:       if (isIn($pQueue, \boldsymbol{x}$)) then
15:          $a \leftarrow$ pop($pQueue, \boldsymbol{x}$)
16:       else
17:          $\hat{\pi} \leftarrow$ getPolicy($sols$)
18:          $a \leftarrow \hat{\pi}(\boldsymbol{x})$
19:       end if
20:    end if
21: until (isTerminal($\boldsymbol{x}$) or $finished$)
22: $\hat{\pi}^* \leftarrow$ getPolicy($sols$)
```

7.4 Trading in the reinforcement learning framework

The continuous time version of the simplified trading domain presented in the previous chapter can be extended in the reinforcement learning framework. In this context, the portfolio manager interacts with the environment to gather new information used to enhance his performance. This interaction is performed online by the selection of an available action, i.e. buy or sell a security or do nothing, while the reinforcement learning signal is based on the current portfolio value according to equation (6.38). The goal of the portfolio manager is to maximize the average return of his portfolio over time.

7.4.1 Proposed solution using structured CTMDPs

The model-based reinforcement learning approach introduced in the previous section can be used to solve the trading problem in the reinforcement learning framework. This method based on structured CTMDPs is straightforward in the context of trading because the real world experience is costly; thus, a better use of the gathered experience is required and it has to scale up to large state spaces as the market size is huge. Moreover, it is a continuous time model and it exploits both additive, as the problem can be decomposed into individual security, and context-specific features, as we assume the existence of a structure among securities. In this approach, we assume that the structure of the model is known, i.e. the portfolio manager is able to represent the relationships among securities, but the parameters of the model are unknown, i.e. the portfolio manager is not able to quantify the values encoded in the conditional intensity matrices.

In the next sections, we perform numerical experiments in order to assess the quality of the theoretical findings. We use as benchmark the structures defined in the previous chapter, i.e. the two-securities topology and its extension to multiple securities connected as a bidirectional ring. In the first set of experiments, we assess the effectiveness of the algorithm-directed exploration against the common types of exploration, where we illustrate the online behavior of Algorithm 7.4 from the average return perspective. In the second set of experiments, we analyze the online behavior of the upper versus lower bounds of the estimated-model average return. In the last set of experiments, we assess the performance of the learned policy against the one calculated using the exact-model.

7.4.2 Online learning

The online behavior of Algorithm 7.4 is analyzed by computing the average return received during learning using three exploration strategies, namely algorithm-directed exploration, e-greedy and random exploration, versus the optimal average return.

Figure 7.1 shows the average return received over time coming from the interaction with the environment against the optimal value (dotted black line) for different number of securities. The algorithm-directed and e-greedy exploration increase their performances over time as they balance between exploration and exploitation, while the random exploration has a flat performance as it always selects a random action. In all cases, the algorithm-directed exploration achieves a higher return compared to other strategies.

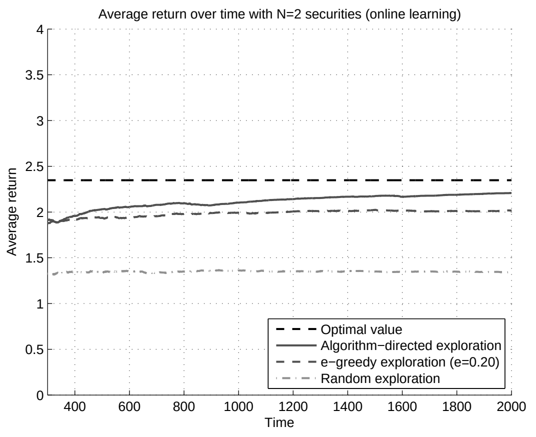

(a)

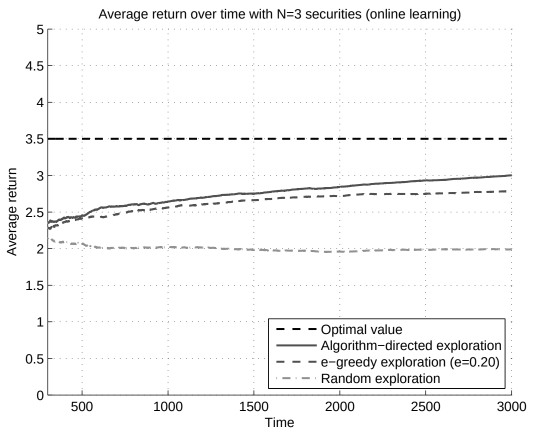

(b)

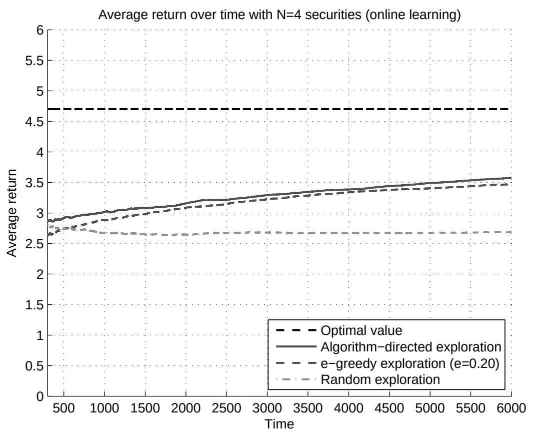

(c)

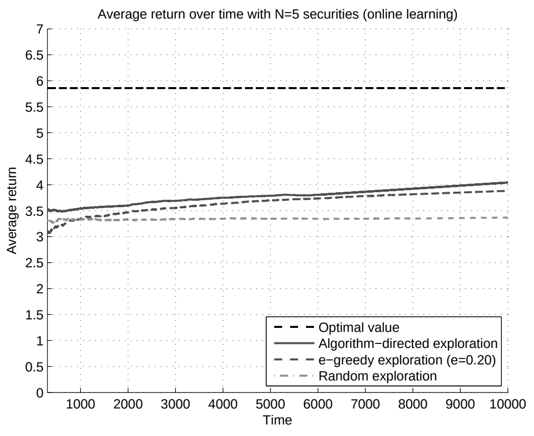

(d)

Figure 7.1: Online behavior of average return over time using two connected securities (a), and three (b), four (c) and five (d) securities connected as a bidirectional ring.

7.4.3 Online behavior of lower and upper bounds

The online behavior of the lower $\underline{\rho}$ and upper $\overline{\rho}$ bounds of the estimated-model average return is assessed by computing the relative difference $\epsilon_\rho = \overline{\rho} - \underline{\rho}$ over time.

Figure 7.2 shows the temporal evolution of ϵ_ρ with $\alpha = 0.05$ for different numbers of securities using the algorithm-directed exploration strategy. Increasing the number of securities leads to a higher difference of the two estimated-model average returns in the first stages and a slower convergence, logarithmically in the size of the problem description.

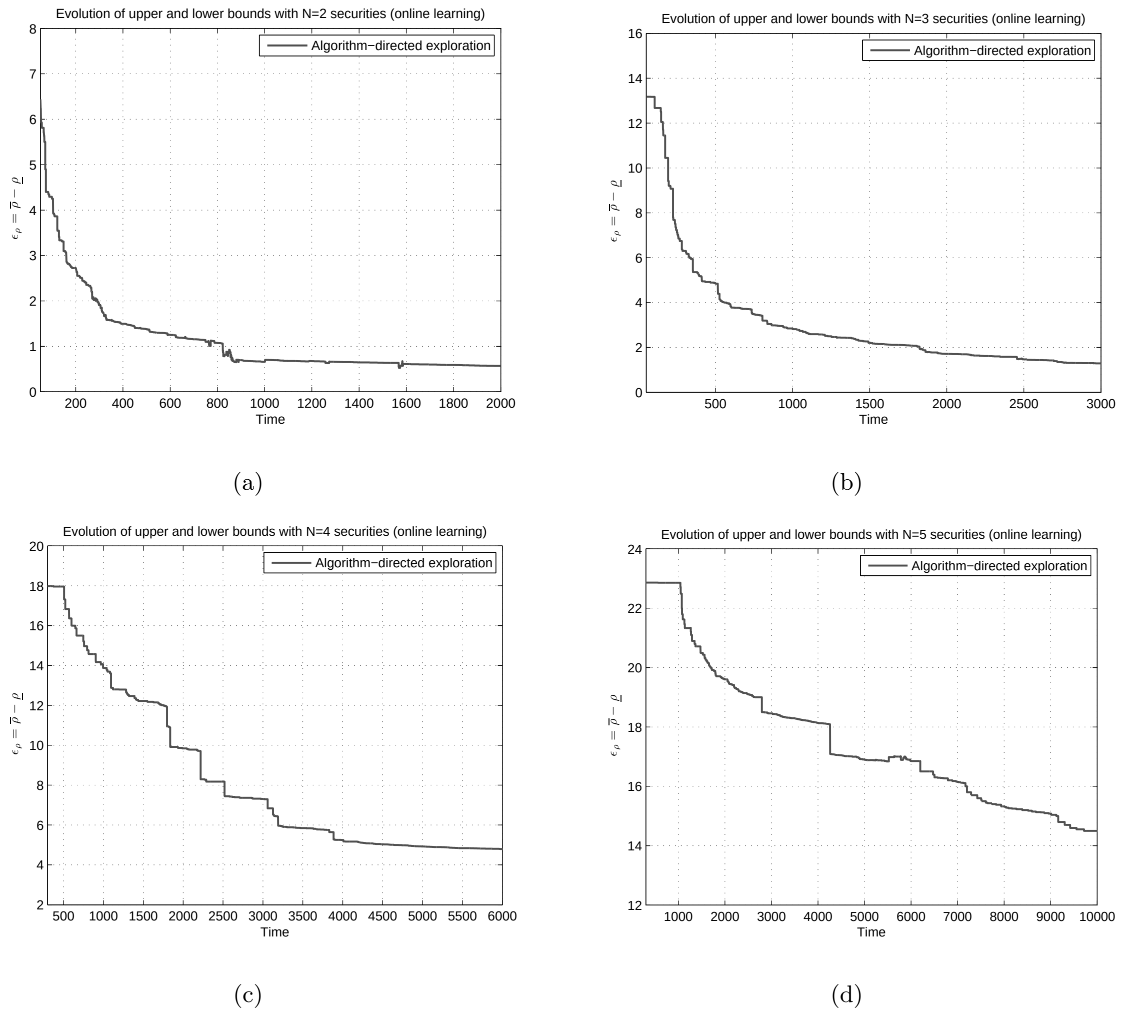

Figure 7.2: Online behavior of lower and upper bounds of the estimated-model average return over time using two connected securities (a), and three (b), four (c) and five (d) securities connected as a bidirectional ring.

7.4.4 Analysis of the learned policy

After the learning period, the policy is extracted and used to interact with the environment.

Figure 7.3 shows the average return received over time coming from the interaction with the environment, using the extracted policy of the algorithm-directed exploration strategy against the optimal value (dotted black line). We note that in all cases the extracted policies act optimally. Therefore, the average return received during learning shown in Figure 7.1 converges to the optimal value.

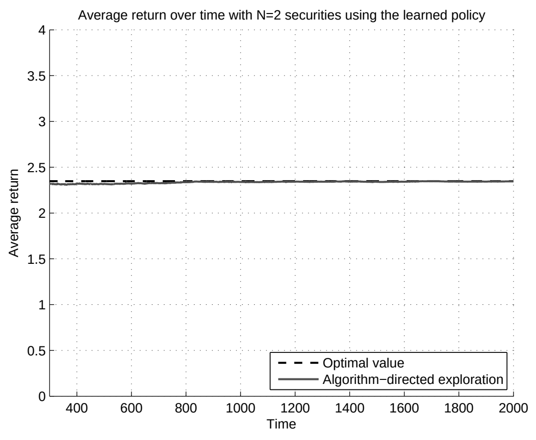

(a)

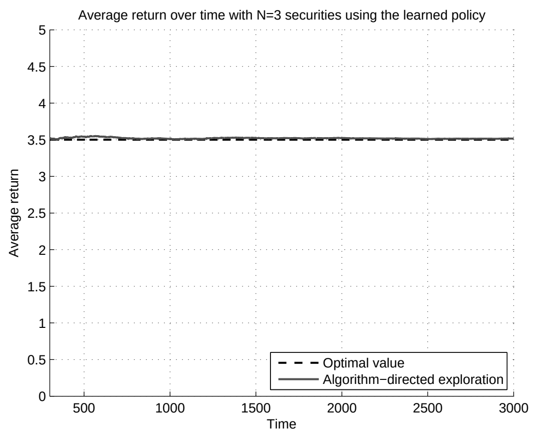

(b)

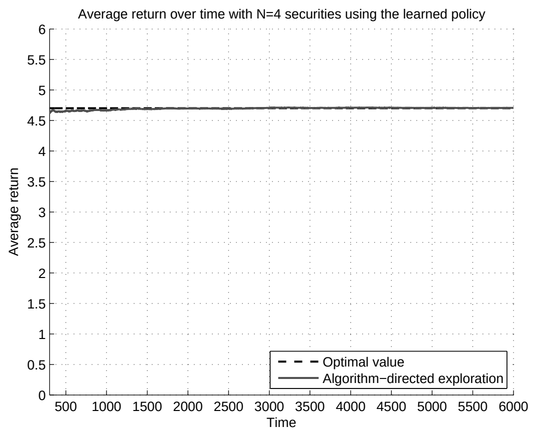

(c)

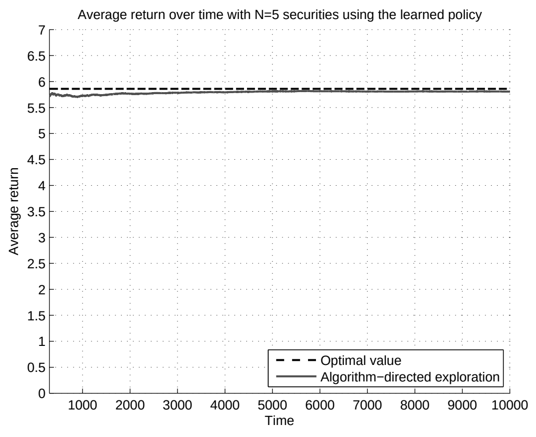

(d)

Figure 7.3: Average return over time of the learned policy corresponding to the algorithm-directed exploration strategy using two connected securities (a), and three (b), four (c), and five (d) securities connected as a bidirectional ring.

7.5 Discussion

We have presented the basic theory about reinforcement learning, a framework that addresses the problem of how a decision-maker can learn a behavior through interactions with an uncertain environment. We have discussed the two main methods used to solve a reinforcement learning problem, namely model-free and model-based, highlighting advantages and disadvantages. We have described how factored MDPs are exploited to manage efficiently the exploration-exploitation trade-off and to effectively scale up to large state spaces in the discrete time settings. We have introduced a novel extension of model-based methods to control continuous time dynamic systems based on structured CTMDPs. This approach leverages on an approximate linear program to efficiently manage the exploration-exploitation trade-off. It learns the critical parts of the model needed to solve the approximate linear program and it achieves a sample efficiency which is logarithmic in the size of the problem description. The proposed approach has performance guarantees in the probably approximately correct framework. Finally, the experimental results on the trading problem have demonstrated the effectiveness of this algorithm.

Chapter 8

Conclusions

This thesis has introduced probabilistic graphical models, specifically Bayesian networks, continuous time Bayesian networks and their extensions, for reasoning and decision-making in finance. Theoretical findings, applications and path-breaking examples have demonstrated their effectiveness and they have opened a substantial amount of potential future work both from theoretical and practical point of views.

8.1 Brief summary

In the first part of this thesis, we have exploited the interplay between modern portfolio theory and Bayesian networks to propose a novel framework for portfolio analysis and optimization. It integrates the investor's market views with a quantitative factor model and it allows efficient evidential reasoning to understand the behavior of the investment portfolio in different economic scenarios. We have described continuous time Bayesian networks, a robust modeling language for structured stochastic processes that evolve over continuous time. We have highlighted advantages and disadvantages of these models, and we have given some insights about their use to tackle real financial problems.

In second part of this thesis, we have presented two extensions of continuous time Bayesian networks to enhance their expressive power and usability: continuous time Bayesian network classifiers, that allow to perform temporal classification in continuous time, and non-stationary continuous time Bayesian networks, that allow to represent dependencies which change over time. We have shown how to learn these classifiers from

Big Data, how to apply them to the foreign exchange rate prediction problem in high frequency domain and how to use non-stationary continuous time Bayesian networks to effectively analyze time-series data.

In the last part of this thesis, we have focused on structured continuous time Markov decision processes that leverage on continuous time Bayesian networks to represent large and structured continuous time systems. We have provided techniques to solve them based on linear programming approximation. Finally, we have introduced a model-based reinforcement learning algorithm to control these systems. It leverages on an approximate linear program to manage the exploration-exploitation trade-off and it achieves a sample efficiency, which is logarithmic in the size of the problem description.

8.2 Future directions

Different directions of the future research will focus on both theoretical and practical challenges. From the theoretical side, we mention the extension of both continuous time Bayesian network classifiers and non-stationary continuous time Bayesian networks to cope with hidden nodes, as well as to handle with missing data. Another issue is related to the design of learning algorithms for continuous time Bayesian networks that can scale well in distributed processing environment for complete and incomplete data. The solution of structured continuous time Markov decision processes, as well as the model-based reinforcement learning algorithm based on them, strongly relies on the efficiency of the approximate linear program. Therefore, the performance can be increased with the design of enhanced versions of this algorithm, such as a clever design of the separation oracle used in the cutting plane algorithm. Moreover, structured continuous time Markov decision processes can be enriched with the modeling of instantaneous rewards for transitioning from one state to another.

From the practical side, the analysis of financial data using continuous time Bayesian networks and their extensions is just at early stages, but there are many possible applications, ranging from scenario analysis, prediction, time-series analysis, optimization of distributions over time, to the design of optimal policies in complex trading environments. This will open the doors to a new way of modeling financial problems.

Bibliography

Aalen, O. O., Borgan, O., and Gjessing, H. K. (2008). *Survival and Event History Analysis*. Springer.

Acerbi, E. and Stella, F. (2014). Continuous time bayesian networks for gene network reconstruction: a comparative study on time course data. In *The 10th International Symposium on Bioinformatics Research and Applications (ISBRA 2013), Zhangjiajie, China*.

Ahmed, A. and Xing, E. P. (2009). Recovering time-varying networks of dependencies in social and biological studies. *Proceedings of the National Academy of Sciences*, 106(29):11878–11883.

Albanese, C., Jackson, K., and Wiberg, P. (2004). A new fourier transform algorithm for value at risk. *Quantitative Finance*, 4(3):328–338.

Andre, D., Friedman, N., and Parr, R. (1998). Generalized prioritized sweeping. *Advances in Neural Information Processing Systems 10*, pages 1001–1007.

Andreassen, S., Woldbye, M., Falck, B., and Andersen, S. K. (1987). Munin - a causal probabilistic network for interpretation of electromyographic findings. In *The 10th International Joint Conference on Artificial Intelligence (IJCAI-87), Milan, Italy*, pages 366–372.

Arnborg, S., Corneil, D. G., and Proskurowski, A. (1987). Complexity of finding embeddings in a k-tree. *SIAM Journal of Algebraic and Discrete Methods*, 8(2):277–284.

Arroyo-Figueroa, G. and Sucar, L. (1999). Temporal bayesian network for diagnosis and prediction. In *The 15th Conference on Uncertainty in Artificial Intelligence (UAI 1999), Stockholm, Sweden*, pages 13–20.

Auer, P., Cesa-Bianchi, N., and Fischer, P. (2002). Finite time analysis of the multiarmed bandit problem. *Machine Learning*, 47(2-3):235–256.

Barto, A. and Mahadevan, S. (2003). Recent advances in hierarchical reinforcement learning. *Discrete Event Dynamic Systems*, 13(1-2):41–77.

Basak, A., Brinster, I., Ma, X., and Mengshoel, O. J. (2012). Accelerating bayesian network parameter learning using hadoop and mapreduce. In *The 1st International Workshop on Big Data, Streams and Heterogeneous Source Mining (BigMine 12), Beijing, China*, pages 101–108.

Bäuerle, N. and Rieder, U. (2011). *Markov Decision Processes with Applications to Finance.* Springer-Verlag.

Baviera, R., Pasquini, M., Serva, M., Vergni, D., and Vulpiani, A. (2002). Antipersistent markov behavior in foreign exchange markets. *Physica A*, 312(3-4):565–576.

Baviera, R., Vergni, D., and Vulpiani, A. (2000). Markovian approximation in foreign exchange markets. *Physica A*, 280(3-4):566–581.

Becker, A. and Geiger, D. (2001). A sufficiently fast algorithm for finding close to optimal clique trees. *Artificial Intelligence*, 125(1-2):3–17.

Bellman, R. and Dreyfus, S. (1959). Functional approximation and dynamic programming. *Mathematical Tables and Other Aids to Computation*, 13(68):247–251.

Bellman, R. E. (1957). *Dynamic Programming.* Princeton University Press.

Bertsekas, D. P. (1987). *Dynamic Programming: Deterministic and Stochastic Models.* Prentice Hall.

Bertsekas, D. P. and Tsitsiklis, J. N. (1996). *Neuro-Dynamic Programming.* Athena Scientific, Belmont, MA.

Bertsimas, D., Mersereau, A. J., and Patel, N. R. (2003). Dynamic classification of online customers. In *The 3rd SIAM International Conference on Data Mining (SMD03), San Francisco, USA*.

Bertsimas, D. and Tsitsiklis, J. (1993). Simulated annealing. *Statistical Science*, 8(1):10–15.

Berzuini, C. (1989). Representing time in causal probabilistic networks. In *The 5th Conference on Uncertainty in Artificial Intelligence (UAI 1989), Ontario, USA*, pages 15–28.

Black, F. and Litterman, R. (1991). Asset allocation: Combining investor views with market equilibrium. *The Journal of Fixed Income*, 1(2):7–18.

Boudali, H. and Dugan, J. B. (2006). A continuous-time bayesian network reliability modeling, and analysis framework. *IEEE Transactions on Reliability*, 55(1):86–97.

Boutilier, C., Dearden, R., and Goldszmidt, M. (1995). Exploiting structure in policy construction. In *The 14th International Joint Conference on Artificial Intelligence (IJCAI-95), Montreal, Canada*.

Boutilier, C., Dearden, R., and Goldszmidt, M. (2000). Stochastic dynamic programming with factored reppresentations. *Artificial Intelligence*, 121(1):49–107.

Boutilier, C., T., D., and S., H. (1999). Decision theoretic planning: Structural assumptions and computational leverage. *Journal of Artificial Intelligence Research*, 11:1–94.

Boyen, X. and Koller, D. (1998). Tractable inference for complex stochastic processes. In *The 14th Conference on Uncertainty in Artificial Intelligence (UAI 1998), Madison, USA*.

Brafman, R. I. and Tennenholtz, M. (2001). R-max - a general polynomial time algorithm for near-optimal reinforcement learning. In *The 17th International Joint Conference on Artificial Intelligence (IJCAI-01), Seattle, USA*.

Cerny, V. (1985). Thermodynamical approach to the traveling salesman problem: An efficient simulation algorithm. *Journal of Optimization Theory and Applications*, 45(1):41–51.

Chakraborty, D. and Stone, P. (2011). Structure learning in ergodic factored mdps without knowledge of the transition function's in-degree. In *The 28th International Conference on Machine Learning (ICML 2011), Bellevue, USA*.

Cheng, J., Greiner, R., Kelly, J., Bell, D., and Liu, W. (2002). Learning bayesian networks from data: An information-theory based approach. *Artificial Intelligence*, 137(1-2):43–90.

Chickering, D. M., Geiger, D., and Heckerman, D. (1994). Learning bayesian networks is np-hard. Technical Report MSR-TR-94-17, Microsoft Research.

Chickering, D. M., Geiger, D., and Heckerman, D. (1995). Learning bayesian networks: Search methods and experimental results. In *The 5th International Workshop on Artificial Intelligence and Statistics (AISTATS 1995), Fort Lauderdale, USA*, pages 112–128.

Chinn, M. and Meese, R. (1995). Banking on currency forecasts: How predictable is change in money? *Journal of International Economics*, 38:161–178.

Chu, C. T., Kim, S. K., Lin, Y. A., Yu, Y. Y., Bradski, G., Ng, A. Y., and Olukotun, K. (2006). Map-reduce for machine learning on multicore. *In Advances in Neural Information Processing Systems 19 (NIPS 2006)*, pages 281–288.

Codecasa, D. and Stella, F. (2014). Learning continuous time bayesian network classifiers. *International Journal of Approximate Reasoning*, 55(8):1728–1746.

Cohn, I., El-Hay, T., Kupferman, R., and Friedman, N. (2009). Mean field variational approximation for continuous-time bayesian networks. In *The 25th Conference on Uncertainty in Artificial Intelligence (UAI 2009), Montreal, Canada*.

Condon, A. (1992). The complexity of stochastic games. *Information and Computation*, 96(2):203–224.

Cooper, G. (1990). Probabilistic inference using belief networks is np-hard. *Artificial Intelligence*, 42:393–405.

Dai, P. and Hansen, E. A. (2007). Prioritizing bellman backups without a priority queue. In *The 17th International Conference on Automated Planning and Scheduling (ICAPS-07), Providence, USA*, pages 113–119.

Dantzig, G. B. (1963). *Linear Programming and Extensions.* Princeton University Press.

Darwiche, A. (1995). Conditioning algorithms for exact and approximate inference in causal networks. In *The 11th Conference on Uncertainty in Artificial Intelligence (UAI 1995), Montreal, Canada*, pages 99–107.

Dayan, P. (1992). The convergence of td(λ) for general λ. *Machine Learning*, 8:341–362.

de Campos, L. M., Fernandez-Luna, J. M., and Huete, J. F. (2004). Bayesian networks and information retrieval: an introduction to the special issue. *Information Processing & Management*, 40(5):727–733.

de Farias, D. P. and van Roy, B. (2003). The linear programming approach to approximate dynamic programming. *Operations Research*, 51(6):850–865.

de Farias, D. P. and van Roy, B. (2004). On constraint sampling in the linear programming approach to approximate dynamic programming. *Mathematics of Operations Research*, 29(3):462–478.

Dean, J. and Ghemawat, S. (2004). Mapreduce: Simplified data processing on large clusters. In *The 6th Conference on Symposium on Opearting Systems Design & Implementation (OSDI '04), San Francisco, USA*.

Dean, T. and Kanazawa, K. (1989). A model for reasoning about persistence and causation. *Computational Intelligence*, 5(2):142–150.

Dearden, R. (2001). Structured prioritised sweeping. In *The 18h International Conference on Machine Learning (ICML 2001), Williamstown, USA*, pages 82–89.

Dearden, R., Friedman, N., and Andre, D. (1999). Model-based bayesian exploration. In *The 15th Conference on Uncertainty in Artificial Intelligence (UAI 1999), Stockholm, Sweden*, pages 150–159.

Dechter, R. (1999). Bucket elimination: A unifying framework for reasoning. *Artificial Intelligence*, 113(1-2):41–85.

Demirer, R., Mau, R., and Shenoy, C. (2006). Bayesian networks: A decision tool to improve portfolio risk analysis. *Journal of Applied Finance*, 16(2):106 – 119.

Dempster, M. A. H. and Jones, C. M. (2001). A real-time adaptive trading system using genetic programming. *Quantitative Finance*, 1:397–413.

D'Epenoux, F. (1963). A probabilistic production and inventory problem. *Management Science*, 10(1):98–108.

Derman, C., Lieberman, G. J., and Ross, S. M. (1975). A stochastic sequential allocation model. *Operations Research*, 23(6):1120–1130.

Dimitrova, E. S., Licona, M. P. V., McGee, J., and Laubenbacher, R. (2010). Discretization of time series data. *Journal of Computational Biology*, 17(6):853–868.

Diuk, C., Li, L., and Leffler, B. R. (2009). The adaptive k-meteorologists problem and its application to structure learning and feature selection in reinforcement learning. In *The 26th International Conference on Machine Learning (ICML 2009), Montreal, Canada*, pages 249–256.

Domingos, P. and Pazzani, M. (1997). On the optimality of the simple bayesian classifier under zero-one loss. *Machine Learning*, 29:103–130.

Dondelinger, F., Lèbre, S., and Husmeier, D. (2013). Non-homogeneous dynamic bayesian networks with bayesian regularization for inferring gene regulatory networks with gradually time-varying structure. *Machine Learning*, 90(2):191–230.

Duda, R. O. and Hart, P. E. (1973). *Pattern Classification and Scene Analysis.* John Wiley & Sons.

Duda, R. O., Hart, P. E., and Stork, D. G. (2000). *Pattern Classification.* John Wiley & Sons.

Durante, D. and Dunson, D. B. (2014). Bayesian dynamic financial networks with time-varying predictors. *Statistics & Probability Letters*, 93:19–26.

El-Hay, T., Cohn, I., Friedman, N., and Kupferman, R. (2010). Continuous-time belief propagation. In *The 27st International Conference on Machine Learning (ICML 2010), Haifa, Israel.*

El-Hay, T., Friedman, N., and Kupferman, R. (2008). Gibbs sampling in factorized continuous-time markov processes. In *The 24th Conference on Uncertainty in Artificial Intelligence (UAI 2008), Helsinki, Finland*, pages 169–178.

Elton, E. J., Gruber, M., Brown, S. J., and Goetzmann, W. N. (2010). *Modern Portfolio Theory and Investment Analysis*. John Wiley & Sons, 8th edition.

Fabozzi, F. J., Kolm, P. N., Pachamanova, D., and Focardi, S. M. (2007). *Robust Portfolio Optimization and Management*. John Wiley & Sons.

Fagiuoli, E., Omerino, S., and Stella, F. (2008). *Mathematical Methods for Knowledge Discovery and Data Mining*, chapter Bayesian Belief Networks for Data Cleaning, pages 204–219. IGI Global.

Fama, E. F. (1965). The behaviour of stock market prices. *Journal of Business*, 38(1):34–105.

Fan, Y. and Shelton, C. (2008). Sampling for approximate inference in continuous time bayesian networks. In *The 10th International Symposium on Artificial Intelligence and Mathematics (ISAIM 2008), Fort Lauderdale, USA*.

Fan, Y. and Shelton, C. R. (2009). Learning continuous-time social network dynamics. In *The 25th Conference on Uncertainty in Artificial Intelligence (UAI 2009), Montreal, Canada*.

Fawcett, T. (2006). An introduction to roc analysis. *Pattern Recognition Letters*, 27(8):861–874.

Fishman, G. (2003). *Monte Carlo: Concepts, Algorithms, and Applications*. Springer Series in Operations Research and Financial Engineering. Springer.

Fletcher, P. and Patty, C. W. (1995). *Foundations of Higher Mathematics*. Cengage Learning, 3rd edition.

Friedman, N., Geiger, D., and Goldszmidt, M. (1997). Bayesian network classifiers. *Machine Learning*, 29(2-3):131–163.

Friedman, N. and Koller, D. (2000). Being bayesian about bayesian network structure: A bayesian approach to structure discovery in bayesian networks. *Machine Learning*, 50(1-2):95–125.

Friedman, N. and Kupferman, R. (2006). Dimension reduction in singularly perturbed continuous-time bayesian networks. In *The 22nd Conference on Uncertainty in Artificial Intelligence (UAI 2006), Cambridge, USA*.

Friedman, N., Linial, M., Nachman, I., and Pe'er, D. (2000). Using bayesian networks to analyze expression data. In *The 4th Annual International Conference on Computational Molecular Biology (RECOMB 2000), Tokyo, Japan*, pages 127–135.

Gatti, E., Luciani, D., and Stella, F. (2011). A continuous time bayesian network model for cardiogenic heart failure. *Flexible Services and Manufacturing Journal*, 24(2):496–515.

Geiger, D. and Heckerman, D. (1997). A characterization of the dirichlet distribution through global and local parameter independence. *Annals of Statistics*, 25(3):1344–1369.

Ghahramani, Z. and Hinton, G. E. (2000). Variational learning for switching state-space models. *Neural Computation*, 12(4):963–996.

Giudici, P. and Castelo, R. (2003). Improving markov chain monte carlo model search for data mining. *Machine Learning*, 50(1-2):127–158.

Gopalratnam, K., Kautz, K., and Weld, D. S. (2005). Extending continuous time bayesian networks. In *The 20th National Conference on Artificial Intelligence (AAAI-05), Pittsburgh, USA*.

Gosavi, A. (2009). Reinforcement learning: A tutorial survey and recent advances. *Journal of Computing*, 21(2):178–192.

Gradojevic, N. (2007). Non-linear, hybrid exchange rate modeling and trading profitability in the foreign exchange market. *Journal of Economic Dynamics & Control*, 31(2):557–574.

Grzegorczyk, M. and Husmeier, D. (2009). Non-stationary continuous dynamic bayesian networks. In *Advances in Neural Information Processing Systems 22 (NIPS 2009)*, pages 682–690.

Guestrin, C., Koller, D., Parr, R., and Venkataraman, S. (2003). Efficient solution algorithms for factored mdps. *Journal of Artificial Intelligence Research*, 19:399–468.

Guestrin, C., Patrascu, R., and Schuurmans, D. (2002). Algorithm-directed exploration for model-based reinforcement learning in factored mdps. In *The 19th International Conference on Machine Learning (ICML 2002), Sydney, Australia.*

Gunawardana, A., Meek, C., and Xu, P. (2011). A model for temporal dependencies in event streams. In *Advances in Neural Information Processing Systems 24 (NIPS 2011)*, pages 1962–1970.

Guo, X. and Hernandez-Lerma, O. (2003). Drift and monotonicity conditions for continuous-time controlled markov chains with an average criterion. *IEEE Transactions on Automatic Control*, 48(2):236–245.

Guo, X. and Hernandez-Lerma, O. (2009). *Continuous-Time Markov Decision Processes*, volume 62 of *Stochastic Modelling and Applied Probability*. Springer-Verlag.

Hanneke, S. and Xing, E. P. (2006). Discrete temporal models of social networks. In *Workshop on Statistical Network Analysis at the 23rd International Conference on Machine Learning (ICML 2006), Pittsburgh, USA*.

Hautsch, N. (2004). *Modelling Irregularly Spaced Financial Data: Theory and Practice of Dynamic Duration Models*. Lecture Notes in Economics and Mathematical Systems. Springer-Verlag.

Heckerman, D., Geiger, D., and Chickering, D. M. (1995). Learning bayesian networks: The combination of knowledge and statistical data. *Machine Learning*, 20:197–243.

Herbrich, R., Graepel, T., and Murphy, B. (2007). Structure from failure. In *The 2nd USENIX workshop on Tackling computer systems problems with machine learning techniques (SYSML 07), Cambridge, USA*, pages 1–6.

Horvitz, E., Suermondt, H., and Cooper, G. (1989). Bounded conditioning: Flexible inference for decisions under scarce resources. In *The 5th Conference on Uncertainty in Artificial Intelligence (UAI 1989), Windsor, USA*, pages 182–193.

Howard, R. A. (1960). *Dynamic Programming and Markov Processes.* The MIT Press.

Hu, Q. and Yue, W. (2007). *Markov Decision Processes with Their Applications.* Advances In Mechanics And Mathematics. Springer.

Ince, H. and Trafalis, T. B. (2006). A hybrid model for exchange rate prediction. *Decision Support Systems*, 42(2):1054–1062.

Jaakkola, T., Jordan, M., and Singh, S. (1994a). Monte-carlo reinforcement learning in non-markovian decision problems. In *Advances in Neural Information Processing Systems 7 (NIPS 1994).*

Jaakkola, T., Jordan, M., and Singh, S. (1994b). On the convergence of stochastic iterative dynamic programming algorithms. *Neural Computation*, 6(6):1185–1201.

Jensen, F., Lauritzen, S., and Olesen, K. (1990). Bayesian updating in recursive graphical models by local computation. *Computational Statistics Quarterly*, 4:269–282.

Jensen, F. V. and Nielsen, T. D. (2007). *Bayesian Networks and Decision Graphs.* Springer-Verlag, 2nd edition.

Kablan, A. and Ng, W. L. (2011). Intraday high-frequency fx trading with adaptive neuro-fuzzy inference systems. *International Journal of Financial Markets and Derivatives*, 2(1):68–87.

Kaelbling, L. P. (1993). *Learning in Embedded Systems.* The MIT Press.

Kaelbling, L. P., Littman, M. L., and Moore, A. W. (1996). Reinforcement learning: A survey. *Journal of Artificial Intelligence Research*, 4:237–285.

Kakade, S. M. (2003). *On the sample complexity of reinforcement learning.* PhD thesis, University College London, UK.

Kakumanu, P. (1971). Continuously discounted markov decision models with countable state and action spaces. *Annals of Mathematical Statistics*, 42:919–926.

Kakumanu, P. (1977). Relation between continuous and discrete markovian decision problems. *Naval Research Logistics Quarterly*, 24(3):431–439.

Kamruzzaman, J., Sarker, R. A., and Ahmad, I. (2003). Svm based models for predicting foreign currency exchange rates. In *The 3rd IEEE International Conference on Data Mining (ICDM 2003), Melbourne, USA*, pages 557–560.

Kan, K. F. and Shelton, C. R. (2008). Solving structured continuous-time markov decision processes. In *International Symposium on Artificial Intelligence and Mathematics (ISAIM 2008), Fort Lauderdale, USA*.

Kanazawa, K. (1992). *Reasoning about Time and Probability*. PhD thesis, Brown University, USA.

Kearns, M. and Koller, D. (1999). Efficient reinforcement learning in factored mdps. In *The 16th International Joint Conference on Artificial Intelligence (IJCAI-99), Stockholm, Sweden*.

Kearns, M. J. and Singh, S. P. (1998). Near-optimal reinforcement learning in polynomial time. In *The 15th International Conference on Machine Learning (ICML 1998), Madison, USA*, pages 260–268.

Kilian, L. and Taylor, M. (2003). Why is it so difficult to beat random walk forecast of exchange rates? *Journal of International Economics*, 60(1):85–107.

Kirkpatrick, S., Gelatt, C. D., and Vecchi, M. P. (1983). Optimization by simulated annealing. *Science*, 220(4598):671–680.

Klee, V. and Minty, G. J. (1972). *Inequalities III*, chapter How Good is the Simplex Algorithm?, pages 159–175. Academic Press Inc.

Koller, D. and Friedman, N. (2009). *Probabilistic Graphical Models: Principles and Techniques*. The MIT Press.

Koller, D. and Parr, R. (1999). Computing factored value functions for policies in structured mdps. In *The 16th International Joint Conference on Artificial Intelligence (IJCAI-99), Stockholm, Sweden*, pages 1332–1339.

Kolter, J. Z. and Ng, A. (2009). Near-bayesian exploration in polynomial time. In *The 26th International Conference on Machine Learning (ICML 2009), Montreal, Canada*, pages 513–520.

Kumar, P. R. and Varaija, P. (1986). *Stochastic Systems: Estimation, Identification, and Adaptive Control*. Prentice Hall, New Jersey.

Kveton, B. and Hauskrecht, M. (2005). An mcmc approach to solving hybrid factored mdps. In *The 19th International Joint Conference on Artificial Intelligence (IJCA-05), Edinburgh, UK*, pages 1346–1351.

Kveton, B. and Hauskrecht, M. (2008). Partitioned linear programming approximations for mdps. In *The 24th Conference on Uncertainty in Artificial Intelligence (UAI 2008), Helsinki, Finland.*

Lai, T. L. and Robbins, H. (1985). Asymptotically efficient adaptive allocation rules. *Advances in Applied Mathematics*, 6(1):4–22.

Langley, P., Iba, W., and Thompson, K. (1992). An analysis of bayesian classifiers. In *The 10th National Conference on Artificial Intelligence (AAAI-92), San Jose, USA*, pages 223–228.

Lauritzen, S. and Spiegelhalter, D. (1988). Local computations with probabilities on graphical structures and their application to expert systems. *Journal of Royal Statistics Society, Series B*, 50(2):157–224.

Lèbre, S., Becq, J., Devaux, F., Stumpf, M. P., and Lelandais, G. (2010). Statistical inference of the time-varying structure of gene-regulation networks. *BMC Systems Biology*, 4(1):130.

Leung, M. T., Chen, A.-S., and Daouk, H. (2000). Forecasting exchange rates using general regression neural networks. *Computers & Operations Research*, 27(11-12):1093–1110.

Lin, J. (2008). Scalable language processing algorithms for the masses: A case study in computing word co-occurrence matrices with mapreduce. In *The 2008 Conference on Empirical Methods in Natural Language Processing (EMNLP 2008), Waikiki, USA*, pages 419–428.

Lin, J. and Dyer, C. (2010). *Data-Intensive Text Processing with MapReduce*. Morgan & Claypool Publishers.

Lions, P. L. (1983). On the hamilton-jacobi-bellman equations. *Acta Applicandae Mathematicae*, 1(1):17–41.

Littman, M., Dean, T., and Kaelbling, L. (1995). On the complexity of solving markov decison problems. In *The 11th Conference on Uncertainty in Artificial Intelligence (UAI 1995), Montreal, Canada*.

Lucas, P. J. F., van der Gaag, L. C., and Abu-Hanna, A. (2004). Bayesian networks in biomedicine and health-care. *Artificial Intelligence in Medicine*, 30(3):201–214.

Luciani, D., Marchesi, M., and Bertolini, G. (2003). The role of bayesian networks in the diagnosis of pulmonary embolism. *Journal of Thrombosis and Haemostasis*, 1(4):698–707.

Madigan, D., York, J., and Allard, D. (1995). Bayesian graphical models for discrete data. *International Statistical Review*, 63(2):215–232.

Mansour, Y. and Singh, S. (1999). On the complexity of policy iteration. In *The 15th Conference on Uncertainty in Artificial Intelligence (UAI 1999), Stockholm, Sweden*, pages 401–408.

Markowitz, H. (1952). Portfolio selection. *The Journal of Finance*, 7(1):77–91.

Mascherini, M. and Stefanini, F. M. (2007). Using weak prior information on structures to learn bayesian networks. In *The 11th International Conference on Knowledge-based Intelligent Information and Engineering Systems (KES 2007), Vietri sul Mare, Italy*, pages 413–420.

Melo, F. S., Meyn, S. P., and Ribeiro, M. I. (2008). An analysis of reinforcement learning with function approximation. In *The 25th International Conference Machine Learning (ICML 2008), Helsinki, Finland*.

Mendelssohn, R. and Sobel, M. J. (1980). Capital accumulation and the optimization of renewable resource models. *Journal of Economic Theory*, 23(2):243–260.

Meucci, A. (2005). *Risk and Asset Allocation.* Springer.

Meucci, A. (2006). Beyond black-litterman in practice: A five-step recipe to input views on non-normal markets. *Risk*, 19:114–119.

Meucci, A. (2009). Enhancing the black-litterman and related approaches: Views and stress-test on risk factors. *Journal of Asset Management*, 10:89–96.

Meucci, A. (2010). Factors on demand. *Risk*, 23(7):84–89.

Meucci, A. (2011). The prayer: Ten-step checklist for advanced risk and portfolio management. *Risk Professional*, (April/June):54–60/55–59.

Mitchell, T. M. (1997). *Machine Learning.* McGraw Hill.

Moler, C. and van Loan, C. (2003). Nineteen dubious ways to compute the exponential of a matrix, twenty-five years later. *SIAM Review*, 45(1):3–49.

Moore, A. W. and Atkeson, C. G. (1993). Prioritized sweeping: Reinforcement learning with less data and less real time. *Machine Learning*, 13:103–130.

Murphy, K. P. (2002). *Dynamic Bayesian Networks: Representation, Inference and Learning.* PhD thesis, University of California, Berkeley, USA.

Murphy, K. P. (2012). *Machine Learning: A Probabilistic Perspective.* The MIT Press.

Neapolitan, R. E. (2003). *Learning Bayesian Networks.* Prentice Hall.

Nielsen, S. H. and Nielsen, T. (2008). Adapting bayes network structures to non-stationary domains. *International Journal of Approximate Reasoning*, 49(2):379–397.

Nodelman, U. (2007). *Continuous Time Bayesian Networks.* PhD thesis, Stanford University.

Nodelman, U. and Horvitz, E. (2003). Continuous time bayesian networks for inferring users' presence and activities with extensions for modeling and evaluation. Technical Report MSR-TR-2003-97, Microsoft Research.

Nodelman, U., Koller, D., and Shelton, C. R. (2005a). Expectation propagation for continuous time bayesian networks. In *The 21st Conference on Uncertainty in Artificial Intelligence (UAI 2005), Edinburgh, UK*, pages 431–440.

Nodelman, U., Shelton, C. R., and Koller, D. (2002). Continuous time bayesian networks. In *The 18th Conference on Uncertainty in Artificial Intelligence (UAI 2002), Edmonton, Canada*, pages 378–387.

Nodelman, U., Shelton, C. R., and Koller, D. (2003). Learning continuous time bayesian networks. In *The 19th Conference on Uncertainty in Artificial Intelligence (UAI 2003), Acapulco, Mexico*, pages 451–458.

Nodelman, U., Shelton, C. R., and Koller, D. (2005b). Expectation maximization and complex duration distributions for continuous time bayesian networks. In *The 21st Conference on Uncertainty in Artificial Intelligence (UAI 2005), Edinburgh, UK*, pages 421–430.

Norris, J. R. (1997). *Markov chains.* Cambridge University Press.

Ohira, T., Sazuka, N., Marumo, K., Shimizu, T., Takayasu, M., and Takayasu, H. (2002). Predictability of currency market exchange. *Physica A*, 308(1-4):368–374.

Owens, J. D., Luebke, D., Govindaraju, N., Harris, M., Krüger, J., Lefohn, A. E., and Purcell, T. (2007). A survey of general-purpose computation on graphics hardware.

Pavlenko, T. and Chernyak, O. (2010). Credit risk modeling using bayesian networks. *International Journal of Intelligent Systems*, 25(4):326–344.

Pearl, J. (1986). Fusion, propagation and structuring in belief networks. *Artificial Intelligence*, 29(3):241–288.

Pearl, J. (1988). *Probabilistic Reasoning in Intelligent Systems: Networks of Plausible Inference.* Morgan Kaufmann.

Plerou, V., Gopikrishnan, V., Rosenau, B., Amaral, L., Guhr, T., and Stanley, E. (2002). Random matrix approach to cross-correlations in financial data. *Physical Review E*, 65:1–17.

Portinale, L. and Codetta-Raiteri, D. (2009). Generalizing continuous time bayesian networks with immediate nodes. In *The 1st IJCAI Workshop on Graph Structures for Knowledge Representation and Reasoning, Pasadena, USA.*

Post, I. and Ye, Y. (2013). The simplex method is strongly polynomial for deterministic markov decision processes. In *The 24th Annual ACM-SIAM Symposium on Discrete Algorithms (SODA13), New Orleans, USA*, pages 1465–1473.

Poupart, P., Vlassis, N., Hoey, J., and Regan, K. (2006). An analytic solution to discrete bayesian reinforcement learning. In *The 23rd International Conference on Machine Learning (ICML 2006), Pittsburgh, USA.*

Proakis, J. G. and Manolakis, D. K. (2006). *Digital Signal Processing: Principles, Algorithms and Applications.* Prentice Hall.

Puterman, M. L. (1994). *Markov decision processes: Discrete stochastic dynamic programming.* Wiley, New York.

Qian, E. and Gorman, S. (2001). Conditional distribution in portfolio theory. *Financial Analyst Journal*, 57(2):44–51.

Rajaram, S., Graepel, T., and Herbrich, R. (2005). A model for structured point processes. In *The 10th International Workshop on Artificial Intelligence and Statistics (AISTATS 2005), Barbados.*

Rao, V. and Teh, Y. W. (2011). Fast mcmc sampling for markov jump processes and continuous time bayesian networks. In *The 27th Conference on Uncertainty in Artificial Intelligence (UAI 2011), Barcelona, Spain.*

Rebonato, R. and Denev, A. (2014). *Portfolio Management under Stress: A Bayesian-Net Approach to Coherent Asset Allocation.* Cambridge University Press.

Reed, B. A. (1992). Finding approximate separators and computing tree width quickly. In *The 24th annual ACM Symposium on Theory of Computing (STOC 1992), Victoria, Canada*, pages 221–228.

Renner, C., Peinke, J., and Friedrich, R. (2001). Evidence of markov properties of high frequency exchange rate data. *Physica A*, 298(3-4):499–520.

Robinson, J. W. and Hartemink, A. J. (2009). Non-stationary dynamic bayesian networks. In *Advances in Neural Information Processing Systems 21 (NIPS 2008)*, pages 1369–1376.

Robinson, J. W. and Hartemink, A. J. (2010). Learning non-stationary dynamic bayesian networks. *Journal of Machine Learning Research*, 11:3647–3680.

Rummery, G. A. and Niranjan, M. (1994). On-line q-learning using connectionist systems. Technical Report CUED/F-INFENG/TR 166, Cambridge University, UK.

Santos, E. and Young, J. D. (1999). Probabilistic temporal networks: A qualitative unified framework for reasoning with time and uncertainty. *International Journal of Approximate Reasoning*, 20(3):263–291.

Saria, S., Nodelman, U., and Koller, D. (2007). Reasoning at the right time granularity. In *The 23rd Conference on Uncertainty in Artificial Intelligence (UAI 2007), Vancouver, Canada*.

Schmidhuber, J. H. (1991). Curious model-building control systems. In *International Joint Conference on Neural Networks (IJCNN 1991), Seattle, USA*.

Schuurmans, D. and Patrascu, R. (2001). Direct value-approximation for factored mdps. In *Advances in Neural Information Processing Systems 14 (NIPS 2001), Vancouver, Canada*, pages 1579–1586.

Schwartz, A. (1993). A reinforcement learning method for maximizing undiscounted rewards. In *The 10th International Conference on Machine Learning (ICML 1993), Amherst, USA*.

Schweitzer, P. and Seidmann, A. (1985). Generalized polynomial approximations in markovian decision processes. *Journal of Mathematical Analysis and Applications*, 110(2):568–582.

Segal, E., Pe'er, D., Regev, A., Koller, D., and Friedman, N. (2005). Learning module networks. *Journal of Machine Learning Research*, 6:557–588.

Shachter, R., D'Ambrosio, B., and del Favero, B. (1990). Symbolic probabilistic inference in belief networks. In *The 6th Conference on Uncertainty in Artificial Intelligence (UAI 1990), Cambridge, USA*, pages 126–131.

Shachter, R. D. and Peot, M. A. (1989). Simulation approaches to general probabilistic inference on belief networks. In *The 5th Conference on Uncertainty in Artificial Intelligence (UAI 1989), Windsor, USA*, pages 221–234.

Sharpe, W. F. (1964). Capital asset prices: a theory of market equilibrium under conditions of risk. *Journal of Finance*, 19(3):425–442.

Shelton, C. R., Fan, Y., Lam, W., Lee, J., and Xu, J. (2010). Continuous time bayesian network reasoning and learning engine. *Journal of Machine Learning Research*, 11:1137–1140.

Shmilovici, A., Kahiri, Y., Ben-Gal, I., and Hauser, S. (2009). Measuring the efficiency of the intraday forex market with a universal data compression algorithm. *Computational Economics*, 33(2):131–154.

Simma, A., Goldszmidt, M., MacCormick, J., Barham, P., Black, R., Isaacs, R., and Mortier, R. (2008). Ct-nor: Representing and reasoning about events in continuous time. In *The 24th Conference on Uncertainty in Artificial Intelligence (UAI 2008), Helsinki, Finland*, pages 484–493.

Simma, A. and Jordan, M. I. (2010). Modeling events with cascades of poisson processes. In *The 26th Conference on Uncertainty in Artificial Intelligence (UAI 2010), Catalina Island, USA*, pages 546–555.

Singh, S., Jaakkola, T., Littman, M., and Szepesvari, C. (2000). Convergence results for single-step on-policy reinforcement learning algorithms. *Machine Learning*, 38(3):287–308.

Smith, A. V., Yu, J., Smulders, T. V., Hartemink, A. J., and Jarvis, E. D. (2006). Computational inference of neural information flow networks. *PLoS Computational Biology*, 2(11):1436–1449.

Song, L., Kolar, M., and Xing, E. P. (2009). Time-varying dynamic bayesian networks. In *Advances in Neural Information Processing Systems 22 (NIPS 2009)*, pages 1732–1740.

Spiegelhalter, D. J., Dawid, A. P., Lauritzen, S. L., and Cowell, R. G. (1993). Bayesian analysis in expert systems. *Statistical Science*, 8(3):219–247.

Spiegelhalter, D. J. and Lauritzen, S. L. (1990). Sequential updating of conditional probabilities on directed graphical structures. *Networks*, 20(5):579–605.

Stella, F. and Amer, Y. (2012). Continuous time bayesian network classifiers. *Journal of Biomedical Informatics*, 45(6):1108–1119.

Stella, F. and Villa, S. (2014). Learning continuous time bayesian networks in non-stationary domains. Working paper.

Strehl, A. L. (2007). Model-based reinforcement learning in factored-state mdps. In *The 2007 IEEE Symposium on Approximate Dynamic Programming and Reinforcement Learning (ADPRL 2007), Honolulu, USA.*

Strehl, A. L., Li, L., and Littman, M. L. (2009). Reinforcement learning in finite mdps: Pac analysis. *Journal of Machine Learning Research*, 10:2413–2444.

Strehl, E. L., Diuk, C., and Littman, M. L. (2007). Efficient structure learning in factored-state mdps. In *The 22nd National Conference on Artificial Intelligence (AAAI-07), Vancouver, Canada.*

Sutton, R. S. (1988). Learning to predict by the method of temporal differences. *Machine Learning*, 3(1):9–44.

Sutton, R. S. (1990). Integrated architectures for learning, planning, and reacting based on approximating dynamic programming. In *The 7th International Conference on Machine Learning (ICML 1990), Austin, USA.*

Sutton, R. S. and Barto, A. G. (1998). *Reinforcement Learning - An Introduction.* The MIT Press.

Sutton, R. S., Szepesvari, C., Geramifard, A., and Bowling, M. P. (2008). Dyna-style planning with linear function approximation and prioritized sweeping. In *The 24th Conference on Uncertainty in Artificial Intelligence (UAI 2008), Helsinki, Finland.*

Szepesvari, C. and Smart, W. D. (2004). Interpolation-based q-learning. In *The 21st International Conference on Machine Learning (ICML 2004), Banff, Canada*, pages 791–798.

Tanaka-Yamawaki, M. (2003). Stability of markovian structure observed in high frequency foreign exchange data. *Annals of the Institute of Statistical Mathematics*, 55(2):437–446.

Tawfik, A. Y. and Neufeld, E. M. (1994). Temporal bayesian networks. In *The International Workshop on Temporal Reasoning (TIME-94), Pensacola, Florida.*

Taylor, J. R. (1996). *An Introduction to Error Analysis: The Study of Uncertainties in Physical Measurements.* University Science Books, 2nd edition.

Thrun, S. B. (1992). *Handbook of Intelligence Control: Neural, Fuzzy, and Adaptive Approaches*, chapter The role of exploration in learning control. Van Nostrand Reinhold, New York.

Treleaven, P., Galas, M., and Lalchand, V. (2013). Algorithmic trading review. *Communications of the ACM*, 56(1):76–85.

Tsitsiklis, J. N. and van Roy, B. (1996). Feature-based methods for large scale dynamic programming. *Machine Learning*, 22(1-3):59–94.

Vanderbei, R. (2001). *Linear Programming: Foundations and Extensions.* Springer-Verlag.

Verma, T. and Pearl, J. (1992). An algorithm for deciding if a set of observed independencies has a causal explanation. In *The 8th Conference on Uncertainty in Artificial Intelligence (UAI 1992), Stanford, USA*, pages 323–330.

Vilasuso, J. R. (2002). Forecasting exchange rate volatility. *Economics Letters*, 76(1):59–64.

Villa, S. and Rossetti, M. (2014). Learning continuous time bayesian network classifiers using mapreduce. *Journal of Statistical Software*, 62(3):1–25.

Villa, S. and Shelton, C. R. (2014a). Model-based reinforcement learning using structured ctmdps. Working paper.

Villa, S. and Shelton, C. R. (2014b). *Package 'ctbn': R Package for Continuous Time Bayesian Networks.* R-LAIR: Riverside Lab for Artificial Intelligence Research, University of California, Riverside, USA.

Villa, S. and Stella, F. (2012). *Financial Decision Making Using Computational Intelligence*, chapter Bayesian Networks for Portfolio Analysis and Optimization, pages 209–232. Optimisation and its Applications. Springer-Verlag.

Villa, S. and Stella, F. (2014). A continuous time bayesian network classifier for intraday fx prediction. *Quantitative Finance*, 14(12):2079–2092.

Vinh, N. X., Chetty, M., Coppel, R., and Wangikar, P. P. (2012). Gene regulatory network modeling via global optimization of high-order dynamic bayesian network. *BMC Bioinformatics*, 13:131.

Watkins, C. J. C. H. (1989). *Learning from Delayed Rewards.* PhD thesis, Cambridge University, UK.

Watkins, C. J. C. H. and Dayan, P. (1992). Q-learning. *Machine Learning*, 8(3-4):279–292.

White, D. (1993). A survey of applications of markov decision processes. *Journal of the Operational Research Society*, 44(11):1073–1096.

White, T. (2009). *Hadoop: The Definitive Guide.* O'Reilly, Sebastopol, California.

Wiering, M. and Schmidhuber, J. (1998). Efficient model-based exploration. In *The 5th International Conference on Simulation of Adaptive Behavior (SAB 1998), Zürich, Switzerland*, pages 223–228.

Wiering, M. and van Otterlo, M., editors (2012). *Reinforcement Learning: State-of-the-Art.* Springer.

Wingate, D. and Seppi, K. D. (2005). Prioritization methods for accelerating mdp solver. *Journal of Machine Learning Research*, 6:851–881.

Xing, Z., Pei, J., and Keogh, E. (2010). A brief survey on sequence classification. *ACM SIGKDD Explorations Newsletter*, 12(1):40–48.

Xing, Z., Pei, J., and Yu, P. S. (2009). Early prediction on time series: A nearest neighbor approach. In *The 21st International Joint Conference on Artifical intelligence (IJCAI-09), Pasadena, USA*, pages 1297–1302.

Xu, J. and Shelton, C. R. (2008). Continuous time bayesian networks for host level network intrusion detection. In *The European Conference on Machine Learning and Principles and Practice of Knowledge Discovery in Databases (ECML PKDD 2008), Antwerp, Belgium*, pages 613–627.

Xuan, X. and Murphy, K. (2007). Modeling changing dependency structure in multivariate time series. In *The 24th International Conference on Machine Learning (ICML 2007), Corvallis, USA*, pages 1055–1062.

Yao, J. and Tan, C. L. (2000). A case study on using neural networks to perform technical forecasting of forex. *Neurocomputing*, 34(1-4):79–98.

Ye, Y. (2011). The simplex and policy-iteration methods are strongly polynomial for the markov decision problem with a fixed discount rate. *Mathematics of Operations Research*, 36(4):593–603.

Yu, L., Wang, S., and Lai, K. K. (2007). *Foreign Exchange Rate Forecasting with Artificial Neural Networks*. International Series in Operations Research & Management Science. Springer-Verlag.

Zhang, Y. (1999). Toward a theory of marginally efficient markets. *Physica A*, 269(1):30–44.

Zou, M. and Conzen, S. D. (2005). A new dynamic bayesian network (dbn) approach for identifying gene regulatory networks from time course microarray data. *Bioinformatics*, 21(1):71–79.